Title
A Combinatorial Peptoid-Based Platform for the Development of Selective Metal Binding Materials

Author
Knight, Abigail

Publication Date
2015

Peer reviewed|Thesis/dissertation

A Combinatorial Peptoid-Based Platform for the Development of Selective Metal Binding Materials

By
Abigail Sheldon Knight

A dissertation submitted in partial satisfaction of the
requirements for the degree of
Doctor of Philosophy
in
Chemistry
in the
Graduate Division
of the
University of California, Berkeley

Committee in charge:

Professor Matthew B. Francis, Chair
Professor Carolyn R. Bertozzi
Professor Lisa Alvarez-Cohen

Spring 2015

A Combinatorial Peptoid-Based Platform for the Development of Selective Metal Binding Materials

By: Abigail Sheldon Knight

Abstract

A Combinatorial Peptoid-Based Platform for the Development of Selective Metal Binding Materials

by

Abigail Sheldon Knight

Doctor of Philosophy in Chemistry
University of California, Berkeley
Professor Matthew B. Francis, Chair

Ligands with the ability to selectively chelate individual metals can be applied in heavy metal remediation, recycling, and metal separations, yet such ligands are currently rare and those processes are avoided or expensive due to the use of nonspecific methods. In order to identify compounds that will selectively chelate metal ions, we designed and synthesized a peptoid library and several screening methods to identify motifs capable of chelating low concentrations of various metal ions in complex sample media. Peptoids, or N-substituted glycine oligomers, are a recently developed class of peptidomimetics that have a variety of new structures and applications. The first target application was the remediation of water contaminated with toxic Cr(VI). Identified structures outperformed commercially available resins and demonstrated the ability to reduce the amount of Cr(VI) to levels within the range of the EPA guidelines. A new library generation was developed for the selective coordination of individual ions in a biological context. One target of this library was lethal Cd(II), and peptoid-based ligands were capable of reducing the concentrations of Cd(II) in human serum to 0.5 μM, comparable to the reported threshold for acute toxicity. After demonstrating the success of this screening platform, the platform has been adapted for many applications with a variety of metal ions described within. Towards the development of inexpensive functional materials, a biorthogonal bioconjugation reaction has been applied to immobilize peptoid sequences after synthesis. This work begins to illuminate the diverse array of applications of selective ligands for individual metal ions and demonstrates the potential for peptoids in highly functional materials.

Dedicated to my friends and family.
I could not have done this without your unfaltering support.

Table of Contents

Chapter 4: Removal of Nickel and Cadmium from Biological Media

Chapter 5: Towards Functional Peptoid-Based Materials for Environmental Applications

Chapter 6: Immobilization of Peptoids on Glass Substrates via Oxidative Coupling to *o*-Aminophenols

Acknowledgments

First and foremost, I would like to acknowledge Matt Francis. I know he hates it when people thank him for "letting me join your lab," but as the sole student joining an overcrowded lab, I am nevertheless appreciative. Matt has always been supportive of new ideas and projects, and the ability to venture into a new research area for the lab has been a challenge, but an invaluable experience in my graduate career. His constant encouragement and enthusiasm for science helped me get through the bumps in the road and have been a driving force for the lab as a whole during my time here.

My home away from home during graduate school has been the Molecular Foundry at Lawrence Berkeley National Lab. I don't know how I would have begun my project without the expertise and instrumentation of the fifth floor. Ron Zuckermann, "the father of peptoids," (I don't think this a thing, but it should be) has become a mentor for me. Through editing an endless review, his consistent involvement and support of Science Leadership and Mentorship (SLAM), and all of our conversations along this journey, I am incredibly thankful that he has been a part of my graduate career.

The people who have defined this experience have been my coworkers in the Francis group. All of them have contributed in some way to the work I have done while here, and have made this experience unique. There a few people I would like to acknowledge in particular. When I joined the lab, Chris and Gary welcomed me into Latimer 733. A room filled with house music and bathroom humor, they were perhaps unprepared for having a first year student in their lives. However, they tolerated my endless questions and qual preparation stress in stride. They are some of the smartest people I have overlapped with, and I'm so glad we have stayed friends since their graduation soon after I joined.

As the only student my year, I quickly became close with many of the older students. The girls of Latimer 743 - Leah, Allie, and Kristen - both helped guide me through joining the lab and selecting a project, and created a fun a relaxed environment filled with "Trader Joe's wine." Leah was the only one to have done combinatorial chemistry in the Francis lab when I joined, and she taught me critical skills including the art of picking 100 μm beads with a pipette. I always admired her kindness and the ease with which she connected with everyone – I know she'll excel in her new position working with undergraduate students at Macalester. Allie was my original lab bestie, and still one of my closest friends. Her generosity and nail polish obsession make her an incredible friend, but her creativity and thoughtful analysis of scientific problems have made her an exceptional mentor. Whenever I was at work late, I could usually count on booming indie music being played by Kristen while she was running some column or another. She was the first to try and bring a bioconjugation twist to my metal-binding peptoid project, and I still have hope that one day someone will continue our peptoid-cerium dream. Finally, although Stacy never sat in 743 while I was there, I always considered her a member of that room. If she wasn't at her bench, it was always assumed that she was out on a 10+ mile run. Her stamina as both a runner and a scientist was always inspiring.

The two people whom with I have shared the south side of 733 are Jelly and Joel. Maybe due to the proximity, these two have become some of my closest friends in the lab. Jelly and her undergraduate student Nielson were always incredibly enthusiastic, and we bonded over working on projects all

on our own. Now that I am moving down to Santa Barbara I can't wait to be somewhat neighbors again! Joel quickly took over Jelly's space when he joined last year, and also rapidly took on my fifth year cynicism. He has also quickly become an essential member of the lab through making posters, maintaining the espresso machine, and by setting lab fashion standards with his 3/4-length sleeves. He is a fantastic scientist and friend, and I know he will continue to improve the lab as a whole.

Many students have joined in the last few years, and brought a fresh energy and excitement. Jess and Jenna both joined from other groups, and brought with them unique expertise in synthetic and inorganic chemistry respectively. Jenna has innate party planning ability, and I will definitely miss her inventive cocktails and "mategria." Am can be easy to look over as she is small and quiet, but she is a talented experimentalist and kind friend. Kristin only recently joined, but has quickly integrated into the lab. I can think of no one better to take over the bench and fume hood that have served me so well in my graduate career.

There are a few students who have joined my project, who I affectionately refer to as "my team." I don't think I can accurately express how much working with all of them has meant to me, but I will do my best. The most recent additions have been Adam and Rachel. Adam was initially hard to read, but as I have gotten to know him he has revealed an incredible sense of humor. I wish I could have continued to get to know him here, but I look forward to our facetime meetings with Rachel in the future. Rachel started working with me the summer before my fifth year, and after breaking a few initial cover slips, she has proved to be an exceptionally motivated and thoughtful scientist. Her bubbling energy, unique word choices (e.g. "brain blast"), and stellar utilization of emoji make her a wonderful coworker and friend.

All of my rotation students, Frances, Jenna, and Rishi, have been great. Unfortunately none of them joined the group, but somehow Rishi never actually left. As someone who remembers everything, and one of the most creative scientists I have met in grad school, I am thankful that he still hangs around. He joined my team as a collaborator interested in making fluorescent peptoids – or as he would like to call them, fleptoids – as heavy metal sensors. Working with him has been a lot of fun, and I'm glad that we have become close friends in addition to collaborators.

Finally, the original and most important member of my team, Effie. When I asked her to work with me I knew that she had mastered the one of the critical skills of general chemistry: making dilutions. However, as Matt Francis finally came to agree, she is "the best undergrad ever". Her academic success speaks for itself, but in the last three years she has significantly contributed to the projects we have pursued. Her kindness, sass, and persistent enthusiasm have made the last three years particularly enjoyable and have spoiled me for mentoring anyone else. I am forever grateful for her, and all of my team – they have taught me at least as much as I taught them.

I'm sure that every class thinks this, but I was lucky to be a member of an amazing graduate class. Perhaps because we were small with only 55 students, we became close very quickly. I have remained close with many of the girls from that year (Jen, Cory, Kate, Ashley, Beatriz, Jordan, Steph, Latisha, and Leah). They have taught me about all fields of chemistry and have been an incredible group with whom to share this experience. Although we make fun of Leah for being "old," she has a worldly wisdom allows her to give the best advice. Latisha has been my nail polish and crafting bestie for years, but in the past few months has provided much needed writing solidarity. I'm so excited for Leah to venture into the world of policy, and for Latisha to take on a "real job." I hope we

can continue to have somewhat frequent cocktails dates.

The two men of the fifth year I have become close with are my roommates, Mike Blaisse and Peter Robinson. They are both incredibly hard working, smart, and fun. I don't know what I'm going to do without our evening scientific conversations or their tolerance of my irrational fear of all bugs. I know that they will both excel wherever they end up, whether as professors or starting companies named after forms of Latin dance.

The longest supporters of my scientific career are my family members. Since I was young, my parents have convinced me that I can succeed at whatever I set my heart on. My mom has always been there to answer the phone and has been incredibly supportive. My dad has been a constant inspiration demonstrating both that a career as a professor isn't all that bad and the importance of solving problems that have a significant impact. Whenever I have felt overwhelmed, I have always been reminded by my younger sister, a vet student, that things could be worse. I am forever grateful for their constant support and love.

An unexpected outcome of graduate school and joining the Francis group was meeting my boyfriend Mike. He has been both a loving and supportive best friend and a constant sounding board for my ideas. Although my life will most likely be filled with mason jars, NPR, and coffee brands no one else has heard of, I consider myself incredibly lucky to have ended up with the smartest and kindest man I have ever met. His sense of humor has brightened my graduate career, and his creativity has inspired many of the ideas described below.

Chapter 1

Peptoid Polymers for Diverse Materials Applications

Abstract

Polymer sequence programmability is required for the diverse structures and complex properties that are achieved by native biological polymers, but efforts towards controlling the sequence of synthetic polymers are, by comparison, still in their infancy. Traditional polymers provide robust and chemically diverse materials, but synthetic control over their monomer sequences is limited. The modular and step-wise synthesis of peptoid polymers, on the other hand, allows for precise control over the monomer sequences, affording opportunities for these chains to fold into well-defined nanostructures. Hundreds of different side chains have been incorporated into peptoid polymers using efficient reaction chemistry, allowing for a seemingly infinite variety of possible synthetically accessible polymer sequences. Combinatorial discovery techniques have allowed the identification of functional polymers within large libraries of peptoids, and newly developed theoretical modeling tools specifically adapted for peptoids enable the future design of polymers with desired functions. Work towards controlling the three-dimensional structure of peptoids, from the conformation of the amide bond to the formation of protein-like tertiary structure, has and will continue to enable the construction of tunable and innovative nanomaterials that bridge the gap between natural and synthetic polymers.

This chapter is based on the publication in *Advanced Materials* entitled "Sequence Programmable Peptoid Polymers for Diverse Materials Applications."

1.1 Advantages of Peptoids in the Development of Functional Materials

The challenge of creating synthetic materials with the structural sophistication and complex function found in biology has been a long-term goal in materials science (Figure 1.1). Research from both the biological and chemical communities has been converging to fill the large gap between synthetic homopolymers and native biological materials. Nature has evolved a variety of sequence programmable polymers that have functions ranging from carrying the genetic code to catalyzing chemical reactions. Natural biopolymers represent the pinnacle of sequence control, and this has allowed for the evolution of a plethora of sophisticated functions. These functions are enabled by the precision control of molecular interactions on the Ångström scale – the length scale of individual bonds. Proteins have complex networks of noncovalent interactions that are necessary for specific molecular recognition (e.g. binding to specific DNA sequences), as well as precisely placed functional groups that are required for catalysis. These exquisite nanoscale architectures are typically folded from absolutely monodisperse linear polymer chains of a precisely defined monomer sequence. Biological research has been moving towards the production of novel materials using the natural biosynthetic machinery; recent work in directed protein evolution[1] and the incorporation of unnatural amino acids[2–4] has made it possible to evolve proteins for non-native functions. However, biopolymers and materials based on proteins or DNA suffer from inherent limitations, including the necessity of water as their solvent, susceptibility to enzymatic degradation, and poor environmental stability to variation in temperature, pH, and ionic strength.

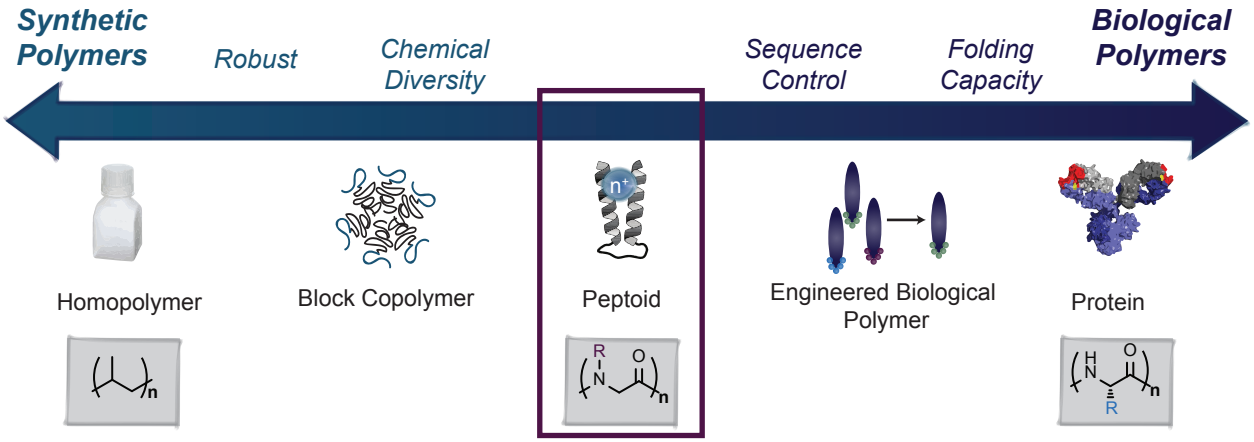

Figure 1.1. The range of characteristics for synthetic and biological polymers reveals a gap that is strategically filled by peptoid-based materials.

The study of synthetic polymeric materials began with homopolymers and copolymers, and has expanded into functional heteropolymers. While polymeric materials tend to be significantly more robust than protein-based materials, they lack the structural sophistication achieved by proteins. In recent years, polymer chemists have sought to improve synthesis methods to emulate biology's degree of sequence control, and the gap between synthetic polymers and native biological materials is beginning to close.[5–7] Many synthetic strategies for polymer sequence control have recently been developed, including templating, kinetic control, orthogonal reactivities, and the linking of structures after polymerization.[5] These techniques have allowed for significant advances in synthetic polymer materials, especially in the development of novel photonics and dynamic materials.[7–9] The demonstrated utility of partial sequence control illuminates the abundance of

opportunities available as the synthetic tools for precise monomer control continue to improve.

Step-wise synthesis provides the opportunity to generate polymers with complete sequence control. This strategy was pioneered using solid supports by Merrifield for peptide synthesis,[10] but has also been developed for the synthesis of DNA, RNA and a variety of resin-bound organic structures.[11] However, the extension of these techniques to create sequence-defined non-natural polymers of significant main chain lengths has been a longstanding challenge. The monomer coupling reactions used to make such polymers need to have nearly quantitative yields in order to synthesize large, well-defined polymer chains. Peptidomimetic *N*-substituted glycine polymers, or peptoids, break this yield barrier and have thus opened up a new class of sequence-defined polymers (Figure 1.2).[12] Peptoid polymers thus straddle the boundary between biological materials and synthetic polymers: their biomimetic structure and precision sequence control provides a breadth of opportunities to produce sequence programmable, folded polymers with the robustness typical of synthetic materials.

Figure 1.2. Peptide versus peptoid structure. Example tetramers are shown of each.

The step-wise solid-phase synthesis of peptoids was developed in 1992,[13] and since then their application to various fields has grown exponentially. This synthesis strategy provides access to an almost infinite diversity of polymer sequences, since each monomer is individually tunable. The large population of potential polymers opens the opportunity to screen for particular sequences with new functionalities using combinatorial chemistry.[14] Moreover, the ability to identify functional structures from such libraries accelerates the discovery of materials with advanced properties. Although this capability exists with genetically-specified biological polymers (e.g. polypeptides and polynucleotides), peptoids are a more versatile option due to their increased chemical diversity, increased stability to degradative enzymes and environmental variables, and a decreased synthetic cost. The step-wise synthesis of peptoid polymers makes the nearly absolute monodispersity encountered with biological polymers accessible, allowing for unique structural control in a synthetic polymer. Recent reviews have described applications of peptoids as small molecules[15–17] and polymers,[18–22] and in the field of biomaterials.[12,23]

1.2. Synthesis and Structural Control of Peptoids

Synthesis

Peptoid polymers have been synthesized using two strategies: an iterative step-wise technique, typically performed on a solid support, that allows precise control of sequence definition, and a polymerization approach, typically completed in solution, that allows access to higher molecular weight polymers. The step-wise submonomer synthesis uses a two-step monomer addition cycle, similar to solid-phase peptide synthesis (Figure 1.3a).[24] Both reactions used in the submomoner synthesis strategy can achieve near quantitative yields, allowing the efficient synthesis of virtually monodisperse sequence-defined polymers. This synthesis, which can be performed

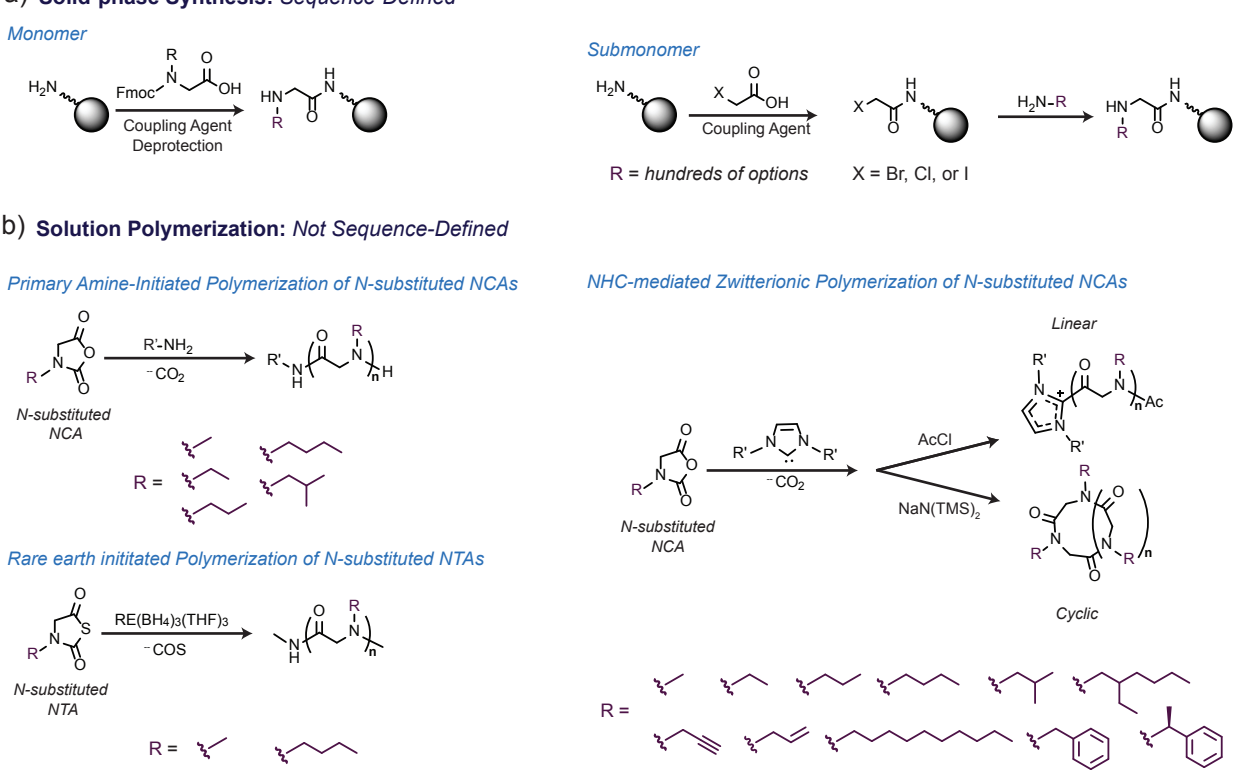

Figure 1.3. An outline of the most common techniques used for the synthesis of α-peptoids. a) Peptoid synthesis techniques used with solid-phase polystyrene resins. Carbodiimides are most commonly used as the coupling agent and piperidine is commonly used for the deprotection step. b) Solution polymerization using N-substituted NCAs and NTAs for peptoid polymer synthesis. For $RE(BH_4)_3(THF)_3$, the rare earth (RE) can be Sc, Y, La, Nd, Dy, or Lu.

manually or by an automated synthesizer, can yield polymers of up to fifty monomer units in length. For larger polymers, the ring-opening polymerization (ROP) of *N*-substituted α-amino acid-*N*-carboxyanhydrides (*N*-substituted NCAs) has been applied to create peptoid homopolymers and copolymers (Figure 1.3b).[22] Less sequence control is available with the polymerization approach, but a large number of different side chains have been incorporated, providing access to a wide variety of polymer structures within the same backbone.

To access sequence-defined peptoid polymers, a step-wise modular synthesis is required. Although the iterative synthesis appears tedious and time consuming in comparison, both synthesis on a solid-support and the automation of the coupling reactions enables rapid and facile synthesis of these polymers. The nearly quantitative yields of the two-step synthesis lead to high yields of very pure polymer material. The modular synthesis begins with the acylation of a resin-bound amine with a haloacetic acid, followed by displacement of the halogen with a primary amine (Figure 1.3a). The nature of this synthesis allows for the use of diverse functional groups as side chains, since nearly any primary amine can be incorporated as a submonomer. Unlike the synthetic strategies used for the synthesis of biological polymers, this synthetic scheme does not require the synthesis of special building blocks. Correspondingly, hundreds of side chains can be easily incorporated at each position directly from commercially available materials. Side chains with reactive functional

groups necessitate protection, but many heterocycles can be used directly with no protection.[25]

Since the first demonstration of the submonomer synthesis technique,[24] hundreds of monomers including ionic, aromatic, heterocyclic, and aliphatic moieties have been incorporated.[26] Almost any primary amine can perform the halogen displacement, providing an unlimited library of functional groups. Functional groups that have been incorporated on the side chains range from small aliphatic groups, to amino acid-like side chains, to larger moieties (e.g. carbohydrates, dyes and cofactors) and individual side chains have been demonstrated to contribute significantly to polymer properties and function. A few examples include azobenzene side chains that lead to photoresponsive polymers[27] and chiral monomers that introduce entropic constraints and promote the formation of secondary structures.[28] The submonomer synthesis method has also been expanded to include chemoselective coupling partners, such as ketones, aldehydes, and thiols, for conjugation of peptoid polymers to other molecules or to substrates.[29] Additionally, Kirshenbaum *et al* demonstrated the incorporation of larger moieties, including hormones and metal complexes, which were added to a fully elongated peptoid using click chemistry.[30] Their work compared the electrochemical properties of ferrocene-peptoid conjugates to the properties of free ferrocene, noting a minimal attenuation of electrochemical properties.

While traditional synthetic techniques allow for rapid and facile synthesis of peptoid polymers, methods relying on biosynthetic pathways could increase the ease of synthesis and enable larger sequence-defined peptoid polymers to be formed. The current techniques only produce small oligomers, but these strategies have huge potential. A ribosomal synthesis has been described for the synthesis of peptoids and peptide-peptoid hybrids by the Suga group.[31] A cell-free translation system was used[32] in addition to flexizymes – artificial aminoacyl-tRNA ribozymes[33] – allowing for the incorporation of *N*-substituted glycines. A variety of functional groups were evaluated, including branched and unbranched alkyl chains and functional chains such as esters, azides, alkenes, and alkynes. Although the yields were low, linear peptoids of up to six monomers were synthesized in addition to cyclic peptide-peptoid hybrids linked with a thioether. Biological machinery has also been applied to the synthesis of β-peptoid homopolymers; a lipase was employed to catalyze the synthesis of poly(*N*-(2-hydroxyethyl)-β-propylamide.[34] The synthesis of hexamers was characterized by MALDI-TOF MS, and the structure was further derivatized to form a brush with polycaprolactone. The copolymer was cast to form films of microstructures characterized by SEM. Although all of the peptoids that have been synthesized with biological machinery are limited in length, these groups have opened up the avenue for enzyme-based synthesis of peptoid-polymers.

A variety of combinatorial platforms using the submonomer synthesis have been developed and employed for identifying functional peptoid sequences. Libraries were initially developed for drug discovery applications such as finding low molecular weight structures that bind specifically to a protein.[35] They have since been used for additional applications including identifying antimicrobial[36] and antifouling[37] molecules and ligands for selective metal coordination.[38] The strength of the combinatorial approach is the ability to screen thousands of molecules for a particular functionality, but once the active compound is identified the structure must be removed from the resin to identify the sequence. Therefore, a cleavable linker such as a methionine (cleavable with CNBr) or a photocleavable linker must be incorporated. Once the peptoid is cleaved, the structure is typically identified using tandem mass spectrometry (MS-MS). In particular, the Kodadek group has contributed to the body of methods for synthesis and screening of combinatorial

peptoid libraries. Techniques that could be applied to materials applications include the design of dimeric[39] and cyclic[40] peptoid libraries that can be sequenced with MS-MS and the development of a two-color quantum dot-based screen.[39] Their work has additionally highlighted the utility of redundant combinatorial libraries to eliminate false positives before post-screening validation.[41] Combinatorial techniques have been applied not only on polystyrene-based resins, but additionally on glass slides[42] and cellulose;[43] this diversity of substrates allows for the development of novel materials such as microarrays that have been used to identify substrates for the early detection of diseases.[44]

While step-wise synthesis is required for sequence control of peptoid polymers and enables the application of combinatorial chemistry, there are still limitations in the length of the polymers that can be accessed. Techniques using traditional living polymerizations have been developed to overcome this limitation. The ring-opening polymerization of *N*-substituted NCAs to form polysarcosine was initially performed in the 1926.[45] In more recent research efforts, the Luxenhofer group has synthesized a variety of polypeptoids using the ROP of *N*-substituted NCAs (Figure 1.3b). They have demonstrated the reliability of living polymerization by making well controlled homopolymers and multiblock copolymers. These copolymers are not accessible via the ROP of NCAs without the *N*-substitution due to irreversible chain termination.[46] Polymerization of *N*-substituted NCAs leads to high monomer conversion and yields polymers with molecular weights of approximately 1 – 10 kg/mol[47] and low polydispersity index ($Đ_M$) values (below 1.1).[48] The polymers are flexible and have a diversity of side chains. Aliphatic side chains with one to four carbons have been evaluated; polymers with shorter side-chains were determined to be water-soluble and those with longer chains were insoluble in water. This allowed for the design of amphiphilic block copolymers. The polymers were characterized by matrix-assisted laser desorption/ionization time of flight mass spectrometry (MALDI-TOF MS), NMR, and GPC. The kinetics of the polymerization were determined to be pseudo first-order with respect to the initiator, allowing for predictable molecular weights.

A few variants of the ring-opening polymerization of *N*-substituted NCAs have also been explored. Zhang and coworkers have described the polymerization of *N*-substituted NCAs using *N*-heterocyclic carbene-mediated ROP (Figure 1.3b), which interestingly can yield either linear or cyclic polymers. [49] The synthesis of the cyclic polymers was determined to proceed with pseudo-first order kinetics and lead to high monomer conversions with narrow weight distributions ($Đ_M$ = 1.03 – 1.15).[50] Cyclic poly(*N*-decylglycine)s were synthesized with an impressive range of molecular weights (4.8 – 31 kg/mol). Block copolymers were synthesized with poly(*N*-methylglycine) achieving similar monomer conversion yields. These block-copolymers were demonstrated to form spherical micelles that transitioned into tubular micelles over time. Ling *et al* used a *N*-substituted glycine *N*-thiocarboxyanhydrides (*N*-substituted NTA), a thio-variant of the *N*-substituted NCAs, to synthesize hydrophilic polymers with sarcosine monomers,[51] hydrophobic polymers with butyl side-chains, and block copolymers which are thermoresponsive.[52] The *N*-substituted NTAs are simpler to synthesize than the corresponding *N*-substituted NCAs and are stable for up to a year at room temperature in an inert atmosphere. Polymerizations of *N*-substituted NTAs required higher temperatures due to lower reactivity, however, the yields, molecular weights, and polydispersities of the synthesized polymers are comparable to those polymerized from *N*-substituted NCAs.

Critical to the development of functional peptoid-based materials is the ability to immobilize

peptoid polymers on various surfaces. There are two fundamental approaches to this: synthesizing polymers from a substrate surface, and ligating structures to a surface after synthesis. Examples of synthesizing polymers directly from a substrate include synthesis on glass surfaces[42,53] and living polymerization on a 1% crosslinked polystyrene beaded solid-support, which is commonly used for solid-phase synthesis.[47] Photolithographic synthesis has been reported using UV-irradiation to unmask a protected surface moiety, allowing spatial and density control over step-wise peptoid synthesis on a glass surface.[42] Additionally, amphiphilic block polypeptoids were synthesized using surface initiated polymerization from a glass surface. [53] The height of the polymer brushes formed was characterized by atomic force microscopy, and the surface was characterized using contact angle measurements. Multiblock copolymers have also been synthesized on a polystyrene resin using ROP of *N*-substituted NCAs, a polymerization typically used in solution.[47] Up to five blocks of polymers with small side chains and low kg/mol molecular weights have been synthesized on a polystyrene resin, then cleaved and characterized with MALDI-TOF MS and ^{1}H-NMR. A strong Brønsted acid (HBF_4) was used to decrease the polydispersity ($Đ_M$ = 1.44) by slowing the polymerization. This synthesis is rapid and cost-efficient and is particularly promising due to the potential to be used in combination with submonomer peptoid synthesis or solid-phase peptide synthesis to create hybrid structures with unique bioconjugation capabilities and various applications.

Modified Primary Structure

Side chain diversity enables structural and functional control, but additional conformations and applications could be accessed by backbone-variants of the traditional α-peptoid. The most

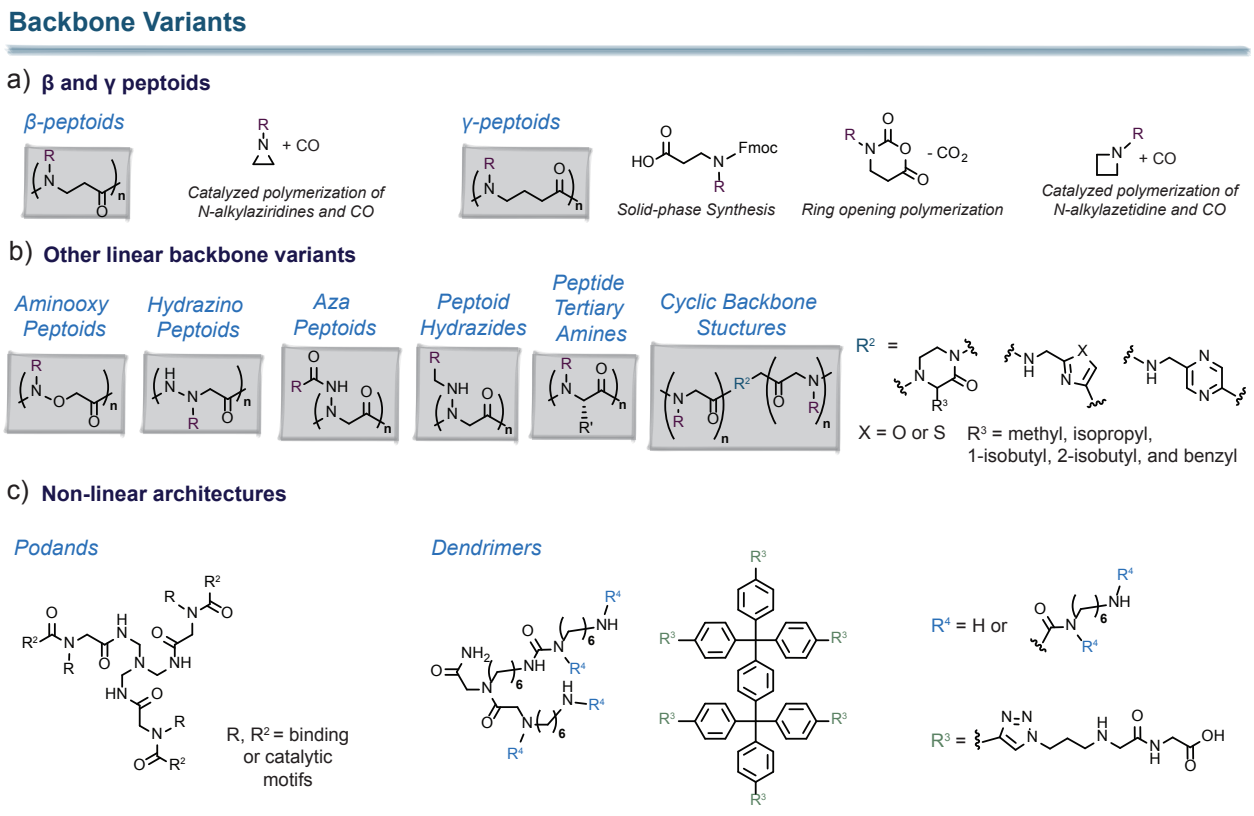

Figure 1.4. An outline of peptoid backbone variants. a) β-peptoid and γ-peptoid structures and synthesis techniques. b) Additional variations on the α-peptoid backbone structures. c) Branching peptoid-based structures. Various side chains were incorporated into the podand, and first, second, and third generation dendrimers were synthesized using the structures on the right.

common variant of the *N*-substituted glycine peptoid backbone is the β-peptoid, or *N*-alkyl-β-alanine oligomer.[54] A variety of synthetic routes have been applied to the synthesis of these structures (Figure 1.4a), including multiple methods of solution phase polymerization. The first catalytic synthesis of poly-β-peptoids was reported by Hanton and coworkers.[55] This copolymerization of *N*-alkylaziridines and carbon monoxide was used to synthesize poly-β-peptoids with quantitative yields and controlled molecular weights (2 – 11 kg/mol with $Đ_M$ = 1.11 – 1.64). The reaction is catalyzed by $BnCOCo(CO)_4$, which is readily synthesized and purified with an extraction before polymerization. The polymers have been characterized by ^1H and ^{13}C-NMR in addition to IR and MALDI-TOF MS. This work was continued by Li Jia's group who investigated the mechanism of the polymerization with various catalysts.[56] Using the aforementioned technique, multiple side-products can form, including a lactam and polyamines instead of the amide based-polymer. To gain a more comprehensive understanding of the mechanism, *in situ* infrared spectroscopy was used to monitor chain growth over time. One of the catalysts, $CH_3C(O)Co(CO)_3P(o\text{-tolyl})_3$, allowed rapid dissociation of the $P(o\text{-tolyl})_3$ ligand, and the remaining cobalt complex efficiently performed the polymerization without catalyzing the formation of a lactam side-product. β-peptoids synthesized using cobalt-based catalysts were characterized using NMR and MALDI-TOF MS, and subsequently immobilized on gold as an anti-fouling material.[57] A similar technique involving the cobalt-catalyzed polymerization of *N*-alkylazetidine and carbon monoxide has been used to synthesize γ-peptoids, which contain one additional methylene in the backbone compared to the β-peptoid.[58,59] This synthesis does not have as high yield as those for β-peptoids due to competing reactions, and therefore the applications of these peptoid variants are rare.

Sequence-defined β-peptoids have also been synthesized using step-wise chemistry (Figure 1.4a). The first approach used a two-step monomer addition cycle involving acylation with an acrylic acid followed by a Michael addition with a primary amine.[60] Further work was done by Arvidsson *et al* optimizing the synthesis and exploring Lewis acid catalysts.[61] They obtained the highest yields using Tentagel S PHB as a solid-support and a solvent system of water and tetrahydrofuran (THF). In this work, a nucleophilic submonomer synthesis similar to that used for α-peptoids was also evaluated and determined to be less efficient. Fmoc-protected monomers were also used to synthesize β-peptoids but led to poor yields.[62] A ring-opening polymerization was first investigated by Birkofer *et al* with the polymerization of *N*-*p*-tolyl-β-alanine-*N*-carboxyanhydride.[63] This reaction has been more recently characterized establishing its living character via kinetic analysis, and the polymerization has been used to synthesize block copolymers.[64] However, further characterization is still required as the molecular weights cannot be reliably predetermined.

The single methylene extension of β-peptoids is not the only backbone variant that has been explored. Aminooxy peptoids have been synthesized in both directions (C→N and N→C) using solution phase synthesis combining nitrobenzenesulfonamide-protected *N*-substituted aminooxyacetate *tert*-butyl esters (Figure 1.4b).[65] Several pentamers with hydrophobic side chains were synthesized using this method. Hydrazino azapeptoids have also been synthesized using a solution phase synthesis.[66] The Kodadek group has additionally worked towards the synthesis of several variants of the typical structure of an α-peptoid. To increase the conformational restraint and functionalization of the peptoid, peptoids with side chains on both the α-carbon (peptide-like) and nitrogen (peptoid-like) have been synthesized using a modification of typical submonomer synthesis.[67] All of these techniques add functional and structural diversity to the peptoid backbone; however, thus far they have been limited to low molecular weight compounds. Fortunately, the

multifunctional submonomers pursued by the Kodadek group are compatible with the typical submonomer technique and could therefore be individually introduced into larger peptoid polymers.

The synthesis of azapeptoids has been achieved by the Kodadek group by using acyl hydrazides in place of the typical primary amine in the submonomer synthesis method.[68] The crystal structure of an acylated monomer indicated that acyl hydrazides tend to prefer *trans* amide bond geometries. Tetramer azapeptoids were synthesized to demonstrate that short structures could be prepared in high yields; however, this chemistry was found to undergo side-reactions under typical peptoid synthesis conditions as a result of intramolecular cyclizations. Further work indicated that these side reactions only occur when a methylene group precedes an aromatic group in the side chains of the azapeptoid.[69] To solve this problem, carbazates and semicarbazides were investigated as alternatives to the acyl hydrazides. These did not perform the undesired cyclization when incorporated with typical peptoid monomers. An octamer library combining typical peptoid monomers and those based on acyl hydrazides, carbazates, and semicarbazides was synthesized, demonstrating the compatibility of these reactions. There are many commercially available carbazates and semicarbazides, making this a promising technique for incorporating backbone diversity. Peptoid hydrazides, which have a similar structure to azapeptoids, have been synthesized using hydrazine as a monomer in the submonomer synthesis. [70] After the cleavage of the peptoid from the resin, modification with an aldehyde and reduction with sodium cyanoborohydride yielded a peptoid hydrazide backbone. This chemistry was used with akyl, aryl, and heterocyclic groups functionalizing the aldehyde.

The Kodadek group has also expanded the variety of peptoid backbone structures by incorporating cyclic molecules. This backbone design leads to unique structures resulting from the additional conformational constraints (Figure 1.4b). This conformational restraint is particularly advantageous as typical peptoid polymers are much more flexible than their corresponding peptides due to the loss of the chiral center.[71,72] The incorporation of heterocycles including oxazole, thiazole, and pyrazine structures into the middle of the backbone was optimized using microwave-assisted conditions.[73] These structures did not prevent sequencing with tandem-mass spectrometry of a combinatorial library. In additional work, 2-oxopiperazine was incorporated in the center of a peptoid backbone.[74] Unlike the heterocycles, which were added as monomers, the 2-oxopiperazine was formed on the solid-support by doing an intermolecular cyclization with an amine side chain and a C-terminal 2-chloroacetamide. The piperazine ring itself was functionalized with alkyl and benzyl side chains.

The primary structure of peptoids has additionally been modified by creating a variety of nanostructures using branching architectures. A one-pot synthesis was used to create peptide-peptoid podands built from tripodal skeletons.[75] Tri-acid, tri-amine, and tri-cyanate scaffolds were used to synthesize a variety of chimeric podands with functional groups including aromatic and heterocyclic rings as well as more complex structures such as steroids (Figure 1.4c). The modularity of the synthesis of these podands and cage structures allows for tunable and versatile structures. For instance, the environment formed by a tri-choline compound yields a unique exterior that changes hydrophobicity depending on the solvent microenvironment. These structures have potential applications in the rapid identification of new catalysts and receptors.

Multiple groups have explored peptoids as the basis for dendrimers (Figure 1.4c).

Bradley and coworkers used *N*-(6-aminohexyl)glycine as the monomer unit of their dendrimer, which was assembled on a solid-phase resin.[76] Microwave irradiation was used to accelerate the coupling reactions of the aminohexylglycine monomer. Three generations of dendrimers were synthesized; double couplings were required to ensure high yield in the second and third generation structures. Mass-spectrometry and HPLC were used to analyze the dendrimer products after ether precipitation, demonstrating an 85% yield for the final generation three dendrimer. These structures were evaluated as transfection agents and found to be non-toxic and able to transfect HEK293T cells. More recently, click chemistry has been used to assemble peptoid dendrimers on a hexaphenylxylylene (HPX) and tetraphenylmethane (TPM) core.[77] Rigid cores were constructed functionalized with alkyne or azide moieties, and peptoid arms were synthesized on solid phase with an N-terminal azide or alkyne-containing monomer and aryl or methoxyethyl side chains. The dendrimers were assembled using Cu-catalyzed click chemistry and washed with a solution of ethylenediaminetetraacetic acid. Dendrimers with the HPX core were found to be insoluble in organic solvents; however, dendrimers with the TPM core were soluble in polar solvents such as acetonitrile allowing HPLC purification. The dendrimers were characterized using electrospray ionization (ESI) MS and NMR diffusion-ordered spectroscopy (DOSY), allowing the calculation of the hydrodynamic radii of the compounds. All of these approaches to synthesizing branched peptoid structures have explored just a few of the potential structures available to *N*-substituted glycine oligomers; these structures could be uniquely useful as nanoarchitectures with more tunability and stability than their peptide counterparts.

Controlling the Secondary Structure

Although peptides primarily favor a *trans* amide bond, peptoid monomers can favor either the *cis* or *trans* orientation of the amide bond depending on local intramolecular interactions (Figure 1.5a). Therefore, many researchers have explored how to control the conformation of the amide bond by varying the size and electronic structure of the side chains and the interactions between the side chains and the backbone. One of the first investigations of the *cis* versus *trans* state was performed by Rabenstein *et al*.[72] They investigated the kinetics of the isomerization of the amide bond with butyl, benzyl, and methyl side chains in solution using NMR. All of the conformational isomers associated with structures containing one, two, and three amide bonds (representing two, four and eight conformations, respectively) were evaluated. The resonances of each isomer were assigned using total correlated spectroscopy (TOCSY) and rotating frame Overhauser effect spectroscopy (ROESY), and inversion-magnetization transfer NMR experiments were used to study the kinetics of exchange. Interestingly, it was observed that the isomerization rate was dependent on the location of the amide bond within the peptoid, and not necessarily just the side group. On average, 35% of the amides were in the *cis* conformation, which is slightly higher than the 10% typically observed with proline, the only proteinogenic *N*-substituted natural amino acid.[78] Additionally, the amide bond isomer tended to be affected by the orientation of neighboring amide bonds: when one amide bond favored a *trans* conformation, the neighboring amide bond demonstrated an increased preference for the *trans* conformation as well.

The control of *cis* versus *trans* amide bond using side chain electronic effects has been investigated in detail. Loca *et al* determined that the $n \rightarrow \pi^*$ interactions that have been characterized in polyproline sequences[79,80] can stabilize amide bond conformations in peptoids as well.[81,82] The $n \rightarrow \pi^*$ interaction between neighboring amides serves to stabilize the *trans* conformation (Figure 1.5c),

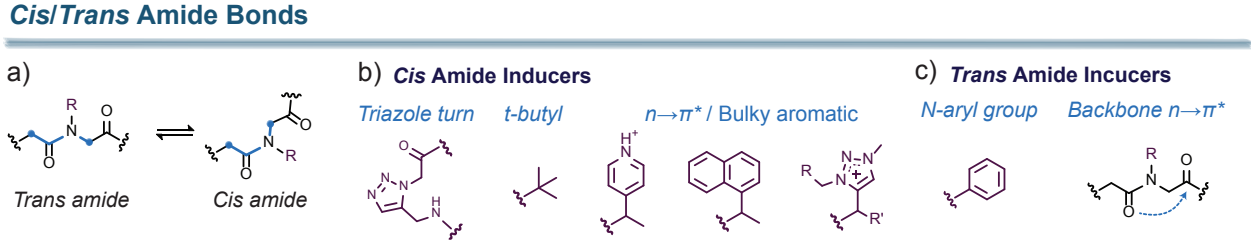

Figure 1.5. Structural features that induce *cis* vs. *trans* amide bonds. a) The equilibrium between the *cis* and *trans* amide bond is depicted with blue circles highlighting the difference in location of the α-carbons with respect to the plane of the amide bond. b) Turn and side chain moieties that will induce *cis* amide bonds. c) Structural features that lead to *trans* amide bonds.

while the n→π* interaction between the amide and aromatic side chains or carbonyl-containing side chains serves to stabilize the *cis* conformation. The unusual *cis* conformation was observed in 89% of the amides using a positively charged α-chiral methylpyridine-containing side chain (Figure 1.5b). Solution phase studies were completed using ^{1}H-NMR and NOESY, and solid-state information was obtained from crystal structures. Gorske and coworkers continued to characterize the n→π* stabilization and found evidence of a "bridged" interaction.[83] In this work over 90% of monomers with an α-chiral naphthyl or pyridine monomer formed a *cis* amide conformation. For the naphthyl compound, there is likely a steric component,[84] but generally computational analysis determined that for electron deficient aromatic side chains, a direct n→π* interaction between the amide and the ring was the driving force stabilizing the *cis* amide bond. However, for rings with a higher electron density that contained an α-methyl group, a "bridged" interaction could contribute to the stabilization. For these cases, the σ* orbital of the methyl group provides a bridge for the electron density from the carbonyl to contribute to the π-system of the aromatic ring.

Kirshenbaum and coworkers performed computational, NMR, and X-ray crystallography studies on *N*-aryl side chains to determine the conformational preferences of ten aniline substituents of varying size and electronic properties.[85] Quantum mechanical calculations on *N*-methylacetanilide-based monomers (the smallest aryl monomers examined) indicated a significant preference for the *trans* geometry (Figure 1.5c), and electron-donating groups tended to increase this preference with the reverse trend for electron-withdrawing groups. These results were confirmed by NMR studies; however, even an aniline with a fluorine substituent maintained a *trans*:*cis* ratio greater than 9:1.

Moieties that lead to an exclusive conformation of the amide bond are rare. Structures have been inserted to create turns in the middle of the peptoid backbone,[86] but only a few functional groups will lead to a single conformation. The Taillefumier group demonstrated that the *tert*-butyl side chain (Figure 1.5b) exerts a purely steric effect, forcing the *cis* conformation of the amide in both water and organic solvents as demonstrated by ^{1}H-NMR and NOE experiments where a *trans* conformation was undetectable.[87] Of particular interest is the research displaying the conformational control provided by the triazole functional group in the side chains of α and β-peptoids.[88] In this work, α and β-peptoids were synthesized with propargylamine and later functionalized with Cu-catalyzed click chemistry. This chemistry has been used for post-synthesis functionalization in other reports;[30,77] however, this work demonstrated how the electron-deficient triazole, even with additional functionalization, can control the amide isomerism. A triazolium linkage led to greater than or equal to 89% of the population with *cis* conformations. With the neutral triazole, the *cis* conformation was still preferred, but to a lesser extent. These measurements were completed

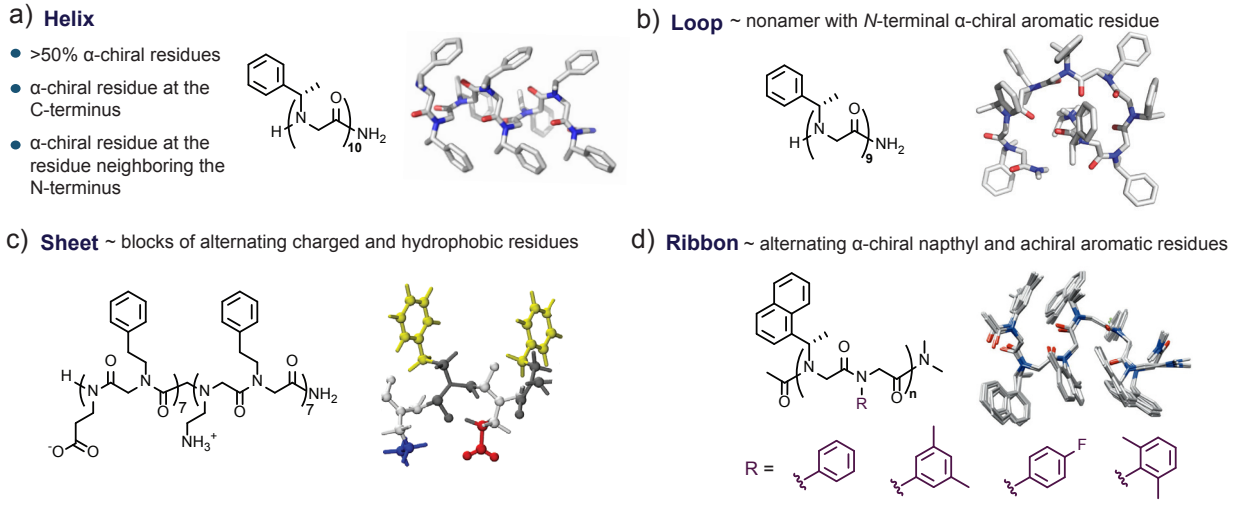

Figure 1.6. Using the primary sequence to control secondary structure. a) A list of primary structure characteristics that encourage the formation of a helix. The structure of a helix as generated using molecular mechanics is shown. b) A "threaded loop" secondary structure observed with peptoid nonamers. c) A sheet structure has been observed within peptoid nanosheets. The structure predicted with coarse-grained modeling is shown. d) The structure of a unique ribbon secondary structure is shown as an overlay of 10 low-energy structures, as determined by NMR spectroscopy. a) and b) reproduced with permission.[96] Copyright 2009, American Chemical Society.

with NOESY, and the effect was investigated with a computational study of the potential energy surface. Their work attributes the stabilization of the *cis* amide to both the $n \rightarrow \pi^*$ interaction and an intramolecular H-bond between the triazole hydrogen and the neighboring carbonyl that is not involved in the $n \rightarrow \pi^*$ interaction.

Secondary structure in a peptoid polymer was first predicted with computational studies of peptoids with chiral side chains.[89] This analysis predicted asymmetric Ramachandran-like plots and therefore indicated the ability of side chains to induce a conformational preference for the amide bond. Barron and coworkers completed some of the initial analysis on forming peptoid helices using chiral aromatic side chains. [90] Since the peptoid structure lacks the amide hydrogen involved in stabilizing peptide helices, other stabilizing interactions are required. However, the incorporation of chiral aromatic monomers in excess of 50% of the total number of side chains was sufficient to confer helicity. Significantly, a chiral aromatic monomer at the C-terminus seemed to be required, though all of these requirements were relaxed with increasing length of the polymer. These helices were able to withstand temperatures up to 75 °C. A continuation of this work displayed the first crystal structure of a peptoid sequence (Figure 1.6a) which was a left-handed helix composed of chiral aliphatic side chains, demonstrating that aromatic monomers were not required for helix formation.[91] The crystal structure indicated an approximate pitch of 6.7 Å and three monomers per turn, results that are comparable to the polyproline type I helix. Both of these studies were important preliminary demonstrations of the capability of secondary structure within peptoid polymers. More recent work verified the significance of a chiral aromatic monomer at the C-terminus demonstrated by Barron *et al* and indicated that in addition to the placement of a chiral monomer at the C-terminus, an α-chiral monomer at the second monomer from the *N*-terminus seems to also have a strong impact on the secondary structure of the peptoid polymer.[92] The presence of only one α-chiral monomer in a heptameric peptoid placed in that position led

to helical character measurable by circular dichroism (CD) spectroscopy. This work highlights the significance of the monomers, and their location in the primary sequence, in directing the peptoid secondary structure. Helices are a fundamental component of protein secondary structure, and therefore the development of peptoid helices is a stepping stone to assembling higher-order structures. Understanding how to control secondary structure formation is critical to the creation of functional peptoid polymer materials.

Research on peptoid helices has been expanded by incorporating functionalized chiral aromatic monomers. The synthesis of α-chiral phenyl monomers with *para*-substituted thiols, carboxylic acids, and amides was completed, and it was demonstrated that these monomers still directed helix-formation.[93] Peptoid sequences with α-chiral pentafluorophenyl monomers were used to specifically probe helix-stabilizing interactions.[94] It was determined using NMR and CD that the hydrogen bonding of the monomer to neighboring heteroatoms was the most significant stabilizing force, and that there was no significant contribution from π-stacking. The placement of the α-chiral pentafluorophenyl monomer at the N-terminus of a nonamer predominantly led to the formation of a "threaded loop" that was previously identified by Radhakrishnan *et al.*[95] In a similar evaluation of a *para*-nitrophenyl α-chiral monomer, this monomer at the N-terminus also stabilized the formation of a threaded loop (Figure 1.6b).[96] However, the *ortho*-nitrophenyl had a destabilizing effect on the secondary structure of the polymer. Even this small chemical difference between the *ortho* and *para* nitro-groups has a significant impact on the folding of the peptoid.

The other canonical secondary structure for peptides, β-sheets, has been observed with peptoids as well. The Blackwell group has crystalized small peptoids with *N*-hydroxyamide peptoid dimers that appear to have β-sheet-like hydrogen bonding interactions between chains.[97] While these are very small structures, it is promising that the hydroxyl side chains could promote β-sheet-like structure in longer polymers. There has been evidence of β-sheet-like structure in longer polymers within the 2D-crystals, or nanosheets, designed by Zuckermann and coworkers (Figure 1.6c).[98] In these assemblies, the intermolecular interactions are hydrophobic forces instead of the typical hydrogen bonding, but powder x-ray diffraction (XRD) has indicated a spacing of 4.5 Å between the polymers, indicating similar packing to peptide beta-sheets that have spacing of 4.7 Å due to hydrogen bonding.[99]

A unique secondary structure rationally designed by Blackwell and coworkers is the peptoid ribbon (Figure 1.6d).[100] This structure was obtained using alternating bulky α-chiral naphthyl monomers and achiral aromatic monomers, which led to alternating *cis* and *trans* orientations of the amide bonds. The ribbon itself had a helical conformation that was parallel to the backbone of the peptoid as characterized by X-ray crystallography, NMR, and CD. This conformation was maintained in protic and aprotic solvents and at different dilutions of the peptoid. This work and the previously described research characterizing the secondary structure of peptoid polymers has created a toolbox of moieties that allow for tunable structures while retaining functionality.

1.3. Surface Immobilized Polymers and Coatings

Antifouling and Antimicrobial Coatings

One important application of sequence specific polymers is to create functional coatings on materials. Maintaining the integrity of surfaces, from instruments as complicated as medical devices to surfaces as large as a ship's hull, has recently become a focus of ongoing research.[101]

Coatings that can prevent the adhesion of proteins, bacteria, and marine microbes are incredibly important in maintaining the useful lifetime of materials. The Messersmith group began the application of polypeptoids as antifouling materials.[37] To achieve this, they focused on a class of peptoid polymers with short, hydrophilic side chains. They used a 25-mer of *N*-(2-methoxyethyl) glycine with a block of five monomers designed to mimic mussel adhesion peptides containing L-3,4-dihydroxyphenylalanine (DOPA) and basic primary amines. The 2-methoxyethyl monomers were chosen to enhance antifouling behavior – namely water solubility, charge neutrality, and the ability to accept hydrogen bonds. Over a period of five months, titanium-modified surfaces modified with these peptoid structures resisted cell adsorption as measured by fluorescence microscopy.

This work was recently expanded by a series of experimental and theoretical analyses. The same anchoring pentamer was used to immobilize varying lengths of 2-methoxyethyl peptoid

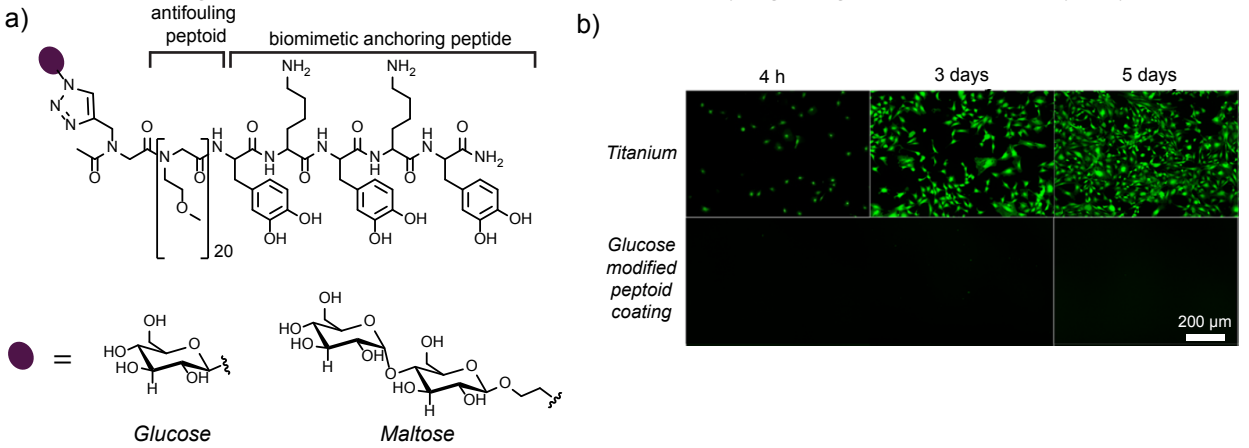

Figure 1.7. Chemical structures and an example application of antifouling peptoids. a) Peptoid structure terminating in a peptide mimetic of a DOPA-containing mussel inspired adhesion peptide linked using click chemistry to carbohydrates as a glycocalyx mimetic. b) Representative images of titanium surfaces with and without the peptoid-carbohydrate antifouling coating treated with fibroblasts demonstrate the ability of the glycocalyx mimic to prevent cell adhesion. Reproduced with permission.[106] Copyright 2013, American Chemical Society.

polymers,[102] monodisperse polysarcosine sequences,[103] homopolymers of hydroxyl-containing monomers,[104] and heteropolymers with alternating charged monomers and 2-methyoxyethyl monomers.[105] Taking advantage of the tunability of the peptoid structures, zwitterionic heteropolymers of different lengths and different spacings between the charged monomers were synthesized and evaluated for antifouling capabilities. Slight differences were observed in the adherence of different cell types, which could be attributed to the aforementioned moieties. In another variation of this work, click chemistry was used to attach sugar units to the previously evaluated methoxyethyl peptoid polymer linked to the anchoring pentamer (Figure 1.7a).[106] These glycocalyx mimicking structures efficiently prevented a series of cells and proteins from adhering to a titanium surface, as demonstrated by fluorescence microscopy (Figure 1.7b). The results of molecular dynamics simulations indicate that sterics are likely the largest contributing factor to the antifouling behavior, in addition to water molecules bound to the terminal sugars. In a unique application of antifouling coatings, the methoxyethyl peptoid polymer and pentamer anchor were used to prevent protein adhesion on the imaging surface used for single-molecule microscopy.[107] Currently poly(ethylene glycol) methyl ether is used for this application, but this coating is labile to hydrolysis and can have unpredictable grafting densities. The peptoid polymer was demonstrated to be more effective at blocking non-specific protein interactions than the typical coating,

demonstrating the practicality for future single molecule studies.

Peptoid polymers synthesized with living polymerizations have also been used as antifouling coatings. Poly(β-peptoids) were synthesized using cobalt catalyzed ring-opening polymerization and adhered to a gold surface using a terminal thiol.[57] Surface plasmon resonance spectroscopy was used to characterize the degree of protein adsorption. This was demonstrated to be an effective and synthetically scalable platform for coating surfaces. Ring-opening polymerization performed directly from the surface has also been applied and provides greater surface polymer densities.[53] An amine-silane was used to functionalize a glass surface, and block copolymers were synthesized directly from the amine moiety. Atomic force microscopy scans of the surface indicated a smooth surface with less than a 1 nm average roughness. Amphiphilic brushes were synthesized using two sequential surface initiated polymerizations and characterized using FTIR spectroscopy and X-ray photoelectron spectroscopy (XPS).

Another approach to anti-fouling is the immobilization of antimicrobial materials on the surface. This approach has been frequently applied with antimicrobial peptides.[108] The Barron group has recently published a number of studies mimicking antimicrobial peptides,[109,110] and the Winter group has applied combinatorial chemistry to this problem.[36,110] However, there is only one report of antimicrobial peptoids being immobilized on a surface.[111] In this work, the immobilized antimicrobial peptoids unfortunately did not prevent adhesion of bacteria to the surface, but the immobilized structures were determined to kill the bacteria that adhered. Although more bacterial adhesion was measured on a surface coated with polymers of methoxyethyl monomers and the antimicrobial peptoids than on a surface coated with the *N*-(2-methyoxyethyl)glycine polymers alone, the antimicrobial retained bactericidal effects. Future studies could involve a more detailed investigation of the ratios and lengths of the polymers, in addition to evaluating other antimicrobial structures.

Chromatography Supports

The ability to separate enantiomers of natural products and synthetic drugs is critical in a wide variety of biomedical applications. A variety of solid supports modified with ligands ranging from small molecules such as amino acids and cyclodextrins to full proteins have been developed to address this concern.[112] Their stability, ability to form secondary structures, and variety of available chiral submonomers make peptoids uniquely useful for this application. The Liang group has published a series of articles evaluating silica modified peptoid structures for these separations. In preliminary studies, polymers of *N*-(*S*)-1-phenylethyl)glycine monomers ranging from three to seven monomers in length were evaluated for their ability to isolate enantiomers of twelve different BINOL (1,1'-bi-2-naphthol) derivatives.[113] A dramatic increase in separation ability was seen with small increases in chain length. For BINOL itself, increasing the chain length significantly enhanced the separation ability, but this reached a maximum at 6 monomers, after which the separation ability started to decline. Methylation of the hydroxyls eliminated the separation ability, and placing bulky groups near the hydroxyls reduced the separation ability, confirming that hydrogen bonding between the substrates and the solid-phase serves as the primary interaction.

Future studies systematically varied the peptoid backbone to assess which other factors contributed to the ability to perform chiral separations. A series of peptoids built on a trimer of (*R*)-*N*-(1-phenylethyl)glycine evaluated the effect of varying the N-terminal moieties (Figure 1.8a).

Various branched and unbranched alkyl chains, in addition to cyclic chiral and aromatic monomers, were evaluated. The chromatographic supports with achiral monomers at the N-terminus outperformed the polymers of (*R*)-*N*-(1-phenylethyl)glycine monomers of the same length. The authors hypothesized that this was due to the removal of unnecessary π-stacking interactions with the aromatic analytes. Additionally, the introduction of additional chiral structures to the N-terminus such as *N*'-phenyl-*L*-proline and *N*'-phenyl-*L*-leucine led to increased peak separation for specific analytes. Another study varied the chirality of the trimer (*R*)-*N*-(1-phenylethyl)glycine monomers and determined that heterogeneous chirality unexpectedly led to increased separation ability.[114]

The study of peptoid-based moieties for the separation of chiral products was expanded by

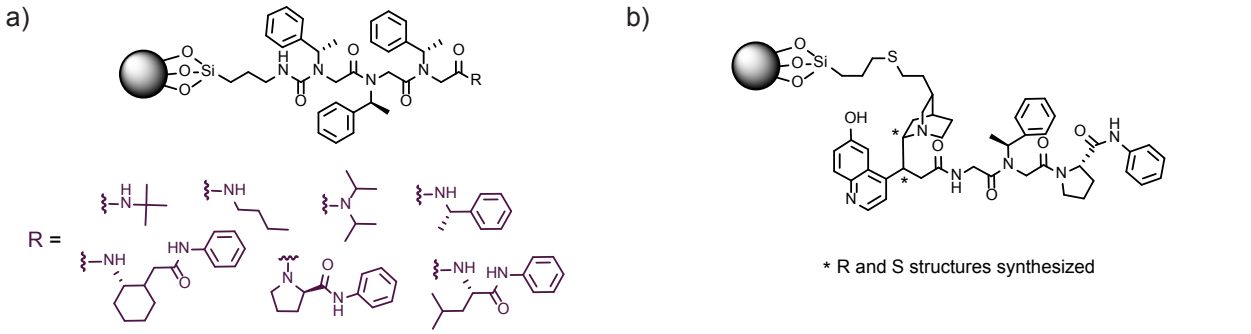

Figure 1.8. Peptoid structures analyzed for their performance in chiral separations. a) The effect of the N-terminal monomer of a trimer of (*R*)-*N*-(1-phenylethyl)glycine groups was investigated. b) The modification of branched peptoid structures with quinine and quinidine moieties was also evaluated.

creating a variety of branched structures. In recent work, a series of six branched structures with six chiral centers was evaluated as chromatography supports; again the chirality was demonstrated to have a large effect on separation ability.[115] Heterogeneity in the chirality of neighboring structures led to increased separation ability, with one structure performing better than some commercial chiral chromatography columns. To increase the efficacy and analyte compatibility, the peptoid-base was expanded by modification with quinine and quinidine moieties, which have been demonstrated to be broadly applicable in chiral separations (Figure 1.8b).[116] These chromatography supports were demonstrated to outperform commercial quinolone-based supports for a variety of analytes. In some separations, the quinolone or quinidine moieties dominated the interactions with the analyte; however, for some of the separations hydrogen bonding and π-stacking with the peptoid played the most significant role in chiral recognition. The series of reports of peptoid-based chromatography supports demonstrate not only the applicability of peptoids for this application, but additionally how the sequence modularity can be used to create a library of supports tunable for the analytes at hand.

Materials Developed with Combinatorial Libraries

Combinatorial chemistry has played an integral part in industrial drug discovery in recent years, and thus a variety of techniques for spatially resolved immobilization of peptoids have been explored. One of the first was an adaption of the SPOT synthesis initially developed for peptides.[117,118] In this method, step-wise synthesis is performed on a cellulose membrane sheet where each individual reaction is spatially separated from its neighbor, leading to a library of thousands

of compounds in a 2D array on the membrane. This technique was applied to the synthesis of a peptoid library in which 8000 peptoid hexamers were synthesized using the a modification of the submonomer method.[43] Due to the prevalence of free hydroxyl groups on the surface of the cellulose, bromoacetic acid 2,4-dinitrophenyl-ester was used for the acylation step. The reliability of the synthesis technique was verified by cleaving individual peptoids and quantifying the purity with LC-MS (on average 44% purity), and the screening capabilities were evaluated by screening the library for antibody affinity.

A more common method of creating a spatially separated array of unique peptoids structures is to create microarrays on functionalized glass. The construction of microarrays from small molecules to proteins has been approached from a variety of perspectives, and there has been significant progress in their construction in recent years.[119,120] A microarray composed of a peptoid library was developed that created unique patterns for individual proteins, demonstrating the promise of peptoid libraries in biomedical detection devices. [121] For high yielding and pure peptoids, the synthesis was completed on a styrene-resin and then adhered to the maleimide-functionalized glass using a SpotArray 72 Microarray Printing System. Using microarrays of over 7500 compounds, they were able to create a "fingerprint" of hybridization unique to individual representative proteins. The protein was either fluorescently labeled or visualized with a fluorescent secondary antibody, and the patterns identified were both unique to the proteins of interest and reproducible (Figure 1.9). This method could reliably detect less than 100 nM of a protein in the presence of *E. coli* cell lysate by subtracting background signal from the lysate proteins (and, when relevant, the secondary antibody). This detection limit is well below the binding affinities previously identified for peptoid-protein interactions, indicating the array itself is critical for the detection of low concentrations of proteins.

In variations of this work, the Kodadek group has also synthesized arrays of unique cyclic peptoids[122] and applied microarrays in the identification of high affinity ligands for proteins of interest.[44,123,124] The immobilization of cyclic peptoids was completed using maleimide-functionalized glass reacted with a cysteine adjacent to the peptoid sequence. The peptoid was cyclized following the on-bead deprotection of a carboxylic acid, which was then reacted with the N-terminus. After cleavage from the resin, the cysteine was robotically spotted onto the glass. A particularly interesting application of the microarrays in the development of diagnostics is the

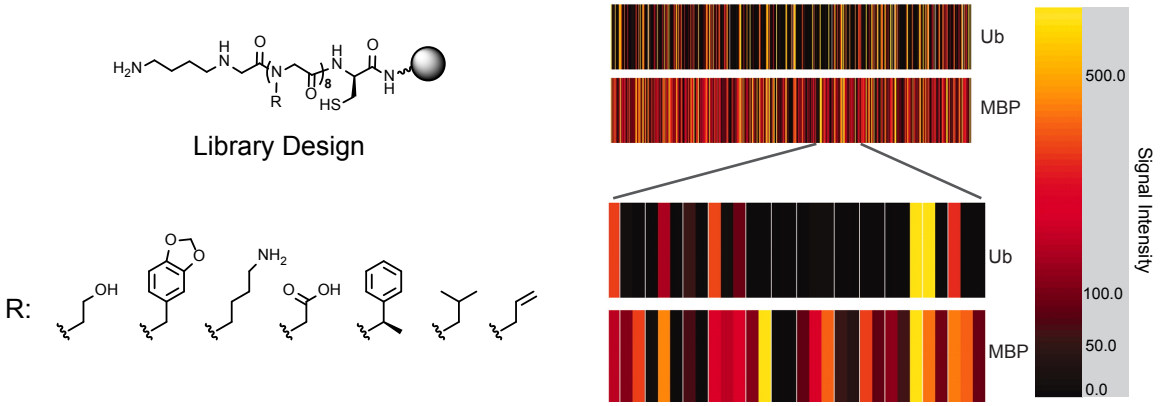

Figure 1.9. Unique protein fingerprints. Peptoid microarrays displaying 7,680 distinct compounds (library schematic shown) were incubated with fluorescently labeled ubiquitin (Ub) and maltose binding protein (MBP). The fluorescence intensities were assigned to a color coding scheme as shown on the right, and depicted as a bar code for ease of visualization of binding. The expanded portion further illuminates the differences in the binding patterns. Reproduced with permission.[121] Copyright 2005, PNAS.

identification of fingerprint patterns for antibodies characteristic of Alzheimer's disease.[44] In this study, blood samples from patients were used to develop diagnostic readouts from a microarray of approximately 15,000 peptoid octamers.

Another unique application that demonstrates the applicability of combinatorial chemistry for materials applications is the identification of peptoid ligands. Some of the first work towards the identification of metal-binding peptoids was completed by Kirshenbaum and coworkers.[125] The binding of a pentamer and hexamer with terminal 8-hydroxy-2-quinoline methylamine monomers, and the affinities for Cu^{2+} and Co^{2+}, were characterized using titrations monitored with UV-vis and CD spectroscopy. The development of peptoid-based ligands has been continued with the development of cyclic peptoids which coordinate Na^{+} and Gd^{3+},[126,127] and combinatorial assays have been established to identify ligands with selective affinity for individual metal ions in a heterogeneous mixture.[38,128] X-ray fluorescence has been used as a screening technique for the identification of multiple metals coordinated to an individual resin-immobilized sequence.[128] As a proof-of-concept, this technique has been used to identify ligands for Ni^{2+} that can remove these ions from a buffered solution. Though the applications of selective ligands are broad (therapeutics, imaging agents, sequestration, etc.) the factors contributing to selective binding are not well understood.[129] Due to the limited precedent for the rational design of selective ligands, these studies demonstrate the value of combinatorial chemistry for rapidly identifying new structures for unique materials properties including selective metal coordination.

1.4. Mimicking Natural Biological Constructs

Lipitoids and Surfactants

The non-viral delivery of nucleic acids into cells is critical for the development of stable, non-toxic, and inexpensive vectors for nucleic acid based pharmaceuticals.[130] With the recently discovered capabilities of the CRISPR/Cas9 system, there seem to be almost limitless applications of these RNA-guided nucleases.[131] Non-viral nucleic acid delivery is usually achieved by forming a complex with a cationic polymer of lipid. The development of lipitoids, or lipid-peptoid conjugates, was inspired by peptide-lipid hybrids, which have frequently been employed as cationic gene delivery agents[132] and drug delivery vehicles.[133] The first lipitoids were polymers of an amine-containing monomer attached to various lipids.[134] The step-wise synthesis of these structures allowed for a systematic evaluation of how the ratio of charge to hydrophobicity impacts the efficacy of the transfection. The peptoids that demonstrated the highest transfection activity also protected DNA from nucleases and contained a repeating trimer of a cationic monomer and two hydrophobic monomers. Interestingly, in a continuation of this work, the transfection efficiency could not be directly correlated with size, surface charge, structure (as characterized by CD), or affinity of the synthetic polymer for DNA (as measured by differential scanning calorimetry or ITC).[135]

Additionally, lipitoids have been used as an siRNA transfection agent, efficiently transfecting a variety of difficult cell lines, including primary human cells.[136] The lack of toxicity to immortalized cell lines was confirmed and efficient siRNA delivery was demonstrated by monitoring the target genes with Western Blots and real-time PCR. Additional SEM and DLS characterization was performed in follow-up work to characterize the particles formed from lipitoids and siRNA.[137] The size of the particles formed was found to vary depending the ionic strength of the environment and the ratio of lipitoid to siRNA.

Another approach to making functional amphiphilic peptoids has been extensively investigated by Barron and coworkers. Their work has focused on the mimicry of amphiphilic peptides and proteins using just the peptoid backbone.[138] Previous work has mimicked antimicrobial peptides by also varying simple arrangements of cationic and hydrophobic monomers.[139] The Barron group has also pioneered higher molecular weight analogs that mimic the helical and amphiphilic nature of lung surfactant protein C. The first peptoid developed for this purpose was a 22-mer containing a 14-mer of chiral aromatic monomers, two positively charged monomers, and a hydrophobic core. These structures served as a functional surfactant without aggregating, demonstrating that a sequence-defined peptoid can mimic a 35-mer protein with additional protease resistance. This work was continued by investigating how adding alkyl chains to the N-terminus of this peptoid affected its activity.[140] These alkyl chains served as lipid anchors and increased dynamic film behavior by decreasing the compressibility, as measured by pulsating bubble surfactometry. Similar strategies have been applied to creating mimics of the larger protein, lung surfactant protein B,[141,142] and the addition of a lipid to the N-terminus of these molecules had a similar increased efficacy.[143] Interestingly, peptide-based mimics of lung surfactant protein B are more effective as dimers, so disulfide and triazole linkages of varying hydrophobicity were explored to dimerize the peptoid mimetic.[144] Dimerization by click chemistry surprisingly led to more surface activity than dimerization by disulfide formation, potentially due to the induction of a hairpin-like turn. The authors hypothesize based on these results that the conformational restraint within the native protein is important for its function. Additionally, the incorporation of achiral hydrophilic monomers into the linker, with 50% aliphatic monomers, led to activity improvement.

Protein-like Polymers and Peptoid-Protein Hybrids

One of the first achievements towards mimicking protein structure and function with peptoid polymers was the development of a protein-like tertiary structure that experienced hydrophobic collapse, leading to the assembly of what was predicted to be a helix bundle.[145] In this work, a combinatorial approach was used to identify that monomers on the face of the helix were responsible for driving the assembly. Twelve hydrophobic monomers were introduced in four positions on the 15-mer peptoid to induce the hydrophobic collapse necessary for the formation of tertiary structure. The assembly of the identified helices into bundles was followed with circular dichroism (CD). This work was continued by linking together 15-mers through disulfide and oxime linkages to conjugate the helix bundles covalently.[146] Fluorophores were attached to each end of the peptoid polymer to allow for the detection of hydrophobic collapse via FRET quenching. Cooperative disassembly was observed upon titrations with various solvents, but the helical structure was unharmed, confirming that the FRET assay was an indicator of tertiary structure. Understanding the hydrophobic driving forces for the assembly of peptoid architectures is important for creating protein-like structures; however, this also fundamentally contributes to the understanding and prediction of protein folding itself.

The fundamental process of hydrophobic chain collapse, the coil-to-globule transition that is common to most protein folding pathways, has also been studied using specific peptoid sequence designs. Work by Zuckermann and coworkers investigated how the sequence of a peptoid polymer containing only one type of hydrophobic monomer and one type of polar monomer contributes to its hydrophobic interactions by synthesizing polymers with the same composition but different sequences (Figure 1.10a).[147] Because computer simulations required a 100-mer chain of defined

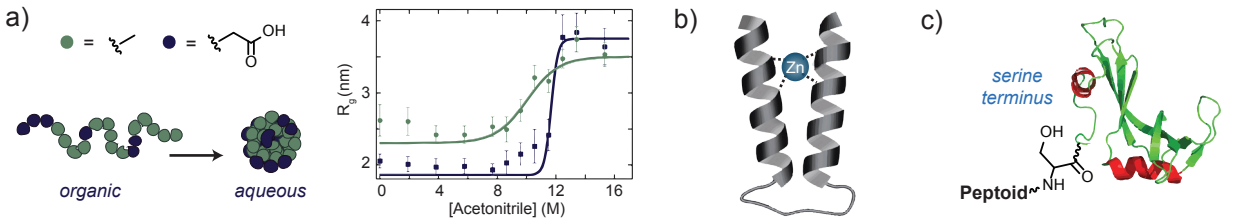

Figure 1.10. Protein-like structures synthesized with peptoid polymers. a) The hydrophobic collapse of polymers into globular structures in water and acetonitrile mixtures was evaluated for "protein-like" and "repeating" sequences with identical compositions but different monomer arrangements. This study indicated that the globular form of the "protein-like" structure was more stable in an organic solvent. b) A peptoid with helix bundle tertiary structure was stabilized with metal coordination. c) A peptoid was attached to ribonuclease S via an N-terminal serine. a) Reproduced with permission.[147] Copyright 2012, American Chemical Society. c) Reproduced with permission.[151] Copyright 2014, ACS.

sequence, two 50-mer peptoids were synthesized and dimerized using click chemistry. One of the structures was designed to be "protein-like" and contained blocks of hydrophobic (*N*-methylglycine) and hydrophilic (*N*-(2-carboxyethyl)glycine) monomers designed using models described by Khokhlov and Khalatur,[148] while the other contained repeating blocks of [(*N*-methylglycine)$_4$-(*N*-(2-carboxyethyl)glycine)]. The stabilities of the assembled globule structures were evaluated by titration with acetonitrile as the unfolding was monitored using SAXS and DLS. The repeating sequence unfolded at lower concentrations of acetonitrile than the protein-like sequence, indicating decreased stability for the repeating structure. This was evidenced by a higher fluorescence signal with the protein-like polymer when probed with Nile red (an environmentally-sensitive dye), indicating a more intact globule. The free energy of the folding transition was calculated in addition to the dependence of that energy on the denaturant (m), both of which were larger for the protein-like sequence. Notably, a 100-mer peptoid polymer was synthesized in this work – one of the largest sequence-defined peptoid polymers that has been synthesized. This also demonstrates the ability to synthesize large polymers using post-synthetic conjugation. It additionally supports the previously mentioned models and demonstrates the utility of sequence controlled polymers in studying fundamental physical properties.

Another way to take on the properties of proteins is to mimic their function. In another report by Zuckermann *et al,* a peptoid helical bundle architecture was designed to mimic a zinc finger motif (Figure 1.10b).[149] Previously identified helical bundle designs[146] were modified with zinc-binding monomer units. The two helices were designed to contain two thirds α-chiral monomers to confer helicity and were built with repeating trimer sequences. The three monomers in the repeating unit were aromatic, acidic, and basic, and a turn sequence between the helices was composed of a Gly-Pro-Gly-Gly sequence or a repeating Gly unit. The zinc coordinating sites were based on an established motif, Cys_2His_2,[150] which was integrated into various sites in the polymer. Eleven peptoids were synthesized with the one of the two linkers and varying locations of the binding motif. A FRET-based assay was used to evaluate the proximity of the two helices in aqueous solution, and the proximity was further evaluated after titration with acetonitrile. Zinc-bound structures did not unfold upon the addition of acetonitrile, indicating the increased structural integrity of the metal-bound structures. This work includes one of few examples of a protein-like tertiary structure and highlights the use of combinatorial chemistry in the development of the precise molecular recognition necessary for higher-order structural control.

Recently, work by Kirshenbaum and coworkers has demonstrated that peptoids can be attached to proteins using a salicylaldehyde functionalized peptoid (Figure 1.10c).[151] Peptoids had

previously been conjugated to small molecules and synthetic homopolymers;[152–154] however, this is the first combination of peptoid sequences and biological polymers. In this work, a ligation strategy developed for the reaction of *C*-terminal salicylaldehyde and an *N*-terminal serine/threonine[155] was applied to conjugate a peptoid and model proteins. The *C*-terminus of the peptoid was functionalized with the salicylaldehyde via an ester, and the model proteins were biosynthesized with the native *N*-terminal serine. The conjugation was completed in a 1:1 ratio of pyridine to acetic acid, which may not be compatible with all proteins of interest, and yielded up to 28% of the desired conjugate with a native amide bond between the peptoid and the protein. CD was applied to confirm that the peptoid did not impact the structure of the protein. In a similar application, individual peptoid monomers have been incorporated into the protein ribonuclease A.[156] These point mutations were incorporated using side-chain translocation mutagenesis. The successful incorporation of peptoid monomers could be used for applications ranging from well-controlled evaluations of the impact of individual monomers on secondary structure to engineering proteins with new functions. The combination of full peptoid sequences and the incorporation of an individual peptoid monomer could be used to combine the advantages of protein and peptoid structures.

1.5. Theoretical Modeling of Peptoid Architectures

A new tool in the development of peptoid polymers is theoretical modeling. It is quickly becoming one of the most useful methods for bridging the gap between synthetic and biological polymers. Due to the tremendous diversity of possible peptoid sequences, modeling is desperately needed to guide the rapid design and discovery of new peptoid-based materials, just as it has proved invaluable to the field of structural biology.[157] Research on peptoid modeling has been approached by adapting peptide force-fields (CHARMM),[158,159] integrating the noncanonical backbone into Rosetta,[160] and using various quantum-mechanical approaches. While there are well-established databases of tens of thousands of protein structures, there are few peptoids with known three-dimensional structures. However, even with the limited available information, models are beginning to be developed and applied, demonstrating the potential of this approach. Early insight into the folding landscape was provided by calculating Ramachandran plots for sarcosine, a model peptoid monomer.[13] Soon after this molecular mechanics predicted the formation of secondary structure by peptoid polymers.[89] A more detailed study characterizing the available peptoid backbone dihedral angles highlighted the impact of six different side chains of various sizes and chemical properties.[161] Density functional theory basis sets were used to evaluate the ability of the peptoid to rotate about each of the bonds in the backbone. As discussed in section 2, peptoids are capable of converting between *cis* and *trans* amide bonds and are less constrained to planarity of the amide bond than canonical peptides, making the isomerization of the amide bond an additional contributor to the number of available conformations. As expected, bulky side-chains can stabilize particular conformations of the peptoid backbones. All of the predicted bond angles were confirmed with the available crystal structures. While most of these structures are of small molecules, an understanding of peptoid topographies on this local scale can likely be extrapolated to larger structures.

The first demonstration of *de novo* structure prediction of a peptoid was demonstrated in 2012 when the structure of a cyclic nonamer was predicted and then confirmed by X-ray crystallography (Figure 1.11a).[162] A combination of Replica Exchange Molecular Dynamics (REMD) and quantum mechanical calculations was able to predict the structure of the nonamer to within 0.2 Å. This method was additionally used to predict the structure of trimers, but the nonamer is

particularly interesting as it approaches the size of functional peptides. While a nonamer is still relatively small, this work was an important advance toward the current capabilities of protein modeling. The authors attribute differences between the predicted and experimental structures to solvent interactions, which were not included in the modeling algorithm. In another molecular dynamics approach, a new force field developed from first principles specifically for the peptoid backbone, called MFTOID, was derived based on the CHARMM simulation package.[163] This allows simulations both in a vacuum and in explicit water (the water was modeled as explicit molecules instead of as a continuous medium). This method was used to simulate a sarcosine dipeptoid and an *N*-(2-phenylethyl)glycine tripeptoid, and demonstrated the significance of solvation in the structure of the peptoid backbone. In this report, the authors suggest that although no modeling of large peptoids had been completed, the small-scale evaluation of individual amide bonds in the peptide backbone has translated to larger proteins; therefore, as structural biology has grown rapidly with the established protein modeling capabilities, peptoid research should similarly be enabled by these computational procedures.

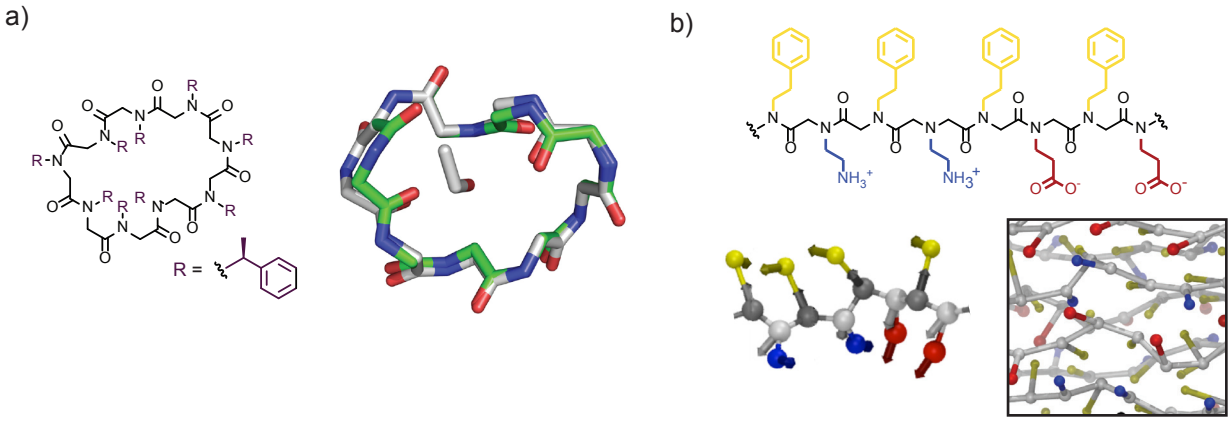

Figure 1.11. Theoretical modeling of peptoid structures. a) Nonamer structure with the experimental (gray) conformation as determined by X-ray crystallography is compared to a conformation predicted by molecular dynamics simulations (green). b) A segment of a peptoid polymer used for nanosheet formation represented as a chemical structure and a coarse-grained model. The nanosheet structure predicted by the model is also shown. a) Reproduced with permission.[162] Copyright 2012, PNAS. b) Reproduced with permission.[167] Copyright 2014, American Chemical Society.

Despite the fact that the surge in peptoid modeling began recently, work towards modeling both large numbers of peptoids and high molecular weight structures is already underway. Some work to integrate experimental and *in silico* approaches has begun by using COSMOS-NMR that allows for three-dimensional modeling based on NMR data without the development of specific force fields.[164] An analysis of a cell-penetrating hexamer with two-dimensional NMR techniques allowed the amide bonds to be characterized as all *cis*, but did not allow for full characterization of the three-dimensional structure. However, with the aid of computational techniques, the structure was determined to be pseudo-helical. To enable entirely theoretical modeling of peptoid structures, recently the peptoid backbones have been integrated into the Rosetta platform typically used for protein modeling.[165] This was then used as a tool to create an *in silico* library of rotamers that represent the conformations available for over fifty side chains.[166]

One demonstration of theoretical modeling that is particularly applicable to materials applications was completed by Whitelam *et al* who used coarse-grained sites to model peptoid polymers that assemble into nanosheets (Figure 1.11b).[167] Of particular interest in this work is

the ability to model not only over longer length scales (which involve non-covalent interactions) but also over longer time scales, and with more polymer chains interacting. All of these features are necessary for understanding supramolecular assembly. To handle these increased demands, some sacrifices must be made in atomic representation – the described model is 10^4 times faster than a model that incorporates every atom. Typically in protein modeling, coarse-grained sites are treated as spherically symmetric. To compensate for this approximation, large numbers of these sites are used. In this work, a different approach was used, with only two sites per monomer fluctuating orientation parameters were incorporated for each of those sites. Due to the flexibility of the backbone compared to typical native biological structures, the models incorporated used independently fluctuating orientations (position and symmetry axes) to evaluate directionally dependent interactions. This model, termed MF-CG-TOID was used to model a 28-mer of alternating hydrophobic and charged monomers as a polymer in solution, as an assembled monolayer at the air-water interface, and as a nanosheet. Work is ongoing to analyze the dynamics of this process. Only with more experimentally determined structures can the accuracy of each of these modeling techniques truly be determined. However, with the diversity of approaches and successes thus far, the widespread modeling of peptoid polymers and assembled materials is certainly on the horizon.

1.6. Conclusion and Overview

As demonstrated in a growing number of examples, peptoid polymers offer wide-ranging opportunities for the construction of advanced biomimetic materials. The efficient and modular step-wise synthesis of these polymers allows monomer-level control and fine-tuning of the polymer structure to precisely engineer polymeric materials for specific applications. Furthermore, it sets the stage for generating and screening vast combinatorial polymer libraries to facilitate the discovery of new materials with desired properties. An underexplored, but imperative application of these materials is in the selective coordination of metal ions. The rapid expansion of peptoid-based materials and integration into a variety of fields has set the stage for this unique application of peptidomimetic materials. In this work, we sought to develop a combinatorial platform for the identification of peptoid ligands with a selective affinity for individual ions and to further integrate these structures into functional materials. This work has both contributed innovative materials for unique applications and expanded our understanding of atomic-scale interactions between peptoid ligands and metal ions.

Herein, the design of a robust and chemically diverse library and screening platform is described. This is followed by the application of this platform to the identification of ligands for the remediation of hexavalent chromium contaminated water. To demonstrate the universal applicability of this strategy, a more complex system was subsequently evaluated. A larger and higher affinity library was screened for ligands that could bind to cadmium in the presence of the proteins, small molecules, and other ions present in human serum. This strategy has additionally been applied to identify ligands for metal separations. Finally, it was demonstrated that a bioconjugation reaction could be used to immobilize ligands on inexpensive glass supports. These studies demonstrate the capabilities of peptoids as metal ligands and highlight the use of combinatorial chemistry in identifying selective ligands and developing functional materials.

1.6 References

1. Nordwald, E. M., Garst, A., Gill, R. T. & Kaar, J. L. Accelerated protein engineering for

chemical biotechnology via homologous recombination. *Curr. Opin. Biotechnol.* **24,** 1017–22 (2013).

2. Hendrickson, T. L., de Crécy-Lagard, V. & Schimmel, P. Incorporation of nonnatural amino acids into proteins. *Annu. Rev. Biochem.* **73,** 147–76 (2004).

3. Noren, C. J., Anthony-Cahill, S. J., Griffith, M. C. & Schultz, P. G. A general method for site-specific incorporation of unnatural amino acids into proteins. *Science* **244,** 182–8 (1989).

4. Van Hest, J. C. M., Kiick, K. L. & Tirrell, D. A. Efficient Incorporation of Unsaturated Methionine Analogues into Proteins in Vivo. *J. Am. Chem. Soc.* **122,** 1282–8 (2000).

5. Lutz, J.-F. Sequence-controlled polymerizations: the next Holy Grail in polymer science? *Polym. Chem.* **1,** 55 (2010).

6. Lutz, J. -F., Ouchi, M., Liu, D. R., Swamoto, M. Sequence-Controlled Polymers. *Science* **341,** 1238149 (2013).

7. Hawker, C. J. & Wooley, K. L. The convergence of synthetic organic and polymer chemistries. *Science* **309,** 1200–1205 (2005).

8. Leibfarth, F. A, Mattson, K. M., Fors, B. P., Collins, H. A. & Hawker, C. J. External regulation of controlled polymerizations. *Angew. Chem. Int. Ed.* **52,** 199–210 (2013).

9. Poelma, J. E., Fors, B. P., Meyers, G. F., Kramer, J. W. & Hawker, C. J. Fabrication of complex three-dimensional polymer brush nanostructures through light-mediated living radical polymerization. *Angew. Chem. Int. Ed.* **52,** 6844–8 (2013).

10. Merrifield, R. B. Solid Phase Peptide Synthesis. I. The Synthesis of a Tetrapeptide. 2149–54 (1963).

11. Cherkupally, P. *et al.* Immobilized coupling reagents: synthesis of amides/peptides. *ACS Comb. Sci.* **16,** 579–601 (2014).

12. Sun, J. & Zuckermann, R. N. Peptoid polymers: a highly designable bioinspired material. *ACS Nano* **7,** 4715–32 (2013).

13. Simon, R. J. *et al.* Peptoids: a modular approach to drug discovery. *Proc. Natl. Acad. Sci. U. S. A.* **89,** 9367–9371 (1992).

14. Potyrailo, R. *et al.* Combinatorial and High-Throughput Screening of Materials Libraries : Review of State of the Art. **13**, 579–633 (2011).

15. Yoo, B. & Kirshenbaum, K. Peptoid architectures: elaboration, actuation, and application. *Curr. Opin. Chem. Biol.* **12,** 714–21 (2008).

16. Fowler, S. A. & Blackwell, H. E. Structure-function relationships in peptoids: recent advances toward deciphering the structural requirements for biological function. *Org. Biomol. Chem.* **7,** 1508–24 (2009).

17. Tedesco, C., Erra, L., Izzo, I. & De Riccardis, F. Solid state assembly of cyclic α-peptoids. *CrystEngComm* **16,** 3667 (2014).

18. Zhang, D., Lahasky, S. & Guo, L. Polypeptoid materials: current status and future perspectives. *Macromolecules* **45**, 5833 (2012).

19. Rosales, A. M., Segalman, R. a. & Zuckermann, R. N. Polypeptoids: a model system to study the effect of monomer sequence on polymer properties and self-assembly. *Soft Matter* **9,** 8400 (2013).

20. Gangloff, N. & Luxenhofer, R. Peptoids for Biomimetic Hierarchical Structures. *Adv. Polym. Sci.* **262**, 389 (2013).

21. Barron, A. E. & Zuckermann, R. N. Bioinspired polymeric materials: in-between proteins and plastics. *Curr. Opin. Chem. Biol.* **3**, 681–7 (2013).

22. Luxenhofer, R., Fetsch, C. & Grossmann, A. Polypeptoids: A perfect match for molecular definition and macromolecular engineering? *J. Polym. Sci. Part A Polym. Chem.* **51,** 2731–52 (2013).

23. Lau, K. H. A. Peptoids for biomaterials science. *Biomater. Sci.* **2,** 627 (2014).

24. Zuckermann, R. N., Kerr, J. M., Kent, S. B. H. & Moos, W. H. Efficient method for the preparation of peptoids [oligo(N-substituted glycines)] by submonomer solid-phase synthesis. *J. Am. Chem. Soc.* **114,** 10646–7 (1992).

25. Burkoth, T. S., Fafarman, A. T., Charych, D. H., Connolly, M. D. & Zuckermann, R. N. Incorporation of unprotected heterocyclic side chains into peptoid oligomers via solid-phase submonomer synthesis. *J. Am. Chem. Soc.* **125,** 8841–5 (2003).

26. Culf, A. S. & Ouellette, R. J. Solid-phase synthesis of N-substituted glycine oligomers (alpha-peptoids) and derivatives. *Molecules* **15,** 5282–335 (2010).

27. Shah, N. H. & Kirshenbaum, K. Photoresponsive peptoid oligomers bearing azobenzene side chains. *Org. Biomol. Chem.* **6,** 2516–21 (2008).

28. Wu, C. W., Sanborn, T. J., Huang, K., Zuckermann, R. N. & Barron, a E. Peptoid oligomers with alpha-chiral, aromatic side chains: sequence requirements for the formation of stable peptoid helices. *J. Am. Chem. Soc.* **123,** 6778–84 (2001).

29. Horn, T., Lee, B.-C., Dill, K. a & Zuckermann, R. N. Incorporation of chemoselective functionalities into peptoids via solid-phase submonomer synthesis. *Bioconjug. Chem.* **15,** 428–35 (2004).

30. Holub, J. M., Jang, H. & Kirshenbaum, K. Clickity-click: highly functionalized peptoid oligomers generated by sequential conjugation reactions on solid-phase support. *Org. Biomol. Chem.* **4,** 1497–502 (2006).

31. Kawakami, T., Murakami, H. & Suga, H. Ribosomal Synthesis of Polypeptoids and Peptoid–Peptide Hybrids. *J. Am. Chem. Soc.* 16861–3 (2008).

32. Shimizu, Y. *et al.* Cell-free translation reconstituted with purified components. *Nat. Biotechnol.* **19,** 751–5 (2001).

33. Goto, Y., Katoh, T. & Suga, H. Flexizymes for genetic code reprogramming. *Nat. Protoc.* **6,**

779–90 (2011).

34. Monsalve, L. N., Petroselli, G., Erra-Ballsells, R., Vázquez, A. & Baldessari, A. Chemoenzymatic synthesis of novel N-(2-hydroxyethyl)-β-peptoid oligomer derivatives and application to porous polycaprolactone films. *Polym. Int.* **63,** 1523–30 (2014).

35. Zuckermann, R. N. Peptoid Origins. *Pept. Sci*. **96**, 545 (2010).

36. Ng, S. *et al.* Combinatorial discovery process yields antimicrobial peptoids. *Bioorg. Med. Chem.* **7,** 1781–5 (1999).

37. Statz, A. R., Meagher, R. J., Barron, A. E. & Messersmith, P. B. New peptidomimetic polymers for antifouling surfaces. *J. Am. Chem. Soc.* **127,** 7972–3 (2005).

38. Knight, A. & Zhou, E. Selective chromium (VI) ligands identified using combinatorial peptoid libraries. *J. Am. Chem. Soc.* **135**, 17488 (2013).

39. Udugamasooriya, D. G., Dineen, S. P., Brekken, R. A. & Kodadek, T. A. Peptoid ' Antibody Surrogate ' That Antagonizes VEGF Receptor 2 Activity A Peptoid ' Antibody Surrogate ' That Antagonizes VEGF Receptor 2 Activity. *J. Am. Chem. Soc.* **130,** 5744–52 (2008).

40. Simpson, L. S. & Kodadek, T. A Cleavable Scaffold Strategy for the Synthesis of One-Bead One-Compound Cyclic Peptoid Libraries That Can Be Sequenced By Tandem Mass Spectrometry. *Tetrahedron Lett.* **53,** 2341–2344 (2012).

41. Doran, T. M. *et al.* Utility of redundant combinatorial libraries in distinguishing high and low quality screening hits. *ACS Comb. Sci.* **16,** 259–70 (2014).

42. Li, S. *et al.* Photolithographic synthesis of peptoids. *J. Am. Chem. Soc.* **126,** 4088–9 (2004).

43. Heine, N. *et al.* Synthesis and screening of peptoid arrays on cellulose membranes. *Tetrahedron* **59,** 9919–30 (2003).

44. Reddy, M. M. *et al.* Identification of candidate IgG biomarkers for Alzheimer's disease via combinatorial library screening. *Cell* **144,** 132–42 (2011).

45. Sisido, M., Imanishi, Y. & Higashimura, T. Molecular Weight Distribution of Polysarcosine Obtained by NCA Polymerization. *Makromol. Chem.* **178,** 3107 (1977).

46. Fetsch, C. & Luxenhofer, R. Highly Defined Multiblock Copolypeptoids : Pushing the Limits of Living Nucleophilic Ring-Opening Polymerization. *Macromol. Rapid Commun.* **33**, 1708–13 (2012).

47. Gangloff, N., Fetsch, C. & Luxenhofer, R. Polypeptoids by living ring-opening polymerization of N-substituted N-carboxyanhydrides from solid supports. *Macromol. Rapid Commun.* **34,** 997–1001 (2013).

48. Fetsch, C., Grossmann, A., Holz, L., Nawroth, J. F. & Luxenhofer, R. Polypeptoids from N -Substituted Glycine N-Carboxyanhydrides : Hydrophilic , Hydrophobic , and Amphiphilic Polymers with Poisson Distribution. *Macromolecules* **44**, 6746–58 (2011).

49. Guo, L., Lahasky, S. H., Ghale, K. & Zhang, D. *N*-heterocyclic carbene-mediated zwitterionic polymerization of N-substituted *N*-carboxyanhydrides toward poly(α-peptoid)s: Kinetic,

mechanism, and architectural control. *J. Am. Chem. Soc.* **134**, 9163-71(2012).

50. Lee, C. -U., Smart, T. P., Guo, L., Epps, T. H. & Zhang, D. Synthesis and Characterization of Amphiphilic Cyclic Diblock Copolypeptoids from *N*-Heterocyclic Carbene-Mediated Zwitterionic Polymerization of N-Substituted *N*-Carboxyanhydride. *Macromolecules* **44**, 9574–85 (2011).

51. Tao, X., Deng, C. & Ling, J. PEG-amine-initiated polymerization of sarcosine *N*-thiocarboxyanhydrides toward novel double-hydrophilic PEG-*b*-polysarcosine diblock copolymers. *Macromol. Rapid Commun.* **35,** 875–81 (2014).

52. Tao, X., Deng, Y., Shen, Z. & Ling, J. Controlled Polymerization of N-Substituted Glycine *N*-Thiocarboxyanhydrides Initiated by Rare Earth Borohydrides toward Hydrophilic and Hydrophobic Polypeptoids. *Macromolecules* **47,** 6173–80 (2014).

53. Schneider, M., Fetsch, C., Amin, I., Jordan, R. & Luxenhofer, R. Polypeptoid Brushes by Surface-Initiated Polymerization of N-Substituted Glycine *N*-Carboxyanhydrides. *Langmuir* **29**, 6983 (2013).

54. Olsen, C. A. Beta-peptoid 'foldamers' - why the additional methylene unit? *Biopolymers* **96,** 561–6 (2011).

55. Jia, L. *et al.* Living Alternating Copolymerization of N-Alkylaziridines and Carbon Monoxide as a Route for Synthesis of Poly-peptoids. *J. Am. Chem. Soc.* **124**, 7282–3 (2002).

56. Darensbourg, D. J., Phelps, A. L., Gall, N. Le & Jia, L. Mechanistic Studies of the Copolymerization Reaction of Aziridines and Carbon Monoxide to Produce Poly-β-peptoids. *J. Am. Chem. Soc.* **126**, 13808–15 (2004).

57. Lin, S. *et al.* Antifouling Poly (β-peptoid)s. *Biomacromolecules* **12**, 2573–82 (2011).

58. Chai, J., Liu, G., Chaicharoen, K., Wesdemiotis, C. & Jia, L. Cobalt-Catalyzed Carbonylative Polymerization of Azetidines. *Macromolecules* **41,** 8980–8985 (2008).

59. Liu, G. & Jia, L. Cobalt-catalyzed carbonylative copolymerization of *N*-alkylazetidines and tetrahydrofuran. *Angew. Chem. Int. Ed.* **45,** 129–31 (2005).

60. Hamper, B. C., Kolodziej, S. A., Scates, A. M. & Smith, R. G. Solid Phase Synthesis of β-Peptoids : N-Substituted β-Aminopropionic Acid Oligomers. *J. Org. Chem.* **63,** 708–18 (1998).

61. Norgren, A. S., Zhang, S. & Arvidsson, P. I. Synthesis and Circular Dichroism Spectroscopic Investigations of Oligomeric β-Peptoids with α-Chiral Side Chains. *Org. Lett,* 8, 4533-6 (2006).

62. Olsen, C. A, Lambert, M., Witt, M., Franzyk, H. & Jaroszewski, J. W. Solid-phase peptide synthesis and circular dichroism study of chiral beta-peptoid homooligomers. *Amino Acids* **34,** 465–71 (2008).

63. Birkofer, L. & Kachel, H. Synthese eines N-Carboxy-β-aminosäureanhydrids. *Naturwissenschaften* **41,** 576 (1954).

64. Grossmann, A. & Luxenhofer, R. Living Polymerization of N-Substituted β-Alanine *N*-Carboxyanhydrides : Kinetic Investigations and Preparation of an Amphilphillic Block Copoly-β-Peptoid. *Macromol. Rapid Commun.* **33**, 1714–9 (2012).

65. Shin, I. & Park, K. Solution-Phase Synthesis of Aminooxy Peptoids in the C to N and N to C Directions. *Org. Lett.* **4**, 869 (2002).

66. Cheguillaume, A., Lehardy, F., Bouget, K., Baudy-Floc'h, M., Le Grel, P. Submonomer Solution Synthesis of Hydrazinoazapeptoids, a New Class of Pseudopeptides. *J Org. Chem.* **64**, 2924–7 (1999).

67. Gao, Y. & Kodadek, T. Synthesis and screening of stereochemically diverse combinatorial libraries of peptide tertiary amides. *Chem. Biol.* **20,** 360–9 (2013).

68. Sarma, B. K., Yousufuddin, M. & Kodadek, T. Acyl hydrazides as peptoid sub-monomers. *Chem. Commun.* **47,** 10590–2 (2011).

69. Sarma, B. K. & Kodadek, T. Submonomer synthesis of a hybrid peptoid-azapeptoid library. *ACS Comb. Sci.* **14,** 558–64 (2012).

70. Liu, F., *et al.* Hydrazone- and Hydrazide-Containing N-Substituted Glycines as Peptoid Surrogates for Expedited Library Synthesis: Application to the Preparation of Tsg101-Directed HIV-1 Budding Antagonists.*Org. Lett.* **8**, 5165 (2006).

71. Rosales, A. M., Murnen, H. K., Kline, S. R., Zuckermann, R. N. & Segalman, R. a. Determination of the persistence length of helical and non-helical polypeptoids in solution. *Soft Matter* **8,** 3673 (2012).

72. Sui, Q., Borchardt, D. & Rabenstein, D. Kinetics and equilibria of *cis*/*trans* isomerization of backbone amide bonds in peptoids. *J. Am. Chem. Soc.* **129**, 12042–8 (2007).

73. Aditya, A. & Kodadek, T. Incorporation of heterocycles into the backbone of peptoids to generate diverse peptoid-inspired one bead one compound libraries. *ACS Comb. Sci.* **14,** 164–9 (2012).

74. Suwal, S. & Kodadek, T. Synthesis of libraries of peptidomimetic compounds containing a 2-oxopiperazine unit in the main chain. *Org. Biomol. Chem.* **11,** 2088–92 (2013).

75. Rivera, D. G., León, F., Concepción, O., Morales, F. E. & Wessjohann, L. a. A multiple multicomponent approach to chimeric peptide-peptoid podands. *Chemistry* **19,** 6417–28 (2013).

76. Diaz-Mochon, J. J., Fara, M. A., Sanchez-Martin, R. M. & Bradley, M. Peptoid dendrimers—microwave-assisted solid-phase synthesis and transfection agent evaluation. *Tetrahedron Lett.* **49,** 923–6 (2008).

77. Peschko, K. *et al.* Dendrimer-Type Peptoid-Decorated Hexaphenylxylenes and Tetraphenylmethanes: Synthesis and Structure in Solution and in the Gas Phase. *Chemistry* **20**, 16273 (2014).

78. Wljthrich, K. & Grathwohl, C. A NOVEL APPROACH FOR STUDIES OF THE MOLECULAR CONFORMATIONS IN FLEXIBLE POLYPEPTIDES. *FEBS Lett.* **43,** 337–

40 (1974).

79. Horng, J. -C. & Raines, R. T. Stereoelectronic effects on polyproline conformation. *Protein Sci.* **43**, 377 (1974).

80. Hodges, J. A. & Raines, R. T. Energetics of an n→π* interaction that impacts protein structure. *Org. Lett.* **8,** 4695–7 (2006).

81. Gorske, B. C., Bastian, B. L., Geske, G. D. & Blackwell, H. E. Local and tunable n-→π* interactions regulate amide isomerism in the peptoid backbone. *J. Am. Chem. Soc.* **129,** 8928–9 (2007).

82. Gorske, B. C., Stringer, J. R., Bastian, B. L., Fowler, S. A. & Blackwell, H. E. New Strategies for the Design of Folded Peptoids Revealed by a Survey of Noncovalent Interactions in Model Systems. *J. Am. Chem. Soc.* **131**, 16555–67 (2009).

83. Gorske, B. C., Nelson, R. C., Bowden, Z. S., Kufe, T. A. & Childs, A. M. 'Bridged' n→π* interactions can stabilize peptoid helices. *J. Org. Chem.* **78,** 11172–83 (2013).

84. Paul, B. *et al. N*-Naphthyl Peptoid Foldamers Exhibiting Atropisomerism. *Org Lett.* **14**, 926 (2012).

85. Shah, N. H. *et al.* Oligo(N-aryl glycines): a new twist on structured peptoids. *J. Am. Chem. Soc.* **130,** 16622–32 (2008).

86. Pkorski, J. K. *et al.* Introduction of a Triazole Amino Acid into a Peptoid Oligomer Induces Turn Formation in Aqueous Solution. *Org. Lett.* **9,** 2381–3 (2007).

87. Roy, O. *et al.* The *tert*-Butyl Side Chain: A Powerful Means to Lock Peptoid Amide Bonds in the Cis Conformation. *Org. Lett.* **15**, 2246-9 (2013).

88. Caumes, C., Roy, O., Faure, S. & Taillefumier, C. The Click Triazolium Peptoid Side Chain: A Strong *cis*-Amide Inducer Enabling Chemical Diversity. *J. Am. Chem. Soc.* **134**, 9553-6 (2012).

89. Armand, P. *et al.* Chiral N-substituted glycines can form stable helical conformations. *Folding Des.* **2**, 369–75 (1997).

90. Wu, C. W., Sanborn, T. J., Zuckermann, R. N. & Barron, a E. Peptoid oligomers with alpha-chiral, aromatic side chains: effects of chain length on secondary structure. *J. Am. Chem. Soc.* **123,** 2958–63 (2001).

91. Wu, C. W. *et al.* Structural and spectroscopic studies of peptoid oligomers with alpha-chiral aliphatic side chains. *J. Am. Chem. Soc.* **125,** 13525–30 (2003).

92. Shin, H.-M., Kang, C.-M., Yoon, M.-H. & Seo, J. Peptoid helicity modulation: precise control of peptoid secondary structures via position-specific placement of chiral monomers. *Chem. Commun.* **50,** 4465–8 (2014).

93. Seo, J., Barron, A. E., Zuckermann, R. N., V, S. U. & James, W. Novel Peptoid Building Blocks : Synthesis of Functionalized Aromatic Helix-Inducing Submonomers. *Org. Lett*, **12**, 492 (2010).

94. Gorske, B. C. & Blackwell, H. E. Tuning peptoid secondary structure with pentafluoroaromatic functionality: a new design paradigm for the construction of discretely folded peptoid structures. *J. Am. Chem. Soc.* **128,** 14378–87 (2006).

95. Huang, K. *et al.* A threaded loop conformation adopted by a family of peptoid nonamers. *J. Am. Chem. Soc.* **128,** 1733–8 (2006).

96. Fowler, S. a, Luechapanichkul, R. & Blackwell, H. E. Synthesis and characterization of nitroaromatic peptoids: fine tuning peptoid secondary structure through monomer position and functionality. *J. Org. Chem.* **74,** 1440–9 (2009).

97. Crapster, J. A., Stringer, J. R., Guzei, I. a. & Blackwell, H. E. Design and conformational analysis of peptoids containing *N*-hydroxy amides reveals a unique sheet-like secondary structure. *Peptide Science* **96,** 604–16 (2011).

98. Nam, K. T. *et al.* Free-floating ultrathin two-dimensional crystals from sequence-specific peptoid polymers. *Nat. Mater.* **9,** 454–60 (2010).

99. Krejchi, M. T. *et al.* Chemical sequence control of beta-sheet assembly in macromolecular crystals of periodic polypeptides. *Science* **265,** 1427–32 (1994).

100. Crapster, J. A., Guzei, I. a & Blackwell, H. E. A peptoid ribbon secondary structure. *Angew. Chem. Int. Ed. Engl.* **52,** 5079–84 (2013).

101. Banerjee, I., Pangule, R. C. & Kane, R. S. Antifouling coatings: recent developments in the design of surfaces that prevent fouling by proteins, bacteria, and marine organisms. *Adv. Mater.* **23,** 690–718 (2011).

102. Lau, K. H. A., Ren, C., Park, S. H., Szleifer, I. & Messersmith, P. B. An Experimental À Theoretical Analysis of Protein Adsorption on Peptidomimetic Polymer Brushes. *Langmuir* **28**, 2288–98 (2012).

103. Lau, K. H. A. *et al.* Surface-grafted polysarcosine as a peptoid antifouling polymer brush. *Langmuir* **28,** 16099–107 (2012).

104. Statz, A. R., Barron, A. E. & Messersmith, P. B. Protein, cell and bacterial fouling resistance of polypeptoid-modified surfaces: effect of side-chain chemistry. *Soft Matter* **4,** 131–9 (2008).

105. Lau, K. H. A. *et al.* Molecular Design of Antifouling Polymer Brushes Using Sequence-Specific Peptoids. *Adv. Mater. Interfaces* **2** (2015).

106. Ham, H. O., Park, S. H., Kurutz, J. W., Szleifer, I. G. & Messersmith, P. B. Antifouling glycocalyx-mimetic peptoids. *J. Am. Chem. Soc.* **135,** 13015–22 (2013).

107. Ryu, J. Y. *et al.* New Antifouling Platform Characterized by Single-Molecule Imaging. *ACS Appl. Mater. Interfaces* **6**, 3553 (2014).

108. Costa, F., Carvalho, I. F., Montelaro, R. C., Gomes, P. & Martins, M. C. L. Covalent immobilization of antimicrobial peptides (AMPs) onto biomaterial surfaces. *Acta Biomater.* **7,** 1431–40 (2011).

109. Chongsiriwatana, N. P. *et al.* Peptoids that mimic the structure, function, and mechanism of

helical antimicrobial peptides. *Proc. Natl. Acad. Sci. U. S. A.* **105,** 2794–9 (2008).

110. Godballe, T., Nilsson, L. L., Petersen, P. D. & Jenssen, H. Antimicrobial β-peptides and α-peptoids. *Chem. Biol. Drug Des.* **77,** 107–16 (2011).

111. Statz, A. R., Park, J. P., Chongsiriwatana, N. P., Barron, A. E. & Messersmith, P. B. Surface-immobilised antimicrobial peptoids. *Biofouling* **24,** 439–48 (2008).

112. Ward, T. J. & Ward, K. D. Chiral separations: fundamental review 2010. *Anal. Chem.* **82,** 4712–22 (2010).

113. Wu, H. *et al.* Enantiorecognition ability of peptoids with α-chiral, aromatic side chains. *Analyst* **136,** 4409–11 (2011).

114. Wu, H., Li, K., Yu, H., Ke, Y. & Liang, X. Investigation of peptoid chiral stationary phases varied in absolute configuration. *J. Chromatogr. A* **1281,** 155–9 (2013).

115. Wu, H. *et al.* Study of stereomeric peptoid chiral stationary phases containing different chiral side chains. *J. Chromatogr. A* **1298,** 152–6 (2013).

116. Wu, H., Wang, D., Song, G., Ke, Y. & Liang, X. Novel chiral stationary phases based on peptoid combining a quinine/quinidine moiety through a C9-position carbamate group. *J. Sep. Sci.* **37,** 934–43 (2014).

117. Frank, R. Spot-synthesis: an easy technique for the positionally addressable, parallel chemical synthesis on a membrane support. *Tetrahedron* **48,** 9217–32 (1992).

118. Blackwell, H. E. Hitting the SPOT: small-molecule macroarrays advance combinatorial synthesis. *Curr. Opin. Chem. Biol.* **10,** 203–12 (2006).

119. Hong, J. A., Neel, D. V, Wassaf, D., Caballero, F. & Koehler, A. N. Recent discoveries and applications involving small-molecule microarrays. *Curr. Opin. Chem. Biol.* **18,** 21–8 (2014).

120. Voskuhl, J., Brinkmann, J. & Jonkheijm, P. Advances in contact printing technologies of carbohydrate, peptide and protein arrays. *Curr. Opin. Chem. Biol.* **18,** 1–7 (2014).

121. Reddy, M. M. & Kodadek, T. Protein 'fingerprinting' in complex mixtures with peptoid microarrays. *Proc. Natl. Acad. Sci. U. S. A.* **102,** 12672–7 (2005).

122. Kwon, Y.-U. & Kodadek, T. Encoded combinatorial libraries for the construction of cyclic peptoid microarrays. *Chem. Commun.* 5704–6 (2008).

123. Lim, H.-S. *et al.* Rapid identification of improved protein ligands using peptoid microarrays. *Bioorg. Med. Chem. Lett.* **19,** 3866–9 (2009).

124. Labuda, L. P., Pushechnikov, A. & Disney, M. D. Small molecule microarrays of RNA-focused peptoids help identify inhibitors of a pathogenic group I intron. *ACS Chem. Biol.* **4,** 299–307 (2009).

125. Maayan, G., Ward, M. D. & Kirshenbaum, K. Metallopeptoids. *Chem. Commun.* 56–8 (2009).

126. Izzo, I., Ianniello, G., Cola, C. De & Nardone, B. Structural Effects of Proline Substitution and Metal Binding on Hexameric Cyclic Peptoids. *Org. Lett.* **15**, 598 (2013).

127. De Cola, C. *et al.* Gadolinium-binding cyclic hexapeptoids: synthesis and relaxometric properties. *Org. Biomol. Chem.* **12,** 424–31 (2014).

128. Nalband, D. M., Warner, B. P., Zahler, N. H. & Kirshenbaum, K. Rapid identification of metal-binding peptoid oligomers by on-resin X-ray fluorescence screening. *Biopolymers* **102,** 407–15 (2014).

129. Hancock, R. & Martell, A. Ligand design for selective complexation of metal ions in aqueous solution. *Chem. Rev.* 1875–1914 (1989).

130. Davis, M. E. Non-viral gene delivery systems. *Curr. Opin. Biotechnol.* **13,** 128–131 (2002).

131. Doudna, J. A. & Charpentier, E. The new frontier of genome engineering with CRISPR-Cas9. *Science.* **346,** 1258096 (2014).

132. Pack, D. W., Hoffman, A. S., Pun, S. & Stayton, P. S. Design and development of polymers for gene delivery. *Nat. Rev. Drug Discov.* **4,** 581–93 (2005).

133. Pearce, T. R., Shroff, K. & Kokkoli, E. Peptide targeted lipid nanoparticles for anticancer drug delivery. *Adv. Mater.* **24,** 3803–22, 3710 (2012).

134. Huang, C. *et al.* Lipitoids - novel cationic lipids for cellular delivery of plasmid DNA in vitro. *Chem. Biol.* **5**, 345 (1998).

135. Lobo, B. a, Vetro, J. a, Suich, D. M., Zuckermann, R. N. & Middaugh, C. R. Structure/function analysis of peptoid/lipitoid:DNA complexes. *J. Pharm. Sci.* **92,** 1905–18 (2003).

136. Utku, Y. *et al.* A peptidomimetic siRNA transfection reagent for highly effective gene silencing. *Mol. Biosyst.* **2,** 312–7 (2006).

137. Konca, Y. Nanometer-scale siRNA carriers incorporating peptidomimetic oligomers: physical characterization and biological activity. *Int. J. Nanomedicine* **9**, 2271–85 (2014).

138. Wu, C. W., Seurynck, S. L., Lee, K. Y. C. & Barron, A. E. Helical Peptoid Mimics of Lung Surfactant Protein C. *Chem. Biol.* **10,** 1057–63 (2003).

139. Patch, J. A. & Barron, A. E. Helical peptoid mimics of magainin-2 amide. *J. Am. Chem. Soc.* **125,** 12092–3 (2003).

140. Brown, N. J., Dohm, M. T., Bernardino de la Serna, J. & Barron, A. E. Biomimetic N-terminal alkylation of peptoid analogues of surfactant protein C. *Biophys. J.* **101,** 1076–85 (2011).

141. Seurynck, S. L., Patch, J. A. & Barron, A. E. Simple, helical peptoid analogs of lung surfactant protein B. *Chem. Biol.* **12,** 77–88 (2005).

142. Seurynck-Servoss, S. L., Dohm, M. T. & Barron, A. E. Effects of including an N-terminal insertion region and arginine-mimetic side chains in helical peptoid analogues of lung surfactant protein B. *Biochemistry* **45,** 11809–18 (2006).

143. Dohm, M. T., Brown, N. J., Seurynck-Servoss, S. L., Bernardino de la Serna, J. & Barron, A. E. Mimicking SP-C palmitoylation on a peptoid-based SP-B analogue markedly improves surface activity. *Biochim. Biophys. Acta* **1798,** 1663–78 (2010).

144. Dohm, M. T., Seurynck-Servoss, S. L., Seo, J., Zuckermann, R. N. & Barron, A. E. Close mimicry of lung surfactant protein B by 'clicked' dimers of helical, cationic peptoids. *Biopolymers* **92,** 538–53 (2009).

145. Burkoth, T., Beausoleil, E., Kaur, S. & Tang, D. Toward the synthesis of artificial proteins: the discovery of an amphiphilic helical peptoid assembly. *Chem. Biol.* **9,** 647–54 (2002).

146. Lee, B., Zuckermann, R. N., Dill, K. A. Folding a Nonbiological Polymer into a Compact Multihelical Structure. *J. Am. Chem. Soc.* **127**, 10999–10009 (2005).

147. Murnen, H. K., Khokhlov, A. R., Khalatur, P. G., Segalman, R. a. & Zuckermann, R. N. Impact of Hydrophobic Sequence Patterning on the Coil-to-Globule Transition of Protein-like Polymers. *Macromolecules* **45,** 5229–36 (2012).

148. Khalatur, Pavel G., Khokhlov, A. R. Conformation-Dependent Sequence Design (Engineering) of AB Copolymers. *Phys. Rev. Lett.* **82**, 3456 (2006).

149. Lee, B., Chu, T. Dill, K. A. & Zuckermann, R. N. Biomimetic nanostructures: Creating a high-affinity zinc-binding site in a folded nonbiological polymer. *J. Am. Chem. Soc.* 8847–55 (2008).

150. Klemba, M. & Regan, L. Characterization of Metal Binding by a Designed Protein: Single Ligand Substitutions at a Tetrahedral Cys2His2 Site. *Biochemistry* **34,** 10094–100 (1995).

151. Levine, P. M., Craven, T. W., Bonneau, R. & Kirshenbaum, K. Semisynthesis of peptoid-protein hybrids by chemical ligation at serine. *Org. Lett.* **16,** 512–5 (2014).

152. Van Zoelen, W., Zuckermann, R. N. & Segalman, R. A. Tunable Surface Properties from Sequence-Specific Polypeptoid–Polystyrene Block Copolymer Thin Films. *Macromolecules* **45,** 7072–82 (2012).

153. Rosales, A. M., McCulloch, B. L., Zuckermann, R. N. & Segalman, R. a. Tunable Phase Behavior of Polystyrene–Polypeptoid Block Copolymers. *Macromolecules* **45,** 6027–6035 (2012).

154. Chen, X., Ding, K. & Ayres, N. Investigation into fiber formation in N-alkyl urea peptoid oligomers and the synthesis of a water-soluble PEG/N-alkyl urea peptoid oligomer conjugate. *Polym. Chem.* **2,** 2635 (2011).

155. Zhang, Y., Xu, C., Lam, H. Y., Lee, C. L. & Li, X. Protein chemical synthesis by serine and threonine ligation. *Proc. Natl. Acad. Sci. U. S. A.* **110,** 6657–62 (2013).

156. Lee, B. & Zuckermann, R. N. Protein Side-Chain Translocation Mutagenesis via Incorporation of Peptoid Residues. *ACS Chem. Biol.* **6,** 1367–74 (2011).

157. Stein, A., Mosca, R. & Aloy, P. Three-dimensional modeling of protein interactions and complexes is going 'omics. *Curr. Opin. Struct. Biol.* **21,** 200–8 (2011).

158. Brooks, B. R. *et al.* CHARMM: A program for macromolecular energy, minimization, and dynamics calculations. *J. Comput. Chem.* **4,** 187–217 (1983).

159. Brooks, B. R. *et al.* CHARMM: the biomolecular simulation program. *J. Comput. Chem.* **30,**

1545–614 (2009).

160. Kaufmann, K. W., Lemmon, G. H., Deluca, S. L., Sheehan, J. H. & Meiler, J. Practically useful: what the Rosetta protein modeling suite can do for you. *Biochemistry* **49,** 2987–98 (2010).

161. Butterfoss, G. L., Renfrew, P. D., Kuhlman, B., Kirshenbaum, K. & Bonneau, R. A preliminary survey of the peptoid folding landscape. *J. Am. Chem. Soc.* **131,** 16798–807 (2009).

162. Butterfoss, G. L. *et al.* De novo structure prediction and experimental characterization of folded peptoid oligomers. *Proc. Natl. Acad. Sci. U. S. A.* **109,** 14320–5 (2012).

163. Mirijanian, D. T., Mannige, R. V, Zuckermann, R. N. & Whitelam, S. Development and use of an atomistic CHARMM-based forcefield for peptoid simulation. *J. Comput. Chem.* **35,** 360–70 (2014).

164. Sternberg, U. *et al.* Structural characterization of a peptoid with lysine-like side chains and biological activity using NMR and computational methods. *Org. Biomol. Chem.* **11,** 640–7 (2013).

165. Drew, K. *et al.* Adding diverse noncanonical backbones to rosetta: enabling peptidomimetic design. *PLoS One* **8,** e67051 (2013).

166. Renfrew, P. D., Craven, T. W., Butterfoss, G. L., Kirshenbaum, K. & Bonneau, R. A rotamer library to enable modeling and design of peptoid foldamers. *J. Am. Chem. Soc.* **136,** 8772–82 (2014).

167. Haxton, T., Mannige, R., Zuckermann, R. N. & Whitelam, S. Modeling sequence-specific polymers using anisotropic coarse-grained sites allows quantitative comparison with experiment. *J. Chem. Theory Comput.* **11**, 303 (2014).

Chapter 2

Development of a Screening Platform for Identifying Metal Ligands

Abstract

Combinatorial chemistry has become a mainstay in the pharmaceutical industry and has demonstrated significant promise in the development of inhibitors and agonists in academic research. This field has grown exponentially in the last couple of decades for biological applications, but the use of combinatorial chemistry to identify ligands for inorganic applications has been limited. Herein the development of a screening platform for identifying ligands capable of metal coordination is described. *N*-substituted glycines, or peptoids, were used for the library scaffold due to their stability to enzymes and variety of functional groups available. Various sequencing strategies and cleavable linkers were evaluated and optimized. This platform will pave the way for future assays to identify ligands with applications in catalysis, environmental remediation, and other fields in which combinatorial chemistry has not been employed to the fullest.

2.1 A Combinatorial Approach to Discovery of Metal Complexes

Since the first efforts to use combinatorial libraries to identify metal ligands, with work by Still *et al* using cyclen-based libraries to develop ionophore mimetics,[1] many groups have used different scaffolds to develop libraries for binding various metal ions.[2] Some examples of applications include the identification of catalysts,[2,3] protein tags,[4] and small molecule probes.[5] Biomolecules (peptides and polynucleotides) are commonly chosen for the library backbone due to the synthetic modularity and established synthesis procedures. *In vitro* synthesis with phage display libraries has also been employed to facilitate the evaluation of larger library sizes.[6–8] The structures identified in these screens have been used in many functional materials and biological applications, but these biomolecules suffer fundamental limitations in stability. Peptides, proteins, and polynucleotides are all sensitive to pervasive enzymes, causing them to have limited efficacy in environmental applications.

Peptoids, or *N*-substituted glycine oligomers, are uniquely applicable to the development of combinatorial metal-binding libraries due to the variety of inexpensive coordinating residues available that may be incorporated via a modular synthesis.[9,10] Additionally, they are resistant to proteolytic cleavage.[9] A limited scope of peptoids have been investigated for metal-binding properties. In work by Zuckermann *et al*, a zinc finger mimetic was developed,[11] and Pirrung *et al* have developed a small library encoded with ^{9}F-tags that was evaluated for iron and copper binding.[12] The ^{19}F-tagged library is limited by the extensive time required to synthesize each of the tagged compounds. This chapter will describe unique approaches to designing a large and easily sequenced library of metal-binding peptoids.

2.2 Monomer Selection

To begin the library design, a synthetic scheme compatible with the incorporation of unprotected heterocyclic side chains was selected (Figure 2.1b). Chloroacetic acid has been demonstrated to be efficient, leading to high yields and purities of peptoids with heterocyclic side chains.[13] Twelve monomers were identified as containing functional groups of interest (Figure 2.1a). Some were selected for their coordinating abilities and others were selected to add structural diversity to the library. To confirm that the monomers of interest could be incorporated with high yields, test pentamers were synthesized with two replicates of the monomer of interest inserted in an alternating fashion between three benzylamine residues. The amines bolded in Figure 2.1a led to high purity products, whereas the italicized amines led to structures yielding significant side products, missing the amine of interest, or causing reduced incorporation of benzylamine.

A variety of solvents have been used for the amination step of the synthesis,[10] and our collaborators at the Molecular Foundry have seen improved incorporation with tetrahydrofuran (THF) over commonly used dimethylformamide (DMF). To evaluate the impact of performing the amination in THF vs DMF, test pentamers were synthesized with the eight bolded amines using THF or DMF as the amination solvent. A decreased reaction time (20 minutes instead of the typical 2 hours) was used to identify the solvent in which the reaction proceeded the fastest. All quantitation was done on an analytical HPLC (C18 column, monitoring at A_{260}). Cysteamine and histamine had limited solubility in THF, and the cysteamine product was not identified by HPLC. Piperonylamine incorporated fully in both solvents, but due to the significant hydrophobicity of the product was not able to be analyzed on by HPLC. The glycine pentamers failed to yield significant

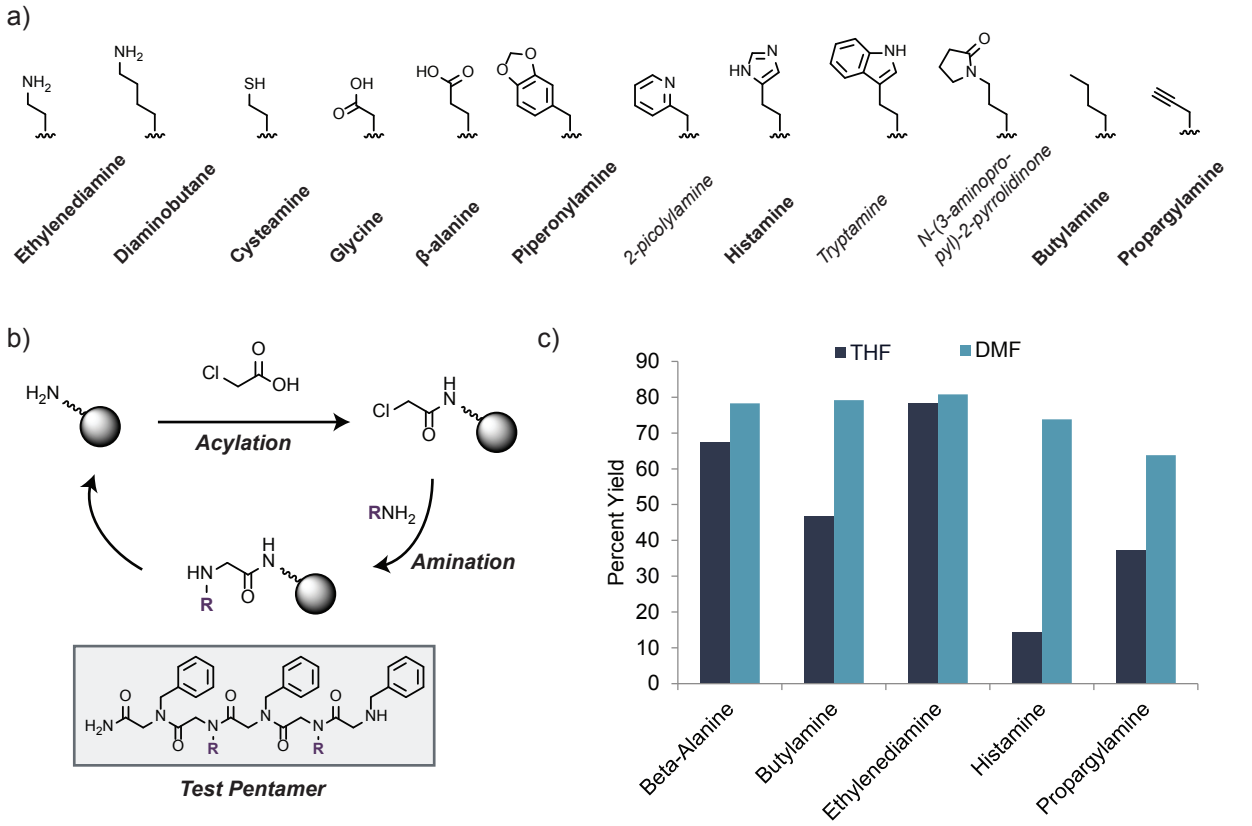

Figure 2.1. Synthetic overview of library development. a) Side chains evaluated in the synthetic scheme outlined in (b). The names of the amines that integrated completely into a test pentamer are bolded, and amines with lower yields are italicized. c) Evaluation of the impact of the solvent used for the amination step.

amounts of the desired product and therefore could not be fully characterized. The incorporation of this amine is likely slower due to steric hindrance from the carboxylic acid. The yield of the remaining pentamers is shown in Figure 2.1c. The results indicate that DMF is comparable to or better than THF for the incorporation of each these amines. The THF solutions tended to have a higher apparently viscosity, which could have led to the slower incorporation.

2.3 Building a Library with a Methionine Linker

A library anticipated to contain metal-ligands was designed with (1) a cleavable methionine linker, (2) a hydrophobic linker, and (3) a peptoid tetramer (schematic in Figure 2.2). The library was synthesized on a pegylated polystyrene resin (Tentagel-NH_2) to allow compatibility with the organic solvents used in peptoid synthesis and water for future screening applications. Methionine was chosen as a cleavable linker due to the success of this strategy in previous peptoid libraries;[10,14]

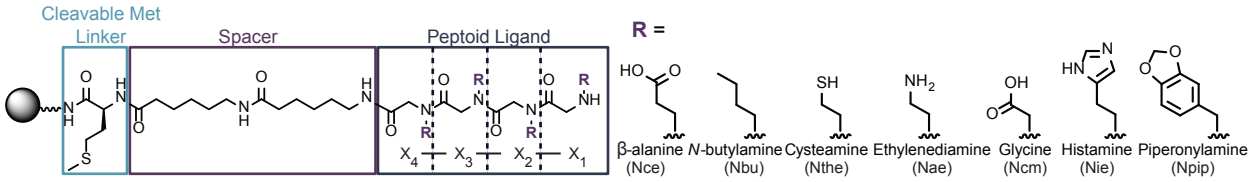

Figure 2.2. Schematic of library synthesized on Tentagel-NH_2 with a cleavable methionine linker. Two aminohexanoic acid residues are included as a spacer and a library of peptoid tetramers was synthesized.

the residue can be cleaved with cyanogen bromide to release the peptoid of interest. Acid and base labile linker moieties are uncommon in the development of peptoid libraries for on-bead screens due to (1) the use of acid labile protection groups for the side chains and (2) the sensitivity of base labile moieties to the high concentrations of primary amine used in the amination step of peptoid synthesis. The hydrophobic spacer is included to increase the mass of the cleaved product and the distance between the resin and the peptoid ligand. The library of peptoid tetramers was synthesized using split-and-pool synthesis creating a one-bead-per-compound library.[15,16] The tetramer size of the ligand was chosen to mimic common small molecule ligands (e.g. ethylenediaminetetraacetic acid). The seven amines incorporated at each variable position (X_1-X_4 in Figure 2.2) were chosen based on their compatibility with the synthetic scheme, and based on the unique masses of the monomers formed. Unique masses were required due to the use of MS-MS as the sequencing technique: each of the peptoid monomers differed by at least two mass units for unambiguous sequencing results.

Following synthesis, the library was incubated with multiple metal-containing solutions to evaluate the metal binding capacity of the tetramer ligands. Aliquots of the library were incubated with metal ions (0.02 M $CoCl_2$, $FeCl_2$, $Ni(OAC)_2$, $Cu(OAc)_2$, or CrO_3) in 4:1 THF: MeOH. Binding was visualized with an optical microscope (Figure 2.3). For some of the metals a dye was used to aid in visualization. Dimethylglyoxime was used to enhance the sensitivity of Ni^{2+} visualization (Figure 2.3b),[17,18] thiocyanate was used to identify complexes with iron that had oxidized to Fe^{3+}(Figure 2.3c),[17] and diphenylcarbazide was used to detect Cr^{6+}(Figure 2.3d).[17,19] The presence of transparent beads in all of the images indicates that the resin itself is not interacting with the metal ions or any of the dyes applied. In Figure 2.3a the different colored beads additionally indicated the presence of a variety of complexes, confirming the diversity of complexes within the library.

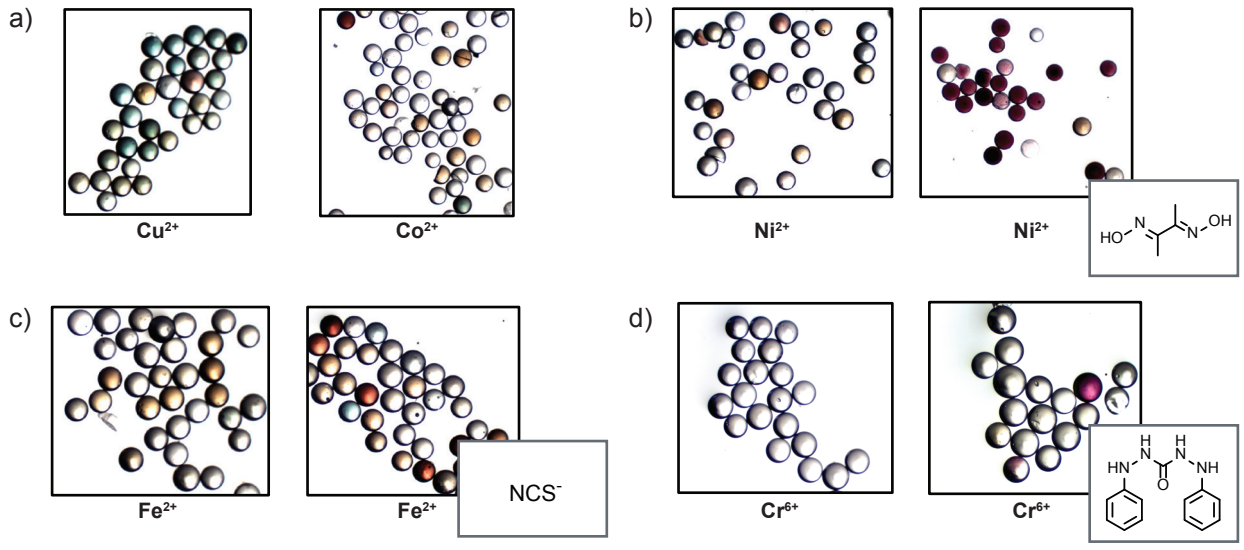

Figure 2.3. Photographs of library members incubated with various metal ions. a) Library members were incubated with Cu^{2+} and Ni^{2+}. b) Dimethylglyoxime was applied to aid in the visualization of Ni^{2+} complexes. c) The library was exposed to Fe^{2+}, but in air some oxidized to Fe^{3+}. This was visualized with the addition of thiocyanate. d) Diphenylcarbazide was used to identify ligands bound to Cr^{6+}.

Inspired by the apparent metal binding in the organic solvent mixture, assays were performed in water to identify ligands that would bind in aqueous applications. To evaluate the impact of these assays on the cleavage and sequencing procedures, a test sequence was synthesized

(Npip-Nthe-Npip-Nie) and cleaved before exposure to metal ions and after exposure to Cr^{6+}. As shown in Figure 2.4 the signal of the sequence of interest was significantly decreased after exposure to Cr^{6+}. To address this, different sequencing and linker options were evaluated.

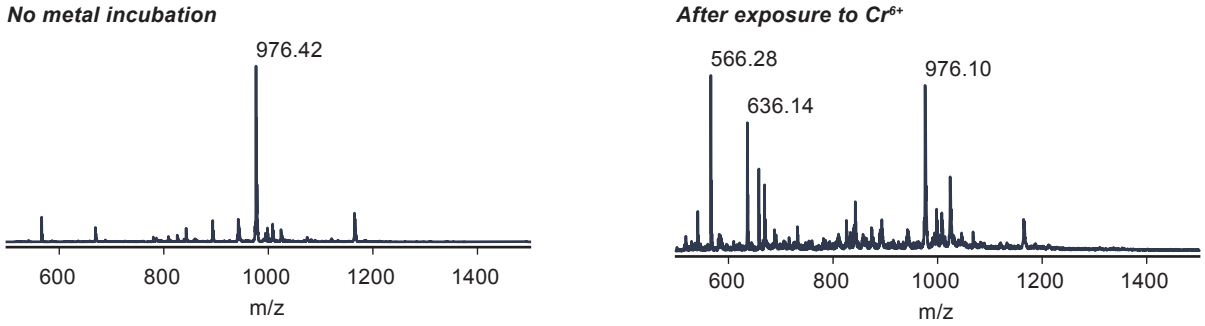

Figure 2.4. To determine whether oxidation of the methionine is impacting the cyanogen bromide cleavage, a test sequence (Npip-Nte-Npip-Nie) was synthesized with a methionine linker. The MALDI-TOF spectrum on the left shows cleavage before any incubation with transition metal ions, and the spectrum on the left shows the decreased signal after exposure to Cr^{6+}.

2.4 Isotope-Tag Sequencing Strategies

One strategy that has been employed for on-resin sequencing is capping 5-10% of the growing structure, so that the sequence can be identified with a single MS instead of MS-MS.[20] This could also be advantageous if the ligands were forming complexes with ions of interest and this was causing decreased ionization. A capping strategy has not been previously applied with peptoid libraries, but an isotope-tagged capping strategy was recently employed by Francis *et al* for a peptide library.[21] To mimic this strategy, a bromophenyl and bromobenzoic acid were selected

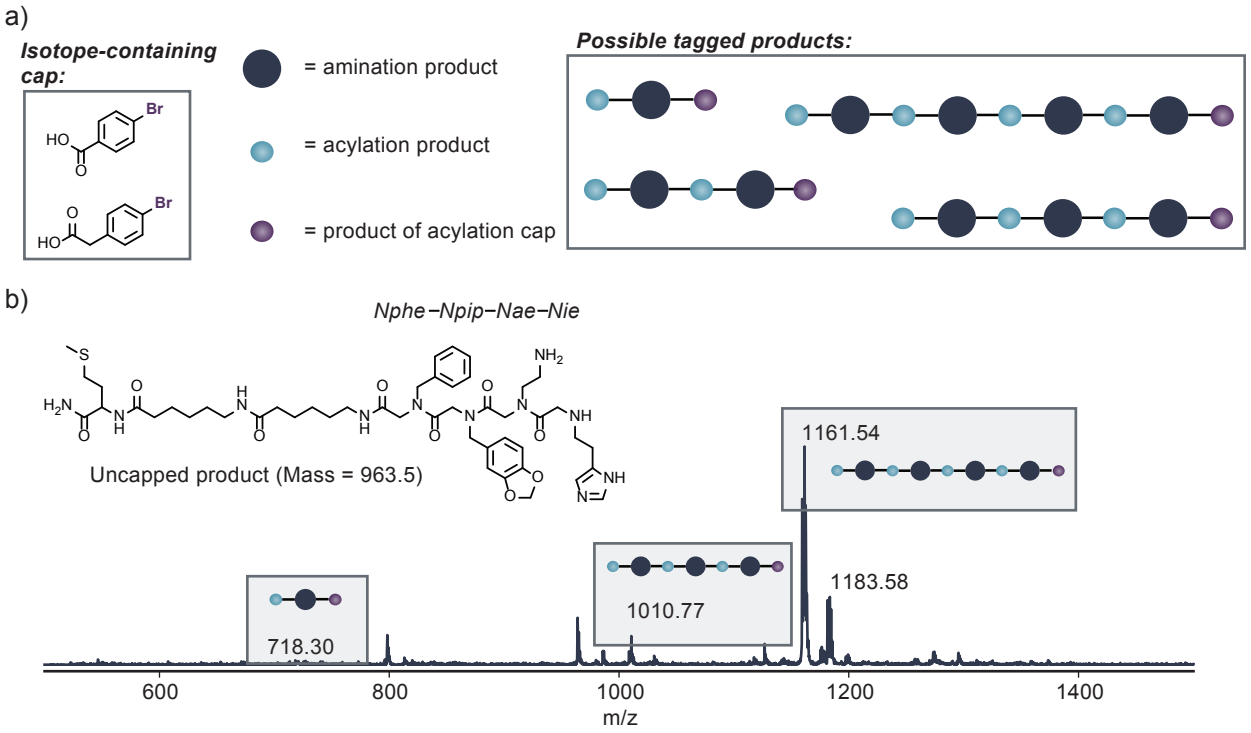

Figure 2.5. Acylation capping strategy. To simplify mass-spectrometry analysis, a bromine-tagged acylation agent was added to cap a small fraction of the growing peptoids at each step. a) A schematic of the possible products containing the bromine-tagged acylation product. b) A MALDI-TOF MS of a test tetramer (Nphe-Npip-Nae-Nie) synthesized with the bromobenzoic acid acylation tag. The bromophenylacetic acid (1 eq) was coupled for 10 min with HCTU as a coupling reagent.

to cap the growing peptoid structures at the acylation step (Figure 2.5a). The potential capped products are shown schematically in Figure 2.5a. Both diisopropylcarbodiimide (DIC) and *O*-(6-chlorobenzotriazol-1-yl)-*N*,*N*,*N*′,*N*′-tetramethyluronium hexafluorophosphate (HCTU) were evaluated. Reaction time, equivalents, and the hydrophobicity of the proceeding amine were also evaluated. The coupling agent seemed to have minimal impact, but a 10 minute coupling gave cleaner products than the 1 hour reaction. Unfortunately, the hydrophobicity of the preceding amine had a significant impact on the reaction. A capping reaction synthetically following an Npip residue had no apparent capping, whereas a reaction synthetically subsequent to an Nie residue led to approximately 50% of the sequence capped with only 0.5 eq. An example of a tetramer with the capping reaction performed after the incorporation of each amine is shown in Figure 2.5b.

A bromine isotope can fortunately be incorporated during either the acylation or the amination synthetic step. Given the limited success with the acylation strategy, a secondary bromine-containing amine was evaluated as a capping reagent (Figure 2.6a). This would lead to the series of structures shown in Figure 2.6a. To ensure that the secondary amine would replace the chloride in the amination reaction, it was added to an existing structure (Met-Ahx-Ahx-Nie) and 100% coupling was characterized by MALDI-TOF MS. Following this, various equivalents and reaction times were screened to identify conditions where 5-10% of the sequence would be capped at each step. Very few equivalents were required (0.1 eq) and a 30 minute reaction led to a detecctable capped product. To test this capping strategy, a Nie-Nae-Npip-Nbu sequence was synthesized where a capping reaction synthetically preceded the incorporation of each of the last three amines. A MALDI-TOF MS of this is shown in Figure 2.6b. Unfortunately it was difficult to identify the capped structures; increasing the reaction time to 2 h did not aid in the visualization of

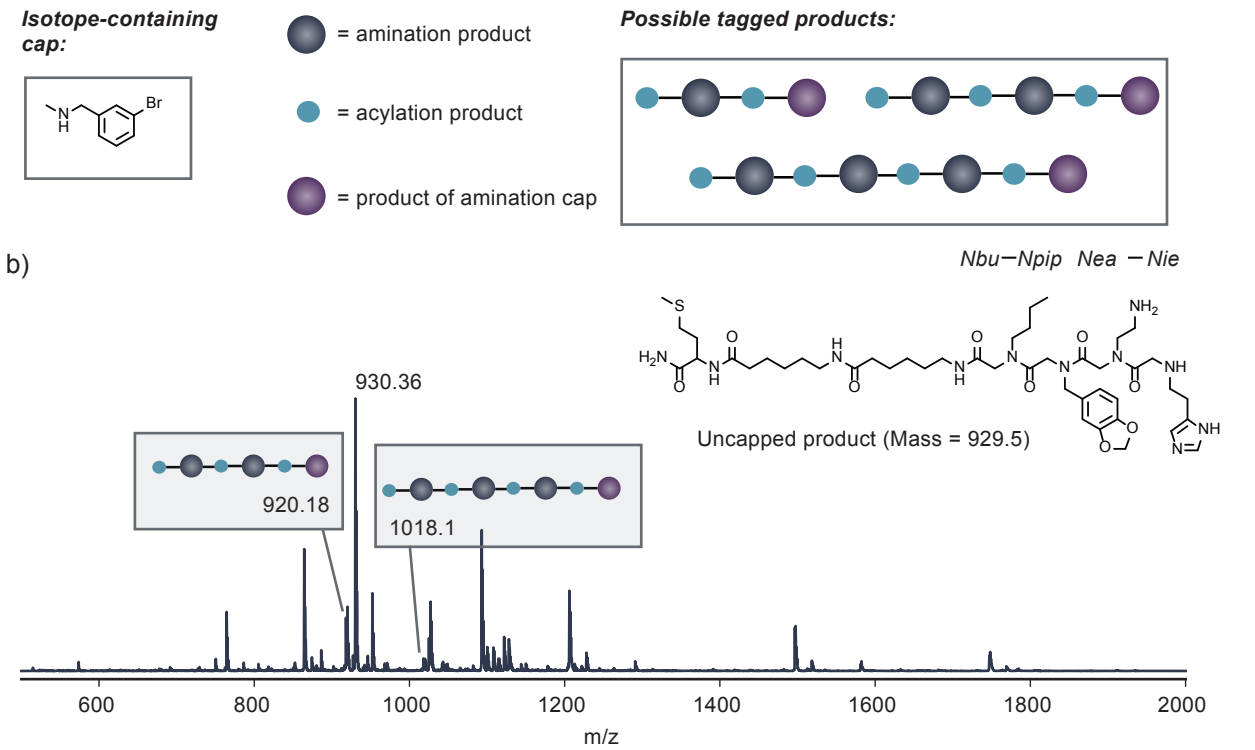

Figure 2.6. Amination capping strategy. a) Schematic of possible bromine-tagged products. b) MALDI-TOF MS of a test tetramer (Nie-Nae-Npip-Nbu) synthesized with a fraction of the growing peptoid sequence capped with the bromine-tagged secondary amine.

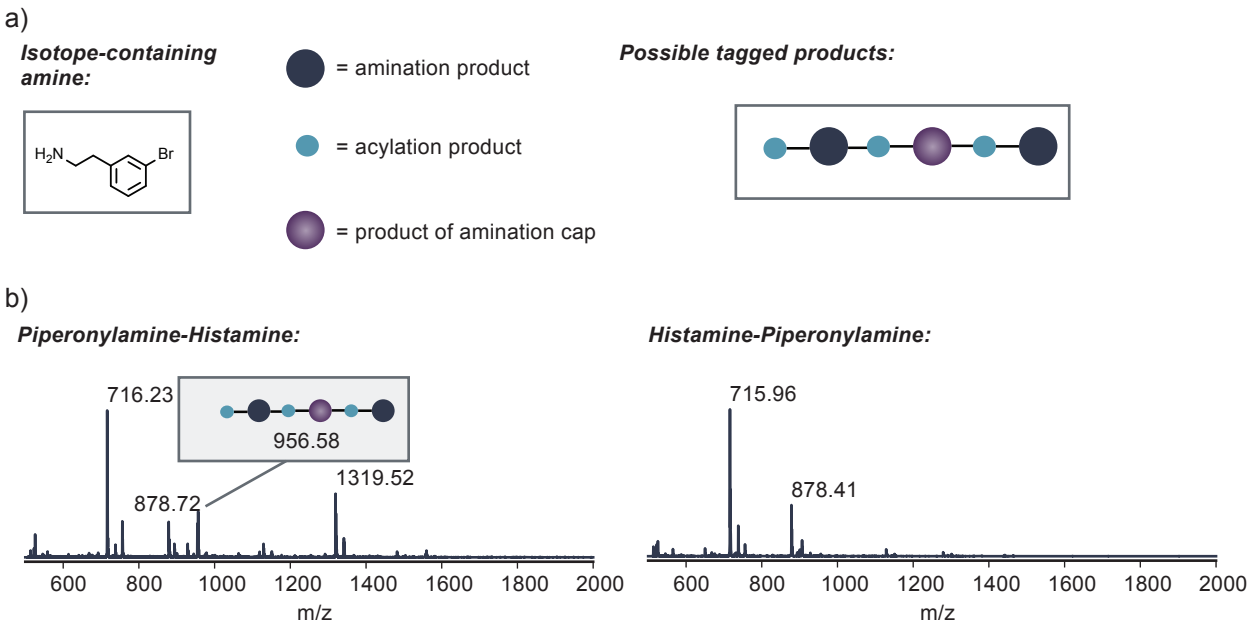

Figure 2.7. Insertion capping strategy. a) Schematic of product with bromine-tagged amine inserted in the middle of a test peptoid dimer. b) MALDI-TOF MS of two test structures with a hyrophobic (Npip) and hydrophilic (Nie) monomer. The comparison of these two spectra shows the different in reactivity of the isotope-containing amine after monomers of varying hydrophobicity.

these products.

A final strategy to provide an isotope tagged structure was to insert a bromine tag into the middle of some of the structures. Any binding should be prevented in this structure, and therefore interactions with metal ions should not prevent ionization. A primary amine containing a bromine was selected (Figure 2.7a) and various equivalents were screened. Similar to what had been previously observed, there was a difference in the incorporation of the residue based on the synthetically preceding residue. Little incorporation was apparent synthetically following Nie, whereas incorporation was apparent after Npip.

2.5 Using a Photocleavable Linker

Another strategy for improving the sequencing efficiency was to replace the methionine linker. Methionine oxidation by metal ions would prevent cleavage and therefore replacing the linker could increase the amount of the structure cleaved and improve the MS signal-to-noise ratio. A photocleavable linker was chosen as the moeity is unaffected by the synthesis and screening procedures (Figure 2.7a). To evaluate preliminarily the cleavage conditions, a test sequence was synthesized and cleaved from the resin. The reaction was complete after three hours in a photobox (Figure 2.7c). Conditions were then evaluated for the cleavage of individual beads. Ethanol and 4:1

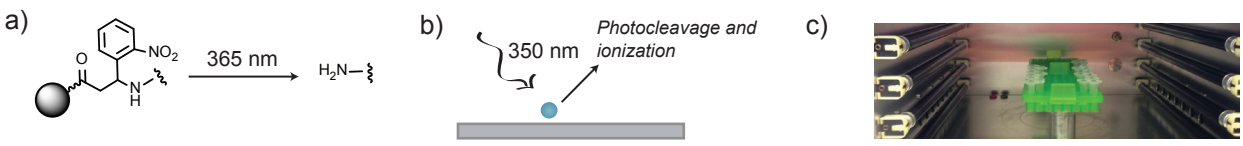

Figure 2.8. Photocleavage strategy. a) Structure of the photolinker and product after cleavage. b) Schematic of cleavage of photolinker immobilized on tentagel resin by MALDI laser. Interaction with the laser leads to photocleavage and ionization. c) Setup employed for cleavage of individual beads in a photobox.

H_2O:MeOH were both evaluated as solvents for the photocleavage, and an eight hour cleavage in ethanol led to a clean MS spectrum. Additionally, immobilization of the beads in the matrix on a MALDI plate allowed both the photocleavage and ionization of the peptoids on the resin. It was determined that the use of phenol in the cleavage of the acid-labile protection groups impeded the photocleavage, but all other reaction conditions were compatible.

2.6 Removing Ions for Sequencing

After the optimization of the photocleavage reaction, it was observed that the screening process led to a decrease in signal, even when the resin was only exposed to a high salt buffer (spectrum in Figure 2.9a). To remove these ions before the cleavage and mass spectrometry, the resin was dialyzed in HCl with ion exchange resin on the opposing side of the dialysis membrane (Figure 2.9b). The acid promotes the dissociation of the ions from the ligands of interest, and an excess of charged residues on the ion-exchange resin provide an excess of additional coordination stites. This de-salting led to a significant improvement in signal, as is apparent in the MALDI-TOF MS spectrum in Figure 2.9c.

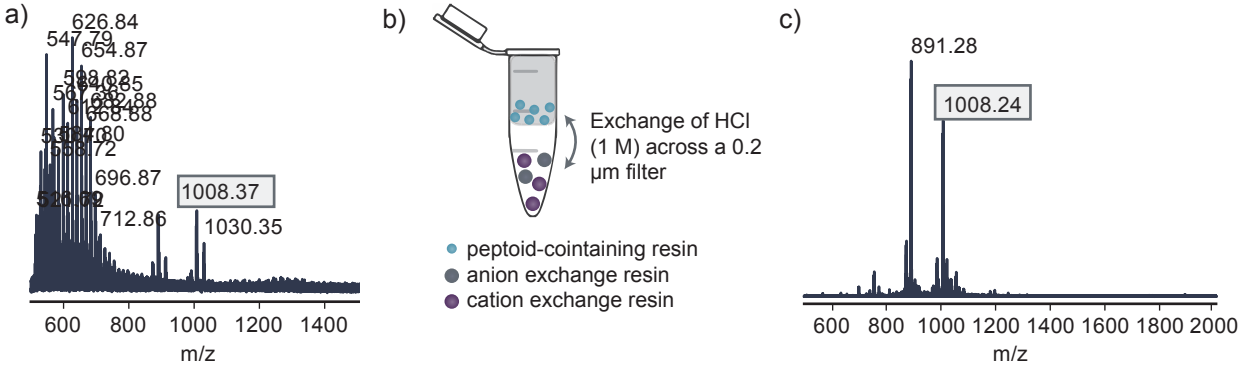

Figure 2.9. Procedure for removing bound ions before photocleavage. a) MALDI-TOF of test tetramer (Npip-Nte- Npip-Nie) after incubation with buffer (NaCl, $MgSO_4$ (1 M) and $NaCO_3$ (20 mM, pH 7)). b) Schematic of strategy employed for removal of ions from peptoid-containing resin after the screening process. c) MALDI-TOF MS of test structure after metal removal procedure (891 mass attributed to incomplete incorporation of Nte residue.

2.7 Conclusions and Future Outlook

Through this work we have designed a metal-binding peptoid library and demonstrated the promise of peptoid libraries in binding various transition metal ions. The synthesis, screening, and sequencing procedures have been individually evaluated and optimized, enabling the use of this platform to screen for metal ligands for almost any application. Further optimization of the capping strategy could lead to a sequencing strategy that would not require access to a MS-MS instrument; however, this synthetic procedure and sequencing technique would likely be more challenging and require optimization for each amine in the library. We look forward to the use of this platform for the identification ligands for new catalysts, small molecule probes, and other cross-disciplinary applications.

2.8 Materials and Methods

General Procedures and Materials

Tentagel MB NH_2 resin (140-170 µm, 0.3 mmol/g), used for library synthesis, was purchased from

Rapp-Polymere (Tuebingen, Germany). Library synthesis steps were performed in fritted disposable chromatography columns (Bio-Rad, Hercules, CA). During the reactions, the resin suspensions were slowly rotated using a nutator (Fisher Scientific, USA). The photolinker (Fmoc-(*R*)-3-amino-3-(2-nitrophenyl)propionic acid) and Fmoc-6-aminohexanoic acid were purchased from Chem-Impex (Wood Dale, IL). Water (dd-H_2O) used was deionized using a Barnstead NANOpure purification system (ThermoFisher, Waltham, MA). All other materials were purchased from commercial sources and used without further purification, except as noted below. All centrifugation was performed in a Galaxy Mini Star (VWR, USA), and lyophilization was performed using a LAB CONCO Freezone 4.5.

Peptoid Synthesis

Of the amine monomers, piperonylamine, butylamine, 2-picolylamine, tryptamine, *N*-(3-aminopropyl)-2-pyrrolidinone, and histamine were used as purchased and incorporated without protecting groups. The glycine and β-alanine monomers were purchased as hydrochloric acid salts with *t*-butyl ester protecting groups. Before use, these compounds were treated with a 1 M NaOH solution that was saturated with NaCl and extracted into a 15:85 v/v isopropanol-chloroform mixture. The organic layers were dried over sodium sulfate and concentrated to yield the monomers as the free bases. *N*-boc-ethylenediamine was purchased and used as received, and cysteamine was protected with a trityl group using a procedure reported by Maltese.[22]

The library was synthesized on Tentagel MB NH_2 resin, which was initially swollen in dichloromethane (DCM). Standard Fmoc solid-phase synthesis (using HCTU as a coupling agent) was used to incorporate the first three members of the linker through amide bond formation. For the first variable position, the resin was split evenly into seven different fritted columns. Acylation and the addition of the first amine were performed according to the procedure developed by Zuckermann *et al.* for the incorporation of heterocyclic amines.[13] Briefly, for each acylation step a solution of chloroacetic acid (6.8 eq, 0.4 mM) was prepared in dimethylformamide (DMF) in addition to a solution of diisopropylcarbodiimide (8 eq, 2 M) in DMF. The resin beads were exposed to both solutions with gentle agitation for 5 min. Following this, the acylation solution was removed via filtration and the resulting beads were rinsed with DMF. Next, the amines were added as 2 M solutions in DMF. After 2 h of gentle agitation at room temperature, the resin samples were isolated via filtration and rinsed with DMF. All of the resin was then pooled and mixed in DCM for five minutes. Subsequently, the resin was isolated via filtration, vacuum dried, and split into a new set of 7 fritted columns. The acylation and amination steps were repeated three more times to add the remaining amines, with pooling and splitting between each round of monomer introduction. After the last amination step, the resin pools were recombined a final time. A 20% solution of 4-methylpiperidine in DMF was next added to each resin sample for 30 min to remove any acylation adducts on the imidazole groups. After isolation via filtration, the resin was rinsed with DMF. The protecting groups were removed by incubation with a cleavage solution (95:2.5:2.5) trifluoroacetic acid:water:triisopropylsilane) for 1.5 h. The resin was then rinsed with DCM, dried under vacuum, and stored at 4 °C until use.

Library Screening

To equilibrate the beads before the screen, a 40 mg portion of the resin (representing more than 8 times the size of the library to ensure inclusion of each sequence) was swelled in 4:1 THF:MeOH

overnight. The library aliquot was then incubated with the metal of interest (0.02 M $CoCl_2$, $FeCl_2$, $Ni(OAC)_2$, $Cu(OAc)_2$, or CrO_3) in 4:1 THF:MeOH for 1 h. The library aliquot was then rinsed with three 1 mL portions of 4:1 THF:MeOH (each with 15 min incubation) to remove any non-specifically bound ions.

For visualization and bead selection, the resin was transferred to a Petri dish. A 50-100 μL portion of the appropriate dye solution was then added to enhance the sensitivity. For chromium, a solution of 0.5 g of 1,5-diphenylcarbazide in 100 mL of acetone was used.[19] For nickel, a solution of 1% (w/v) dimethylglyoxime in methanol was applied.[18] Iron(III) was visualized with a solution of KSCN (20 μL of 1% KSCN in MeOH).[17] The volume of solution that was added was chosen such that the solvent would rapidly evaporate from the Petri dish, trapping the dye and the metal within the individual beads. After 15 min, the Petri dish was examined using a Leica S6D Microscope (Leica, Germany) equipped with a Moticam 2300 3.0 MP camera and Micromanager Software[23] for capturing images. The individual beads with the most intense colors were selected for ligand identification.

Cyanogen Bromide Cleavage

Selected beads were placed in 0.6 mL Eppendorf tubes with 2 mg/mL CNBr in 1:1 AcN:0.25 N HCl (20 μL for an individual bead) and incubated for 18-22 hr. The solution was then evaporated by heating the samples in the fume hood. After the solution had fully evaporated the beads were dissolved in 1:1 H_2O:AcN with 0.5 mM TCEP to reduce any potential disulfides.

Photocleavage

The beads bearing hit sequences were removed from the filter unit and once again placed in a Petri dish using ethanol (approx. 500 μL). The individual beads were captured using a pipet and placed into individual 0.6 mL Posi-Click tubes (Denville Scientific, South Plainfield, NJ). The volume in each tube was brought to 5 μL with absolute ethanol. To cleave the peptoids from single resin beads, the tubes were placed in a computer controlled ICH-2 photoreactor with UVA bulbs (Luzchem, Ottawa, Canada) for 8 h (various incubation times were screened). For characterization of bulk samples of resin, photocleavage time was limited to 10 min.

Metal Ion Removal

The selected beads were combined on top of the membrane of a 0.5 mL 0.2 μm centrifugal filter unit (Millipore, Billerica, MA). A mixture of Amberlite cation (Na^+ form, 0.5 mg) and anion (Cl^- form, 0.5 mg) exchange resins was then added to the filtrate collection tube of the centrifugal filter unit. The filter and the collection tube were then filled with 1 M HCl (both 0.1 M and 1 M HCl were evaluated). This setup was incubated with gentle agitation on a nutator for 2 h, allowing diffusion to occur through the 0.2 μm filter. The Amberlite beads and acidic solution in the lower collection tube were removed, and the solution in the filter unit was removed by brief centrifugation. Water (500 μL) was added to the filter unit, and the unit was gently agitated on a nutator for 15 min. The water was then removed by centrifugation. This process was repeated twice to ensure that the residual HCl had been rinsed from the beads.

2.9 References

1. Burger, M. T. & Still, W. C. Synthetic Ionophores. Encoded Combinatorial Libraries of

Cyclen-based Receptors for Cu^{2+} and Co^{2+}. *J. Org. Chem*. **60**, 7382–3 (1995).

2. Francis, M. B., Jamison, T. F. & Jacobsen, E. N. Combinatorial libraries of transition-metal complexes, catalysts and materials. *Curr. Opin. Chem. Biol.* **2,** 422–8 (1998).

3. Francis, M. B., Finney, N. S. & Jacobsen, E. N. Combinatorial Approach to the Discovery of Novel Coordination Complexes. *J. Am. Chem. Soc*. **118**, 8983–4 (1996).

4. Nitz, M., Franz, K. J., Maglathlin, R. L. & Imperiali, B. A Powerful Combinatorial Screen to Identify High-Affinity Terbium (III)-Binding Peptides. *ChemBioChem* **4**, 272–6 (2003).

5. Vendrell, M., Zhai, D., Er, J. C. & Chang, Y. T. Combinatorial strategies in fluorescent probe development. *Chem. Rev.* 112, 4391–420 (2012).

6. Mejàre, M., Ljung, S. & Bülow, L. Selection of cadmium specific hexapeptides and their expression as OmpA fusion proteins in Escherichia coli. *Protein Eng.* **11**, 489–94 (1998).

7. Day, J. W., Kim, C. H., Smider, V. V & Schultz, P. G. Identification of metal ion binding peptides containing unnatural amino acids by phage display. *Bioorg. Med. Chem. Lett.* **23**, 2598–600 (2013).

8. Nam, K. T. et al. Virus-enabled synthesis and assembly of nanowires for lithium ion battery electrodes. *Science 312*, 885–8 (2006).

9. Simon, R. J. et al. Peptoids: a modular approach to drug discovery. *Proc. Natl. Acad. Sci. U. S. A*. **89**, 9367–71 (1992).

10. Culf, A. S. & Ouellette, R. J. Solid-phase synthesis of N-substituted glycine oligomers (alpha-peptoids) and derivatives. *Molecules* **15**, 5282–335 (2010).

11. Lee, B. C., Chu, T. K., Dill, K. A. & Zuckermann, R. N. Biomimetic nanostructures: Creating a high-affinity zinc-binding site in a folded nonbiological polymer. *J. Am. Chem. Soc.* **130**, 8847–55 (2008).

12. Pirrung, M. C., Park, K. & Tumey, L. N. ^{19}F-encoded combinatorial libraries: discovery of selective metal binding and catalytic peptoids. *J. Comb. Chem.* **4**, 329–44 (2002).

13. Burkoth, T. S., Fafarman, A. T., Charych, D. H., Connolly, M. D. & Zuckermann, R. N. Incorporation of unprotected heterocyclic side chains into peptoid oligomers via solid-phase submonomer synthesis. *J. Am. Chem. Soc.* **125**, 8841–5 (2003).

14. Udugamasooriya, D. G., Dineen, S. P., Brekken, R. A. & Kodadek, T. A Peptoid ' Antibody Surrogate' That Antagonizes VEGF Receptor 2 Activity. *J. Am. Chem. Soc*. **130**, 5744–52 (2008).

15. Lam, K. S. *et al*. A new type of synthetic peptide library for identifying ligand-binding

activity. *Nature* **354**, 82–84 (1991).

16. Lam, K. S., Lebl, M. & Krchnák, V. The 'One-Bead-One-Compound' Combinatorial Library Method. *Chem. Rev.* **97**, 411–48 (1997).

17. Feigl, F., Anger, V. & Koslow, R. H. Spot Tests in Inorganic Analysis. *Elsevier* 158 (1973).

18. Godycki, L. E. & Rundle, R. E. The structure of nickel dimethylglyoxime. *Acta Crystallogr.* **6**, 487–495 (1953).

19. Pflaum, R. T. & Howick, L. C. The Chromium-Diphenylcarbazide Reaction. *J. Am. Chem. Soc.* **78**, 4862–66 (1956).

20. Thompson, L. A. & Ellman, J. A. Synthesis and Applications of Small Molecule Libraries. *Chem. Rev.* **96**, 555–600 (1996).

21. Witus, L. S. et al. Identification of highly reactive sequences for PLP-mediated bioconjugation using a combinatorial peptide library. *J. Am. Chem. Soc.* **132**, 16812–7 (2010).

22. Maltese, M. Reductive demercuration in deprotection of trityl thioethers, trityl amines, and trityl ethers. *J. Org. Chem. 66,* 7615–25 (2001).

23. Edelstein, A., Amodaj, N., Hoover, K., Vale, R. & Stuurman, N. Computer control of microscopes using μManager. *Curr. Protoc. Mol. Biol.* Chapter 14, Unit 14.20 (2010).

Chapter 3

Selective Coordination of Cr(VI) for Water Remediation

Abstract:

Hexavalent chromium (Cr(VI)) is a world-wide water contaminant that is currently without cost-effective and efficient remediation strategies. This is in part due to a lack of ligands that can bind it amid an excess of innocuous ions in aqueous solution. We present herein the design and application of a peptoid-based library of ligand candidates for toxic metal ions. A selective screening process was used to identify members of the library that can bind to Cr(VI) species at neutral pH and in the presence of a large excess of spectator ions. Eleven sequences were identified, and their affinities were compared using titrations monitored with UV-Vis spectroscopy. To identify the interactions involved in coordination and specificity, we evaluated the effects of sequence substitutions and backbone variation in the highest affinity structure. Additional characterization of the complex formed between this sequence and Cr(VI) was performed using NMR spectroscopy. To evaluate the ability of the developed sequences to remediate contaminated solutions, the structures were synthesized on a solid-phase resin and incubated with environmental water samples that contained simulated levels of chromium contamination. The synthetic structures demonstrated the ability to reduce the amount of toxic chromium to levels within the range of the EPA contamination guidelines. In addition to providing some of the first selective ligands for Cr(VI), these studies highlight the promise of peptoid sequences as easily-prepared components of environmental remediation materials.

This chapter is based on the publication in the *Journal of the American Chemical Society* entitled "Selective Chromium(VI) Ligands Identified Using Combinatorial Peptoid Libraries."

3.1 Introduction

Water contamination from manufacturing and mining activities has been a problem since the industrial revolution, providing a constant need for new technologies that can remove toxic chemicals from drinking water supplies and purify industrial waste streams. While there are practical methods currently in use, there remain many pollutants that are very difficult to remove in a cost-effective fashion. As a particularly notable example, chromium(VI) species produced by leather tanning, chrome plating, and other industrial activities have polluted water supplies in communities world-wide.[1] In some locations, drinking water contamination can reach up to 250 times the limit dictated by the world health organization.[2] Though the biological mechanism is unknown, the demonstrated health effects of Cr(VI) exposure include sensitization of the skin and an elevated risk of lung cancer.[3] A variety of methods have been explored for the removal of Cr(VI) and other heavy metal contaminants, including activated carbon adsorption, biosorpents, inorganic particles and membranes, electrochemical treatment, and ion-exchange resins.[4–6] However, many of these methods are expensive due to physical sensitivity of the materials or a lack of selectivity that requires large quantities for effective chromium removal. These limitations have prevented the widespread adoption of a cost effective strategy for the removal of Cr(VI) and other heavy metals from contaminated areas.

The major challenge in developing materials for remediation is selectivity. Heavy metal contaminants are often found in concentrations that are orders of magnitude lower than innocuous ions in water (e.g. Na^+, Cl^-, Mg^{2+}, SO_4^{2-}, CO_3^{2-}, etc.). Therefore, for the materials to be efficient, they must have a substantially higher affinity for the contaminating ions than for the harmless ones. A few selective metal chelators have been identified for use in biological applications,[7–11] but otherwise ligands have rarely been designed to discriminate between ions. The rational design of a selective ligand for Cr(VI) is particularly difficult due to the limited number of ligands that are currently known.[12] Additionally, because of its potent oxidative reactivity, the pursuit of well-defined Cr(VI) complexes is uncommon. For these reasons, combinatorial chemistry, which has previously been applied to identify new transition-metal complexes and catalysts,[9,10,13,14] provides a particularly attractive approach for the identification of selective binders for Cr(VI) species.

Peptoids, or *N*-substituted glycine oligomers, are uniquely appropriate for this application due to their modular synthesis, wide variety of potential monomers, resistance to enzymatic degradation, and relatively low synthetic cost.[15,16] Previous work has, in fact, shown that peptoids can be designed to bind to metals.[14,17–19] However, neither their selective binding abilities nor their ability to bind to Cr(VI) species have been explored. In this work, we have developed a library of peptoids that can bind to a wide variety of metal ions. We have also developed a screening method that selectively reports the members of the library that can bind to Cr(VI) ions even in a complex mixture of other ions. This has resulted in a new class of binders for this toxic metal that can be prepared easily on solid supports for use in remediation applications.

3.2 Library Design and Synthesis

To identify new peptoid-based ligands for metal ions, the solid-phase library depicted in Figure 3.1a was first synthesized. Because of its compatibility with both the peptoid synthesis conditions and the acid-induced cleavage of the side chain protecting groups, a photocleavable moiety[20,21] was chosen to link the library members to the 140-170 μm PEG-grafted polystyrene beads.

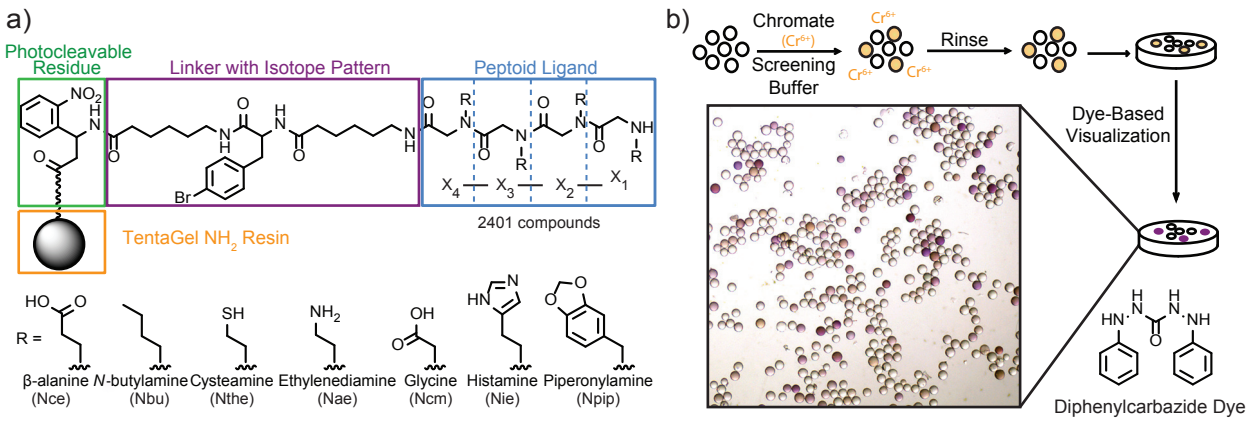

Figure 3.1. Outline of the peptoid library design and overall screening procedure. (a) The diagram depicts the linking groups and variable positions, as well as the amine monomers that were incorporated into each of the "X_n" sites. (b) The library was screened for metal ion binding as shown. A representative photograph shows a portion of the library after incubation with $Cr(VI)_{aq}$, rinsing, and treatment with a diphenylcarbazide dye.

To facilitate library sequencing using MALDI-TOF MS/MS spectrometry, two 6-aminohexanoic acid residues and a 4-bromo-D-phenylalanine residue were also included. These spacing groups added a distinctive isotopic tag ($^{79}Br/^{81}Br$) to each structure[22,23] while simultaneously increasing the overall mass of the compounds. The peptoid segment was synthesized using the submonomer method[24] with chloroacetic acid.[25] Amine monomers were incorporated at each of four variable positions to generate structures with the potential to form metal ion binding pockets. Seven different amines were selected for incorporation: five with heteroatoms capable of metal ion coordination (Nce, Nthe, Nae, Ncm, and Nie in Figure 3.1a) and two chosen to add nonbonding interactions to the library (Nbu and Npip). Before inclusion, the incorporation ability of each amine monomer was validated through the synthesis of repetitive "sandwich" sequences with benzylamine, as previously described.[26] Using split-and-pool synthesis techniques,[27,28] a library of 2401 unique structures was produced. Following synthesis, the side chain protecting groups were cleaved using trifluoroacetic acid.

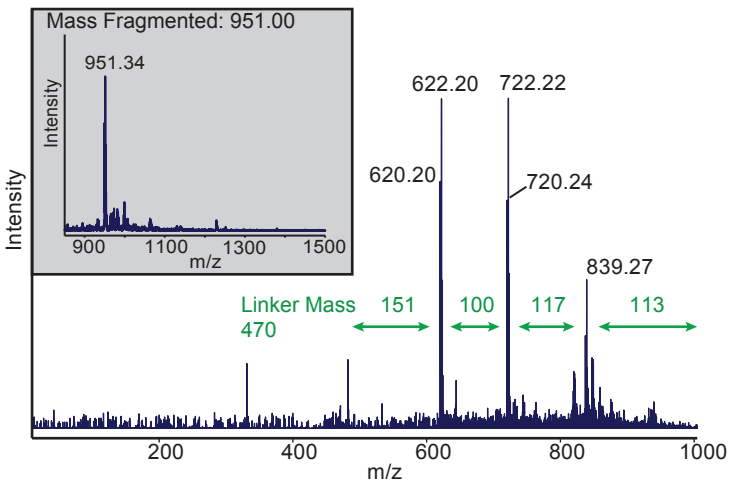

Residue	Monomer Fragment Mass
Nce	129
Nbu	113
Nthe	117
Nae	100
Ncm	115
Nie	151
Npip	191

Figure 3.2. Representative MS and MS/MS spectra of an identified $Cr(VI)_{aq}$ binding sequence. MALDI-TOF spectrum of single bead cleavage of Sequence 10, which will be described in detail below, after being selected from the chromate screen. MALDI-TOF-TOF analysis of the same sample was used to identify the Nbu - Nthe - Nae - Nie sequence.

3.3 Screening for Selective Metal Affinity

The key objective of this work was the identification of ligands that could bind chromium(VI) ions in complex ionic solutions with high affinity. This was achieved using the screening procedure outlined in Figure 3.1b. Portions of the library were first incubated with solutions containing 2 mM CrO_3 and a high salt screening buffer (1 M NaCl, 1 M $MgSO_4$, 20 mM $NaHCO_3$, pH 7). Upon dissolving CrO_3 in water, a mixture of chromate and dichromate ions is formed,[29] which will be referred to as $Cr(VI)_{aq}$ in this work. After 1 h, the beads were isolated via filtration and rinsed briefly with water. A number of the library members were observed to have taken on a pale yellow color at this point. To facilitate the unambiguous identification of the chromium complexes, a solution of diphenylcarbazide[30] was next added. This resulted in the formation of a bright pink precipitate, which remained trapped in the resin matrix.[31] As this detection method relies on the oxidation of the carbazide group to generate the color,[32] it also confirmed that the bound metal ions were in the (VI) oxidation state. The darkest pink beads were individually selected from the library for metal removal, photocleavage, and sequencing by mass spectrometry (Figure 3.2), as described in the materials and methods.

Eleven sequences were identified in the screen (Figure 3.3), with Sequence 5 being identified twice. There was a substantial degree of similarity among the ligands, with the Nthe monomer consistently being present in position X_2 or X_3. This is consistent with previous studies of the interactions of Cr(VI) ions with thiol containing metabolites.[12] However, the absence of structures in which this monomer was in position X_1 or X_4 suggested that other interactions were also participating. Additionally, each sequence contained at least one non-chelating residue, and almost always in position X_1. To confirm that the coordination of the isolated structures was metal-specific, the library was also screened for nickel(II) binding under similar conditions. In this case,

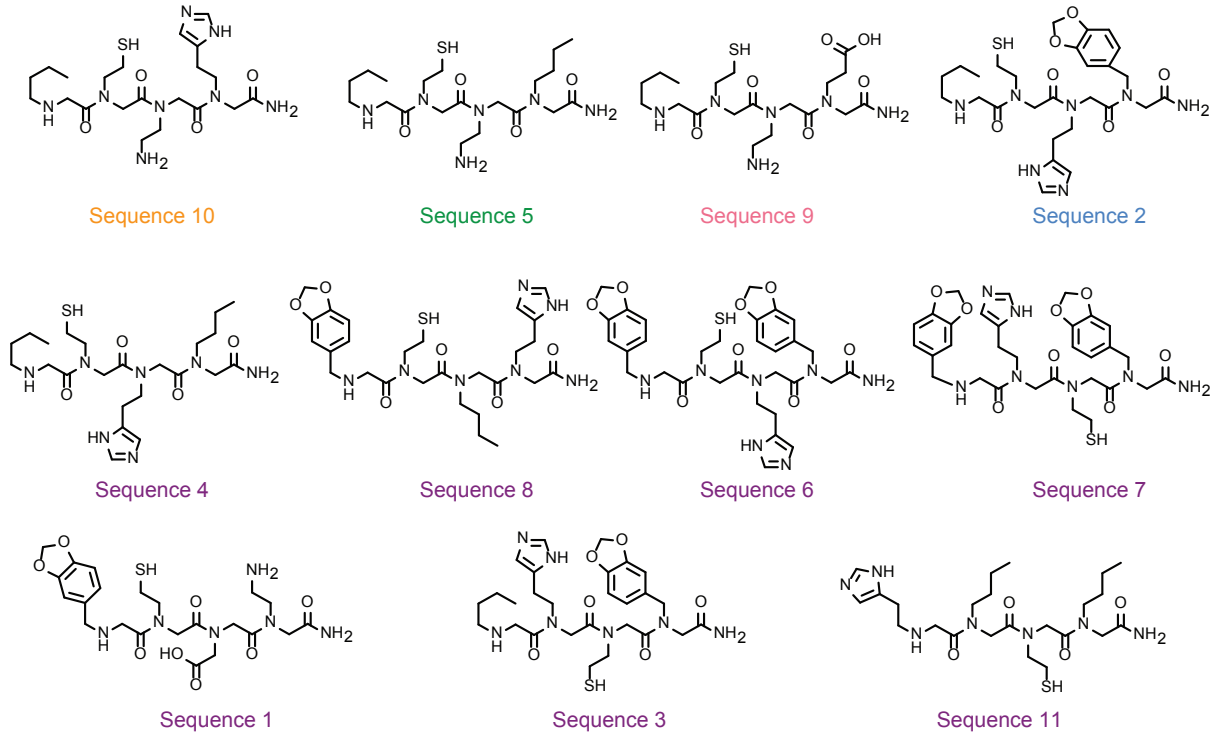

Figure 3.3. Identified sequences and evaluated for $Cr(VI)_{aq}$ binding.

dimethylglyoxime was used to visualize the complexes.[33] As would be expected from previous studies involving peptide-based ligands,[31] the identified peptoids contained a large number of imidazole groups (Figure 3.4). They bore no resemblance to the $Cr(VI)_{aq}$-binding ligands, confirming the ability of the library design and screening approach to provide successful coordination motifs for widely varying species.

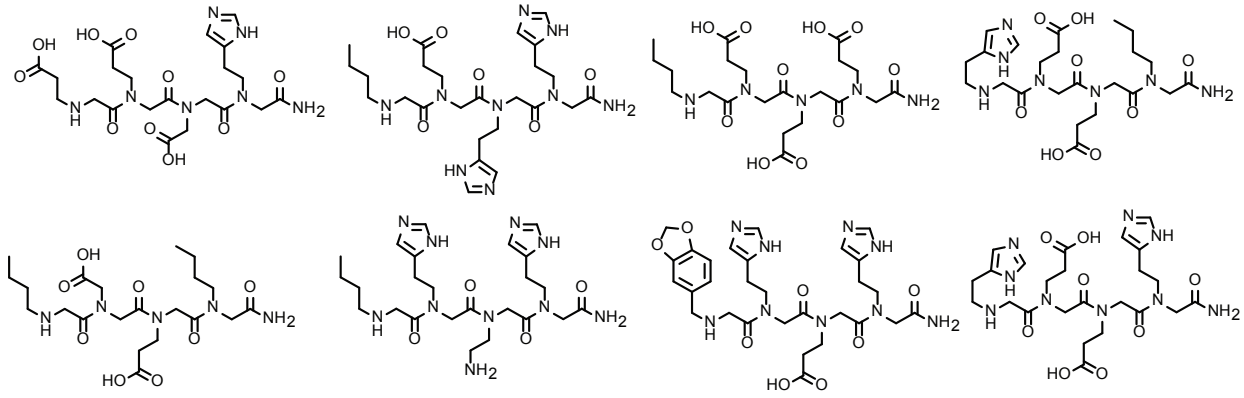

Figure 3.4. Sequences identified to bind nickel (Ni(II)) selectively in the presence of excess sodium and magnesium ions using similar screening conditions to those used for chromium (1 M NaCl, 1 M $MgSO_4$, 20 mM $NaHCO_3$, 2 mM $Ni(OAc)_2$, pH 8)

3.4 Binding Affinity Characterization

To validate the ability of the identified peptoids to interact with Cr(VI) species and to compare their relative affinities, all of the 11 identified sequences were resynthesized for use in titration experiments. The ligand candidates were prepared on Rink Amide resin and purified by reverse-phase HPLC (Figure 3.5). Each of the sequences was characterized through the addition of $Cr(VI)_{aq}$ while monitoring complex formation using UV-Vis spectroscopy. At each concentration, the spectrum of the peptoid-$Cr(VI)_{aq}$ mixture was compared to a control sample that lacked the ligand. An increased absorbance due to complex formation was found at 457 nm (Figure 3.6), similar to wavelengths previously established for a S→Cr charge-transfer.[12] A corresponding decrease in the absorbance of free Cr(VI) was also observed. The dissociation constants were approximated as the midpoints of sigmoidal fits to the data assuming one-to-one association of the peptoid and Cr(VI). It is recognized the accuracy of these values may be confounded by competing processes, such as the oxidation of the thiols to disulfides or sulfonates, but the NMR spectra discussed below suggest that complex formation is the most significant reason for the observed spectral shifts. The measured values should be taken as approximations; nonetheless, they provide a ready means by which to compare the performance of the identified binding sequences.

The structures, binding curves, and estimated dissociation constants for the highest affinity sequences are shown in Figure 3.7, and the full set of binding data appears in Figure 3.8. To confirm the precision of the titrations, the experiment was repeated three times with Sequence 5 and displayed a consistent estimate of the K_d (Figure 3.9a). Each of the best sequences possessed a side chain group in position X_3 that is positively charged at pH 7, an Nthe in position X_2, and an Nbu in position X_1. The significance of the positively charged residues can be rationalized by interactions with the negatively charged chromate and dichromate anions in neutral solution. To support this assertion, we evaluated the binding affinity of Sequence 10, the sequence with the highest affinity, at various pH values. As expected, a lower pH of 5.5 resulted in stronger observed binding between

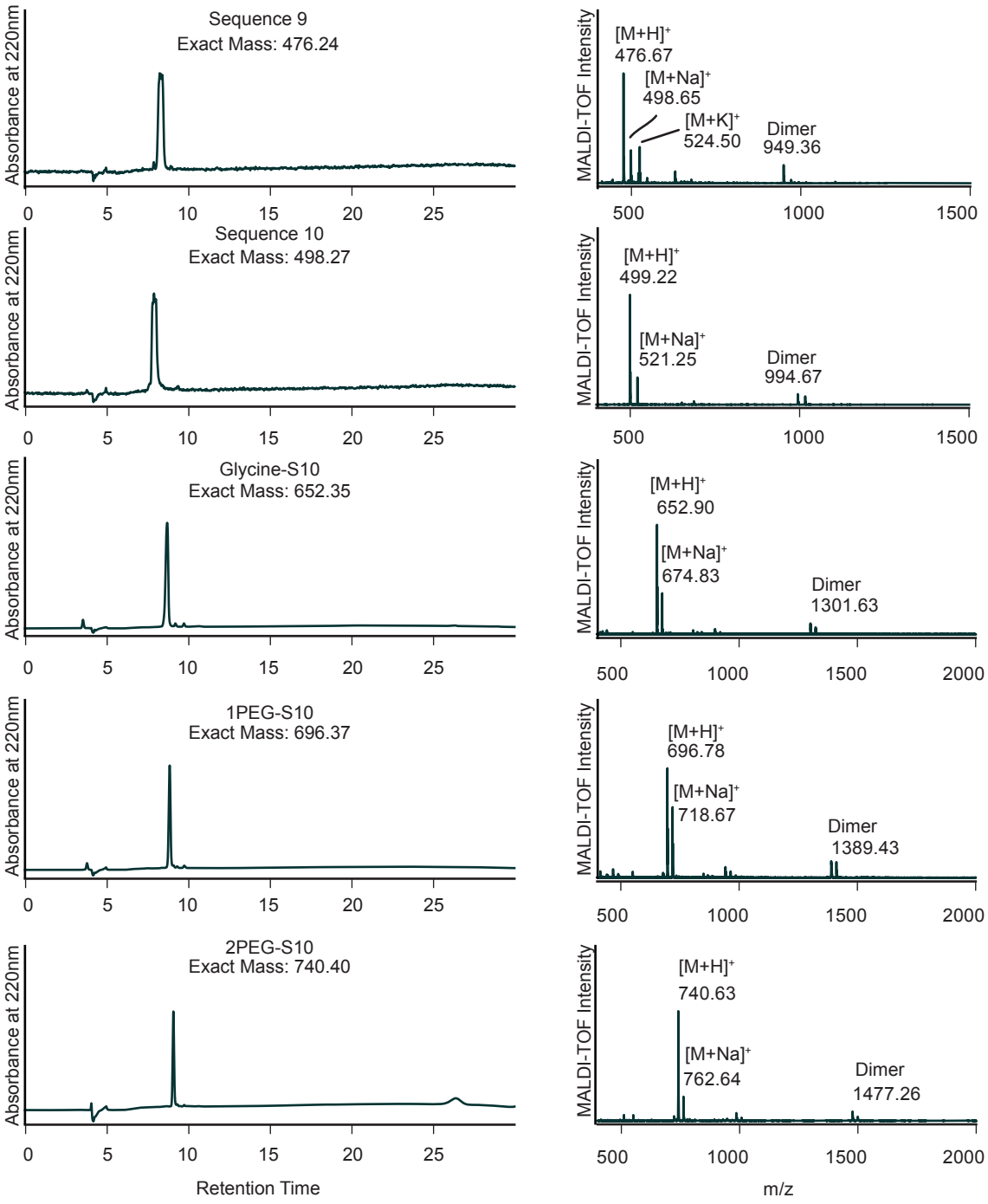

Figure 3.5. Representative purity and mass confirmation for re-synthesized peptoids (see Figure 3 for structures), as evaluated by reverse phase HPLC (left) and MALDI-TOF MS (right).

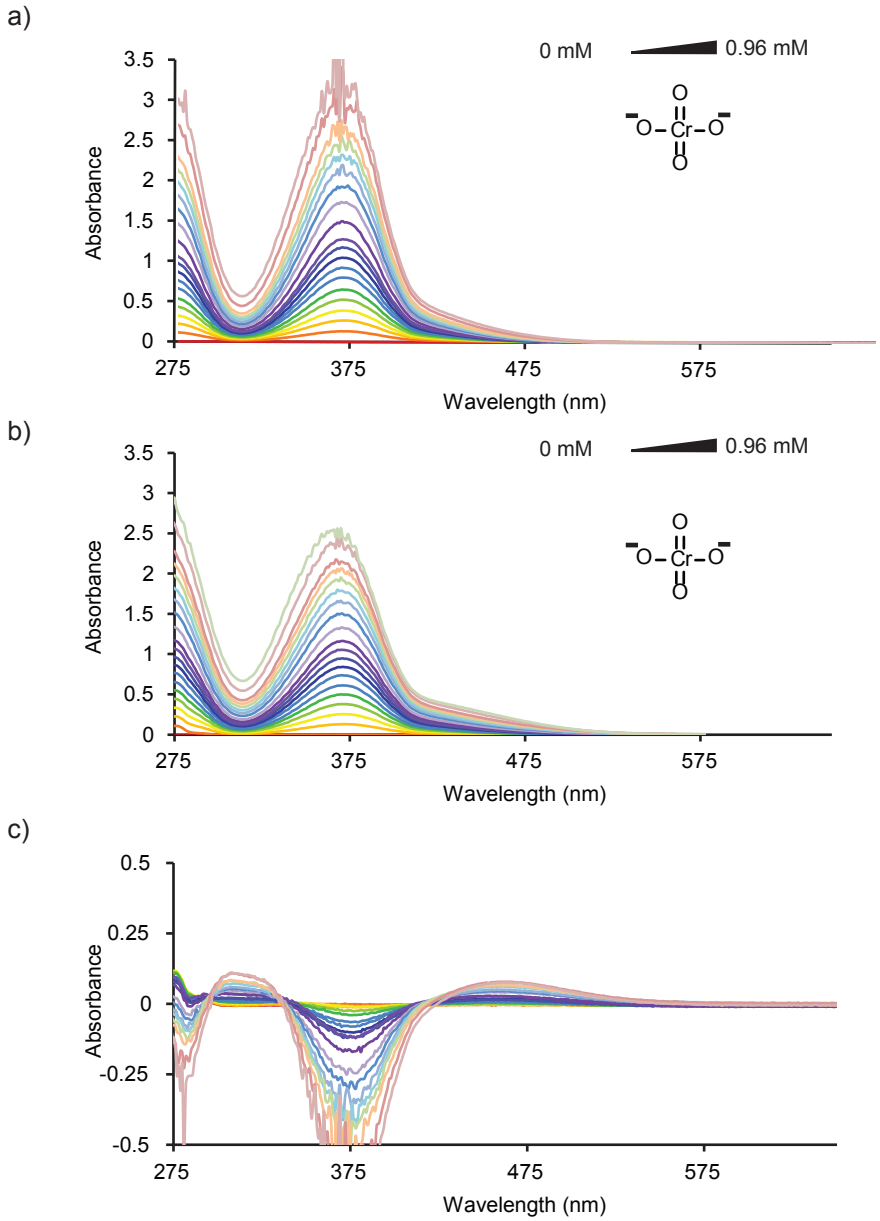

Figure 3.6. Determination of the binding affinity of peptoid ligands for chromium(VI). All titrations were performed in 10 mM HEPES, pH 7. (a) Control titration of Cr(VI)aq with no added ligand. (b) Titration of $Cr(VI)_{aq}$ into Sequence 9 (300 μM). (c) Spectra in (a) were subtracted from spectra in (b) in order to account for the background absorbance from $Cr(VI)_{aq}$. The decrease at 370 nm is due to the depletion of free chromate, and the increase at 457 nm is due to the formation of a new complex.

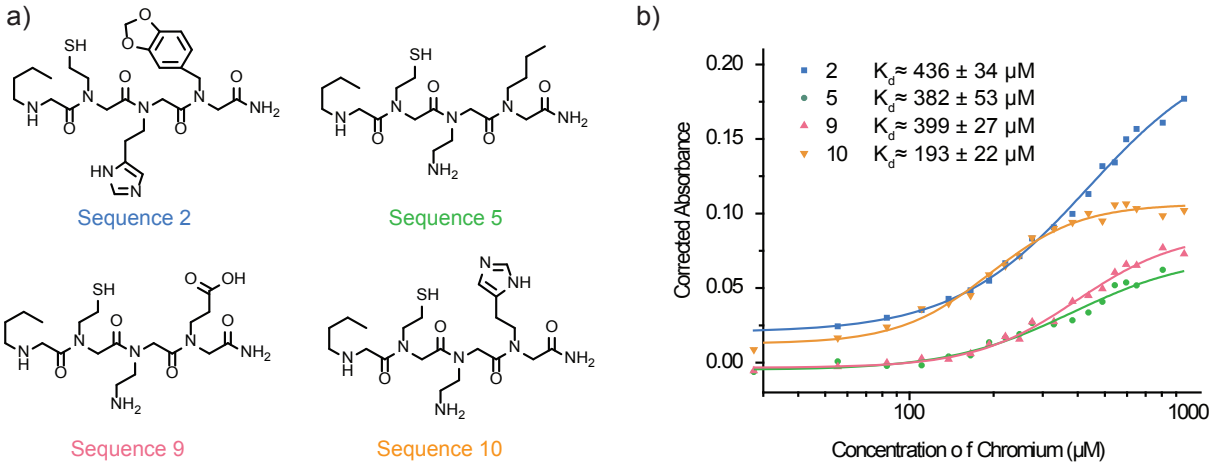

Figure 3.7. Summary of identified sequences and their Cr(VI) binding affinities. Using UV-vis spectroscopy, binding constants were determined for each sequence at 300 µM in 10 mM HEPES buffer (pH 7). a) The four highest affinity sequences identified from the screen are shown. b) Binding curves are plotted for each of the four sequences in HEPES buffer as $Cr(VI)_{aq}$ was added. The absorbance has been corrected by subtracting the absorbance of chromium alone. The data were fit using a logistic function and the K_d values were approximated by the inflection points of the curves.

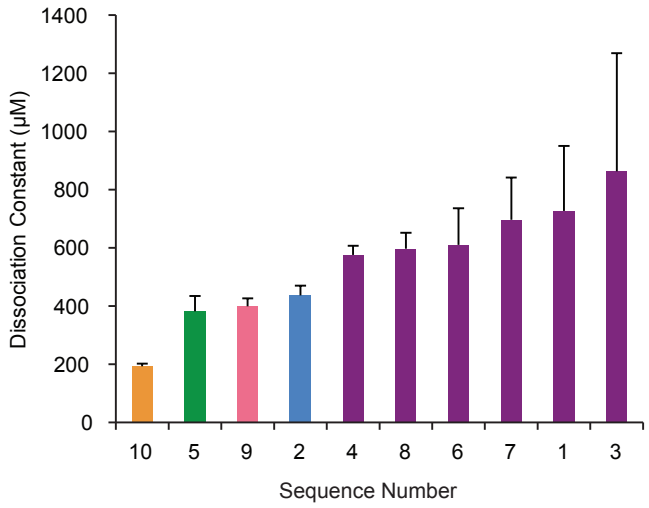

Sequence #	K_D(µM)	Error	χ^2	R^2
10	193	22	2.02E-5	0.949
5	382	53	1.53E-5	0.970
9	399	27	9.53E-6	0.988
2	436	34	1.41E-5	0.995
4	575	32	8.31E-6	0.998
8	597	55	2.06E-5	0.997
6	610	126	2.21E-5	0.986
7	696	145	1.50E-5	0.990
1	727	223	1.84E-5	0.978
3	863	406	3.01E-5	0.979
11	>1 mM	-	-	-

Figure 3.8. Dissociation constants, as determined by UV-vis titrations with Cr(VI)aq. The error bars represent the standard error in the logistic fit.

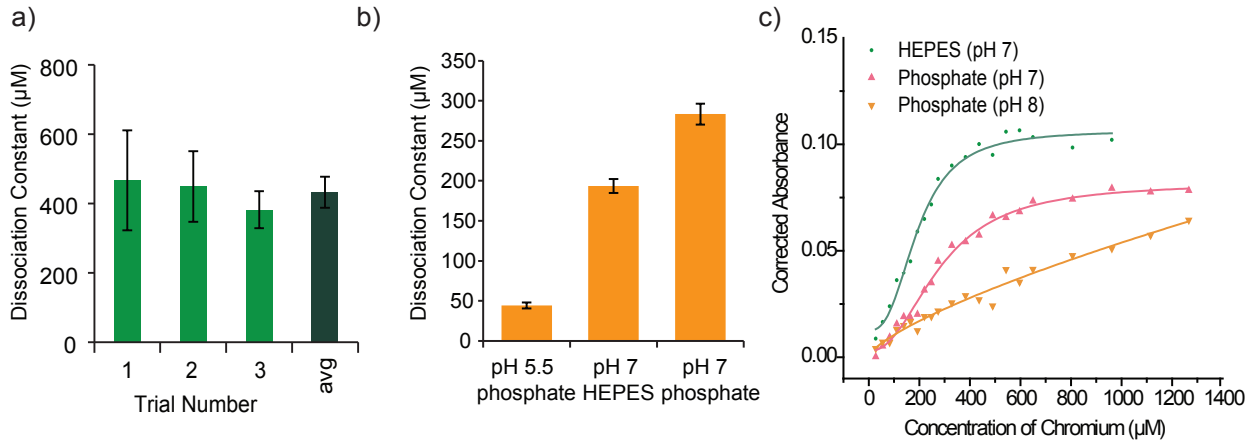

Figure 3.9. a) Binding constant for Sequence 5 measured three times to ensure repeatability of binding experiments. The error bars represent the standard error of the logistic fit, with the exception of the average which displays the standard error of the three trials. (b), (c) The affinity of Sequence 10 for Cr(VI)aq was also measured in phosphate buffer at pH 5.5 and 7 (shown) and pH 8 (not shown). he absorbance has been corrected by subtracting the absorbance of chromium alone. All error bars represent the standard error in the logistic fit.

the ligand and the metal, whereas the affinity at pH 8 was too low to measure accurately with this technique (Figure 3.9b,c).

Previous examples of $Cr(VI)_{aq}$ complexes have involved thiol ligands.[34] To verify that additional moieties of Sequence 10 were also required for binding, a solution of glutathione was evaluated using the same titration method. A dissociation constant above 1 mM was observed at pH 7, and a dissociation constant of 708 ± 170 μM was measured at pH 5.5 (Figure 3.10). The affinity has been previously reported at low pH, measuring a dissociation constant of 673 ± 23 μM at pH 1.[35] This dissocation constant is ten-fold higher than that of Sequence 10 under the same conditions, confirming the importance of non-thiol residues in the structures.

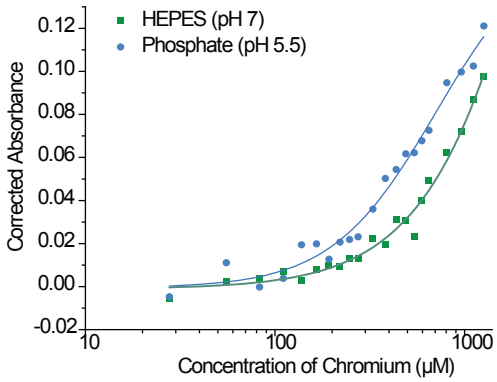

Buffer	Estimated K_d (μM)
HEPES (pH 7)	n.d.
Phosphate (pH 5.5)	708±170

Figure 3.10. Evaluation of glutathione (300 μM) binding to $Cr(VI)_{aq}$. Note the use of a logarithmic scale for the x-axis.

3.5 Varying Peptoid Structure to Elucidate Binding Interactions

As a first step toward probing the interactions of Sequence 10 with Cr(VI)aq, we synthesized a series of sequence analogs with different monomer orders and substitutions (Figure 3.11). Since the sequences shown in Figure 3.7 had a consistent order for the X_2-X_3 groups, we first looked at the impact of switching the Nae and the Nthe residues. The binding affinity appeared to be negligibly affected by this change; however, when the entire sequence was reversed the measured dissociation

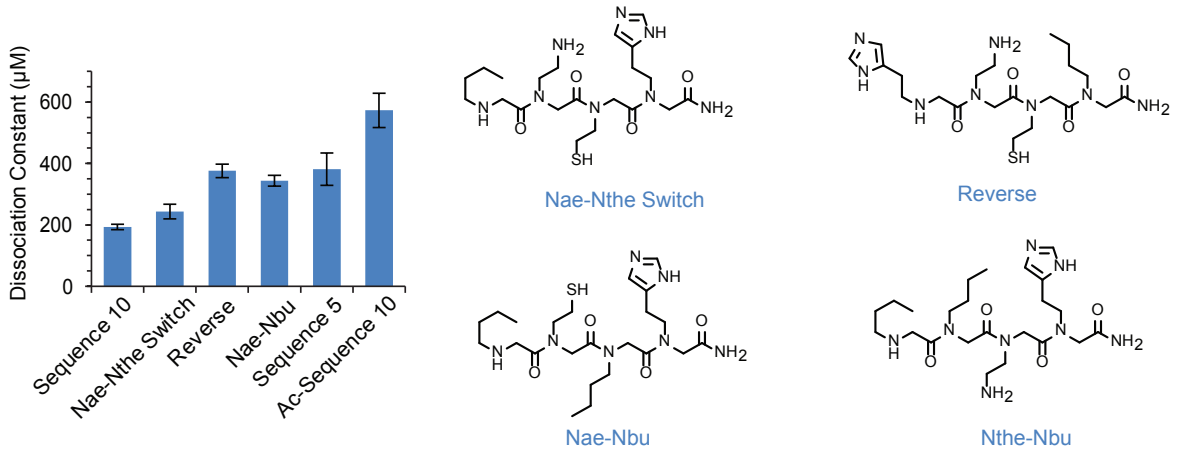

Figure 3.11. Evaluating binding affinity through variations of Sequence 10. A series of Sequence 10 variants was synthesized to examine the importance of sequence order and to verify the binding contributions of the individual residues. The binding affinity of each ligand was determined at 300 μM in 10 mM HEPES buffer (pH 7) through titration with $Cr(VI)_{aq}$.

constant increased by nearly two-fold. Since the peptoid backbone is achiral, this is likely due to the N-terminal residue switch from Nbu to Nie. To confirm the involvement of this component, the affinity of Sequence 10 was measured after acylation of the secondary amine in position X_1. The dissociation constant was even higher than that of the reversed sequence. To investigate the contribution of the X_4 and X_3 residues, they were sequentially replaced with non-binding Nbu. One of these substitutions (Nbu in place of the initial Nie) was identified from the screen (Sequence 5), but the other substitutions were not identified from the screen and were therefore additionally synthesized. The sequences with Nbu substituted for Nae and Nie retained their affinity, with measured dissociation constants similar to that of the reversed sequence; however, the sequence in which the Nthe had been replaced had a significantly decreased affinity that could not be determined with the titration. This and the prevalence of the Nthe in the identified sequences suggested that the thiol is more directly involved in the metal binding than the other residues.

Relative to peptides, which contain chiral α-amino acids, peptoids can sample a substantially greater conformational space. This could be viewed as both a positive and a negative feature: the additional conformations could allow multidentate binding interactions that peptides cannot accommodate, but a significant entropic penalty could accompany complex formation. In an effort

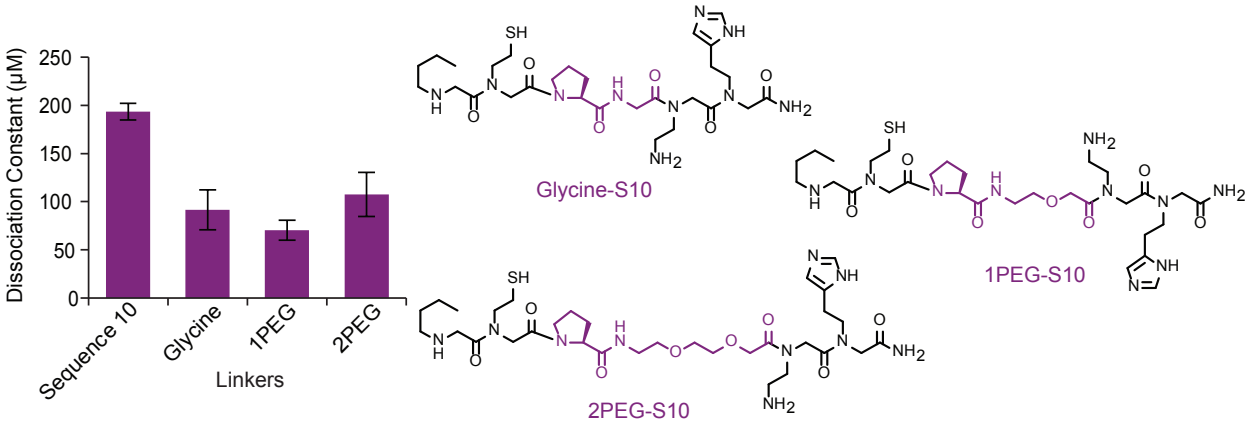

Figure 3.12. To explore the influence of enhanced flexibility, several Sequence 10 derivatives were prepared with a D-proline turn and a glycine, 1PEG, or 2PEG linker. The affinity of the synthesize sequences is compared to the original Sequence 10. The binding affinity of each new ligand (measured at 150 μM) was determined by titration with $Cr(VI)_{aq}$ in 10 mM HEPES buffer (pH 7).

to introduce some degree of conformational bias into the structures, a "turn" sequence, similar to the D-Pro-Gly sequence used in peptides,[36–38] was introduced into the identified binding motif of Sequence 10, Figure 3.12. A pair of extended glycine analogs with internal ethylene glycol groups (1PEG and 2PEG) were also incorporated to explore the effects of conformational flexibility further. The binding of each of the three structures was evaluated with UV-Vis, and indicated that all of them possessed a two-fold improvement in affinity over the parent peptoid (Sequence 10). The similarity of the measured dissociation constants suggested that the D-proline was the main contributor to the increased affinity, but more characterization would be necessary to determine the specific role of the moiety. For example, the simple extension of the backbone chain could also allow a better binding pocket to be formed and thus produce increased affinity.

3.6 Complex Characterization by NMR

Several Cr(VI) complexes have been structurally characterized,[12] and the interactions of peptoids with other metal ions (such as Zn^{2+}) have been studied.[17,19] However, these previously evaluated ligands bear little resemblance to peptoid Sequence 10 and therefore this complex

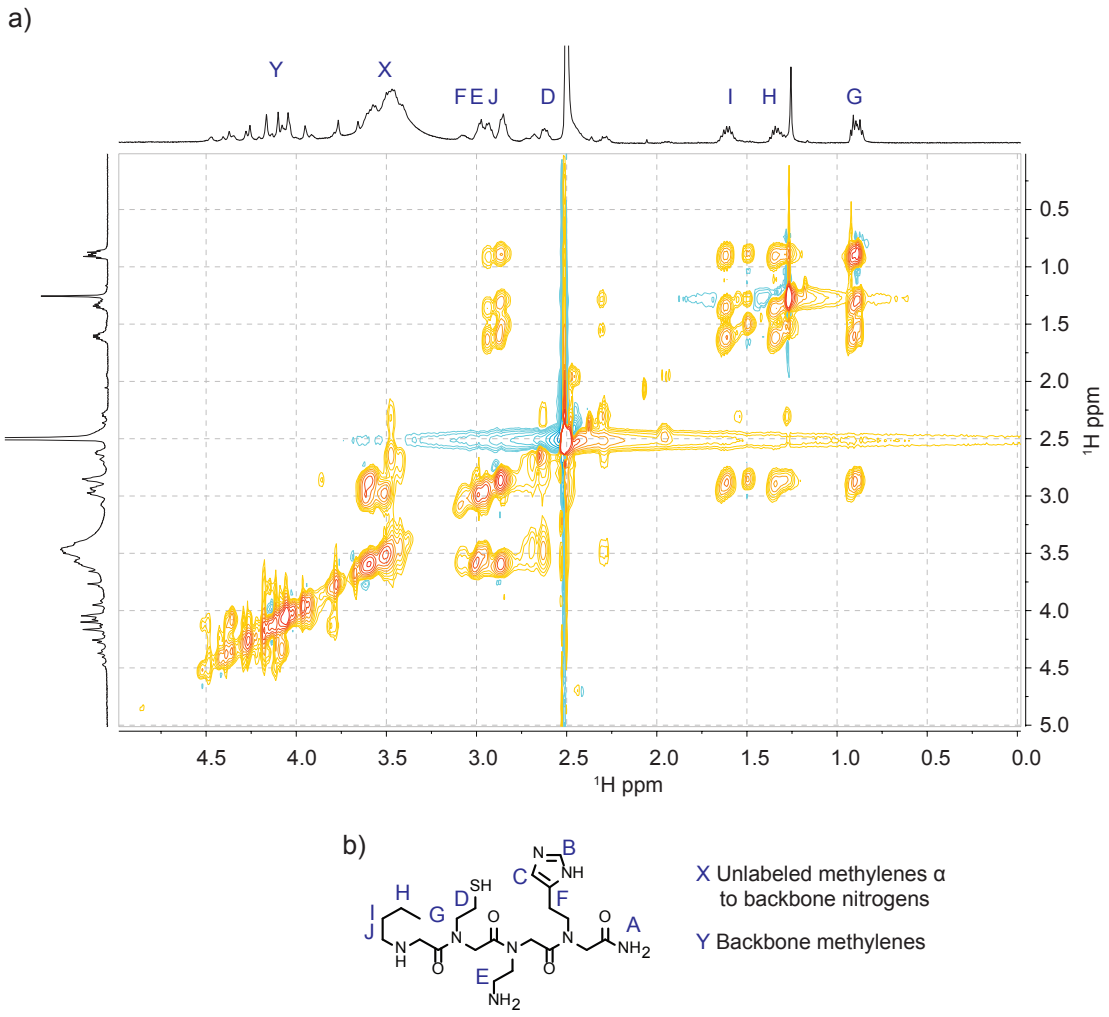

Figure 3.13. NMR characterization of Sequence 10 for the purpose of peak assignment (500 MHz, 60 °C). a) TOCSY spectrum. Peak annotation on top ^{1}H NMR spectrum. b) HSQC spectrum. (c) Key resonances appearing in the NMR spectra of Sequence 10 are annotated.

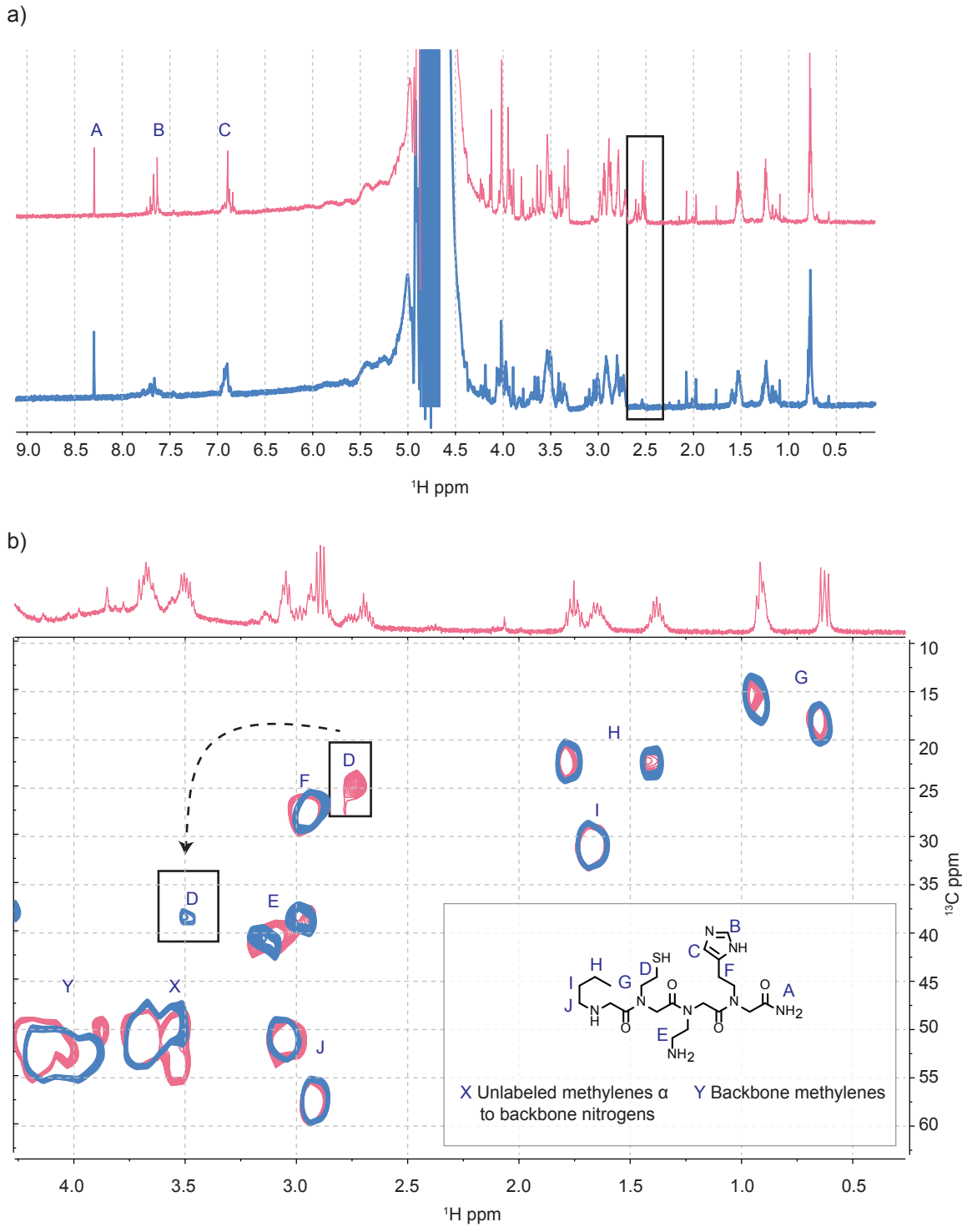

Figure 3.14. NMR characterization of sequence 10 binding $Cr(VI)_{aq}$. All spectra were obtained in 10 mM phosphate buffer (pH 7) with 10% D_2O. a) 1H NMR (900M Hz, 25 °C) spectrum of sequence 10 alone (pink) and in the presence of excess $Cr(VI)_{aq}$ (blue). b) Overlayed HSQC (500M Hz, 90 °C) spectra of sequence 10 alone (pink) and with excess $Cr(VI)_{aq}$ (blue). Key resonances appearing in the NMR spectra of sequence 10 are annotated.

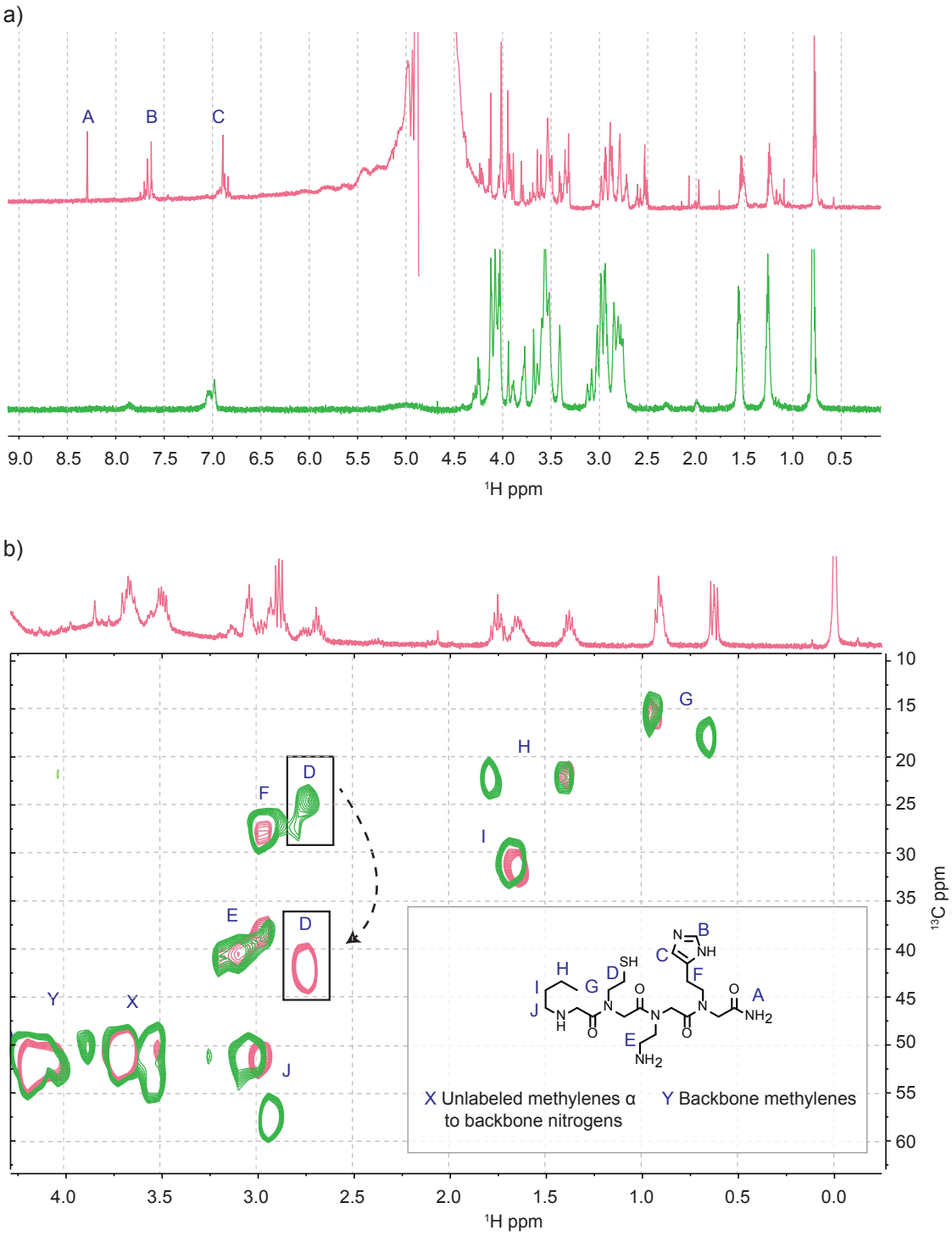

Figure 3.15. NMR characterization of sequence 10. All spectra were obtained in 10 mM phosphate buffer (pH 7) with 10% D_2O unless otherwise noted. a) ^1H NMR (900 MHz, 25 °C) spectrum of sequence 10 alone (green) and after disulfide formation (D_2O, pink). b) Overlayed HSQC spectra (500 MHz, 60 °C) of Sequence 10 alone (pink) and after disulfide formation (green). Key resonances appearing in the NMR spectra of Sequence 10 are annotated.

was characterized using NMR spectroscopy. Overall, the large number of conformers and overlapping signals in the ^{1}H-NMR spectrum of Sequence 10 severely limited interpretation of the backbone resonances (Figure 3.13). However, the spectrum revealed multiple singlets that clearly corresponded to the two aromatic protons of the imidazole group (resonances B and C in Figure 3.14a), as well as a distinct signal for the protons alpha to the thiol group (resonance D at 2.6 ppm). The latter assignment was confirmed by the shift of the resonance upon disulfide formation (Figure 3.15). An HSQC spectrum with fewer equivalents of $Cr(VI)_{aq}$ (approx. 0.4 equiv) was evaluated and that signal disappeared indicating ligand exchange on the NMR time scale (Figure 3.16). After the addition of $Cr(VI)_{aq}$ the imadazole peaks broadened, suggesting weak interactions with the chromate. In addition, the peak at 2.6 ppm shifted substantially, as would be expected if the thiol were directly involved in metal ion binding. Most notably, the peaks in the overall spectrum remained sharp, indicating that a diamagnetic Cr(VI) species was being bound and that minimal amounts of paramagnetic chromium ions (which would result if the ligand had been oxidized) were present.

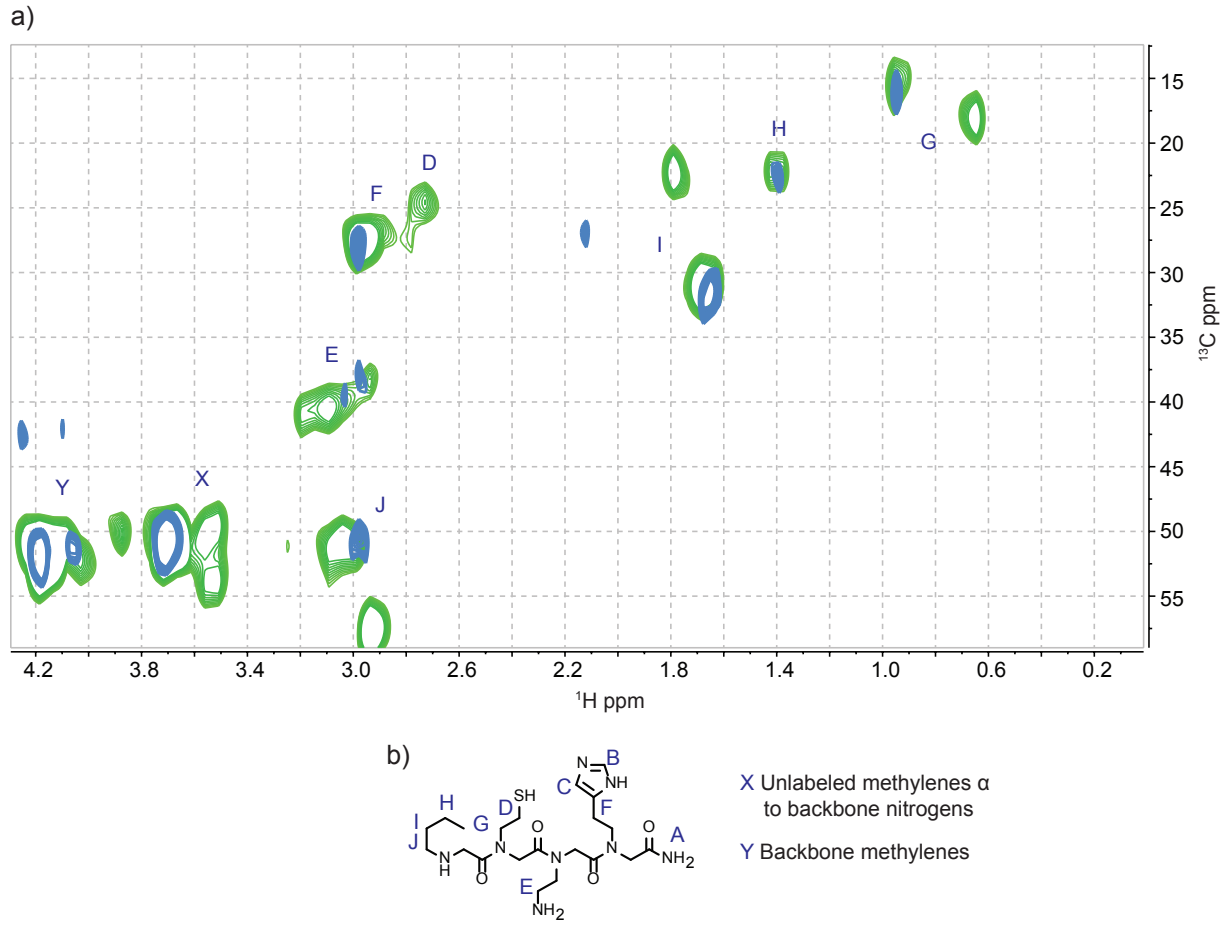

Figure 3.16. NMR characterization of Sequence 10 for the purpose of characterizing the complex formation equilibrium (500 MHz, 60 °C). a) Overlayed HSQC spectra (500 MHz, 60 °C) of Sequence 10 alone (green) and after disulfide formation (blue). b) Key resonances appearing in the NMR spectra of Sequence 10 are annotated.

A second round of high-temperature HSQC analysis was performed in phosphate buffer (10 mM, pH 7) for samples both with and without $Cr(VI)_{aq}$ (Figure 3.14). Analysis of the spectra showed that the methylene neighboring the thiol (Figure 3.14, signal D) had shifted from 2.6 ppm

to 3.5 ppm. The new peak position is similar to previously reported characterizations of thiol-Cr(VI) complexes.[39,40] Additionally, the formation of two equivalent peaks corresponding to the methylene alpha to the primary amine appeared upon addition of $Cr(VI)_{aq}$ (Figure 3.14, signal E). This could be due to differentiation of the two hydrogens upon the formation of a new chiral center when the terminal amine binds to the chromate, or due to stabilization of two different rotamers. Furthermore, shifts in the remaining methylenes that were alpha to the side chain nitrogens (Figure 3.14, signal X) and the backbone methylenes (Figure 3.14 signal Y) were also apparent, possibly due to a change in the shift of the methylene group beta to the thiol.

3.7 Chromium Depletion Assays

As the peptoid ligands were prepared on polymer supports, a convenient platform was already available for the selective solid phase extraction of $Cr(VI)_{aq}$ species from contaminated water sources. This ability was tested using water samples taken from Strawberry Creek (Berkeley, CA) and Ocean Beach (San Francisco, CA). Contamination was simulated by adding $Cr(VI)_{aq}$ to the samples at concentrations of 20 μM and 200 μM (1 ppm and 10 ppm). A third pair of chromium-containing samples was prepared using 10 mM phosphate buffer (pH 7) with the same $Cr(VI)_{aq}$ concentrations to evaluate metal ion removal under more controlled conditions. Sequence 10, the

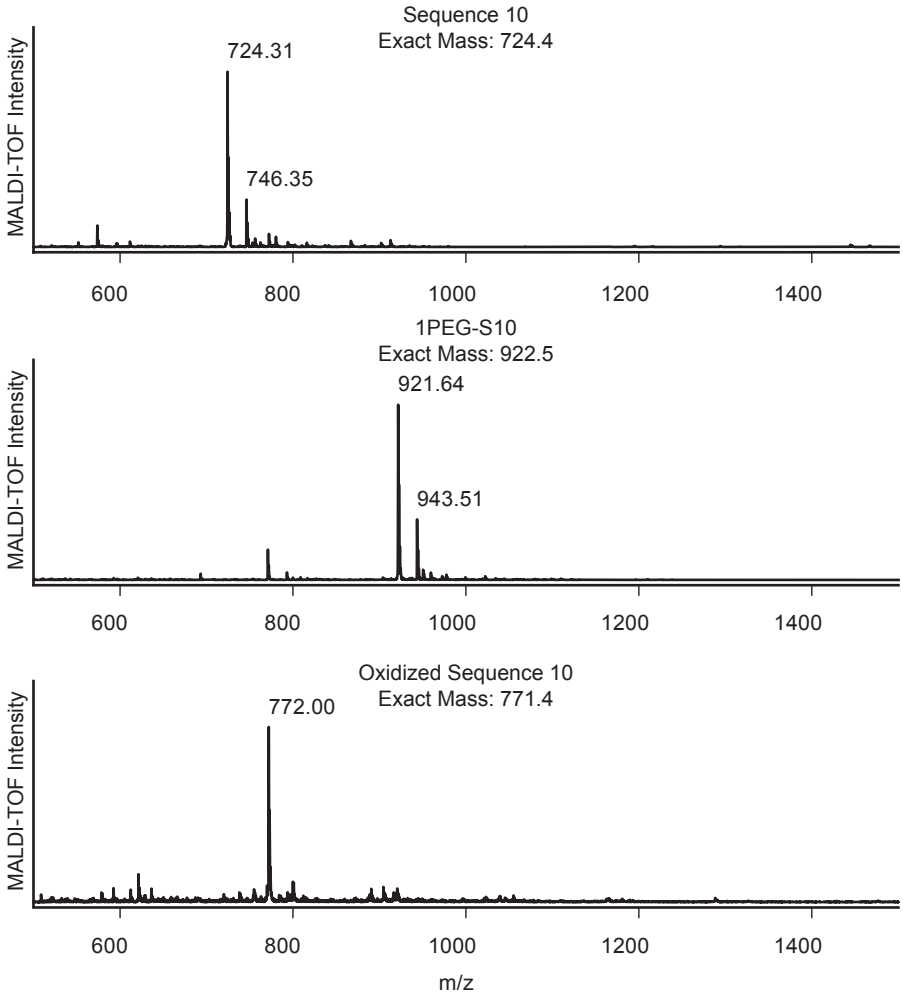

Figure 3.17. Characterization and evaluation of Sequence 10 for metal ion removal. An oxidized variant was also generated and tested. MALDI-TOF MS spectra confirming that the sequences were successfully synthesized.

highest affinity ligand of the identified sequences, and 1PEG-S10 (Sequence 10 with the D-Pro and 1PEG turn) were synthesized on water-compatible TentaGel beads. The sequence identities were again confirmed by photocleavage of a small portion of each resin, followed by MALDI-TOF MS (Figure 3.17). In addition to the Sequence 10 and 1PEG-S10 ligands, a commercially available anion-exchange resin, DOWEX Monosphere 550A, was evaluated for comparison. Each $_{resin}$ sample was incubated with each of the different contaminated solutions. The ligands were added in approximately 10-fold molar excess of the $Cr(VI)_{aq}$ in solution. After a 2 h incubation period, the

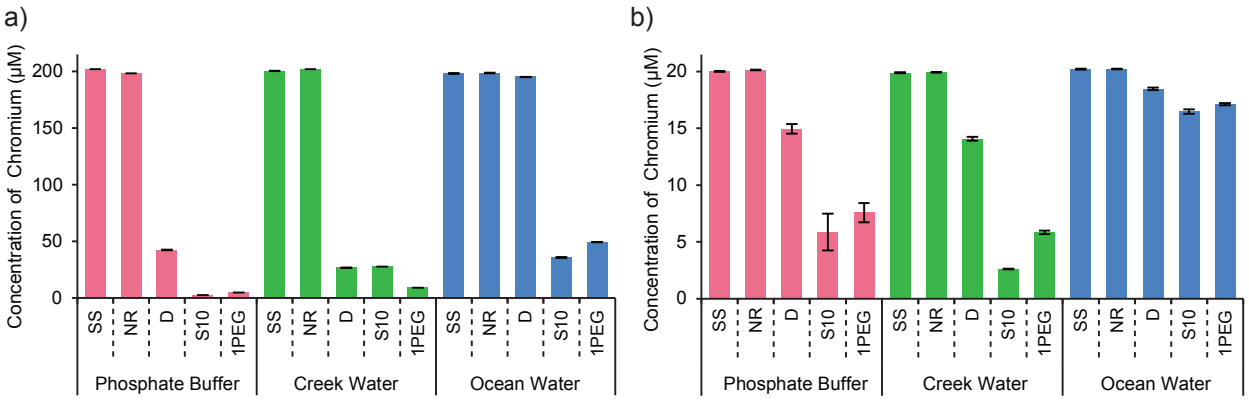

Figure 3.18. Use of peptoid ligands for the depletion of Cr(VI) species from environmental samples. After exposure to various resin samples, the supernatants were analyzed using ICP-OES with five replicates. The error bars represent the standard error of each sample set (n = 5). SS = starting solution, NR = no resin added, D = Dowex Monosphere 550A, S10 = Sequence 10, and 1PEG = 1PEG-S10. Data are shown for initial Cr(VI)aq concentrations of (a) 200 μM and (b) 20 μM.

concentration of chromium in the supernatant was measured using ICP-OES (Figure 3.18).

In nearly every solution, Sequence 10 and 1PEG-S10 were substantially more effective than the DOWEX resin for $Cr(VI)_{aq}$ removal. This effect was particularly evident as the ionic strength of the solution increased relative to the metal ion concentration, which was consistent with the selection criteria used in the binding screen. In many cases, the peptoid ligands reduced the metal ion concentrations to values close to the EPA limit for drinking water, 2 μM.[41] Even in the ocean water sample with 200 μM $Cr(VI)_{aq}$, where competing ions such as sodium and chloride are in ~10,000-fold excess, more than 80% of the chromium was removed. The remediation ability of Sequence 10 was inhibited only when the chromium concentration in the ocean water sample was reduced to 20 μM. Interestingly, the binding ability was still retained at 20 μM in the freshwater and phosphate buffer samples. In the Strawberry Creek water sample, the 1PEG-S10 ligand was more effective than Sequence 10 at 200 μM $Cr(VI)_{aq}$, which corresponds with its lower dissociation constant. However, as the ratio of chromium to other ions decreased in the 20 μM samples, Sequence 10 became more effective than 1PEG-S10. A possible explanation is the loss of some selectivity when the turn was incorporated. This observation reinforces the necessity of screening all of the ligands with an excess of competing ions to achieve maximum selectivity.

To remove the Cr(VI) from the beads in order to recycle the ligands, immobilized Sequence 10 bound to Cr(VI) was exposed to a reductant followed by an acid to remove the bound ion. Ethanol and dithionite were explored as reductants to convert Cr(VI) to Cr(III) and hydrochloric and acetic acids were added to protonate the ligands, freeing the metal ion from the resin. None of these initially seemed promising – after this treatment the ligands were only able to remove 50% of the $Cr(VI)_{aq}$ solution (Figure 3.19).

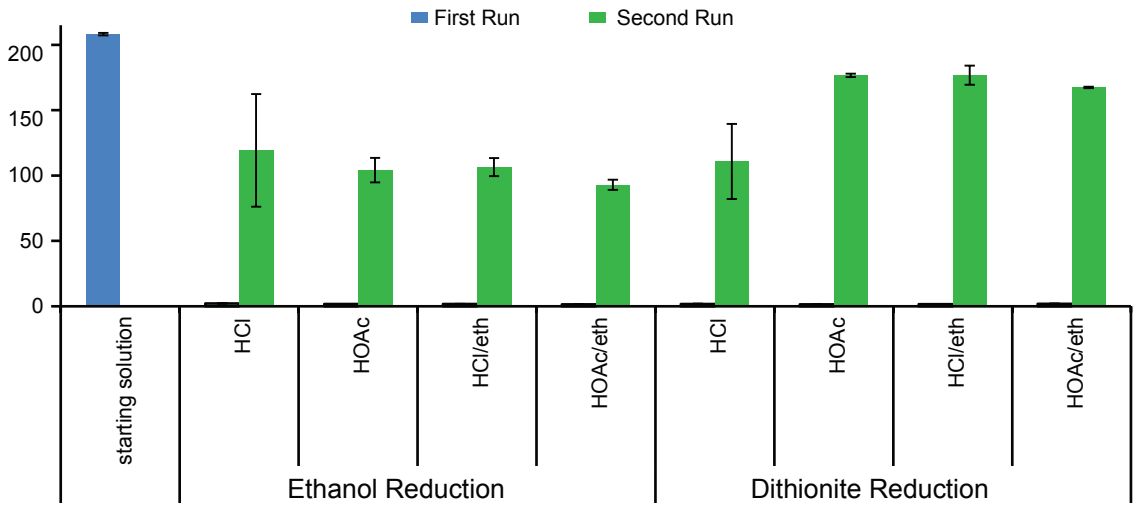

Figure 3.19. Following initial remediation of phosphate buffer containing $Cr(VI)_{aq}$ with immobilized Sequence 10, the resin was treated with ethanol or dithionite (10 eq) to reduce the Cr(VI) to Cr(III) and then treated with 1 M acid (HCl or HOAc) +/- 1% ethanol.

Final experiments sought to confirm our previous analysis of the binding moieties. The first task was to demonstrate that the thiol group, and not a sulfonate group produced through oxidation, was interacting with the Cr(VI) species. When Sequence 10 was pre-oxidized using sodium periodate (confirmed to produce the sulfonate group, as shown in Figure 3.20), the resulting beads were ineffective in removing the metal ions.

There are many other commercially available products that contain thiols and thioureas; however, our results clearly indicated that the additional components supplied by the peptoid significantly contribute to the binding. As further confirmation, we incubated the resin with solutions of chromium and glutathione, both at a concentration equal to that of the $Cr(VI)_{aq}$ and additionally at a 1:1 molar ratio with the peptoid (Figure 3.20). Our sequence retained its ability to remove more than 80% of the chromium in both solutions, reaffirming the increased effectiveness of the identified structure.

3.8 Conclusions

Through this work, we have developed a new platform for the identification of selective ligands using a combinatorial peptoid library. The chromium(VI) ligands that were identified provide some of the first examples of selective binders for this pollutant, and they demonstrate the promise of peptoid sequences as easily-prepared components of environmental remediation materials. Further improvements in binding affinity may be achievable through further exploration of the backbone structures, including the introduction of conformationally-restricted spacing groups. This strategy is currently being explored in ongoing studies. Moreover, the chromogenic screening method is likely to be successful for the identification of selective binders for a wide variety of different metal ions. We are currently applying this method to the discovery of new chelators for lanthanides, actinides, and other species that would benefit from the availability of new ligand structures.

3.9 Materials and Methods

General Procedures and Materials

Tentagel MB NH_2 Resin (140-170 μm, 0.3 mmol/g), used for library synthesis, was purchased from Rapp-Polymere (Tuebingen, Germany). Library synthesis steps were performed in fritted disposable chromatography columns (Bio-Rad, Hercules, CA). During the reactions, the resin suspensions were slowly rotated using a nutator (Fisher Scientific, USA). The photolinker (Fmoc-(*R*)-3-amino-3-(2-nitrophenyl)propionic acid) and Fmoc-6-aminohexanoic acid were purchased from Chem-Impex (Wood Dale, IL). The 1PEG ((2-(Fmoc-amino)ethoxy)acetic acid) and 2PEG ((2-(2-(Fmoc-amino)ethoxy)ethoxy)acetic acid) linkers were purchased from Iris Biotech GMBH (Marktredwitz, Germany). Water (dd-H_2O) used was deionized using a Barnstead NANOpure purification system (ThermoFisher, Waltham, MA). All other materials were purchased from commercial sources and used without further purification, except as noted below. All centrifugation was performed in a Galaxy Mini Star (VWR, USA), and lyophilization was performed using a LAB CONCO Freezone 4.5.

NMR Characterization

^1H spectra were obtained on a Bruker Biospin (900 MHz) spectrometer and high temperature ^1H and ^{13}C spectra were obtained on a Bruker DRX-500 (500MHz) spectrometer. Peaks were calibrated using a DSS (4,4-dimethyl-4-silapentane-1-sulfonic acid) standard and spectra were analyzed using TopSpin software. For 1D ^1H experiments, water was suppressed with excitation sculpting.[42] ^1H-^{13}C HSQC spectra were collected at 60 °C recorded with the hsqcetgp sequence provided by the manufacturer. A total of 128 scans were collected for 128 complex ^{13}C increments. The ^{13}C spectral width was set to 80 ppm and the carrier frequency was set to 46 ppm.

Library Synthesis

Of the seven amine monomers, piperonylamine, butylamine, and histamine were used as purchased and incorporated without protecting groups. The glycine and β-alanine monomers were purchased as hydrochloric acid salts with *t*-butyl ester protecting groups. Before use, these compounds were treated with a 1 M NaOH solution that was saturated with NaCl and extracted into a 15:85 v/v isopropanol-chloroform mixture. The organic layers were dried over sodium sulfate and concentrated to yield the monomers as the free bases. *N*-boc-ethylenediamine was purchased and used as received, and cysteamine was protected with a trityl group using a procedure reported by Maltese.[43] The ability of each amine to incorporate into a peptoid using the chemistry described below was verified by synthesizing pentamers with alternating benzylamine groups and test monomers.[25]

The library was synthesized on Tentagel MB NH_2 resin, which was initially swollen in dichloromethane (DCM). Standard Fmoc solid-phase synthesis (using HCTU as a coupling agent) was used to incorporate the first four members of the linker through amide bond formation. For the first variable position, the resin was split evenly into seven different fritted columns. Acylation and the addition of the first amine were performed according to the procedure developed by Zuckermann *et al.* for the incorporation of heterocyclic amines.[25] Briefly, for each acylation step a solution of chloroacetic acid (6.8 eq, 0.4 M) was prepared in dimethylformamide (DMF) in addition to a solution of diisopropylcarbodiimide (8 eq, 2 M) in DMF. The resin beads were exposed to both solutions with gentle agitation for 5 min. Following this, the acylation solution was removed via filtration and the resulting beads were rinsed with DMF. Next, the amines were added as 2 M solutions in DMF. After 2 h of gentle agitation at room temperature, the resin samples

were isolated via filtration and rinsed with DMF. All of the resin was then pooled and mixed in DCM for five minutes. Subsequently, the resin was isolated via filtration, vacuum dried, and split into a new set of 7 fritted columns. The acylation and amination steps were repeated three more times to add the remaining amines, with pooling and splitting between each round of monomer introduction. After the last amination step, the resin pools were recombined a final time. A 20% solution of 4-methylpiperidine in DMF was next added to each resin sample for 30 min to remove any acylation adducts on the imidazole groups. After isolation via filtration, the resin was rinsed with DMF. The protecting groups were removed by incubation with a cleavage solution (95:2.5:2.5) trifluoroacetic acid:water:triisopropylsilane) for 1.5 h. The resin was then rinsed with DCM, dried under vacuum, and stored at 4 °C until use.

Screening to Identify Selective Metal-Binding Sequences

To equilibrate the beads before the screen, a 40 mg portion of the resin (representing more than 8 times the size of the library to ensure inclusion of each sequence) was swelled in water overnight. The library aliquot was then incubated with the metal of interest (2 mM CrO_3 or 2 mM $Ni(OAc)_2$) in the screening buffer (1 M NaCl, 1 M $MgSO_4$, 20 mM $NaHCO_3$, pH 7) for 1 h. The library aliquot was then rinsed with three 1 mL portions of water (each with 15 min incubation) to remove any non-specifically bound ions.

For visualization and bead selection, the resin was transferred to a Petri dish. A number of the beads had taken on a distinct pale yellow color, but provided insufficient contrast for unambiguous identification. A 50-100 μL portion of the appropriate dye solution was then added to enhance the sensitivity. For chromium, a solution of 0.5 g of 1,5-diphenylcarbazide in 100 mL of acetone was used,[30] and for nickel, a solution of 1% (w/v) dimethylglyoxime in methanol[33] was applied. The volume of solution that was added was chosen such that the solvent would rapidly evaporate from the Petri dish, trapping the dye and the metal within the individual beads. After 15 min, the Petri dish was examined using a Leica S6D Microscope (Leica, Germany) equipped with a Moticam 2300 3.0 MP camera and Micromanager Software[44] for capturing images. The individual beads with the most intense colors were selected for ligand identification.

Metal Ion Removal and Photocleavage

The removal of the metal ions was found to be essential before usable MALDI-TOF MS sequencing data could be obtained. This was done by combining the selected beads on top of the membrane of a 0.5 mL 0.2 μm centrifugal filter unit (Millipore, Billerica, MA). A mixture of Amberlite cation (Na^+ form, 0.5 mg) and anion (Cl^- form, 0.5 mg) exchange resins was then added to the filtrate collection tube of the centrifugal filter unit. The filter and the collection tube were then filled with 1 M HCl (several concentrations were screened to optimize ion removal). This setup was incubated with gentle agitation on a nutator for 2 h, allowing diffusion to occur through the 0.2 μm filter. The Amberlite beads and acidic solution in the lower collection tube were removed, and the solution in the filter unit was removed by brief centrifugation. Water (500 μL) was added to the filter unit, and the unit was gently agitated on a nutator for 15 min. The water was then removed by centrifugation. This process was repeated twice to ensure that the residual HCl had been rinsed from the beads.

The beads bearing hit sequences were removed from the filter unit and once again placed in a Petri dish using ethanol (approx. 500 μL). The individual beads were captured using a pipet and placed into individual 0.6 mL Posi-Click tubes (Denville Scientific, South Plainfield, NJ). The volume in

each tube was brought to 5 μL with absolute ethanol. To cleave the peptoids from single resin beads, the tubes were placed in a computer controlled ICH-2 photoreactor with UVA bulbs (Luzchem, Ottawa, Canada) for 8 h (various incubation times were screened). For characterization of bulk samples of resin, photocleavage time was limited to 10 min.

Single Bead Sequencing

After photocleavage, the ethanol was evaporated and replaced with 1:1 water:acetonitrile containing tris(2-carboxyethyl)phosphine (0.5 mM). The sample (0.5 μL) was mixed with matrix solution (0.5 μL, 5 mg α-cyano-4-hydroxycinnamic acid in 1:1 water:acetonitrile with 0.1% trifluoroacetic acid and 0.6 M ammonium phosphate) and spotted directly on a stainless steel MALDI plate. MALDI-TOF MS (Voyager-DE instrument, Applied Biosystems) was used to identify the mass of each selected sequence, and MALDI-TOF-TOF MS/MS (AB Sciex TF4800, Applied Biosystems) was used to fragment the peptoids for sequencing.

Binding Constant Evaluation via UV-vis Titration

Each of the identified sequences was prepared using the protocols described for library synthesis with Fmoc-Rink Amide MBHA resin (Anaspec, Fremont, CA) in place of the Tentagel MB NH2 resin. The initial fluorenylmethyloxycarbonyl (Fmoc) group was removed with 20% 4-methylpiperidine in DMF. To insert the linker and proline monomers into the peptoid backbone (Figure 3.12), solutions of the linker (20 eq, 0.6 mM in DMF) and diisopropylcarbodiimide (19 eq, 3.2 mM in DMF) were incubated with the resin for 30 min with gentle agitation. The proline was attached using standard solid-phase peptide synthesis (with HCTU as the coupling agent), after which the standard peptoid synthesis procedure was resumed to couple the remaining amines. The acylated N-terminus of Ac-sequence 10 (for use in Figure 3.11) was incorporated by the addition of acetic anhydride (50 eq) and DIPEA (50 eq) for 30 min. Following synthesis, a cleavage cocktail (95:2.5:2.5 trifluoroacetic acid:water:triisopropylsilane) was used to remove the peptoids from the resin, while also removing the protecting groups from the monomers. After evaporating the trifluoroacetic acid, the peptoids were precipitated from ether. The resulting precipitates were resuspended in water and purified using reversed phase chromatography on a semi-preparatory scale HPLC column (Agilent). The isolated fractions were concentrated using a speed vacuum (Labconoco, USA) and then lyophilized. The resulting sequences were stored dry at -20 °C before use in order to minimize disulfide formation. HPLC and MALDI-TOF MS characterizations of the purified peptoids appear in Figure 3.5.

For each binding constant determination, a control titration with $Cr(VI)_{aq}$ was performed using the sample buffer on the same day of the experiment. A 25 mM or 5 mM solution of CrO_3 was then added in 0.1, 0.2, and 0.6 μL increments to each peptoid sample (300 or 150 μM, 90 μL). The absorbance spectrum was measured at each increment using a Cary 50 spectrophotometer (Varian). In order to obtain a spectrum specific to the complex, the control titration was subtracted from the experimental titration at each set of concentrations. The maximum absorbance of the peptoid-metal complex was determined to be at 457 nm, and the absorbance was plotted against the concentration of chromium and fit to a logistic binding curve using Origin software. The model used to fit the data is displayed in Equation 1, where A_1 and A_2 are the asymptotes of the data, p correlates to the slope of the curve, and x_0 is the inflection point used to approximate the dissociation constant.

$$y=(A_1-A_2)/(1+x/x_0)^p+A_2$$

Equation 1

Chromium Depletion Analysis with ICP-OES

Water samples were collected from Strawberry Creek (Berkeley, CA, Latitude: 37.871052, Latitude: -122.257214) and Ocean Beach (San Francisco, CA, Latitude: 37.760232, Latitude: -122.512227). An appropriate amount of CrO_3 was added in order to simulate chromium contamination at concentrations of 20 μM and 200 μM. To prepare a separate set of solutions under more controlled conditions, CrO_3 was added to phosphate buffer (10 mM, pH 7) at concentrations of 20 μM and 200 μM.

To evaluate the ability of sequence 10 and 1PEG-S10 to remove the chromium from the contaminated samples, the sequences were synthesized on Tentagel MB NH2 (0.3 mmol/g) using the procedures described in the "library synthesis" section. A photolinker and two aminohexanoic acid residues were used to link the peptoid structures to the resin. The sequence identities were confirmed via MALDI-TOF MS after photocleavage of a bulk sample (approx. 1 mg) in ethanol (50 μL) using a computer-controlled ICH-2 photoreactor with UVA bulbs (Luzchem, Ottawa, Canada) for 10 min. Assuming 100% modification of the resin, the sequences were added to each chromium-containing solution such that the ligands were in a ten-fold molar excess to the chromium ions. A commercially available anion exchange resin, DOWEX Monosphere 550A (1.0 meq/mL by wetted bed volume, Sigma Aldrich, USA), was compared at the same ratio to the metal ions. All depletion experiments were run as a series of 5 experimental replicates. For the 200 μM samples, 0.75 mL portions of the solution were incubated with the sequences synthesized on Tentagel MB NH2 (5 mg) and the DOWEX 550A (0.7 mg). The same amount of resin was incubated with 7.5 mL portions of solution for the 20 μM samples. Each solution was exposed to each type of resin for 2 h. Following this, a sample of the supernatant was removed and diluted with nitric acid to make a final solution of 2% HNO_3. The concentration of chromium in those samples, each measured in triplicate, was determined with a Perkin Elmer 5300 DV optical emission ICP using scandium as an internal standard. For the ocean water samples, standards were made with comparable salt concentrations.

The oxidized sequence 10 sample was synthesized by exposing beads bearing sequence 10 to sodium periodate (10 eq) in water for 10 min. The beads immediately turned darker yellow. The mass of the resulting sulfonate ligand was confirmed using MALDI-TOF MS following photocleavage (Figure 3.17).

3.7 References

1. Booker, S. & Pellerin, C. Reflections on hexavalent chromium. *Environ. Health Perspect.* **108,** 402–7 (2000).

2. Sharma, P. *et al.* Groundwater contaminated with hexavalent chromium [Cr (VI)]: a health survey and clinical examination of community inhabitants (Kanpur, India). *PLoS One* **7,** e47877 (2012).

3. Saha, R., Nandi, R. & Saha, B. Sources and toxicity of hexavalent chromium. *J. Coord.*

Chem. **64,** 1782–806 (2011).

4. Owlad, M., Aroua, M. K., Daud, W. A. W. & Baroutian, S. Removal of Hexavalent Chromium-Contaminated Water and Wastewater: A Review. *Water. Air. Soil Pollut.* **200,** 59–77 (2008).

5. Roundhill, D. M. & Koch, H. F. Methods and techniques for the selective extraction and recovery of oxoanions. *Chem. Soc. Rev.* **31,** 60–7 (2002).

6. Hernandez-Ramirez, O. & Holmes, S. M. Novel and modified materials for wastewater treatment applications. *J. Mater. Chem.* **18,** 2751 (2008).

7. Walkup, G. K., Burdette, S. C., Lippard, S. J. & Tsien, R. Y. A New Cell-Permeable Fluorescent Probe for Zn^{2+}. *J. Am. Chem. Soc.* **2000**, 5644–5 (2000).

8. Radford, R. J. & Lippard, S. J. Chelators for investigating zinc metalloneurochemistry. *Curr. Opin. Chem. Biol.* **17,** 1–8 (2013).

9. Nitz, M., Franz, K. J., Maglathlin, R. L. & Imperiali, B. A Powerful Combinatorial Screen to Identify High-Affinity Terbium (III)-Binding Peptides. *ChemBioChem* **4,** 272–6 (2003).

10. Martin, L. J., Sculimbrene, B. R., Nitz, M. & Imperiali, B. Rapid Combinatorial Screening of Peptide Libraries for the Selection of Lanthanide-Binding Tags (LBTs). *QSAR Comb. Sci.* **24,** 1149–1157 (2005).

11. Zeng, L., Miller, E. W., Pralle, A., Isacoff, E. Y. & Chang, C. J. A selective turn-on fluorescent sensor for imaging copper in living cells. *J. Am. Chem. Soc.* **128,** 10–1 (2006).

12. Cieślak-Golonka, M. & Daszkiewicz, M. Coordination geometry of Cr(VI) species: Structural and spectroscopic characteristics. *Coord. Chem. Rev.* **249,** 2391–407 (2005).

13. Francis, M. B., Jamison, T. F. & Jacobsen, E. Combinatorial libraries of transition-metal complexes, catalysts and materials. *Curr. Opin. Chem. Biol.* **2,** 422–8 (1998).

14. Pirrung, M. C., Park, K. & Tumey, L. N. 19F-encoded combinatorial libraries: discovery of selective metal binding and catalytic peptoids. *J. Comb.Chem.* **4,** 329–44 (2002).

15. Simon, R. J. *et al.* Peptoids: a modular approach to drug discovery. *Proc. Natl. Acad. Sci. U. S. A.* **89,** 9367–71 (1992).

16. Sun, J. & Zuckermann, R. N. Peptoid polymers: a highly designable bioinspired material. *ACS Nano* **7,** 4715–32 (2013).

17. Lee, B.-C., Chu, T. K., Dill, K. a & Zuckermann, R. N. Biomimetic nanostructures: creating a high-affinity zinc-binding site in a folded nonbiological polymer. *J. Am. Chem. Soc.* **130,** 8847–55 (2008).

18. Maayan, G., Ward, M. D. & Kirshenbaum, K. Metallopeptoids. *Chem. Commun.* 56–8 (2009).

19. Izzo, I. *et al*. Structural Effects of Proline Substitution and Metal Binding on Hexameric Cyclic Peptoids. *Org. Lett.* **15** 598-601 (2013).

20. Brown, B. B., Wagner, D. S. & Geysen, H. M. A single-bead decode strategy using electrospray ionization mass spectrometry and a new photolabile linker: 3-amino-3-(2-nitrophenyl)propionic acid. *Mol. Divers.* **1,** 4–12 (1995).

21. Franz, A. H., Liu, R., Song, A., Lam, K. S. & Lebrilla, C. B. High-throughput one-bead-one-compound approach to peptide-encoded combinatorial libraries: MALDI-MS analysis of single TentaGel beads. *J. Comb. Chem.* **5,** 125–37 (2003).

22. Paulick, M. G. *et al.* Cleavable hydrophilic linker for one-bead-one-compound sequencing of oligomer libraries by tandem mass spectrometry. *J. Comb. Chem.* **8,** 417–26 (2006).

23. Witus, L. S. *et al.* Identification of highly reactive sequences for PLP-mediated bioconjugation using a combinatorial peptide library. *J. Am. Chem. Soc.* **132,** 16812–7 (2010).

24. Zuckermann, R. N., Kerr, J. M., Kent, S. B. H. & Moos, W. H. Efficient method for the preparation of peptoids [oligo(N-substituted glycines)] by submonomer solid-phase synthesis. *J. Am. Chem. Soc.* **114,** 10646–7 (1992).

25. Burkoth, T. S., Fafarman, A. T., Charych, D. H., Connolly, M. D. & Zuckermann, R. N. Incorporation of unprotected heterocyclic side chains into peptoid oligomers via solid-phase submonomer synthesis. *J. Am. Chem. Soc.* **125,** 8841–5 (2003).

26. Figliozzi, G., Goldsmith, R. & Ng, S. Synthesis of N-substituted glycine peptoid libraries. *Methods Enzymol.* **267,** 437–47 (1996).

27. Lam, K. S. *et al.* A new type of synthetic peptide library for identifying ligand-binding activity. *Nature* **354,** 82–4 (1991).

28. Lam, K. S., Lebl, M. & Krchnák, V. The 'One-Bead-One-Compound' Combinatorial Library Method. *Chem. Rev.* **97,** 411–48 (1997).

29. Kotaś, J. & Stasicka, Z. Chromium occurrence in the environment and methods of its speciation. *Environ. Pollut.* **107,** 263–83 (2000).

30. Pflaum, R. T. & Howick, L. C. The Chromium-Diphenylcarbazide Reaction. *J. Am. Chem. Soc.* **78,** 4862–6 (1956).

31. Francis, M.B., Finney, Nathaniel S., Jacobsen, E. N. Combinatorial approach to the discovery of novel coordination complexes. *J. Am. Chem. Soc.* **118,** 8983–4 (1996).

32. Willems, G. J., Blaton, N. M., Peeters, O. M. & De Ranter, C. J. The interaction of chromium (VI), chromium (III) and chromium (II) with diphenylcarbazide, diphenylcarbazone and diphenylcarbadiazone. *Anal. Chim. Acta* **88,** 345–52 (1977).

33. Godycki, L. E. & Rundle, R. E. The structure of nickel dimethylglyoxime. *Acta Crystallogr.*

6, 487–495 (1953).

34. Levina, A. & Lay, P. A. Solution structures of chromium(VI) complexes with glutathione and model thiols. *Inorg. Chem.* **43,** 324–35 (2004).

35. Adecboyeca, M. & Olatnb, M. B. Metal-ion oxidations in solution. Part XV1II.l Characterization, rates, and mechanism of formation of the intermediates in the oxidation of thiols by chromium(V1). *Can. J. Chem.* 55, 3328-34 (1977).

36. Haque, Tasir S, Little, Jennifer C., Gellman, S. H. ' Mirror Image ' Reverse Turns Promote ß-Hairpin Formation. *J. Am. Chem. Soc.* **116,** 4105–6 (1994).

37. Haque, T. S., Little, J. C. & Gellman, S. H. Stereochemical Requirements for ß-Hairpin Formation: Model Studies with Four-Residue Peptides and Depsipeptides. *J. Am. Chem. Soc.* **118,** 6975–6985 (1996).

38. Venkatraman, J., Shankaramma, S. C. & Balaram, P. Design of folded peptides. *Chem. Rev.* **101,** 3131–52 (2001).

39. Brauer, S. & Wetterhahn, K. Chromium (VI) forms a thiolate complex with glutathione. *J. Am. Chem. Soc.* 3001–7 (1991).

40. Brauer, S. & Hneihen, A. Chromium (VI) forms thiolate complexes with γ-glutamylcysteine, N-acetylcysteine, cysteine, and the methyl ester of N-acetylcysteine. *Inorg. Chem* 373–81 (1996).

41. Environmental Protection Agency. Chromium in Drinking Water. (2012). at <http://water.epa.gov/drink/info/chromium/#one>

42. Hwang, T. & Shaka, A. Water suppression that works. Excitation sculpting using arbitrary wave-forms and pulsed-field gradients. *J. Magn. Reson. Ser. A* **112,** 275–9 (1995).

43. Maltese, M. Reductive demercuration in deprotection of trityl thioethers, trityl amines, and trityl ethers. *J. Org. Chem.* **66,** 7615–25 (2001).

44. Edelstein, A., Amodaj, N., Hoover, K., Vale, R. & Stuurman, N. Computer control of microscopes using μManager. *Curr. Protoc. Mol. Biol.* **Chapter 14,** Unit 14.20 (2010).

Chapter 4

Removal of Nickel and Cadmium from Biological Media

Abstract:

The balance of metal ions in biological systems is critical to their function, but this balance is poorly understood and therefore designing therapeutics to target individual metal ions is a challenge. In this chapter two targets will be highlighted: (1) selectively binding nickel as a tuberculosis treatment and (2) the treatment of cadmium poisoning. Our work studying tuberculosis has been in collaboration with Prof. Deborah Hung (Broad Institute of MIT and Harvard) who has identified an aminothiazole molecule that can treat active and latent strains of *Mycobacterium tuberculosis*. We characterized the binding to transition metal ions and identified a ligand that can bind to nickel selectively in the presence of relevant ions and biomolecules in human serum. Cadmium poisoning was chosen as the second target as it poses a serious health concern due to cadmium's increasing industrial use, yet there is currently no recommended treatment. The selective coordination of cadmium in a biological environment—i.e. in the presence of serum ions, small molecules, and proteins—is a difficult task. To address these challenges, a combinatorial library of peptoid-based ligands has been evaluated to identify structures that selectively bind to nickel and cadmium in human serum with minimal chelation of essential metal ions. Ligands were identified in this screening procedure, and the binding affinity of each was measured using metal titrations monitored by UV-vis spectroscopy. The cadmium binding ligands were characterized by NMR spectroscopy and in depletion assays. In one of these depletion experiments, the peptoid sequence was able to deplete the cadmium to a level comparable to the reported acute toxicity limit. Evaluation of the metal selectivity in buffered solution and in human serum was performed to verify minimal off-target binding. These studies highlight a screening platform for the identification of metal-ligands that are capable of binding in a complex environment. This additionally demonstrates the potential utility of biologically-compatible ligands for the treatment of heavy metal poisoning.

This chapter contains data from the publication in *Chemical Science* entitled "Development of Peptoid-Based Ligands for the Removal of Cadmium from Biological Media."

4.1 Targeting tuberculosis

In 2013, 1.5 million people died from tuberculosis and 9 million people contracted the disease.[1] Drug resistance is a significant hurdle in the development of effective therapeutic strategies. To develop small molecule inhibitors that have unique therapeutic targets, the Hung group has applied a high-throughput screening strategy.[2,3] Their whole-cell screening strategy is designed to improve the fraction of relevant hits discovered in the screening process by effectively mimicking the natural biological environment.[2] Their recent work identified a panel of inhibitors that target both replicating and non-replicating *M. tuberculosis*.[3] Experimental evidence indicated that after treatment with an aminothiazole-based inhibitor identified from the screen (Figure 4.1) bacterial growth could be restored upon the addition nickel or cobalt. Though there is no current evidence that *M. tuberculosis* uses nickel dependent enzymes, there is evidence of nickel dependent enzymes in a variety of bacteria.[4] To confirm the binding of the aminothiazole compound to cobalt and nickel, we performed titrations of both nickel and cobalt into the aminothiazole (3:1 water:methanol) and monitored complex formation using UV-vis. (Figure 4.1a). Dissociation constants were calculated by fitting these data, and a slightly higher affinity was measured for cobalt (K_d = 29 μM) than nickel (K_d = 36 μM). However, no affinity was measured for other biologically relevant ions (Mn^{2+} and Fe^{2+}). In this chapter the identification of ligands selective for nickel binding over other relevant ions, including cobalt, is described. Expanding on a previously developed combinatorial platform,[5] a screen was completed in a serum-like environment. The selectivity of the ligands of interest are explored through titrations in buffer as well as a biological medium, demonstrating the significant potential of this platform in identifying ligands with application relevant selectivity.

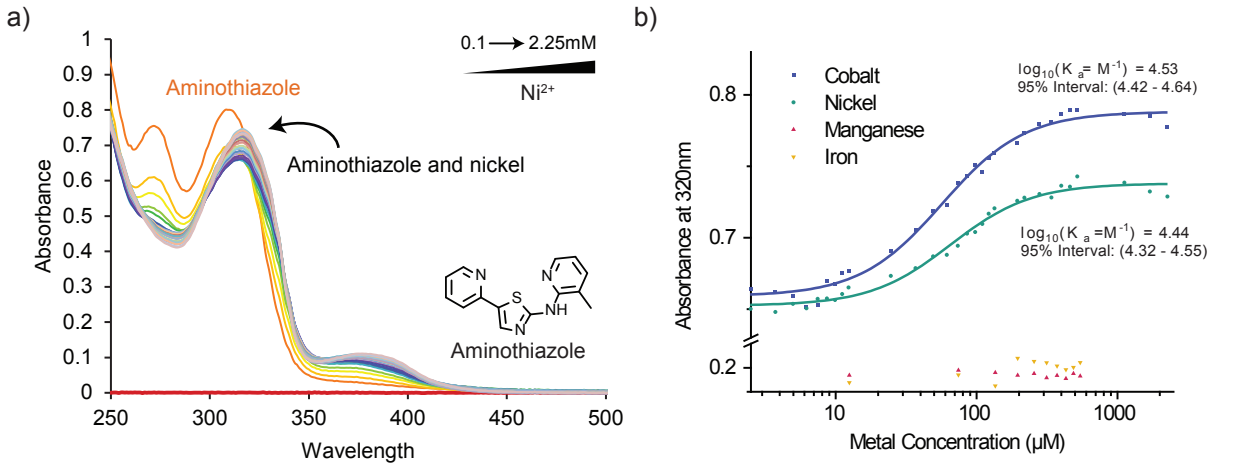

Figure 4.1. An aminothiazole compound identified by the Hung group to have antitubercular activity was determined to have reduced potency in the presence of additional nickel and cobalt. a) Representative titration of $Ni(OAc)_2$ into the aminothiazole (50 μM in 25% MeOH, 75% ddH_2O). The concentrations of Ni(II) ranged from 0.1 mM to 2.25 mM. b) Binding of $Ni(OAc)_2$and $Co(OAc)_2$ to the aminothiazole was quantified. Negligable binding to Mn(II) and Fe(II) was observed.

4.2 Cadmium poisoning

For the past fifty years it has been well established that cadmium is hazardous to human health, but the industrial use of this metal has continued to increase world-wide.[6] Cadmium exposure leads to a particularly problematic form of heavy metal poisoning due to the lack of current treatment options.[7] Cadmium has been identified by the International Agency for Cancer as a group-1 carcinogen, and it is listed by the Environmental Protection Agency as one of 126 priority pollutants.[8] Despite this toxicity being well accepted, it is not fully understood how

cadmium interacts with biological molecules to produce these deleterious effects.[9] One current hypothesis reports that Cd^{2+} can interfere with DNA repair and protein function, and that it can mediate the production of reactive oxygen species despite not acting directly as an oxidant.[9–11] Two biological molecules, metallothionein proteins and glutathione, can aid in the clearance of Cd^{2+}. Unfortunately, metallothioneins can increase the circulation time of cadmium ions,[12] and the glutathione depletion can have debilitating effects on cells, potentially including the observed oxidative stress responses.[13]

Evolution does not appear to have provided a strategy for clearing Cd^{2+}, and unfortunately there is also no therapeutic solution to cadmium poisoning. Chelation therapy has been proven to be beneficial for some heavy metals including lead and mercury, and has become the mainstay of treatment for acute poisoning with these metals.[14] Simple small molecules, including EDTA, dimercaptosucininc acid, and 2,3-dimercaprol, are commonly used for these purposes. One major concern with the administration of chelation therapy is that despite the increased affinity of many small molecule chelators for their heavy metal targets, the significant excess of other biological ions makes ions such as Ca^{2+} their primary target. This leads to a variety of hazardous side effects.[15] There exists a clear need for non-toxic ligands with selective affinity for cadmium that could be introduced as a chelation therapy alternatives. Additionally, such ligands could be integrated into other blood treatment strategies, such as dialysis platforms.

Selective chelation of Cd^{2+} in blood is a considerable challenge due to the significant excess of competing ions and small molecule and protein chelators, including serum small molecules and proteins. The rational design of a ligand for this application is particularly difficult due to the chemical similarity between Cd^{2+} and biologically essential Zn^{2+}. Peptide-based combinatorial approaches have been demonstrated to successfully identify ligands as catalysts and metal tags,[16–19] and pioneering work on peptide-based synthetic ionophores was completed by W.C. Still.[20] However, peptoids, or *N*-substituted glycine oligomers,[21] offer distinct advantages for the treatment of cadmium poisoning. The ability of these peptidomimetics to access unique conformations and the variety of available monomers make peptoids particularly valuable as ligands, and their metal binding capacity has been recently demonstrated.[5,22–25] Additionally, their improved *in vivo* stability provide exceptional advantages for a therapeutic application.[26–28] In this work, we have developed an expanded peptoid-based library and used it to identify multiple ligands with the ability to bind Cd^{2+} in human serum. One of these structures was found to reduce the concentration of Cd^{2+} to a level comparable with the reported limit of acute toxicity.[29] These studies therefore reinforce the unique capabilities of peptoid-based ligands through the development of structures with unparalleled ion-selectivity in a particularly complex biological medium.

4.3 Library Design and Synthesis.

To approach the challenge of developing a high affinity ligand that can bind to cadmium and nickel in the complex medium of human blood, we synthesized a peptoid-based library designed to decrease the number of available conformations and form a binding "pocket."[30] In our previous work, a peptoid tetramer was synthesized and demonstrated to have the potential for selective binding; additionally it was discovered that the incorporation of a D-proline-based turn increased the metal affinity of the ligand.[5] Based on this observation a library incorporating D-proline and three turn motifs (Glycine, 1PEG, and 2PEG) was designed (Figure 4.2), with the objective of discovering higher affinity and more selective structures. The library members were synthesized on 140-170 μm PEG-grafted polystyrene resin, which is compatible with both organic solvents and water for the synthesis and screening steps, respectively. The first residue incorporated was a photocleavable moiety to allow for cleavage and sequence identification using MALDI-TOF MS/MS. This residue and the following three linker residues were added using standard solid-phase peptide chemistry.

Previously, a residue with an isotopic tag ($^{79}Br/^{81}Br$) was included to uniquely identify library member mass signals; however, due to the decreased signal-to-noise ratio we chose not to include this residue for this screen. To increase the mass of the cleaved structures and the distance between the ligands and the resin, three aminohexanoic acid residues were combined to form a linker. The ligand itself was synthesized using a combination of the submonomer method of peptoid synthesis[31] with chloroacetic acid to allow incorporation of heterocyclic side chains[32] and standard Fmoc-peptide synthesis. Split-and-pool synthesis was used to create a library of 7203 members. Adducts between the histamine and chloroacetic acid were cleaved with 4-methylpiperidine[32] and acid labile protecting groups on the monomers were cleaved with trifluoroacetic acid.

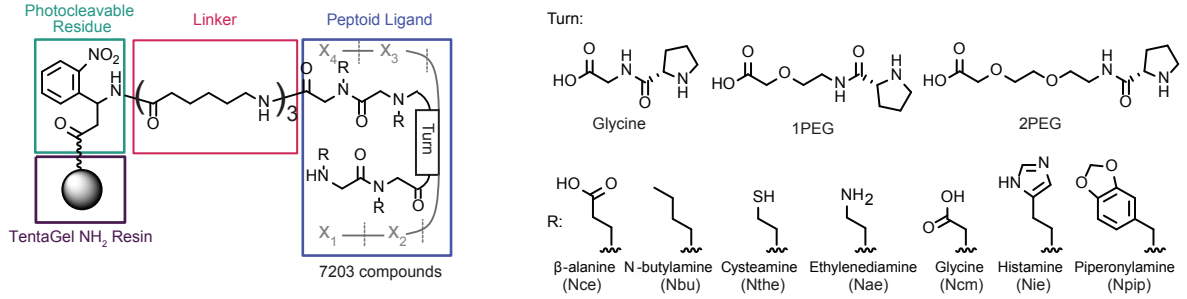

Figure 4.2. Peptoid library schematic. The diagram depicts the photocleavable residue, linker, and peptoid ligand structure with variable positions represented as "X_n" and "Turn". The seven "R" residues were incorporated into each of the four peptoid positions, and the three D-Proline based turns were incorporated into the "Turn" position. The overall library consists of 7203 compounds.

4.4 Screening for Selective Cadmium and Nickel Affinity

To identify ligands that could bind nickel or cadmium in the presence of the proteins, small molecules, and other ions in human serum, a screening medium that contained reproducible concentrations of these components was designed. A serum replacement, intended as a media supplement for mammalian cell culture, was obtained from Life Technologies. Excess biologically relevant transition metals (Fe^{2+}, Mn^{2+}, Zn^{2+}), typically present in high concentrations or unbound in serum,[33,34] were considered to be the main competing ions; these were added to the serum replacement (2.5 mM each) in addition to Cd^{2+} or Ni^{2+} (250 μM). An outline of the screening procedure with cadmium is shown in Figure 4.3. A library aliquot pre-swelled in water was exposed to this screening medium for 1-4 h before being isolated via filtration and rinsed with water. Cadmium typically forms colorless complexes; therefore, to identify complexed ligands, a commercially available dye that forms a pink complex with cadmium was applied. The dye was applied in ethanol, which after evaporation left the metal and cadion dye[35,36] trapped within the bead. The cadion dye is yellow in water and blue in ethanol, leading to the yellow, blue, and green beads apparent in Figure 4.3. However, the pink color only occurs with the complexation of cadmium

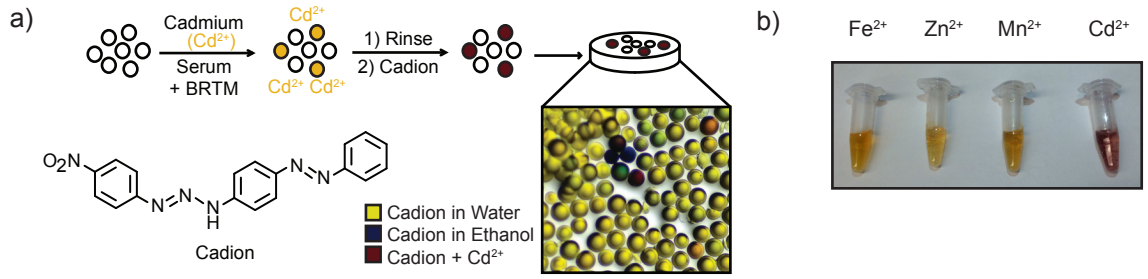

Figure 4.3. a) An outline of the screening procedure is shown with a representative photograph of the library members after the staining procedure. The screening medium included serum replacement, added transition metal ions found in blood (BRTM - Fe^{2+}, Mn^{2+}, and Zn^{2+}, 250 μM) and cadmium (25 μM). After incubation of the library with the screening medium, the library was rinsed and treated with cadion dye. b) Cadion dye added to relvant transition metals (4 mM).

a)

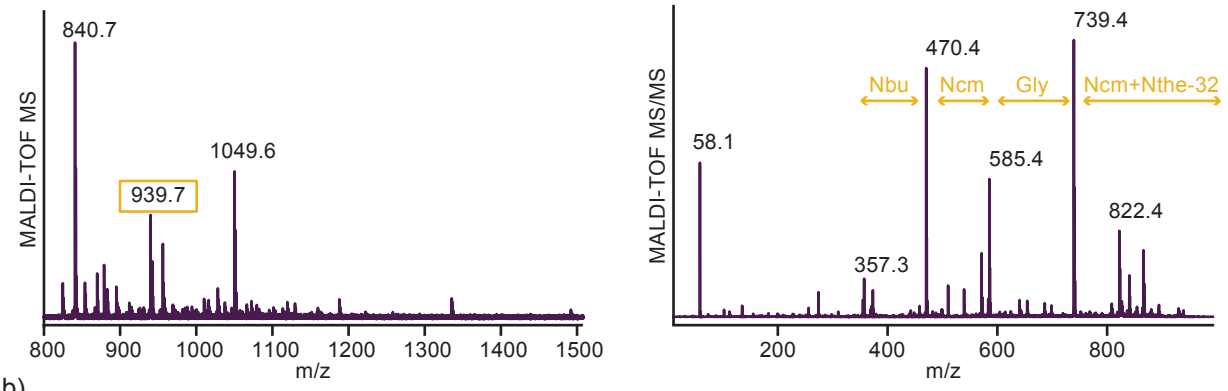

b)

Residue	Monomer Fragment Mass
Nce	129
Nbu	113
Nthe	117
Nae	100
Ncm	115
Nie	151
Npip	191

Residue	Mass of Turn plus Monomer Fragment	
	1PEG	2PEG
Nce	298	342
Nbu	311	355
Nthe	313	357
Nae	315	359
Ncm	327	371
Nie	349	393
Npip	389	433

Figure 4.4. a) MALDI-TOF MS and MALDI-TOF MS/MS of Sequence 2 after screening and photocleavage. b) Table of masses of monomer fragments and the masses of the sum of the turn and the third monomer. The fragmentation that would lead to the intermediate is not visible due the decreased stability of the fragmented secondary amide verses a tertiary amide.

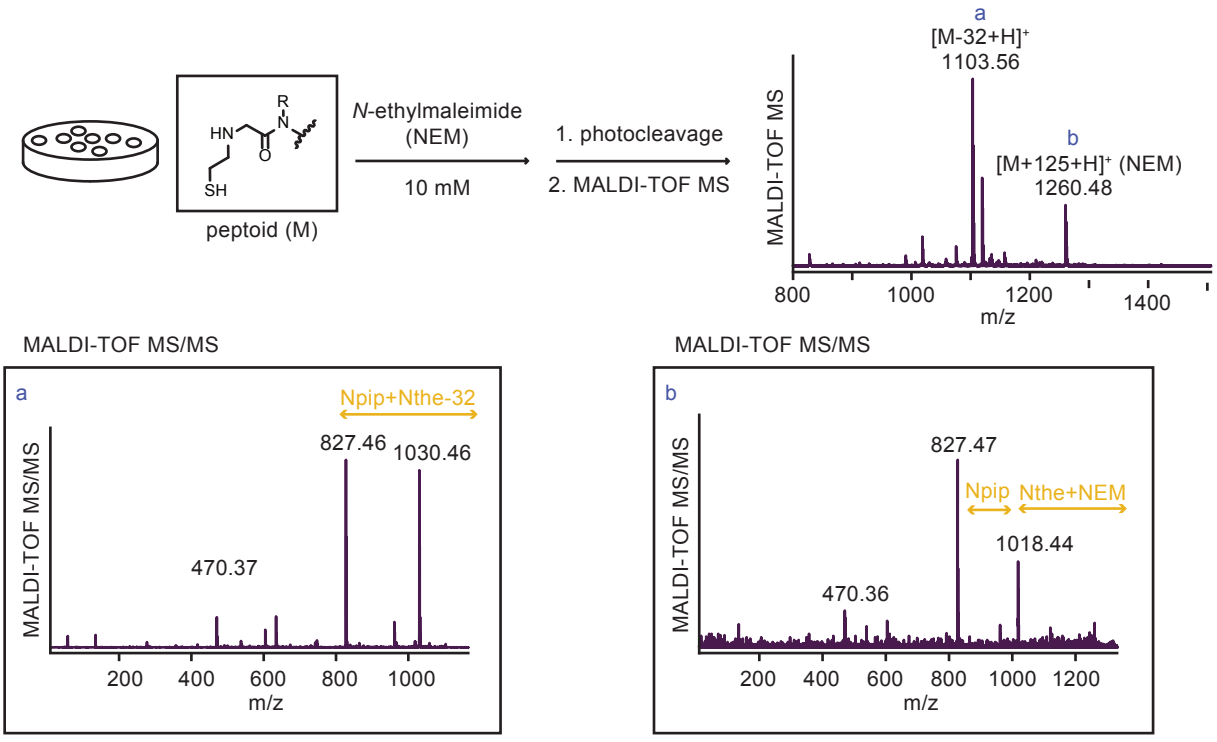

Figure 4.5. Schematic of the *N*-ethylmaleimide (NEM) capping used to determine the mass of the peptoid before photocleavage. MALDI-TOF MS of an individual bead with both the NEM capped mass and the M-32 mass is shown in addition to the MS/MS spectrum for both masses.

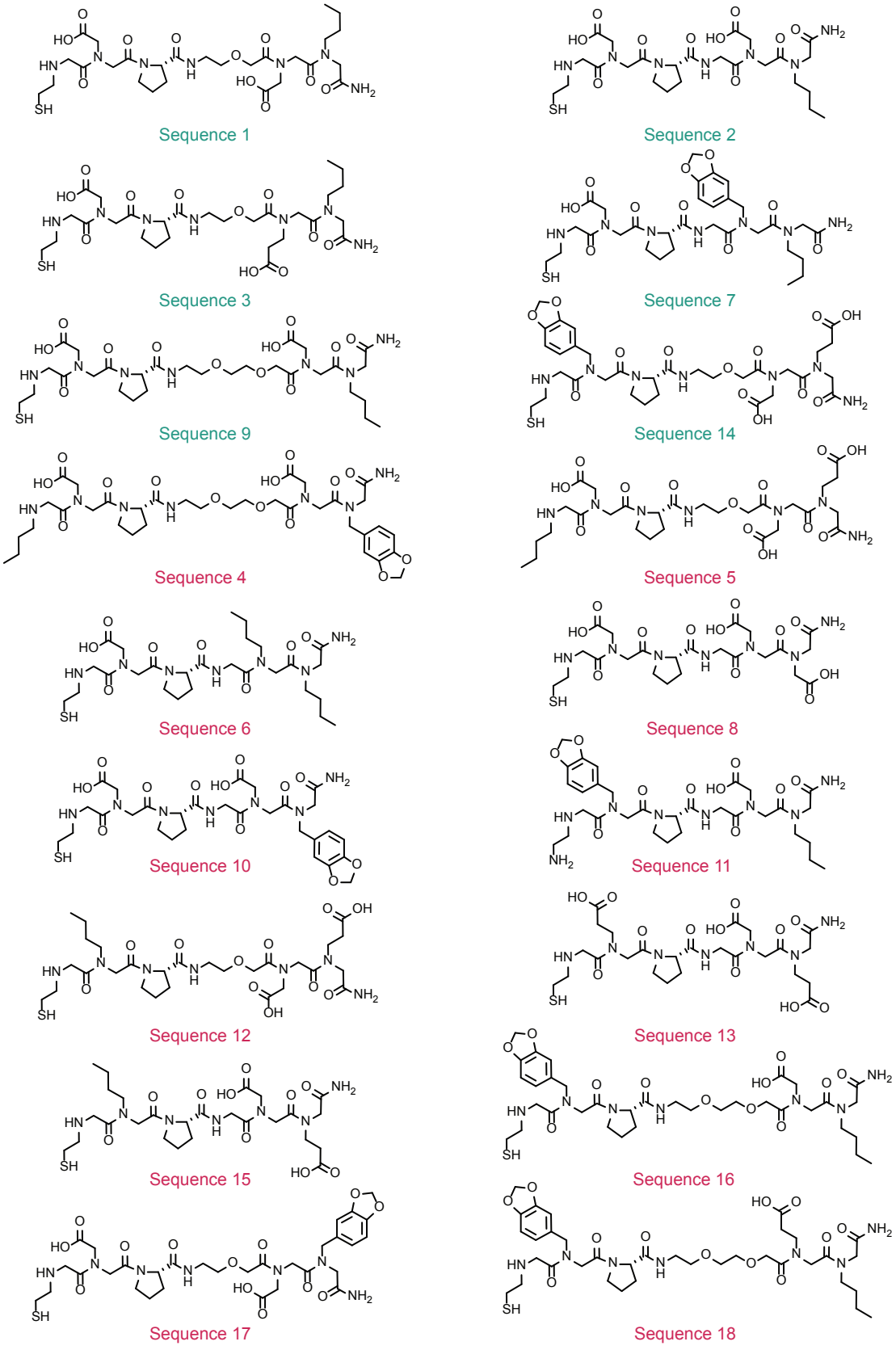

Figure 4.6. Structures of each of the unique peptoids identified in the cadmium screens. The structures labeled in teal are highlighted in the main text.

and cadion, allowing unambiguous identification of cadmium chelators using a light microscope. A similar strategy was applied in the identification of selective nickel ligands. Dimethylglyoxime, which forms a pink precipitate when complexed with nickel, was used to visualize the complexes.[37]

The dye and complexed ions were removed from the selected beads to prepare for sequencing using MS/MS. Photocleavage was performed, but, as depicted in Figure 4.4, this led to a mass loss of 32 with the cadmium hit sequences. It was assumed that this loss corresponded to desulfurization under the photolysis conditions. To verify the mass of the original structure, the screening procedure was repeated and the selected beads were incubated with *N*–ethylmaleimide (NEM) before photocleavage to cap the thiol residues and prevent any undesired photochemical reactions (Figure 4.5). This procedure yielded an individual bead with both the NEM capped structure and the uncapped structure. By comparing the MS/MS fragmentation patterns of the two structures, it was clear that the mass of 32 was lost from an N-terminal Nthe residue during the photocleavage.

After multiple rounds of screening, eighteen unique cadmium chelating sequences were identified (Figure 4.6). All but two of these structures contained an N-terminal Nthe residue, with the negatively charged residues (Ncm and Nce) common in positions X_2 and X_3. Interestingly, the Nthe group was not identified in other positions. There was no consensus for the linker in the turn sequence and many of the unique ligands varied only by that residue. The final position, X_4, was mostly filled by hydrophobic residues (Nbu and Npip).

4.5 Binding Affinity Characterization of Nickel Ligands

To evaluate the affinity of the six sequence identified from the nickel screen (Figure 4.7), titrations were performed with relevant ions (Co^{2+}, Ni^{2+}, Mn^{2+}, Zn^{2+}, and Fe^{2+}) and complex

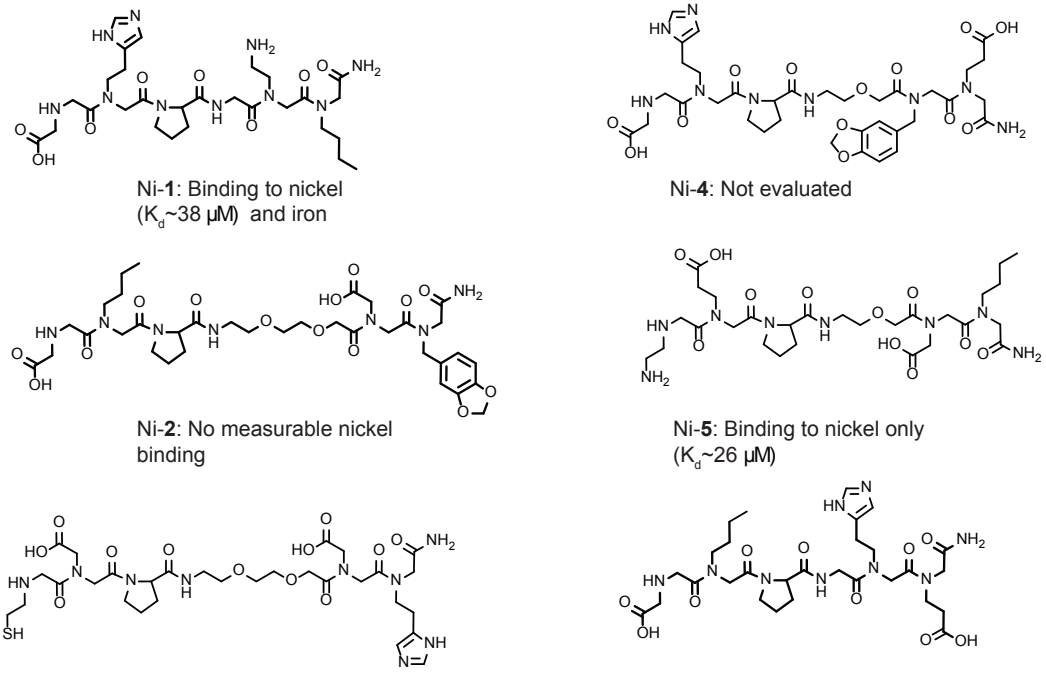

Figure 4.7. Structures of each of the unique peptoids identified in the nickel screens. Binding to cadmium was characterized, and affinities are listed. For each structure determined to bind to cadmium the affinities for zinc, iron, and manganese were also characterized.

formation was monitored by UV-vis. Complex formation for nickel was visible for Ni-**1** and Ni-**5** at 230 nm and for Ni-**5** complex formation was visible at 268 nm. The affinities were approximated by using the inflection point of a logistic fit and ranged from 16-38 μM (values in Figure 4.7). Unfortunately, Ni-**1** had comparable affinity for iron and Ni-**3** for zinc. However, Ni-**5** promisingly displayed no affinity for the ions evaluated with the exception of nickel.

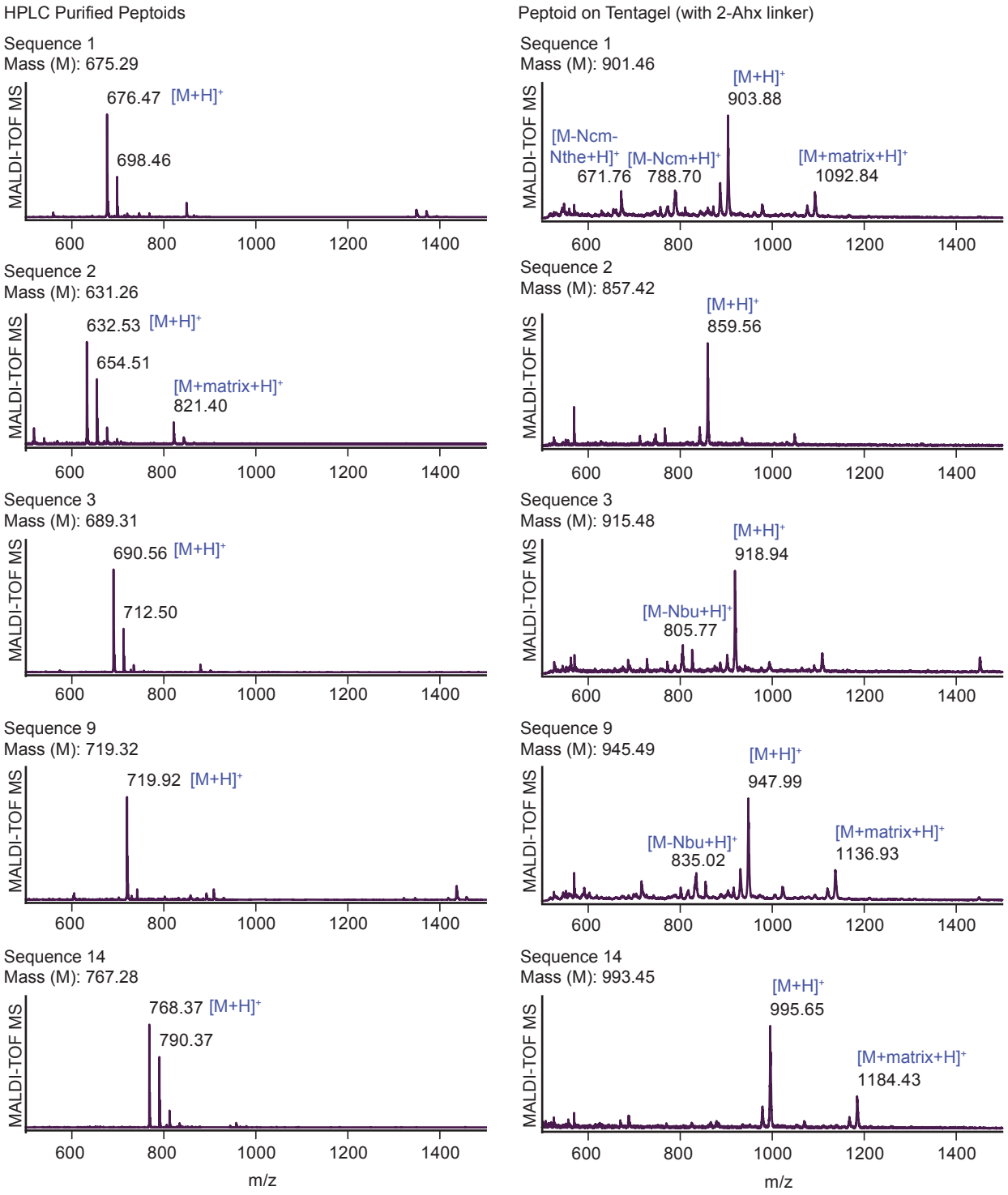

Figure 4.8. Representative MALDI-TOF MS spectra of HPLC purified peptoids and peptoids on Tentagel MB NH2, directly cleaved with the MALDI-TOF MS laser. Corresponding structures are featured in Figure 4.6.

4.6 Binding Affinity Characterization of Cadmium Ligands

To compare the affinity of each of the structures for Cd^{2+}, titrations of Cd^{2+} into each peptoid were completed and monitored by UV-vis spectroscopy. The peptoid structures were prepared by synthesis on Rink Amide resin and purified by reverse phase HPLC after cleavage from the resin. Example mass-spectra of sequences after purification are shown in Figure 4.8. The titrations were monitored at a wavelength of 245 nm. A broad peak spanning from 260 nm through the lowest wavelength scanned (220 nm) was apparent (Figure 4.9); 245 nm was chosen to avoid wavelengths where the solvent and isolated peptoid would absorb. Absorbance at these low wavelengths is characteristic of cadmium thiolate clusters.[38] The data sets were fit to logistic curves and the inflection points were used to determine the dissociation constants. The K_d for the highest affinity peptoid, Sequence 2, and the highest affinity structures that were identified multiple times in the screen (Sequences 1, 3, 9, and 14) are shown in Figure 4.10. Generally, the K_d values ranged from 5 – 40 μM (Figure 4.11). As a preliminary evaluation of the selectivity of the peptoids, the same titration was performed with Sequence 2 and Zn^{2+}, and an eight-fold lower affinity was observed (Figure 4.12). To compare the identified sequences to a similar biological compound, a titration was performed with glutathione and cadmium. Glutathione had an affinity too poor to characterize with the titration (Figure 4.13).

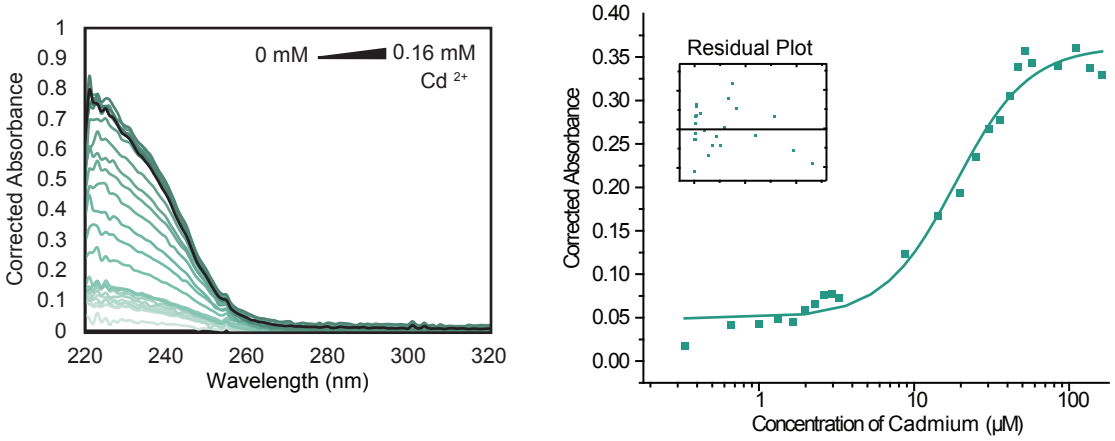

Figure 4.9. Example of a UV-vis titration of Cd^{2+} into a peptoid (Sequene 3, 150 μM) in HEPES (10 mM, pH 7). The curve was fit to a logistic function and the inflection point was used to approximate the K_d. The absorbance values have been normalized for all binding data by subtracting the spectrum of the peptoid alone.

To understand the mode of Cd^{2+} binding and inform any future ligand evolution, the specific interactions of each residue with Cd^{2+} were probed. To begin, the location of the Nthe residue (at the N-terminus) was switched with each of the other residues in the highest affinity ligand (Sequence 2). The structures and measured K_d values are shown in Figure 4.14 as variants

#	X1	X2	Turn	X3	X4	Replicates
2	Nthe	Ncm	Gly	Ncm	Nbu	-
14	Nthe	Npip	1PEG	Ncm	Nce	2
9	Nthe	Ncm	2PEG	Ncm	Nbu	2
3	Nthe	Ncm	1PEG	Nce	Nbu	2
1	Nthe	Ncm	1PEG	Ncm	Nbu	3

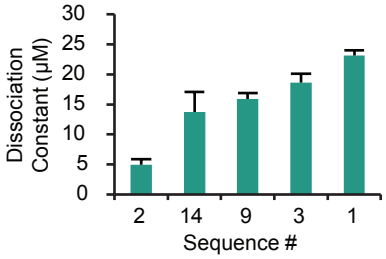

Figure 4.10. Five of the eighteen identified sequences are listed. All dissociation constants displayed were measured using titrations in HEPES buffer (10 mM, pH 7) monitored by UV-vis spectroscopy. A logistic fit was applied to the data and the inflection point was used to approximate the K_d values. A 1:1 binding mode was assumed.

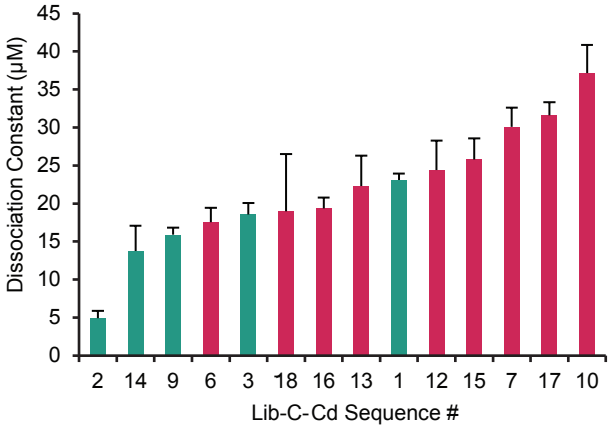

#	Replicates	K_d (μM)	Error	X^2	R^2
2		4.9	0.9	0.0001	0.963
14	2	13.7	3.3	0.0004	0.975
9	2	15.9	0.9	0.0002	0.988
6		17.5	1.9	0.0007	0.988
3	2	18.6	1.5	0.0003	0.981
18		19.0	7.5	0.0003	0.984
16		19.4	1.4	0.0018	0.978
13		22.3	4.0	0.0002	0.971
1	3	23.1	0.9	0.0001	0.990
12		24.4	3.9	0.0006	0.951
15		25.8	2.8	0.0003	0.987
7	3	30.1	2.5	0.0011	0.986
17		31.6	1.7	0.0003	0.988
10		37.2	3.7	0.0005	0.986

Figure 4.11. Graph and table of the measured Kd values. Error bars represent the standard errors in the logistic fits.

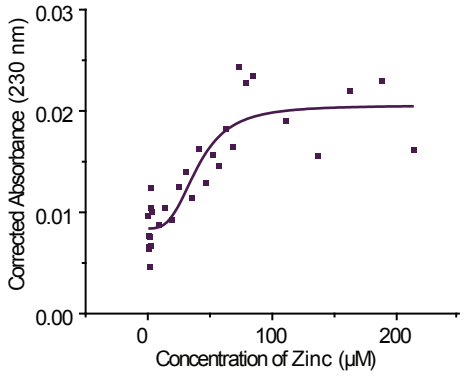

	K_d (μM)	Error	X^2	R^2
Zinc	40	7	0.000008	0.763

Figure 12. inding data from titration of Zn^{2+} into Sequence 2 (150 μM) in HEPES (10 mM, pH 7). The absorbance values have been normalized for all binding data by subtracting the spectrum of the peptoid alone.

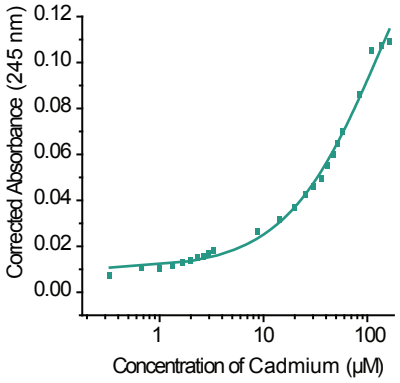

Glutathione

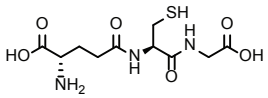

	K_d (μM)	Error	X^2	R^2
Glutathione	134	61	0.000008	0.993

Figure 4.13. Structue and cadmium binding curve for glutathione (150 μM) in HEPES (10 mM, pH 7). The absorbance values have been normalized for all binding data by subtracting the spectrum of the peptoid alone.

a)

#	X1	X2	Turn	X3	X4	Variant
2A	Ncm	Nthe	Gly	Ncm	Nbu	Scramble
2B	Ncm	Ncm	Gly	Nthe	Nbu	Scramble
2C	Nbu	Ncm	Gly	Ncm	Nthe	Scramble
2Y	Nthe	Nbu	Gly	Ncm	Nbu	Substitution
2Z	Nthe	Ncm	Gly	Nbu	Nbu	Substitution

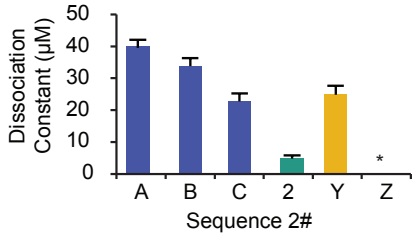

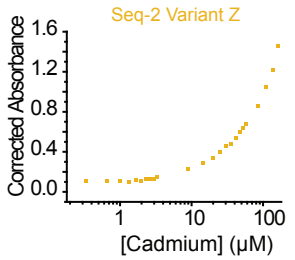

b)

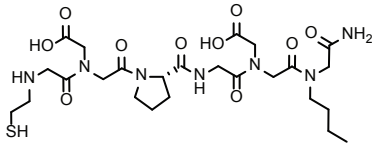
Sequence 2

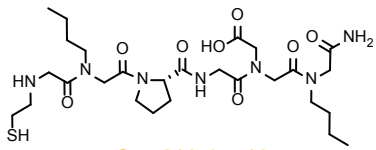
Seq-2 Variant Y

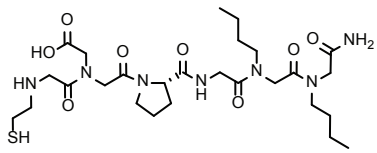
Seq-2 Variant Z

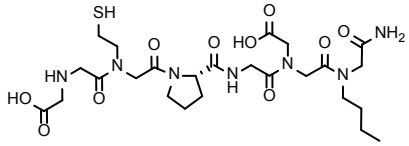
Seq-2 Variant A

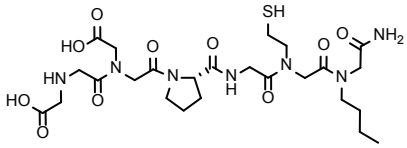
Seq-2 Variant B

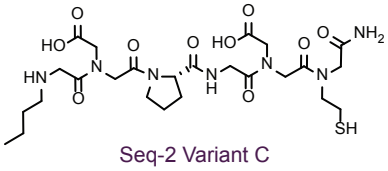
Seq-2 Variant C

Figure 4.14. a) Variants of the highest affinity sequence, Sequence 2, are shown. 2A-C are scrambled sequences in which the thiol containing monomer (Nthe) was switched with each residue. 2Y and 2Z are structures in which the acid containing moieties (Ncm) were replaced with Nbu to investigate the significance of each residue. The binding of each variant was characterized, however, for Z, the affinity was too low to measure. Titration data for Sequence 2 Variant Z, (150 μM) in HEPES (10 mM, pH 7) is shown. All error bars represent the standard error of the logistic fit. b) Structures of Sequence 2 variants.

2A, 2B, and 2C. These rearrangements yielded four- to eight-fold decreases in affinity, indicating not only the necessity of the Nthe residue, but also the importance of its location in the ligand. To analyze the importance of each of the two carboxylic acids, variants were synthesized with Nbu residues replacing the Ncm functionalities (variants 2Y and 2Z). Each of these had a significantly decreased affinity, and 2Z (containing Nbu at the X_3 position) had a K_d value larger than what could be determined with the titration (Figure 4.14).

4.7 Cadmium Complex Characterization with NMR

Synthesizing variants confirmed the importance of the peptoid moieties, but NMR was necessary to identify which residues were directly coordinating the Cd^{2+}. Cadmium is commonly used as a surrogate for other divalent cations when studying proteins by NMR, but few complexes have been characterized in order to probe small molecule ligand-Cd^{2+} interactions.[39] Sequence 2 was selected for this analysis, as it was identified as the highest affinity sequence. An initial ^{1}H-NMR spectrum of the peptoid alone had notably fewer rotamers than the tetramers we have previously studied.[5] A 3:1 ratio of two distinct conformers was apparent instead of the overlapping signals of many rotamers. This conformational restriction could be due to the unique tertiary amines in this structure, but we propose that the two conformers result from the *cis* and *trans* states available to the D-Proline.[40] There have been many previous reports of the structure of peptoids with chiral centers in the side chains.[41,42] However, an evaluation of the available rotamers has not been previously reported.

From ^{1}H TOCSY (Figure 4.15) and ^{1}H-^{13}C HMBC (Figure 4.16 and Figure 4.17) spectra, each of the relevant signals from Sequence 2 was assigned. The HSQC spectrum shown in Figure 18 displays the behavior of Sequence 2 upon titration with Cd^{2+}. With increasing equivalents of Cd^{2+}

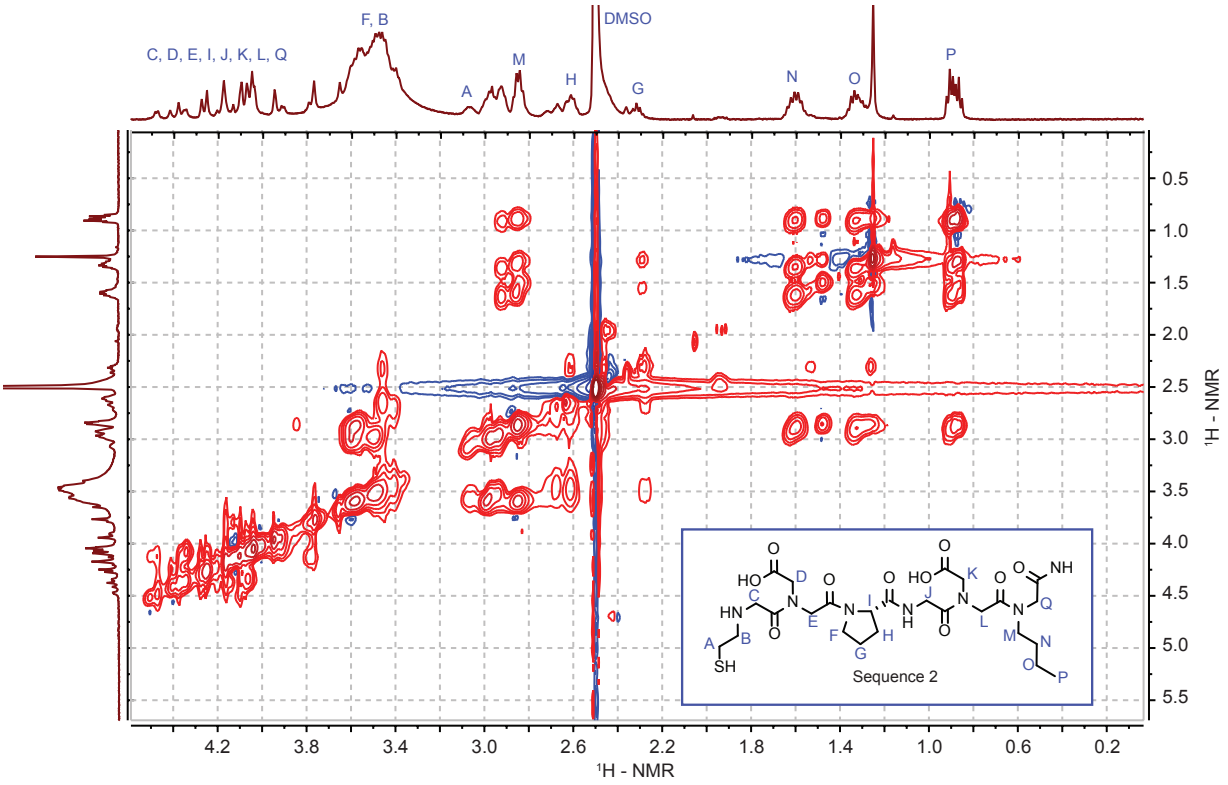

Figure 4.15. ^{1}H TOCSY (900 MHz) of Sequence 2. Spectra were obtained in 10 mM phosphate buffer (pH 7) with 10% D_2O and 500 μM peptoid.

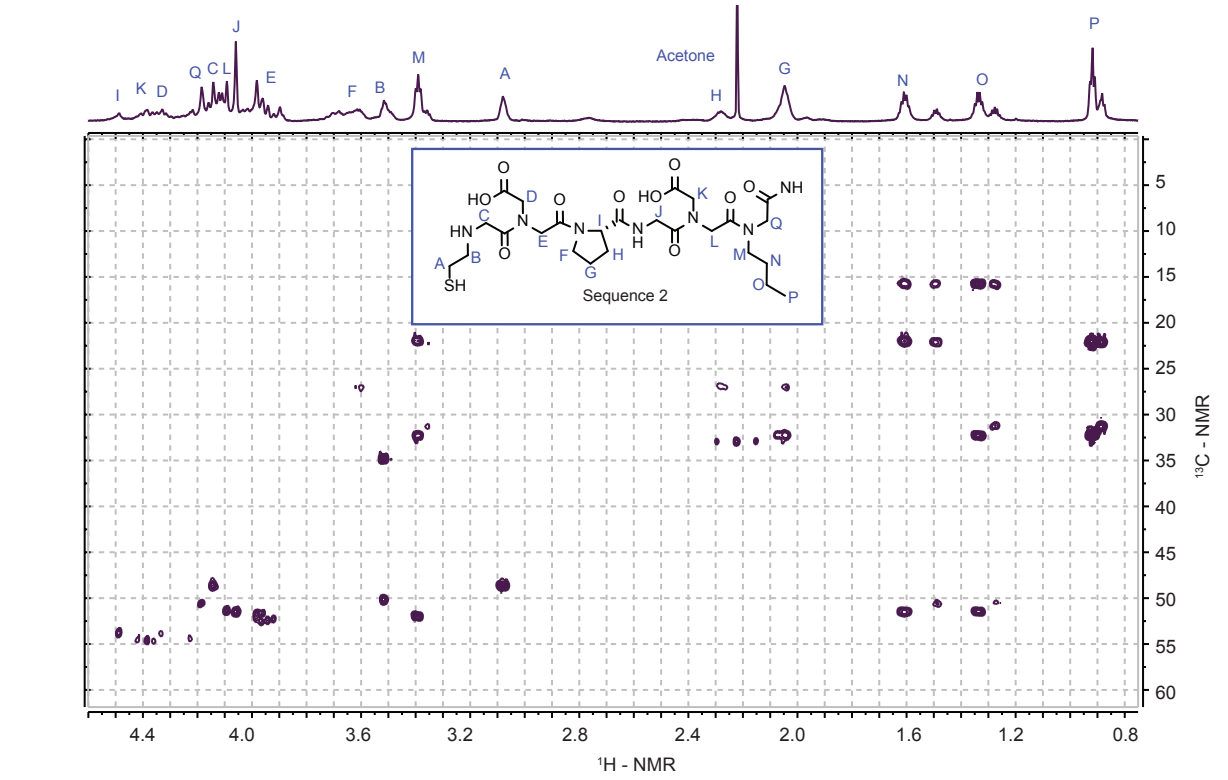

Figure 4.16. ^{1}H-^{13}C HMBC of Sequence 3 with cadmium (2 eq). Spectra were obtained in 10 mM phosphate buffer (pH 7) with 10% D_2O and 500 μM peptoid.

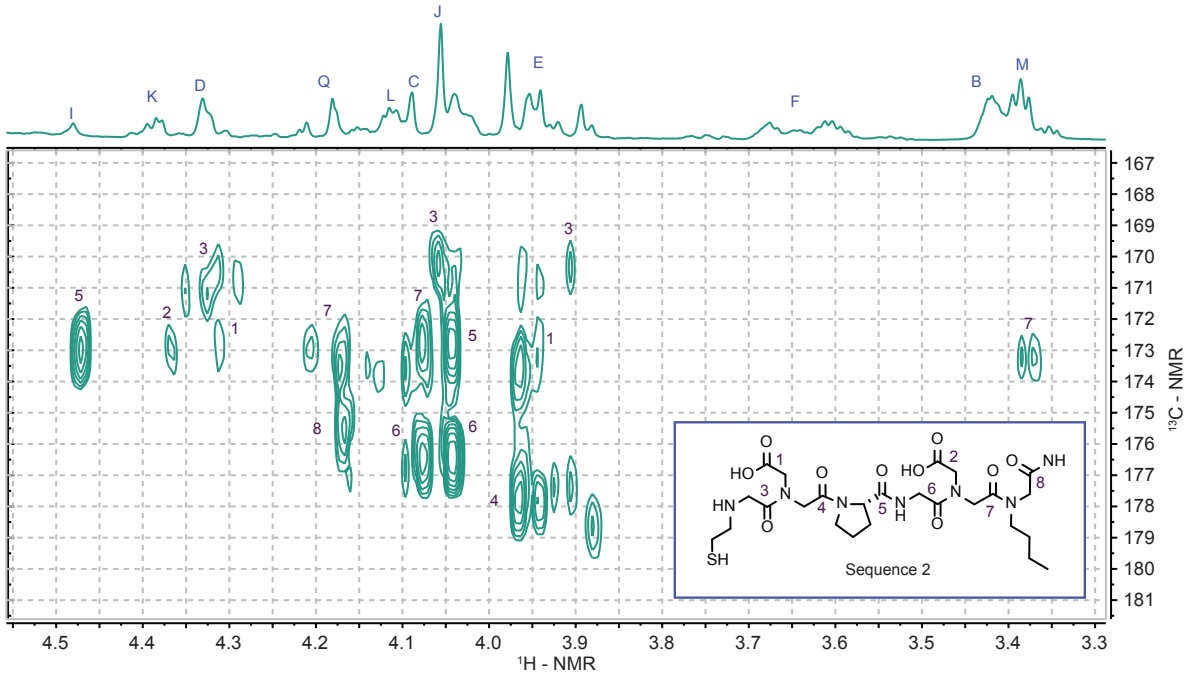

Figure 4.17. ^{1}H-^{13}C HMBC (900 MHz) spectrum of Sequence 2.

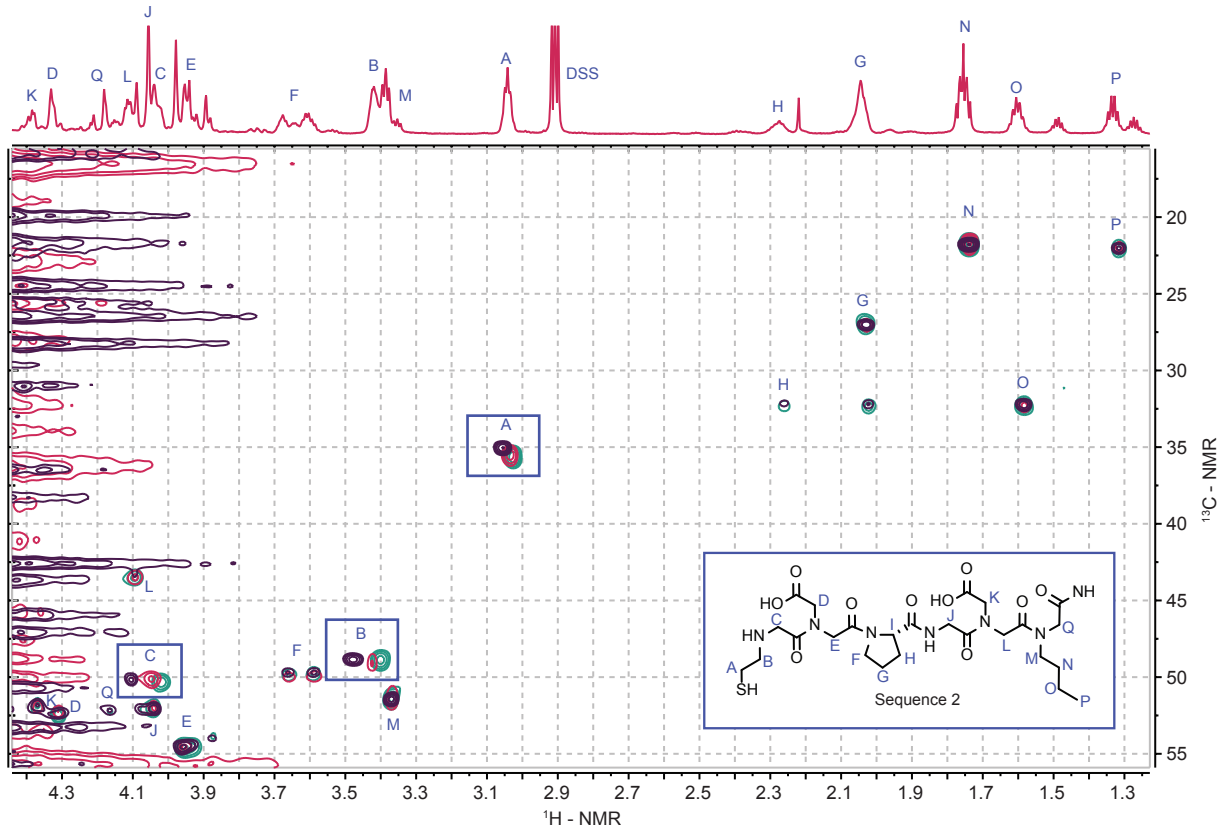

Figure 4.18. ^{1}H-^{13}C HSQC NMR (900 MHz) spectrum of Sequence 2 (500 μM) in the presence of Cd^{2+}. Resonances that shift upon the addition of Cd^{2+} are highlighted. All spectra were obtained in 10 mM phosphate buffer (pH 7) with 10% D_2O.

the methylene peaks of the Nthe residue (Figure 18, signals A and B), in addition to those alpha to the N-terminus (Figure 4.18, signal C), displayed distinct chemical shifts. These changes, and the importance of the N-terminal Nthe residue, indicate that the N-terminus and thiol were both likely coordinating the cadmium. The shifts observed in the protons in the Nthe residue are comparable to those observed for the methylene hydrogens in glutathione.[43] However, the methylene hydrogens in glutathione display separate diastereotopic signals whereas the corresponding methylene hydrogens in Sequence 2 are identical. A possible binding mode supported by this observation is that the thiol and carboxylic acids coordinate the Cd^{2+} in a symmetrical fashion.

4.8 Evaluation of Nickel Ligands in Biological Environments

To evaluate the selectivity of each of the nickel ligands in a biological environment, depletion experiments were performed in the serum replacement used in the screen. In one set of samples the biologically relevant metal ions used in the initial screen were added to the serum replacement and in the other only nickel was added. After incubation of the immobilized peptoid ligands with the samples, the amount of nickel remaining was measured using ICP-OES (Figure 4.19a). Although in this initial study very little of the nickel was depleted, it was clear that Ni-**5** was the most effective structure.

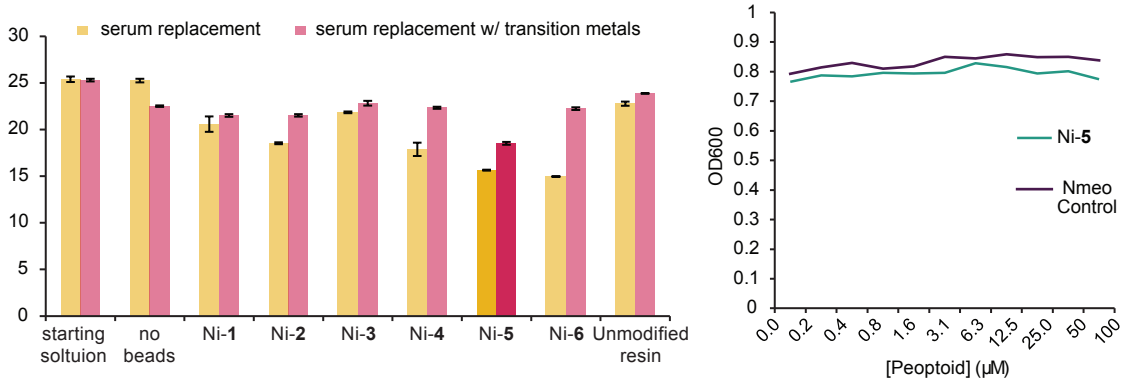

Figure 4.19. Evaluation of the efficacy of nickel binding peptoids in biological environments. a) Tentagel NH_2 resin modified with peptoid sequences of interest were incubated with serum replacement or serum replacement with additional transition metals. The concentration of nickel remaining was measured with ICP-OES. Error bars represent the standard error of three samples. b) Evaluation of the growth of *M. tuberculosis* after fourteen days of treatment with Ni-**5** and a water soluble control (Nmeo control).

Preliminary evaluation of the efficacy of the peptoid structures as a therapeutic for *M. tuberculosis* was performed by Samantha Wellington in the laboratory of Professor Deborah Hung. This preliminary study indicated minimal impact of Ni-**5** against *M. tuberculosis*. The mycobacteria were treated with Ni-**5** in addition to a water soluble peptoid control (Nmeo control), and the absorbance at 600 nm was measured after fourteen days (Figure 4.19b). While Ni-**5** had a limited impact, this could be due to poor cell permeability. Future evaluations of these ligands should include ester protecting groups on the carboxylic acids. These esters would be cleaved by esterases upon entering the cell cytoplasm.

4.9 Depletion of Cadmium from Biological Media

The initial characterization confirmed the affinity of the identified structures for Cd^{2+}. The next step was to confirm the selectivity of the ligands within the complex mixture of ions, small molecules, and proteins present in human serum. Since affinity does not necessarily correlate with selectivity, the four highest affinity peptoids that were repeatedly identified in the screening process (Sequences 1, 3, 9, and 14) and the overall highest affinity ligand (Sequence 2) were resynthesized on the PEG-grafted resin compatible with both organic solvents and water (sequences are listed in Figure 4.6**,** and MALDI-TOF spectra are displayed in Figure 4.8). Each of these ligands was exposed

to three biological mixtures: (1) serum replacement, (2) serum replacement with the addition of relevant transition metals (100 μM: Fe^{2+}, Mn^{2+}, Zn^{2+}), and (3) human serum from AB clotted whole blood. Each of these experiments contained an added cadmium concentration of 10 μM with a ten molar equivalent excess of the peptoid ligands on the resin.

Similar trends were apparent in each of the serum solutions evaluated (Figure 4.20). The most cadmium was depleted from the serum replacement alone, and most of the peptoids were comparably effective in the serum replacement with transition metals and the human serum, validating the selection of the former as a screening medium. Notably, Sequence 2, the ligand with the highest affinity for Cd^{2+}, was outperformed by the other sequences in the serum replacement and human serum. Since the addition of the transition metals did not affected the efficacy of Sequence 2, it is likely that the binding was impeded by additional components of the serum, such as other ions or proteins. Sequence 14 deviated from the consensus exhibited by the other sequences evaluated (thiol – carboxylic acid – carboxylic acid – butyl) by including Npip in the middle of the structure; therefore, it is unsurprising that it was not as selective as the other ligands. Sequences 1, 3 and 9 appeared to perform equivalently, as might be expected by the minor differences in their structures.

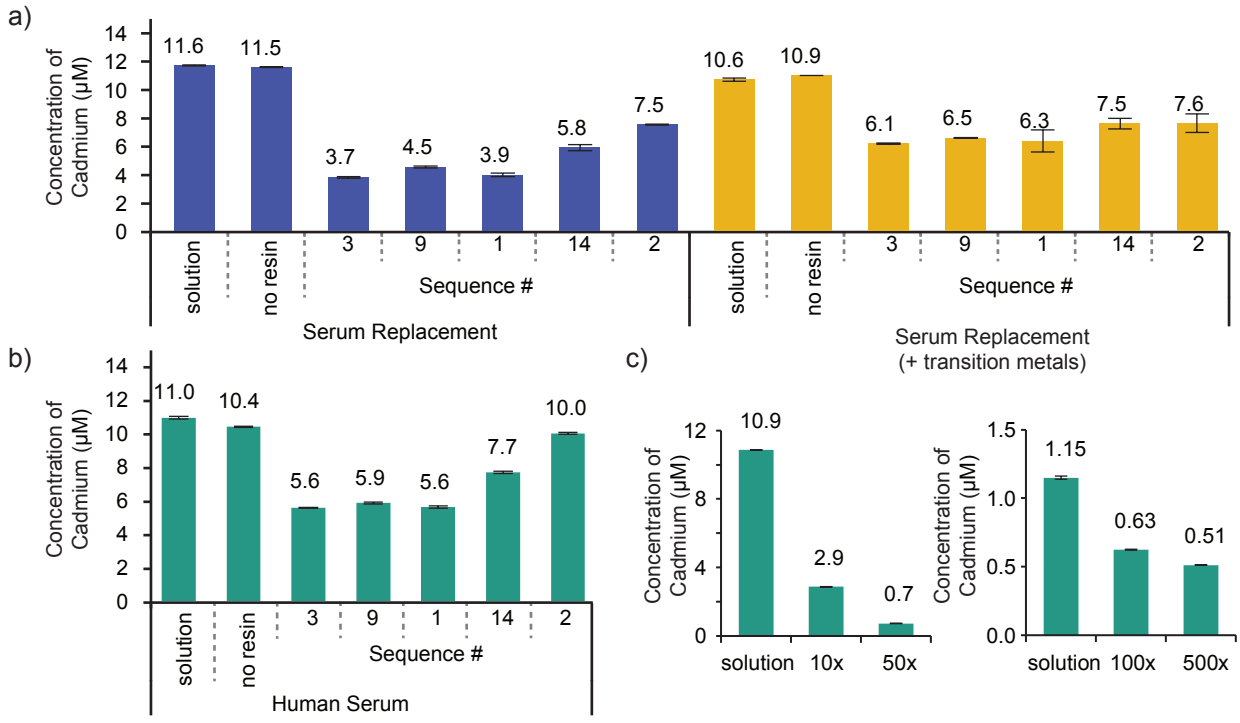

Figure 4.20. Evaluation of Cd^{2+} binding efficacy of peptoid ligands in human serum and mimetic solutions. a) Serum replacement with and without the addition of biologically relevant transition metals (Fe^{2+}, Mn^{2+}, Zn^{2+}, 100 μM) and b) human serum were prepared with a toxic level of Cd^{2+} (10 μM) and exposed to five peptoid sequences attached to the resin (10 eq relative to Cd^{2+}). The amount of cadmium remaining after a 24 h incubation was measured with ICP-OES. The cadmium concentration in the initial solution and a sample with no resin are reported, in addition to those exposed to ligands. c) The depletion ability of Sequence 3 in human serum was additionally evaluated with more equivalents (x = eq relative to Cd^{2+}) of the ligand and at a lower concentration of Cd^{2+} (1 μM). All error bars represent the standard errors of each sample set (n = 3).

In chelation therapies, it is feasible and common to use large excesses of chelating agents. As one example, studies investigating EDTA as a chelation therapy used up to 500 equivalents (1.5 g/kg) of the small molecule relative to the cadmium concentration in an *in vivo* study.[40] To determine how effective the peptoids could be at higher molar ratios, Cd^{2+} was added to human serum at concentrations of 1 and 10 μM and exposed to various amounts of Sequence 3 on resin (Figure 4.4c). Sequence 3 (structure in Figure 4.5b) was chosen as a representative ligand, but we anticipate

similar results with Sequences 1 and 9. Penicillin and streptomycin were added to these serum samples to prevent the growth of bacteria, which could accumulate in the resin and block ligand access. In the 10 μM Cd^{2+} serum samples, 10 and 50 molar equivalents of Sequence 3 on resin were incubated with the samples and removed 73% and 94%, respectively, of the cadmium. More equivalents of the peptoid could not be added to these samples while still allowing full swelling of the resin. Therefore, to demonstrate further the depletion ability of the ligand, Sequence 3 was added to human serum samples with 1 μM Cd^{2+}. The same quantities of resin containing Sequence 3 were added to these samples, and up to 56% of the Cd^{2+} was removed.

Although antibiotics were added to the samples to prevent bacteria from growing and accumulating in the resin used for the assay, it is still likely that larger proteins in the serum prevented the access of some ligands in the pores of the resin. Notably, even with the limitations of this assay, we were able to bring the cadmium concentration down to 0.51 μM—comparable to the limit for acute toxicity in whole blood reported by the Mayo Clinic (0.45 μM).[25] If these ligands were integrated into dialysis systems that have been optimized for blood treatment, it is likely that blood cadmium concentration could be reduced to well below this limit.

4.10 Evaluation of Cadmium Ligand Selectivity

We next sought to evaluate the selectivity of the identified peptoid ligands more directly. To explore this, each of the five peptoid sequences evaluated in the serum depletion experiment were exposed to a solution with relevant ions (K^{+}, Fe^{2+}, Mg^{2+}, Mn^{2+}, Ca^{2+}, Zn^{2+}, Cu^{2+}, Ni^{2+}, Cd^{2+} - approximately 10 μm) in a buffer compatible with each of these ions, bis(TRIS) (10 mM, pH 7.4). The samples were agitated with the beads using a nutator for 24 h at room temperature. The ligands were at a lower molar excess than in the serum assays (5 equiv instead of 10 equiv). In this solution, the ligands were still able to deplete the solution of over 70% of the Cd^{2+}. As depicted in Figure 4.21, cadmium was the most significantly depleted with the concentrations of the later transition metals also being impacted.

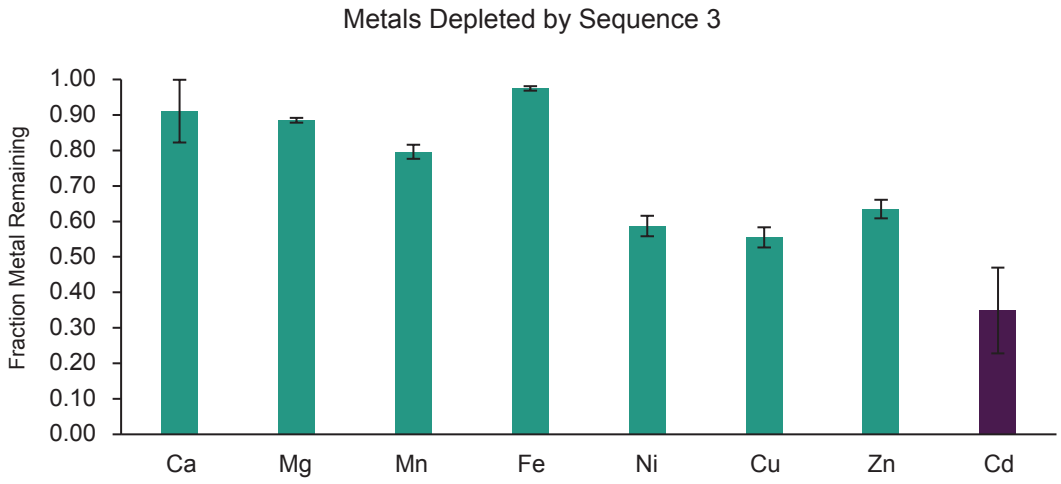

	Ca	Mg	Mn	Fe	Ni	Cu	Zn	Cd
starting solution (μM)	10.37	14.34	10.13	10.82	10.37	10.51	10.15	9.44
depleted soltuion (μM)	9.44	12.69	8.06	10.55	6.09	5.83	6.44	3.29

Figure 4.21. Comparison of depletion of Cd^{2+} verses biological cations. a) Sequence 3 was exposed to each ion (Ca^{2+}, Fe^{2+}, K^{+}, Mn^{2+}, Mg^{2+}, Zn^{2+}, Cd^{2+}, Cu^{2+}, Ni^{2+}) at concentrations of approximately 10 μM and the remaining metal concentrations were measued with ICP-OES. The error bars represent the standard errors of each sample set (n=5).

These depletion selectivity experiments were next repeated in human serum using the native concentrations of the metal ions (Figure 4.22). Serum samples with Cd^{2+} added at 1 and 10 μM Cd^{2+} were exposed to Sequence 3 on resin, and the remaining concentrations of Ca^{2+}, Fe^{2+}, Mg^{2+}, Cu^{2+}, Zn^{2+}, and Cd^{2+} were measured. No significant change was measured for Mg^{2+}, Ca^{2+}, Cu^{2+}, and Fe^{2+}. Although the original concentration of Cu^{2+} and Zn^{2+} measured in the serum samples were close to 10 μM, much less was depleted from the serum samples than in the buffer samples. This is possibly due to native interactions of the ions with serum proteins and small molecules. Due to the chemical similarities between Cd^{2+} and Zn^{2+} (both d^{10} transition metal ions) there are very few ligands with a selective affinity for cadmium.[45] While a variety of small molecules have been developed as fluorescent sensors for cadmium, many are incompatible with water or have fluorescence variance due to factors other than specificity.[46]

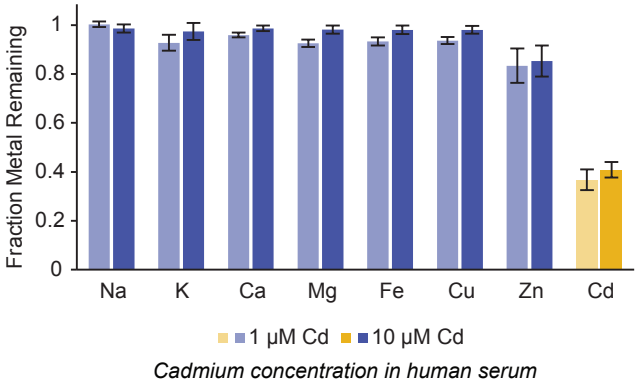

Human serum with 1 μM Cd								
	K	Na	Fe	Zn	Ca	Mg	Cd	Cu
original solution (μM)	3812	14944	10.9	8.8	2250	144	0.6	11.5
Seq 3 depleted (μM)	3534	14991	10.2	7.3	2158	133	0.2	10.8
Human serum with 10 μM Cd								
	K	Na	Fe	Zn	Ca	Mg	Cd	Cu
original solution (μM)	3812	14944	10.9	8.8	2250	144	10.9	11.5
Seq 3 depleted (μM)	3710	14742	10.7	7.5	2219	142	4.5	11.3

Figure 4.22. Evaluation of selectivity of peptoid ligands for Cd^{2+} in the presence of biological divalent cations in human serum. Two concentrations of cadmium (1 μM and 10 μM) were exposed to Sequence 3 (100 μM on resin) for 24 h, and the remaining concentrations of each of the divalent cations were measured using ICP-OES. All error bars represent the standard errors of each sample set (n = 5).

4.11 *In Vitro* Evaluation of Cadmium Ligand

To develop *in vitro* assay, the viability of MDA-MB-231 and Huh7 cell lines were evaluated when treated with cadmium. The Huh7 cell line was chosen for future assays due to (1) its biological relevance as a liver cancer cell line and (2) the range of toxicity observed at an 8-hour time point for cadmium concentrations from approximately 1 to 100 μM. Cadmium toxicity was significantly lower for the MDA-MB-231 cells at the same time point. To evaluate the ability of Sequence 3 to reduce the toxicity of cadmium, Huh7 cells were incubated with no treatment, cadmium and Sequence 3 (100 μM), or cadmium and EDTA (100 μM). Viability of the cells was evaluated with an MTS assay. Figure 4.23 shows the viability of cells under each of the conditions evaluated. The green and purple traces both represent cells treated with Sequence 3 and cadmium, but the

green trace is compared to a control with cells alone and the purple trace is compared to a control treated with the peptoid alone. These data demonstrate that the presence of a chelator reduces the observed toxicity of cadmium, but the peptoid is less effective than EDTA alone. Unfortunately, it is challenging to evaluate the long term impact of removing the other ions coordinated by EDTA, so it was difficult to demonstrate the improved efficacy of the peptoid structure. The media used for growing immortalized cell lines contains different components in different concentrations than the serum in which the other assays were performed. A media more representative of the relevant biological environment could be used for future studies.

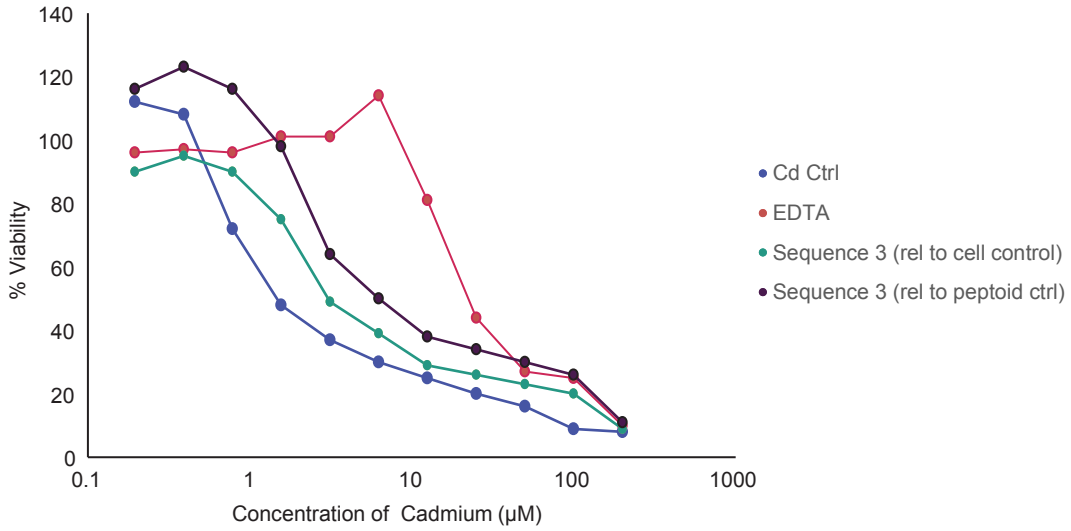

Figure 4.23. Evaluation of the impact of Sequence 3 on Huh7 cells exposed to Cd^{2+} for 8 hours compared to EDTA. The blue plot represents the viability of the cells explosed to just Cd^{2+}, the red plot is the viability of cells exposed to Cd^{2+}in the presence of EDTA (100 μM) and the green and purple plots represent cells in the presence of $Cd^{2+}$and Sequence 3. Control viability assays were performed with not treatment and cells treated with peptoid alone. The green plot shows the viability of the Cd^{2+}treated cells relative to the control with no treatment while the purple is with respect to the control with the peptoid alone.

4.12 Conclusions

Through this work, we have demonstrated a the use of a combinatorial platform for the identification of readily-synthesized ligands capable of selectively chelating Cd^{2+} and Ni^{2+} in complex biological environments. Using the identified ligands, we demonstrated the capacity to remove cadmium from human serum samples with unprecedented selectivity. Identified molecules can be applied not only to the treatment of cadmium poisoning, but also to the ongoing investigations of the mechanisms of its toxicity. We are currently exploring the development of simple economical devices for the detection and treatment of cadmium poisoning by immobilizing these ligands on larger supports. Additionally, we are continuing to explore the applications of this platform in a variety of fields, including metal separations and actinide sequestration.

4.13 Materials and Methods

General Procedures and Materials

Tentagel MB NH_2 resin (140-170 μm, 0.3 mmol/g), used for library synthesis, was purchased from Rapp-Polymere (Tuebingen, Germany). Library synthesis steps were performed in fritted disposable chromatography columns (Bio-Rad, Hercules, CA). During the reactions, the resin suspensions were slowly rotated using a nutator (Fisher Scientific, USA). The photolinker (Fmoc-(*R*)-3-amino-3-(2-nitrophenyl) propionic acid) and Fmoc-6-aminohexanoic acid were purchased from Chem-Impex (Wood Dale, IL). The 1PEG ((2-(Fmoc-amino)ethoxy)acetic acid) and 2PEG ((2-(2-(Fmoc-

amino)ethoxy)ethoxy)acetic acid) linkers were purchased from Iris Biotech GMBH (Marktredwitz, Germany). Water (dd-H_2O) used was deionized using a Barnstead NANOpure purification system (ThermoFisher, Waltham, MA). Serum replacement (KnockOut Serum Replacement) was purchased from Life Technologies (Carlsbad, CA) and human serum was obtained from AB clotted whole blood (Sigma, St Louis, MO). All other materials were purchased from commercial sources and used without further purification, except as noted below. Small scale centrifugation was performed in a Galaxy Mini Star (VWR, USA) and lyophilization was performed using a Labconco Freezone 4.5.

NMR Characterization

^{1}H and ^{13}C spectra were obtained on a Bruker Biospin (900 MHz) spectrometer. Peaks were calibrated using a DSS (4,4-dimethyl-4-silapentane-1-sulfonic acid) standard, DMSO (2.500, q), or H_2O (4.790, s) and spectra were analyzed using TopSpin software. For experiments in water, water was suppressed with excitation sculpting.[47]

Library Synthesis

Of the seven amine monomers, piperonylamine, butylamine, and histamine were used as purchased and incorporated without protecting groups. *N*-boc-ethylenediamine was purchased and used as received. Before use, the glycine and β-alanine monomers (purchased as hydrochloric acid salts with *t*-butyl ester protecting groups) were treated with 1 M NaOH and extracted into a 15:85 v/v isopropanol-chloroform mixture which was dried over sodium sulfate and concentrated, yielding the monomers as the free bases. Cysteamine was protected with a trityl group using a procedure reported by Maltese.[48] The ability of each amine to incorporate into a peptoid using the chemistry described below was previously verified by synthesizing pentamers with alternating benzylamine groups and test monomers.[5,32] The library was synthesized on Tentagel MB NH_2 resin, which was initially swollen in dichloromethane (DCM). Standard Fmoc solid-phase synthesis (using HCTU as a coupling agent) was used to incorporate the three residues in the linker through amide bond formation. For the first variable position, the resin was split evenly into seven different fritted columns. Acylation and the addition of the first amine were performed according to the procedure developed by Zuckermann *et al.* for the incorporation of heterocyclic amines.[31] Acylation was achieved by gently agitating resin beads for 5 min with a solution of chloroacetic acid (6.8 eq, 0.4 mM) in dimethylformamide (DMF) and a solution of diisopropylcarbodiimide (8 eq, 2 M) in DMF. The acylation solution was removed via filtration and the resin beads were rinsed with DMF. Next, the amines were added as 2 M solutions in DMF. After 2-12 h of gentle agitation at room temperature, the resin samples were isolated via filtration and rinsed with DMF. All 7 resin aliquots were then pooled and mixed in DCM for 5 min. Subsequently, the resin was isolated via filtration, vacuum dried, and split into a new set of 7 fritted columns. The acylation and amination steps were repeated to add amines at the second variable position. The library was pooled and split into three separate containers for the addition of the turn sequences. To insert the linker and proline monomers into the peptoid backbone, solutions of the linker (20 eq, 0.6 mM in DMF) and diisopropylcarbodiimide (19 eq, 3.2 mM in DMF) were incubated with the resin for 30 min with gentle agitation. The proline was attached using standard solid-phase peptide synthesis (with HCTU as the coupling agent), after which the standard peptoid synthesis procedure was resumed to couple the remaining amines. After the final amination, the resin pools were recombined and agitated gently in a 20% solution of 4-methylpiperidine in DMF to remove any acylation adducts on the imidazole groups. After isolation via filtration, the resin was rinsed with DMF and DCM, then dried under a vacuum. The protecting groups were removed by incubation with a cleavage solution (95:2.5:2.5) trifluoroacetic acid:water:triisopropylsilane) for 1.5 h. The resin was then rinsed with DCM, dried under vacuum, and stored, protected from light, at 4 °C until use.

Screening to Identify Selective Metal-Binding Sequences

To equilibrate the beads before the screen, a 50 mg portion of the resin (representing more than 3 times the size of the library to ensure inclusion of each sequence) was swelled in water (1 h). The library aliquot was then incubated with $CdCl_2$ (250 μM) in 20-40 mL of screening solution (2.5 mM in $ZnCl_2$, $MnCl_2$, and $FeCl_2$ in serum replacement) for 1 h. The aliquot was then rinsed three times by incubation with 1 mL water in order to facilitate removal of ions retained by non-specific binding.

For visualization and bead selection, the resin was transferred to a Petri dish. Approximately 500 μL of cadmium-specific dye, cadion, (0.23 mM cadion and 20 mM potassium hydroxide in ethanol) was applied, and the solvent was evaporated from the Petri dish under a gentle flow of nitrogen in order to trap the dye and the metal within the individual beads. The aliquot in the Petri dish was examined using a Leica S6D Microscope (Leica, Germany). The beads with the most intense colors were manually selected for ligand identification. All photographs were taken with an iPhone (model 4 or 5).

Metal Ion Removal and Photocleavage

The removal of the metal ions was found in previous work to be essential before interpretable MALDI-TOF MS sequencing data could be obtained. Beads selected from the library screen were deposited onto the membrane of a 0.5 mL 0.2 μm centrifugal filter unit (Millipore, Billerica, MA). A mixture of Amberlite cation (Na^+ form, 5 mg) and anion (Cl^- form, 5 mg) exchange resins was then added to the filtrate collection tube of the centrifugal filter unit. The filter and the collection tube were then filled with 1 M HCl. This setup was incubated with gentle agitation on a nutator for 2 h, allowing diffusion to occur through the 0.2 μm filter. The selected library members were isolated from the exchange resins and acidic solution by centrifugation of the filtration unit. Water (500 μL) was added to the filter unit, and the unit was gently agitated on a nutator for 15 min to rinse the library members. The water was then removed by centrifugation. This process was repeated twice to ensure removal of residual HCl.

The beads bearing hit sequences were removed from the filter unit and transferred to a Petri dish using ethanol (approx. 500 μL). The individual beads were captured using a pipet and placed into individual 0.6 mL Posi-Click tubes (Denville Scientific, South Plainfield, NJ). The volume in each tube was brought to 5 μL with absolute ethanol. To cleave the peptoids from single resin beads, the tubes were placed in a computer controlled ICH-2 photoreactor with UVA bulbs (Luzchem, Ottawa, Canada) for 8 h (various incubation times were screened). For mass verification of bulk peptoid samples, the beads were able to be directly cleaved with the nitrogen laser (337 nm) on the MALDI-TOF MS (Voyager-DE Pro, Applied Biosystems) in addition to the Nd:YAG laser (355 nm) on the MALDI-TOF-TOF MS/MS (4800 plus MALDI-TOF-TOF Analyzer, Applied Biosystems)

To determine whether unintended photoreactions were occurring with the unprotected N-terminal thiol, after one screen the library members were incubated in *N*-ethylmaleimide (25 μL, 10 mM, in dd-H_2O) for 30 min before photocleavage.

Single Bead Sequencing

After single-bead photocleavage, the ethanol was evaporated and replaced with 1:1 water:acetonitrile containing tris(2-carboxyethyl)phosphine (0.5 mM). The sample (0.5 μL) was mixed with 0.5 μL matrix solution (5 mg α-cyano-4-hydroxycinnamic acid in 1:1 water:acetonitrile with 0.1% trifluoroacetic acid and 0.6 M ammonium phosphate) and spotted directly on a stainless steel MALDI plate. MALDI-TOF MS (AB Sciex TF4800, Applied Biosystems) was used to identify the mass of each selected sequence, and MS/MS was used to fragment the peptoids for sequencing.

Eighteen unique sequences were identified from this screening process.

Binding Constant Evaluation via UV-vis Titration

Each of the identified sequences was synthesized using the protocols described for library synthesis with Fmoc-Rink Amide MBHA resin (Anaspec, Fremont, CA) in place of the Tentagel MB NH_2 resin. The initial fluorenylmethyloxycarbonyl (Fmoc) group was removed with 20% 4-methylpiperidine in DMF. Following synthesis, a cleavage cocktail (95:2.5:2.5 trifluoroacetic acid:water:triisopropylsilane) was used to remove the peptoids from the resin, while also removing the protecting groups from the monomers. After evaporating the trifluoroacetic acid, the peptoids were precipitated from ether. The resulting precipitates were resuspended in water and purified using reversed phase chromatography on a semi-preparatory scale HPLC column (Agilent). The isolated fractions were concentrated using a speed vacuum (Labconoco, USA) and then lyophilized. The resulting sequences were stored dry at -20 °C before use in order to minimize disulfide formation. MALDI-TOF MS characterizations of the purified peptoids appear in Figure 4.8.

To evaluate binding constants for each hit sequence, $CdCl_2$ (0.3 - 5 mM) was titrated into a solution of peptoid (90 µL, 150 µM in 10 mM HEPES buffer, pH 7) in increments of 0.1-1 µL. The visible absorbance spectrum was measured at each increment using a Cary 50 spectrophotometer (Varian). The absorbance at the monitored wavelength (245 nm) was plotted against the concentration of cadmium and fit to a logistic binding curve using Origin software. The model used to fit the data is displayed in Equation 1, where A_1 and A_2 are the asymptotes of the data, p correlates to the slope of the curve, and x_0 is the inflection point used to approximate the dissociation constant.

$$y = (A_1\text{-}A_2)/(1+x/x_0)^p+A_2$$

Equation 1

Cadmium Depletion Analysis with ICP-OES

Five of the original eighteen hit sequences were carried forward to depletion experiments: Sequence 2 (which demonstrated the best binding constant from the UV-vis assay) and Sequence 1, Sequence 3, Sequence 9 and Sequence 14, which were all identified multiple times in the initial screens. These sequences were synthesized on Tentagel MB NH_2 (0.3 mmol/g) using the procedures described in the "library synthesis" section. A photolinker and two aminohexanoic acid residues were used to link the peptoid structures to the resin. The sequence identities were confirmed via MALDI-TOF MS by directly cleaving beads with the MALDI laser.

To evaluate these sequences' ability to remove cadmium from serum replacement and human serum samples, several solutions were evaluated: serum replacement was artificially contaminated with either (1) $CdCl_2$ (10 µM) or (2) $CdCl_2$ (10 µM), $ZnCl_2$, $MnCl_2$, and $FeCl_2$ (100 µM); and human blood serum was contaminated with 10 µM $CdCl_2$. Three replicate samples of each of the five hit sequences were each incubated for 24 h in the depletion solutions, such that the ligands were initially in ten-fold molar excess to the cadmium ions (assuming 100% modification of the resin). Following this incubation period, an aliquot from each sample was removed and diluted with nitric acid to a final concentration of 2% HNO_3; samples containing human blood serum were centrifuged (30 min, 4 ˚C, 4000 rpm) to aid in precipitation of denatured proteins. The concentration of cadmium remaining in those samples was determined by averaging five measurements of each sample with a Perkin Elmer 5300 DV optical emission ICP using scandium as an internal standard.

Further depletion assays were carried out to determine the full potential of the peptoid ligands to deplete cadmium from human serum. Sequence 3 on resin was added to human blood serum with 10 µM cadmium (with 10-fold molar excess peptoid) and 1 µM cadmium (with 100-fold molar excess peptoid). In these samples penicillin (100 units mL^{-1}) and streptomycin (0.1 mg mL-1) were

added to prevent bacterial growth during the assays. This experiment was repeated to determine the selectivity of the binding, and the concentration of the biological cations (Na^+, K^+, Zn^{2+}, Mn^{2+}, Mg^{2+}, Fe^{2+}, Cu^{2+}, and Ca^{2+}) was measured in addition to cadmium. The Na+ and K^+ ions were measured at 1:1000 dilution and the other ions were measured at a 1:10 dilution into nitric acid (final concentration 2%). One of the data points for the measurement of Na^+ and K^+ in untreated serum was determined to be a statistical outlier and was not included.

Finally, to evaluate selective binding of cadmium verses biological divalent cations at comparable concentrations, a solution of $CdCl_2$, $ZnCl_2$, $MnCl_2$, $FeCl_2$, $CuCl_2$, $Ni(OAc)_2$, $Mg(OAc)_2$, calcium lactate (10 μM) and bis(TRIS) (10 mM, pH 7.4, BioXtra, Sigma-Aldrich (St Lous, MO)) was exposed to each of the resin-bound peptoids.

Culturing of immortalized cell lines

MDA-MB-231 and Huh7 cells were purchased from ATCC and grown in media recommended by the supplier with 1% penicillin and streptomycin. To passage the cells, the cells were first rinsed with phosphate buffered saline (PBS) and then treated with trypsin and incubated at room temperature for approximately 3-5 min. The cells were grown at 37 °C with an atmosphere of 95% air and 5% CO_2.

Cell viability assay

To measure the viability of the cells, they were treated with 3-(4,5-dimethylthiazol-2-yl)-5-(3-carboxymethoxyphenyl)-2-(4-sulfophenyl)-2H-tetrazolium (MTS) according to the instructions provided. Briefly, the after exposure to $Cd^{2+}$for 8 h with no treatment, EDTA, or the peptoid of interest (100 μM) the cells were washed and treated with a solution of 20% MTS in media. After a 1-3 h incubation period the absorbance was measured at 490 nm.

4.14 References

1. WHO | Global tuberculosis report 2014. at <http://www.who.int/tb/publications/global_report/en/>

2. Stanley, S. A. *et al.* Identification of Novel Inhibitors of M. tuberculosis Growth Using Whole Cell Based High-Throughput Screening. *ACS Chem. Biol.* **7,** 1377–84 (2012).

3. Grant, S. S. *et al.* Identification of novel inhibitors of nonreplicating Mycobacterium tuberculosis using a carbon starvation model. *ACS Chem. Biol.* **8,** 2224–34 (2013).

4. Boer, J. L., Mulrooney, S. B. & Hausinger, R. P. Nickel-dependent metalloenzymes. *Arch. Biochem. Biophys.* **544,** 142–52 (2014).

5. Knight, A. S., Zhou, E. Y., Pelton, J G. & Francis, M. B. Selective chromium (VI) ligands identified using combinatorial peptoid libraries. *J. Am. Chem. Soc.* **135**, 17488-93 (2013).

6. Moulis, J.-M. & Thévenod, F. New perspectives in cadmium toxicity: an introduction. *Biometals* **23,** 763–8 (2010).

7. Agency for Toxic Substances and Disease Registry. Cadmium (Cd) Toxicity: How Should Patients Exposed to Cadmium Be Treated and Managed? *Cadmium Toxic. How Should Patients Expo. to Cadmium Be Treat. Manag.* at <http://www.atsdr.cdc.gov/csem/csem.asp?csem=6&po=16>

8. US EPA, O. Priority Pollutants. at <http://water.epa.gov/scitech/methods/cwa/pollutants.cfm>

9. Bertin, G. & Averbeck, D. Cadmium: cellular effects, modifications of biomolecules, modulation of DNA repair and genotoxic consequences (a review). *Biochimie* **88**, 1549-59 (2006).

10. Nawrot, T. S. *et al.* Cadmium exposure in the population: from health risks to strategies of prevention. *Biometals* **23,** 769–82 (2010).

11. Waisberg, M., Joseph, P., Hale, B. & Beyersmann, D. Molecular and cellular mechanisms of cadmium carcinogenesis. *Toxicology* **192,** 95–117 (2003).

12. Waalkes, M. P. Cadmium carcinogenesis in review. *J. Inorg. Biochem.* **79,** 241–4 (2000).

13. Cuypers, A. *et al.* Cadmium stress: an oxidative challenge. *Biometals* **23,** 927–40 (2010).

14. Flora, S. J. S. & Pachauri, V. Chelation in metal intoxication. *Int. J. Environ. Res. Public Health* **7,** 2745–88 (2010).

15. Flora, S. J. S., Mittal, M. & Mehta, A. Heavy metal induced oxidative stress & its possible reversal by chelation therapy. *Indian J. Med. Res.* **128,** 501–23 (2008).

16. Nitz, M., Franz, K. J., Maglathlin, R. L. & Imperiali, B. A Powerful Combinatorial Screen to Identify High-Affinity Terbium (III)-Binding Peptides. *ChemBioChem* **4,** 272–6 (2003).

17. Martin, L. J. L. J., Sculimbrene, B. R. B. R., Nitz, M. & Imperiali, B. Rapid Combinatorial Screening of Peptide Libraries for the Selection of Lanthanide-Binding Tags (LBTs). *QSAR Comb. Sci.* **24,** 1149–1157 (2005).

18. Francis, M. B., Jamison, T. F. & Jacobsen, E. Combinatorial libraries of transition-metal complexes, catalysts and materials. *Curr. Opin. Chem. Biol.* **2,** 422–8 (1998).

19. Pirrung, M. C., Park, K. & Tumey, L. N. 19F-encoded combinatorial libraries: discovery of selective metal binding and catalytic peptoids. *J. Comb. Chem.* **4,** 329–44 (2002).

20. Burger, M. T. & Still, W. C. Synthetic Ionophores. Encoded Combinatorial Libraries of Cyclen-based Receptors for Cu^{2+} and Co^{2+}. *J. Org. Chem.* **60,** 7382–3 (1995).

21. Simon, R. J. *et al.* Peptoids: a modular approach to drug discovery. *Proc. Natl. Acad. Sci. U. S. A.* **89,** 9367–71 (1992).

22. Lee, B.-C., Chu, T. K., Dill, K. a & Zuckermann, R. N. Biomimetic nanostructures: creating a high-affinity zinc-binding site in a folded nonbiological polymer. *J. Am. Chem. Soc.* **130,** 8847–55 (2008).

23. Maayan, G., Ward, M. D. & Kirshenbaum, K. Metallopeptoids. *Chem. Commun.* 56–8 (2009).

24. Izzo, I., *el al.* Structural Effects of Proline Substitution and Metal Binding on Hexameric

Cyclic Peptoids. *Org. Lett.* **15,** 4–7 (2013).

25. Nalband, D. M., Warner, B. P., Zahler, N. H. & Kirshenbaum, K. Rapid identification of metal-binding peptoid oligomers by on-resin X-ray fluorescence screening. *Biopolymers* **102,** 407–15 (2014).

26. Astle, J. M., Udugamasooriya, D. G., Smallshaw, J. E. & Kodadek, T. A VEGFR2 Antagonist and Other Peptoids Evade Immune Recognition. *Int. J. Pept. Res. Ther.* **14,** 223–7 (2008).

27. Zuckermann, R. N. & Kodadek, T. Peptoids as potential therapeutics. *Curr. Opin. Mol. Ther.* **11,** 299–307 (2009).

28. Seo, J., Ren, G., Liu, H., Miao, Z. & Park, M. In vivo biodistribution and small animal PET of 64Cu-Labeled antimicrobial peptoids. *Bioconjug. Chem.* **24,** 1069-79 (2012).

29. Heavy Metals Screen with Demographics, Blood. at <http://www.mayomedicallaboratories.com/test-catalog/Clinical+and+Interpretive/34506>

30. Francis, M. B., Finney, N. S. & Jacobsen, E. N. Combinatorial Approach to the Discovery of Novel Coordination Complexes. *J. Am. Chem. Soc.* **118,** 8983-4 (1996).

31. Zuckermann, R. N., Kerr, J. M., Kent, S. B. H. & Moos, W. H. Efficient method for the preparation of peptoids [oligo(N-substituted glycines)] by submonomer solid-phase synthesis. *J. Am. Chem. Soc.* **114,** 10646–7 (1992).

32. Burkoth, T. S., Fafarman, A. T., Charych, D. H., Connolly, M. D. & Zuckermann, R. N. Incorporation of unprotected heterocyclic side chains into peptoid oligomers via solid-phase submonomer synthesis. *J. Am. Chem. Soc.* **125,** 8841–5 (2003).

33. Heumann, K. G. *Handbook of Elemental Speciation: Techniques and Methodology*. (John Wiley & Sons, 2004), 38-41.

34. Jackson, G. E. & Byrne, M. J. Metal Ion Speciation in Blood Plasma : Gallium-67-Citrate and MRI Contrast Agents. *J. Nucl. Med.* **37**, 379–86 (2014).

35. Verma, M. R. & Paul, S. D. SPOT-TEST METHOD FOR THE DETECTION OF CADMIUM IN PRESENCE OF COPPER, LEAD AND TIN. *Analyst* **80,** 399-401 (1955).

36. Feigl, F. & Anger, V. Spot Tests in Inorganic Analysis. *Elsevier* **80,** 399-401 (1973).

37. Godycki, L. E. & Rundle, R. E. The structure of nickel dimethylglyoxime. *Acta Crystallogr.* **6,** 487–95 (1953).

38. Liu, H., Hupp, J. T. & Ratner, M. A. Electronic Structure and Spectroscopy of Cadmium Thiolate Clusters. **3654,** 12204–12213 (1996).

39. Sigel, A., Sigel, H. & Sigel, R. K. O. *Cadmium: From Toxicity to Essentiality*. (Springer Science & Business Media, 2013), 118-137.

40. Deber, C. & Bovey, F. Nuclear magnetic resonance evidence for cis-peptide bonds in

proline oligomers. *J. Am. Chem. Soc.* **35,** 6191–8 (1970).

41. Armand, P. *et al.* NMR determination of the major solution conformation of a peptoid pentamer with chiral side chains. *Proc. Natl. Acad. Sci.* **95,** 4309–14 (1998).

42. Wu, C. W. *et al.* Structural and spectroscopic studies of peptoid oligomers with alpha-chiral aliphatic side chains. *J. Am. Chem. Soc.* **125,** 13525–30 (2003).

43. Delalande, O. *et al.* Cadmium-glutathione solution structures provide new insights into heavy metal detoxification. *FEBS J.* **277,** 5086–96 (2010).

44. Jr, L. C. & Klaassen, C. Decreased effectiveness of chelation therapy with time after acute cadmium poisoning. *Toxicol. Appl. Pharmacol.* **180,** 173–80 (1982).

45. Mejàre, M., Ljung, S. & Bülow, L. Selection of cadmium specific hexapeptides and their expression as OmpA fusion proteins in *Escherichia coli. Protein Eng.* **11,** 489–94 (1998).

46. Kim, H. N., Ren, W. X., Kim, J. S. & Yoon, J. Fluorescent and colorimetric sensors for detection of lead, cadmium, and mercury ions. *Chem. Soc. Rev.* **41,** 3210–44 (2012).

47. Hwang, T. & Shaka, A. Water suppression that works. Excitation sculpting using arbitrary wave-forms and pulsed-field gradients. *J. Magn. Reson. Ser. A* **112,** 275–9 (1995).

48. Maltese, M. Reductive demercuration in deprotection of trityl thioethers, trityl amines, and trityl ethers. *J. Org. Chem.* **66,** 7615–25 (2001).

Chapter 5

Towards Functional Peptoid-Based Materials for Environmental Applications

Abstract

Inspired by the success of identifying ligands for removing chromium from water and cadmium from blood, we have been working towards developing peptoid-based materials for additional environmental applications. In this chapter a screen for identifying a ligand for separating the lanthanide ions is described in addition to work towards creating a polymer-based mercury sensor. The lanthanide screen employs europium and terbium; their proximity on the periodic table correlates with their chemical similarity. Therefore, this assay, which looks for a differential affinity between europium and terbium, should extrapolate to the whole series. A two-step screen was used to identify mercury ligands, which encouragingly deplete mercury selectively in the presence of other toxic metal ions. Finally, reactions for attaching the peptoids to a new type of support, methacrylate polymers, were evaluated.

5.1 Separating Lanthanide Ions

Recently, the application of lanthanides in a variety of fields including catalysis and clean energy has grown significantly.[1] Lanthanides remain expensive and the process taking the ore from the mine to the market is environmentally detrimental.[2] A critical step in this process is the separation of the lanthanide ions from each other, as the natural ores exist as mixtures of the metals.[3] The separation is currently completed with counter-current extractions using caustic acids. Many other approaches have been evaluated (e.g. liquid and gas chromatography), but this separation remains a significant challenge due to the extreme chemical similarity of the lanthanide ions. The identification of an efficient and green separation strategy would eliminate the environmental damage caused by the current processes, but could also decrease the cost and thereby increase the availability of these metals that are critical for green energy applications.

Liquid chromatography methods have demonstrated success in the separation of the lanthanide ions,[4] but the most common drawbacks of these processes are the use of strong acids in the mobile phase or non-scalable high pressure liquid chromatography. The resins used in these separations have some selectivity that is enhanced by an acidic gradient mobile phase or by high pressure. This chapter will describe the design of a combinatorial library to identify ligands with enhanced selectivity such that separations can be completed without additional pressure or an acidic mobile phase. Peptoids, or *N*-substituted glycine oligomers, are uniquely applicable for this combinatorial approach due to their modular synthesis and the diversity of inexpensive monomers available.[5,6] Peptoid-based metal ligands have been identified previously from combinatorial screens.[7,8] However, a screen to identify a ligand with a differential affinity among a mixture of ions is unprecedented. Herein, we will describe the development of a screen designed to identify a peptoid ligand with a differential affinity for lanthanide ions in water.

5.2 Screening for Lanthanide Ligands

To preliminarily evaluate the ability of oligomeric peptoids to bind to lanthanides, a library previously designed in Chapter 2 (schematic in Figure 5.1a) was evaluated. Given the previous

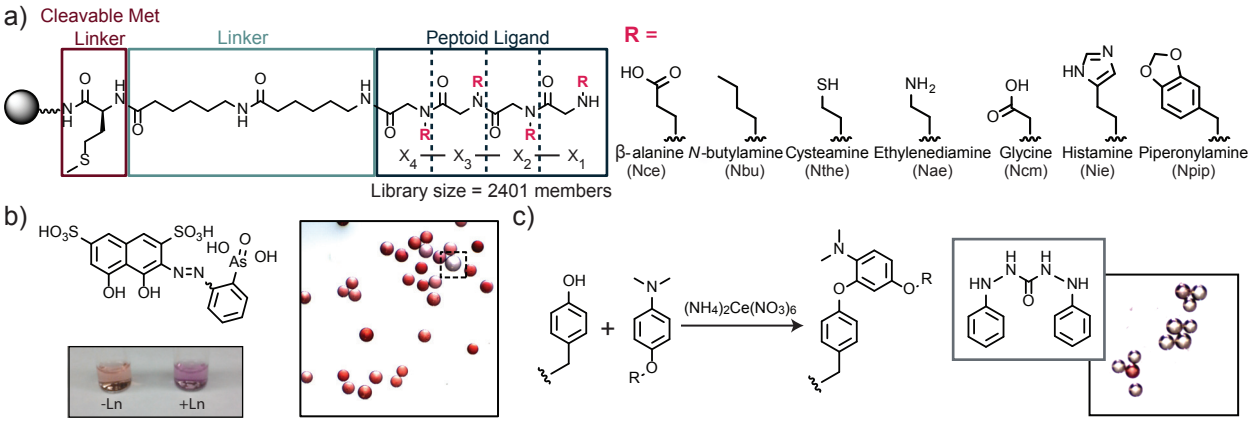

Figure 5.1. Screening for lanthanide binding peptoids. a) Library schematic. The synthesis was completed on Tentagel-NH_2 resin with a linker of two aminohexanoic acid residues before a tetramer peptoid library. At each of the four variable positions, one of the seven variable side chains shown were incorporated. b) Neothorin (structure shown) was used to visualize lanthanide binding. The photograph of the vials shows color of neothorin alone and complexed with La^{3+}. The library members shown in the remaining photograph were incubated with 2 mM La^{3+} and visualized with neothorin (0.001% in EtOH). A purple bead is highlighted. c) In an attempt to identify ligands for Ce(IV) for the reaction shown, the library was screened with cerium ammonium nitrate (2 mM) and binding was visualized with diphenylcarbazide.

success of colorimetric assays, neothorin, a dye used to identify lanthanides, was used to visualize the library after incubation with lanthanum (2 mM).[9] The neothorin solution (0.001% in EtOH) is red in solution, but purple when complexed with lanthanide ions (Figure 5.1b). The photograph of the library in Figure 5.1b shows interaction of the library members with the lanthanum, but the difference between the red and purple on resin is too subtle to be characteristic.

A similar assay was performed to identify ligands capable of Ce(IV) coordination. A reaction recently developed by Seim *et al* uses cerium ammonium nitrate as an oxidant in a bioconjugation reaction (Figure 5.1c).[10] The reaction is sensitive to buffer and pH, and in collaboration with Kristen Seim, we designed a screen to look for ligands for Ce(IV). Diphenylcarbazide, which had previously been used to visualize Cr(VI),[7,11,12] was determined to also form a bright pink complex with cerium. Although this assay was successful, preliminary screening did not reveal any sequences, likely due to the use of the methionine linker (see Chapter 2).

Developing a screen that involved each of the fourteen naturally occurring lanthanide ions would be a significant challenge. To simplify the system, only two ions were chosen for evaluation in the screen. Europium and terbium both luminesce at visible wavelengths when coordinated. They also have very similar ionic size (relative ionic radii of lanthanide ions shown in Figure 5.2b). We therefore hypothesized that a ligand with a differential affinity for europium and terbium would have a differential affinity for the other lanthanides as well. DELFIA is a commercially available time resolved fluorescence assay[13] that has been previously used for immunodetection and receptor-ligand binding assays with europium and terbium tagged proteins simultaneously. This assay could therefore be adapted to simultaneously measure the concentrations europium and terbium bound to an individual bead.

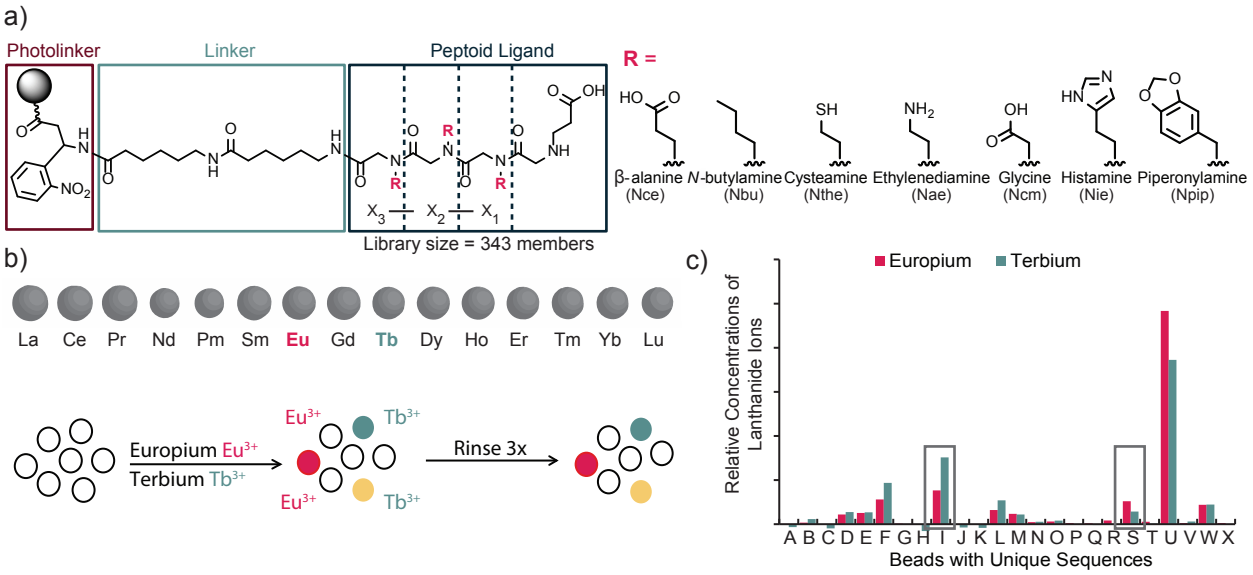

Figure 5.2. Identifying ligands for lanthanide separation. a) Schematic of library designed for lanthanide separation. A photocleavable residue and a two aminohexanoic acid linker connected the peptoid library to the Tentagel-NH_2 resin. Due to the complexity of the screen, a small library was designed with a constant *N*-terminal residue. b) A diagram showing the relative ionic size of each of the lanthanides. Europium and terbium are highlighted as they were chosen for the screen outlined below. c) Twenty-four individual beads from the library in (a) were screened to identify the relative lanthanide concentrations bound. This bar graph shows the relative concentrations of each ion for each of the 24 beads. The boxes highlight beads with significant differences between the concentrations of europium and terbium bound.

5.3 Developing Selective Sensors for Mercury Contamination

Current methods for detecting the presence of heavy metal contaminants in water require expensive equipment and trained technicians. Although many sensors have been developed in research laboratories, many are ineffective in actual samples due to interference from other organic or inorganic compounds.[14] A different approach to the development of functional materials was developed based on previous work constructing dynamic hydrogels as metal sensors completed by Francis *et al.*[15] In this work a metallothionein protein was used to crosslink a water-soluble polymer. Upon metal binding the protein crosslinkers would contract, leading to an overall contraction of the hydrogel. Although the change in size of the protein as a response to metal coordination is likely more significant than the corresponding change in a peptoid crosslinker, we hypothesized that with a higher percentage of peptoid crosslinker we could create a hydrogel that would contract upon metal binding.

Although we had previously demonstrated the selectivity of Sequence 10 (structure in Figure 5.3a) from chromium in the presence of innocuous ions, the affinity for other heavy metal toxins had not been previously evaluated. We evaluated the binding to Cd^{2+}, Pb^{2+}, and Hg^{2+} using

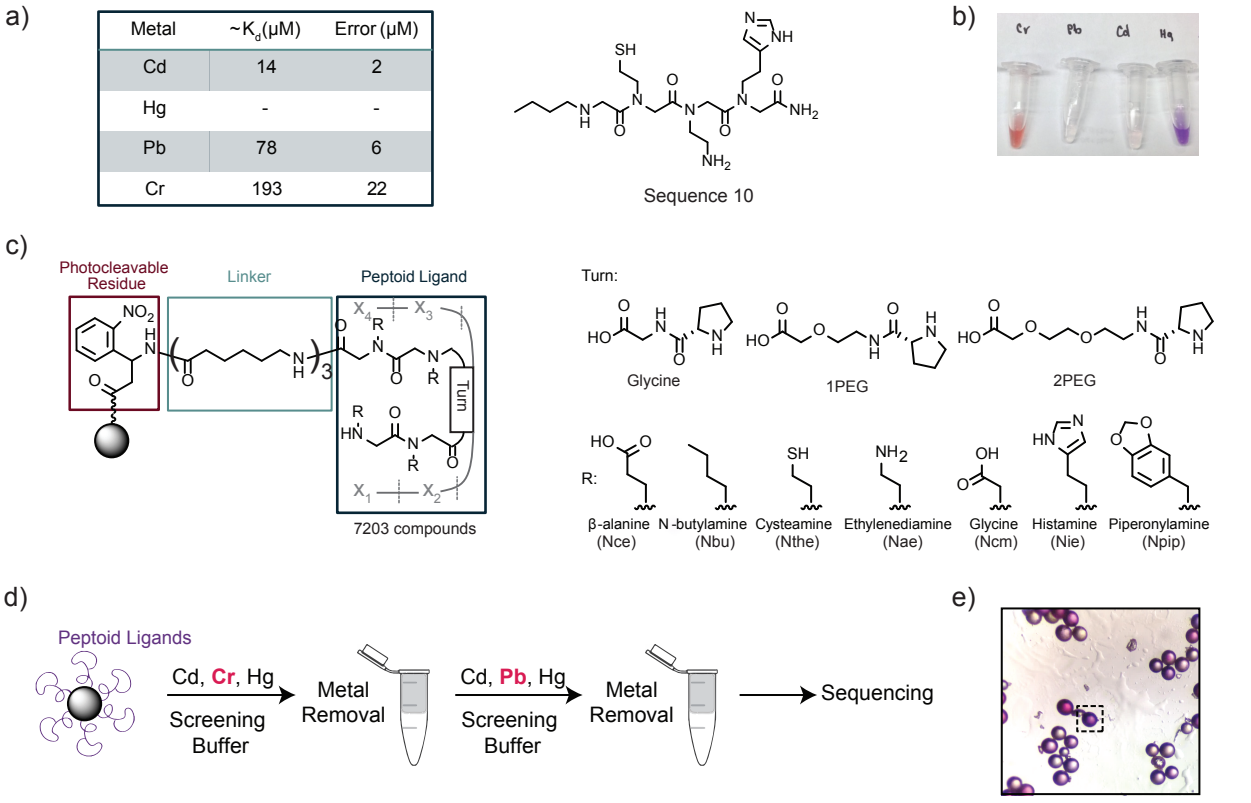

Figure 5.3. Selective mercury ligands. a) Sequence 10 (structure shown), previously identified as a selective ligand for Cr^{6+} in the presence of ions common in natural water, was determined to also have affinity for cadmium and lead. Mercury affinity was not measurable, but due to the significant affinity of thiols for mercury, it's possible that the affinity was too strong to detect with the titrations monitored by UV-vis spectroscopy. b) To identify a ligand with affinity for mercury in the presence of chromium, lead, and cadmium, diphenylcarbazide was identified to have a unique colorimetric response. c) The same library as is shown in Figure 3.2 was used for this assay. d) Due to the extremely low solubility of lead chromate, the screen for mercury affinity had to be completed in two steps. As the schematic shows, a screen was completed in the presence of chromium and then the ions were removed from the hit sequences and the screen was repeated with lead instead of chromium. e) A photograph of the first step in the screening process. A purple bead (indicating bound mercury) is highlighted.

titrations into the peptoid solution (300 uM Sequence 10 in 10 mM HEPES, pH 7) monitored with UV-vis. Affinity for Cd^{2+} and Pb^{2+} was detected, but no affinity for Hg^{2+} was detected. Given the strong interactions of mercury with thiols, it is likely that there is a significant affinity of Sequence 10 for Hg^{2+} that could be evaluated with competition assays. To approximate the dissociation constant of the complexes formed between Sequence 10 and Cd^{2+} and Pb^{2+}, the absorbance at a wavelength attributed to complex formation was plotted verses the concentration of metal, and the data was fit to a logistic curve (see Chapter 2 for examples). The inflection point of the curve was used to approximate the dissociation constants (assuming 1:1 binding) listed in Figure 5.3a. While the affinity of Sequence 10 for many toxic metals may facilitate the development of a sensor for detecting heavy metals, we additionally wanted to identify a ligand that could specifically detect the targeted contaminant. We chose to target Hg^{2+}, as (1) mercury in water bioaccumulates and can cause significant renal problems[16,17] and (2) inorganic mercury can be converted to neurotoxic methylmercury by marine organisms.[18,19]

First, several dyes were examined to identify a dye that could be used to detect mercury complexes in the presence of Cr^{6+}, Pb^{2+}, and Cd^{2+}. Diphenylcarbazide forms a purple complex with Hg^{2+} that is distinctly different from the pink complex formed with Cr^{6+} and does not form a colored complex with Pb^{2+} or Cd^{2+} (Figure 5.3b). Using a peptoid library previously developed for identifying high affinity selective ligands (see Chapter 3 and Figure 5.3c), a screen was designed to identify ligands that would bind to Hg^{2+} in the presence of other toxic metal ions. Unfortunately, lead and chromium form incredibly insoluble lead chromate in aqueous solution, so the screen

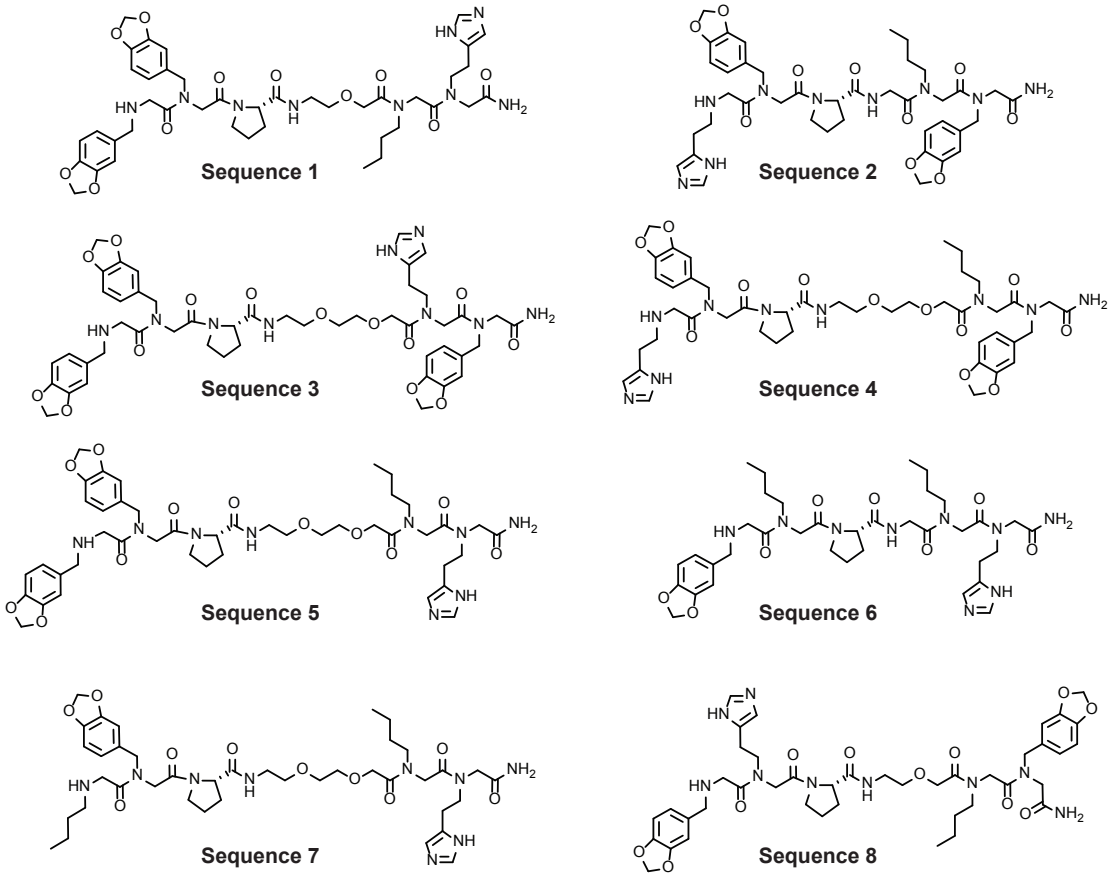

Figure 5.4. Structures identified in the mercury screen.

had to be completed in two parts (schematic in Figure 5.3d). The library was first incubated with Pb^{2+} and Cd^{2+} (2.5 mM) and Hg^{2+} (250 μM) in a screening buffer (50 mM bis(TRIS) pH 7, Na^{+} and Mg^{2+} - 25 mM, and Ca^{2+} - 2.5 mM). After rinsing, mercury ligands were visualized with diphenylcarbazide, selected, and placed in a 0.2 μm filter. Approximately 50 beads were selected, and the ions were removed from the ligands using dialysis in acid (1 M HNO_3). These hit sequences were then incubated an analogous solution with Pb^{2+} being replaced with Cr^{6+}. A photograph of the library after rinsing and treatment with diphenylcarbazide is shown in Figure 5.3e. After the second stage of this screen approximately twelve beads remained; from these, eight sequences were identified using MALDI-TOF-TOF MS (structures in figure 5.4).

The structures identified in this screen displayed different trends than those identified as chromium or cadmium ligands in previous work. The aromatic residue, Npip, was much more prevalent than anticipated. Each of the sequences contains a single imidazole, a functionality which has been known to have a selective affinity for mercury.[20] Although these sequences contain little variety in residues, we hypothesized that the arrangement of these residues could form different binding pockets enhancing the selectivity of the ligands. To evaluate this, two of the ligands were resynthesized on Tentagel-NH_2 to compare their ability to deplete mercury form a solution containing an excess of other toxic metals (Cd^{2+}, Cr^{6+}, and Pb^{2+}) and ions typically in high concentrations in water (Na^{+}, Ca^{2+}, and Mg^{2+}). Ten equivalents of each of the sequences were incubated with each solution with respect to the concentration of mercury. The amount of remaining mercury was measured with ICP-OES, and the results are shown in Figure 5.5. Both Sequence 4 and 7 are able to selectively remove mercury from solution and a slight difference in the efficacy of the two sequences is apparent. This could be due to different levels of modification; future studies with all of the structures will allow a more in depth contrast of the efficacy of the various structures.

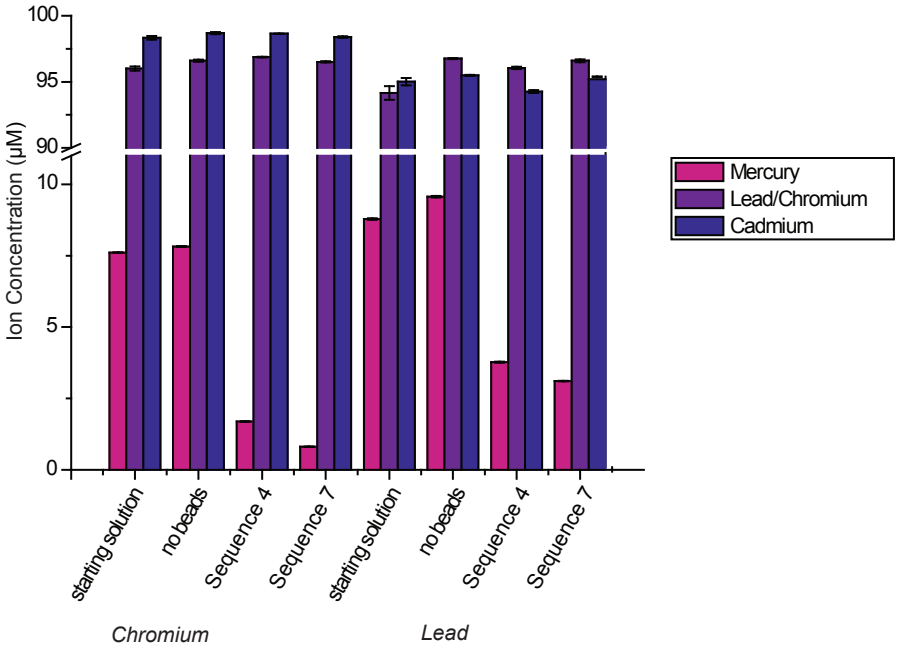

Figure 5.5. Sequences 4 and 7 were evaluated for their ability to deplete Hg in the presence of other heavy metal ions. This graph shows the depletion of mercury with a 10-fold excess of cadmium and chromium and then a 10-fold excess of lead and cadmium in bis(TRIS) (50 mM, pH 7) with native ions (Na^{+}, Mg^{2+} - 25 mM and Ca^{2+}- 2.5 mM).

After determining that Sequence 10 can likely be used to bind any of the toxic heavy metals and the identification of at least two sequences with a selective affinity for mercury, we began evaluating methods of using peptoids to form hydrogel-based sensors. Inspired by previous work with metallothionein proteins with the proteins cross-linking the polymers,[15] strategies to crosslink the polymers with peptoids were investigated. Oxime formation was used to attach the proteins to the polymers, but incorporating an aldehyde into the peptoid as an acetal proved to be challenging. One approach employed click chemistry to attach the peptoid to the polymer. A 1:1 *N*-(2-hydroxypropyl)methacrylamide (HPMA) : *N*-(3-aminopropyl)methacrylamide (APMA) polymer was synthesized using free radical polymerization and reacted with an azido-NHS-ester to form the polymer shown in Figure 5.6a. The ^{1}H-NMR spectrum before and after the reaction with the NHS-ester demonstrates full conversion from the amine-containing polymer to the azide-containing polymer. A peptoid crosslinker was synthesized with two terminal propargyl moieties. With the small amount of peptoid synthesized we were unable to confirm crosslinking via heat or copper catalyzed click chemistry.

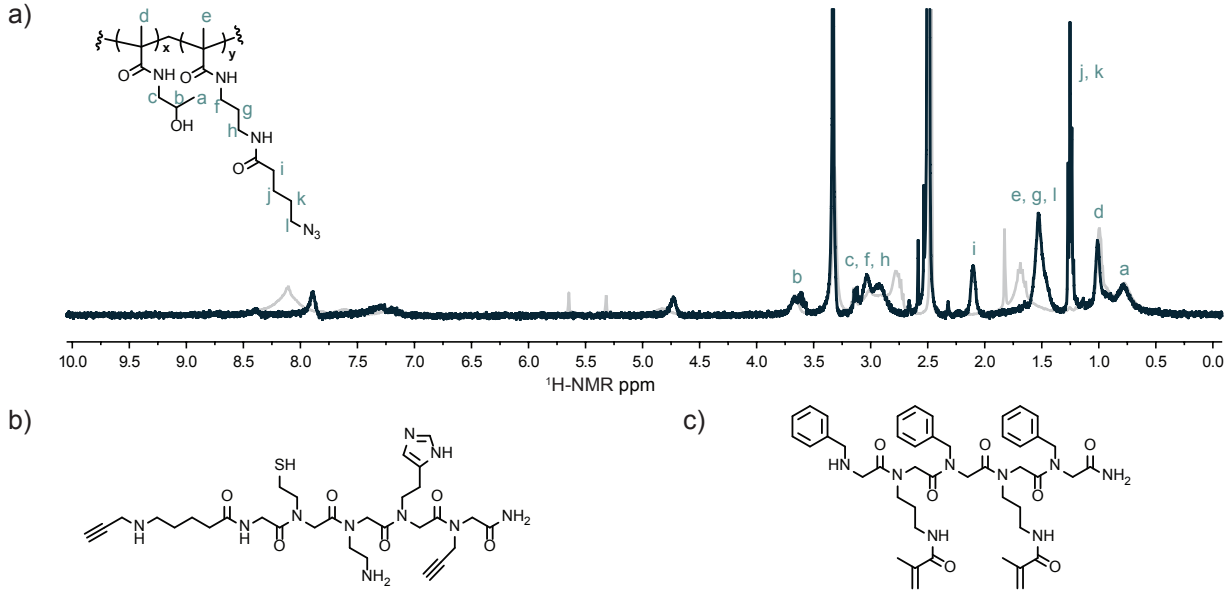

Figure 5.6. Peptoid incorporation into hydrogels. a) A copolymer of 1:1 HPMA:APMA was modified with an azido-NHS ester to form the polymer structure shown. The grey spectrum is the ^{1}H-NMR spectrum before modification and the dark teal spectrum shows the ^{1}H-NMR spectrum after the addition of the azide. b) Sequence 10 appended with two propargyl monomers was synthesized and purified by HPLC to crosslink the polymer shown in (a). c) A test peptoid was synthesized with the APMA monomer to allow for polymer cross-linking during the radical synthesis.

In a final attempt to synthesize a peptoid capable of crosslinking polymers, APMA was incorporated as a monomer in a peptoid test pentamer (a sandwich compound used to test the efficiency of incorporation of new amine submonomers).[6] While side products were visible by MALDI-TOF MS, the desired pentamer was the major product. The peptoid was purified by reverse-phase HPLC and polymerized with HPMA at 1 wt%. Following the free-radical polymerization, ether precipitation and centrifugal filtration against a 3k membrane were used to isolate the polymer from any remaining monomers. Incorporation of the peptoid into the polymer was confirmed by measuring the absorbance at 260 nm.

5.4 Conclusions and Future Directions

The work highlighted in this section displays the potential for developing peptoid-based materials with environmental impact. Both the lanthanide separations and mercury sensors have only preliminary results, but the results for both applications are extremely promising. Future work sequencing the peptoids from the lanthanide screen could identify promising structures for separations. Additionally, more detailed evaluation of the mercury sequences could provide insight into the significance of the order of the residues. Finally the incorporation of these structures into polymeric materials could provide an inexpensive method for detection of mercury contamination.

5.5 Materials and Methods

General Procedures and Materials

Tentagel MB NH_2 resin (140-170 μm, 0.3 mmol/g), used for library synthesis, was purchased from Rapp-Polymere (Tuebingen, Germany). Library synthesis steps were performed in fritted disposable chromatography columns (Bio-Rad, Hercules, CA). During the reactions, the resin suspensions were slowly rotated using a nutator (Fisher Scientific, USA). The photolinker (Fmoc-(*R*)-3-amino-3-(2-nitrophenyl) propionic acid) and Fmoc-6-aminohexanoic acid were purchased from Chem-Impex (Wood Dale, IL). The 1PEG ((2-(Fmoc-amino)ethoxy)acetic acid) and 2PEG ((2-(2-(Fmoc-amino)ethoxy)ethoxy)acetic acid) linkers were purchased from Iris Biotech GMBH (Marktredwitz, Germany). *N*-(2-hydroxypropyl)methacrylamide (HPMA) and *N*-(3-aminopropyl) methacrylamide (APMA) were purchased from Polysciences (Warrington, PA). Water (dd-H_2O) used was deionized using a Barnstead NANOpure purification system (ThermoFisher, Waltham, MA). Serum replacement (KnockOut Serum Replacement) was purchased from Life Technologies (Carlsbad, CA) and human serum was obtained from AB clotted whole blood (Sigma, St Louis, MO). All other materials were purchased from commercial sources and used without further purification, except as noted below. Small scale centrifugation was performed in a Galaxy Mini Star (VWR, USA) and lyophilization was performed using a Labconco Freezone 4.5.

NMR Characterization

^1H spectra were obtained on a Bruker AVQ-400 (400 MHz) spectrometer. Peaks were calibrated using DMSO (2.500, q) and spectra were analyzed using TopSpin software.

Library Synthesis

Of the amine submonomers, piperonylamine, butylamine, and histamine were used as purchased and incorporated without protecting groups. *N*-boc-ethylenediamine was purchased and used as received. Before use, the glycine, β-alanine, and APMA monomers (purchased as hydrochloric acid salts with *t*-butyl ester protecting groups) were treated with 1 M NaOH and extracted into a 15:85 v/v isopropanol-chloroform mixture which was dried over sodium sulfate and concentrated, yielding the monomers as the free bases. Cysteamine was protected with a trityl group using a procedure reported by Maltese.[48] The ability of each amine to incorporate into a peptoid using the chemistry described below was previously verified by synthesizing pentamers with alternating benzylamine groups and test monomers.[21,32] The library was synthesized on Tentagel MB NH_2 resin, which was initially swollen in dichloromethane (DCM). Standard Fmoc solid-phase synthesis (using HCTU as a coupling agent) was used to incorporate the three residues in the linker through amide bond formation. For the first variable position, the resin was split evenly into seven different fritted columns. Acylation and the addition of the first amine were performed according

to the procedure developed by Zuckermann *et al.* for the incorporation of heterocyclic amines.[31] Acylation was achieved by gently agitating resin beads for 5 min with a solution of chloroacetic acid (6.8 eq, 0.4 mM) in dimethylformamide (DMF) and a solution of diisopropylcarbodiimide (8 eq, 2 M) in DMF. The acylation solution was removed via filtration and the resin beads were rinsed with DMF. Next, the amines were added as 2 M solutions in DMF. After 2-12 h of gentle agitation at room temperature, the resin samples were isolated via filtration and rinsed with DMF. All 7 resin aliquots were then pooled and mixed in DCM for 5 min. Subsequently, the resin was isolated via filtration, vacuum dried, and split into a new set of 7 fritted columns. The acylation and amination steps were repeated to add amines at the second variable position. The library was pooled and split into three separate containers for the addition of the turn sequences. To insert the linker and proline monomers into the peptoid backbone, solutions of the linker (20 eq, 0.6 mM in DMF) and diisopropylcarbodiimide (19 eq, 3.2 mM in DMF) were incubated with the resin for 30 min with gentle agitation. The proline was attached using standard solid-phase peptide synthesis (with HCTU as the coupling agent), after which the standard peptoid synthesis procedure was resumed to couple the remaining amines. After the final amination, the resin pools were recombined and agitated gently in a 20% solution of 4-methylpiperidine in DMF to remove any acylation adducts on the imidazole groups. After isolation via filtration, the resin was rinsed with DMF and DCM, then dried under a vacuum. The protecting groups were removed by incubation with a cleavage solution (95:2.5:2.5) trifluoroacetic acid:water:triisopropylsilane) for 1.5 h. The resin was then rinsed with DCM, dried under vacuum, and stored, protected from light, at 4 °C until use.

Screening to Identify Lanthanide Ligands

To equilibrate the beads before the screen, a 50 mg portion of the resin (representing more than 3 times the size of the library to ensure inclusion of each sequence) was swelled in water (1 h). The library aliquot was then incubated with $LaCl_3$ or $(NH_4)_2Ce(NO_3)_6$ for 1 h. The aliquot was then rinsed three times by incubation with 1 mL water in order to facilitate removal of ions retained by non-specific binding.

For visualization and bead selection, the resin was transferred to a Petri dish. Approximately 500 µL of neothorin (0.001% in EtOH) or 1, 5 diphenylcarbazide (0.5 g in 100 mL of acetone) was applied, and the solvent was evaporated from the Petri dish under a gentle flow of nitrogen in order to trap the dye and the metal within the individual beads. The aliquot in the Petri dish was examined using a Leica S6D Microscope (Leica, Germany). The beads with the most intense colors were manually selected for ligand identification. All photographs were taken with an iPhone (model 4 or 5).

Screening to Identify a Ligand with Differential Affinity for Lanthanide Ions

An aliquot of the library was incubated with 1 mL of 100 µM $EuCl_3$ and $TbCl_3$, rinsed 3x with water, and individually isolated into a 96-well plate. DELFIA enhancement solution was added to each well (200 µL) and the plate was incubated for 5 min. A SpectroMax M2 plate reader was used to read the time resolved fluorescence using an excitation of 320 nm, emission of 615 nm, and a delay of 400 µsec. After reading, DELFIA enhancement solution (50 µL) was added to each of the wells. After a 2 min incubation the plate was read at an excitation of 340 nm, emission of 545 nm, and a delay of 500 µsec.

Screening to Identify Selective Mercury Ligands

In the first step of the screen the library was incubated with the lead-containing solution (25 mM – NaOAc, $Mg(OAc)_2$, 2.5 mM – $Ca(C_3H_5O_6)_2$, $Pb(NO_3)_2$, $Cd(OAc)_2$, and $HgCl_2$ 250 μM in bis(TRIS) 50 mM pH 7). Sequences bound to mercury were identified using 1, 5 diphenylcarbazide (0.5 g in 100 mL of acetone) that turns purple when bound to Hg^{2+}. The beads were selected and the ions were removed using the process described below. The sequences were then incubated with the chromium-containing solution (25 mM – NaOAc, $Mg(OAc)_2$, 2.5 mM – $Ca(C_3H_5O_6)_2$, CrO_3, $Cd(OAc)_2$, and $HgCl_2$ 250 μM in bis(TRIS) 50 mM pH 7) and mercury ligands were again visualized with diphenylcarbazide. The aliquot in the Petri dish was examined using a Leica S6D Microscope (Leica, Germany). The beads with the most intense colors were manually selected for ligand identification. All photographs were taken with and iPhone (model 4 or 5).

Metal Ion Removal and Photocleavage

The removal of the metal ions was found in previous work to be essential before interpretable MALDI-TOF MS sequencing data could be obtained. Beads selected from the library screen were deposited onto the membrane of a 0.5 mL 0.2 μm centrifugal filter unit (Millipore, Billerica, MA). A mixture of Amberlite cation (Na^+ form, 5 mg) and anion (Cl^- form, 5 mg) exchange resins was then added to the filtrate collection tube of the centrifugal filter unit. The filter and the collection tube were then filled with 1 M HCl. This setup was incubated with gentle agitation on a nutator for 2 h, allowing diffusion to occur through the 0.2 μm filter. The selected library members were isolated from the exchange resins and acidic solution by centrifugation of the filtration unit. Water (500 μL) was added to the filter unit, and the unit was gently agitated on a nutator for 15 min to rinse the library members. The water was then removed by centrifugation. This process was repeated twice to ensure removal of residual HCl.

The beads bearing hit sequences were removed from the filter unit and transferred to a Petri dish using ethanol (approx. 500 μL). The individual beads were captured using a pipet and placed into individual 0.6 mL Posi-Click tubes (Denville Scientific, South Plainfield, NJ). The volume in each tube was brought to 5 μL with absolute ethanol. To cleave the peptoids from single resin beads, the tubes were placed in a computer controlled ICH-2 photoreactor with UVA bulbs (Luzchem, Ottawa, Canada) for 8 h (various incubation times were screened). For mass verification of bulk peptoid samples, the beads were able to be directly cleaved with the nitrogen laser (337 nm) on the MALDI-TOF MS (Voyager-DE Pro, Applied Biosystems) in addition to the Nd:YAG laser (355 nm) on the MALDI-TOF-TOF MS/MS (4800 plus MALDI-TOF-TOF Analyzer, Applied Biosystems)

To determine whether unintended photoreactions were occurring with the unprotected N-terminal thiol, after one screen the library members were incubated in *N*-ethylmaleimide (25 μL, 10 mM, in dd-H_2O) for 30 min before photocleavage.

Single Bead Sequencing

After single-bead photocleavage, the ethanol was evaporated and replaced with 1:1 water:acetonitrile containing tris(2-carboxyethyl)phosphine (0.5 mM). The sample (0.5 μL) was mixed with 0.5 μL matrix solution (5 mg α-cyano-4-hydroxycinnamic acid in 1:1 water:acetonitrile with 0.1% trifluoroacetic acid and 0.6 M ammonium phosphate) and spotted directly on a stainless steel MALDI plate. MALDI-TOF MS (AB Sciex TF4800, Applied Biosystems) was used to identify the mass of each selected sequence, and MS/MS was used to fragment the peptoids for sequencing. Eighteen unique sequences were identified from this screening process.

Binding Constant Evaluation via UV-vis Titration

Each of the identified sequences was synthesized using the protocols described for library synthesis with Fmoc-Rink Amide MBHA resin (Anaspec, Fremont, CA) in place of the Tentagel MB NH_2 resin. The initial fluorenylmethyloxycarbonyl (Fmoc) group was removed with 20% 4-methylpiperidine in DMF. Following synthesis, a cleavage cocktail (95:2.5:2.5 trifluoroacetic acid:water:triisopropylsilane) was used to remove the peptoids from the resin, while also removing the protecting groups from the monomers. After evaporating the trifluoroacetic acid, the peptoids were precipitated from ether. The resulting precipitates were resuspended in water and purified using reversed phase chromatography on a semi-preparatory scale HPLC column (Agilent). The isolated fractions were concentrated using a speed vacuum (Labconoco, USA) and then lyophilized. The resulting sequences were stored dry at -20 °C before use in order to minimize disulfide formation. MALDI-TOF MS characterizations of the purified peptoids appear in Figure S3.

To evaluate binding constants for Sequence 10, $CdCl_2$, $HgCl_2$, $Pb(NO_3)_2$ (0.3 - 5 mM) was titrated into a solution of peptoid (90 µL, 150 µM in 10 mM HEPES buffer, pH 7) in increments of 0.1-1 µL. The visible absorbance spectrum was measured at each increment using a Cary 50 spectrophotometer (Varian). The absorbance at the monitored wavelength (245 nm) was plotted against the concentration of cadmium and fit to a logistic binding curve using Origin software. The model used to fit the data is displayed in Equation 1, where $A_1$and A_2 are the asymptotes of the data, p correlates to the slope of the curve, and x_0 is the inflection point used to approximate the dissociation constant.

$$y = (A_1\text{-}A_2)/(1+x/x_0)^p+A_2$$

Equation 1

Mercury Depletion Analysis with ICP-OES

Two of the original eight hit sequences were carried forward to depletion experiments: Sequences 4 and 7. These sequences were synthesized on Tentagel MB NH_2 (0.3 mmol/g) using the procedures described in the "library synthesis" section. A photolinker and two aminohexanoic acid residues were used to link the peptoid structures to the resin. The sequence identities were confirmed via MALDI-TOF MS by directly cleaving beads with the MALDI laser.

The selectivity of these sequences was evaluate by adding the sequences to solutions similar to those used in the selection process. (Lead: 25 mM – NaOAc, $Mg(OAc)_2$, 2.5 mM – $Ca(C_3H_5O_6)_2$, $Pb(NO_3)_2$, $Cd(OAc)_2$, and $HgCl_2$ 250 µM in bis(TRIS) 50 mM pH 7 and Chromium: CrO_3 instead of $Pb(NO_3)_2$). After a 2 h incubation, an aliquot from each sample was removed and diluted with nitric acid to a final concentration of 2% HNO_3. The concentration of mercury, cadmium, lead, and chromium remaining in those samples was determined by averaging five measurements of each sample with a Perkin Elmer 5300 DV optical emission ICP using scandium as an internal standard.

Synthesis Azido-NHS ester.

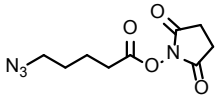

N,N'-dicyclohexylcarbodiimide (722 mg, 3.5 mmol) was added to a stirring solution of azidopentanoic acid (500 mg, 3.5 mmol) and *N*-hydroxysuccinimide (402 mg, 3,5 mmol) in 20 mL of CH_2Cl_2 on ice. The reaction was warmed to room temperature and after two hours filtered through Celite before removing

the solvent *in vacuo*. ^{1}H NMR (400 MHz, $CDCl_3$): δ 3.34 (t, 2H), 2.94 (s, 4H), 2.66 (t, 2H, J = 6.8), 1.85 (dd, 2H), 1.71 (dd, 2H).

Synthesis of HPMA : azide copolymer.

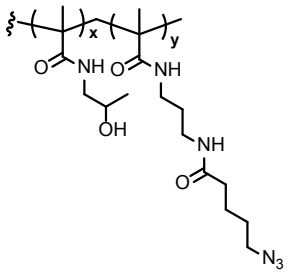

Before polymerization, azobisisobutyronitrile (AIBN) was recrystallized from EtOH. A 1:1 wt% ratio of *N*-(2-hydroxypropyl)methacrylamide (179 mg) and *N*-(3-aminopropyl) methacrylamide (130 mg) and AIBN (15 mg) were added to a vial which was purged with N_2. Methanol (2.7 mL, 12.5:0.6:86.9 monomers : AIBN : MeOH) was sparged with N_2 before being transferred to the solids. The vials were heated at 60 °C for 6-12 h under N_2. Following the reaction, the polymer was purified via precipitation from diethyl ether and centrifugation. The polymer (100 mg, 411 mmol) was combined with, *N,N*-diisopropylethylamine (290 µL, 1644 mmol), and **1** (170 mg, 822 mmol) in 3:2 MeOH : CH_2Cl_2 and stirred for 2 h. The polymer was purified again via precipitation from diethyl ether and centrifugation.

5.6 References

1. Gschneidner Jr, K. A. The rare earth crisis–the supply/demand situation for 2010–2015. *Mater. Matters* **6**, 32–7 (2011).

2. Fryxell, G. E., Chouyyok, W. & Rutledge, R. D. Design and synthesis of chelating diamide sorbents for the separation of lanthanides. *Inorg. Chem. Commun.* **14,** 971–4 (2011).

3. Robards, K., Clarke, S. & Patsalides, E. Advances in the analytical chromatography of the lanthanides. *Analyst* **113,** 1757-79 (1988).

4. Yang, Y. & Alexandratos, S. D. Affinity of Polymer-Supported Reagents for Lanthanides as a Function of Donor Atom Polarizability. *Ind. Eng. Chem. Res.* **48,** 6173–87 (2009).

5. Zuckermann, R. N., Kerr, J. M., Kent, S. B. H. & Moos, W. H. Efficient method for the preparation of peptoids [oligo(N-substituted glycines)] by submonomer solid-phase synthesis. *J. Am. Chem. Soc.* **114,** 10646–7 (1992).

6. Simon, R. J. *et al.* Peptoids: a modular approach to drug discovery. *Proc. Natl. Acad. Sci. U. S. A.* **89,** 9367–71 (1992).

7. Knight, A. S., Zhou, E. Y., Pelton, J G. & Francis, M. B. Selective chromium (VI) ligands identified using combinatorial peptoid libraries. *J. Am. Chem. Soc.* **135**, 17488-93 (2013).

8. Nalband, D. M., Warner, B. P., Zahler, N. H. & Kirshenbaum, K. Rapid identification of metal-binding peptoid oligomers by on-resin X-ray fluorescence screening. *Biopolymers* **102,** 407–15 (2014).

9. Feigl, F. & Anger, V. Spot Tests in Inorganic Analysis. *Elsevier* **80,** 399-401 (1973).

10. Seim, K. L., Obermeyer, A. C. & Francis, M. B. Oxidative modification of native protein

residues using cerium(IV) ammonium nitrate. *J. Am. Chem. Soc.* **133,** 16970–6 (2011).

11. Pflaum, R. T. & Howick, L. C. The Chromium-Diphenylcarbazide Reaction. *J. Am. Chem. Soc.* **78,** 4862–6 (1956).

12. Willems, G. J., Blaton, N. M., Peeters, O. M. & De Ranter, C. J. The interaction of chromium (VI), chromium (III) and chromium (II) with diphenylcarbazide, diphenylcarbazone and diphenylcarbadiazone. *Anal. Chim. Acta* **88,** 345–52 (1977).

13. Diamandis, E. P. Immunoassays with time-resolved fluorescence spectroscopy: Principles and applications. *Clin. Biochem.* **21,** 139–50 (1988).

14. Li, M., Gou, H., Al-Ogaidi, I. & Wu, N. Nanostructured Sensors for Detection of Heavy Metals: A Review. *ACS Sustain. Chem. Eng.* **1**, 713-23 (2013).

15. Esser-Kahn, A. P., Iavarone, A. T. & Francis, M. B. Metallothionein-cross-linked hydrogels for the selective removal of heavy metals from water. *J. Am. Chem. Soc.* **130,** 15820–2 (2008).

16. U.S. EPA. Inorganic Mercury. *TEACH Chemical Summary* 1–19 (2007).

17. Stacchiotti, A. *et al.* Stress proteins and oxidative damage in a renal derived cell line exposed to inorganic mercury and lead. *Toxicology* **264,** 215–24 (2009).

18. Fitzgerald, W. F., Lamborg, C. H. & Hammerschmidt, C. R. Marine Biogeochemical Cycling of Mercury Marine Biogeochemical Cycling of Mercury. *Chem. Rev.* **107,** 641-62 (2007).

19. Blum, J. D., Popp, B. N., Drazen, J. C., Anela Choy, C. & Johnson, M. W. Methylmercury production below the mixed layer in the North Pacific Ocean. *Nat. Geosci.* **6,** 879–84 (2013).

20. Brooks, P. & Davidson, N. Mercury(II) Complexes of Imidazole and Histidine. *J. Am. Chem. Soc.* **82,** 2118–23 (1960).

Chapter 6

Immobilization of Peptoids on Glass Substrates via Oxidative Coupling to *o*-Aminophenols

Abstract

Glass and other SiO_2-based surfaces are commonly functionalized with peptides and other biomolecules for various applications including drug delivery, the construction of biosensors, and the development of high-throughput assays. Many of the methods currently available involve the conjugation of a nucleophile common to biomolecules (–SH, –OH, or –NH). Herein we describe the use of mild oxidative coupling for the immobilization of *N*-substituted glycine oligomers (peptoids) on a glass substrate. Since their development, peptoids have demonstrated significant promise as therapeutic molecules and their immobilization is critical for the development of functional materials. Additionally, the bioconjugation reaction has been demonstrated previously to be compatible with a variety of substrates, and therefore we envision this strategy to be generally applicable to all biomolecules.

6.1 Immobilization of Small Molecules and Biomolecules on SiO_2 Surfaces

The immobilization of small molecules and biomolecules on SiO_2 surfaces has become increasingly important with the growing implementation of microarrays and high-throughput screening techniques,[1–4] silica-based drug-delivery,[5] biosensors,[6,7] and biocatalysis.[7,8] For these applications, covalent attachment is preferable to non-covalent adsorption to obtain a stable and uniform coating of high-densities of biomolecules. Common techniques for covalent immobilization include an amine or thiol containing biomolecule conjugated to a surface that has been silanized with an electrophilic (e.g. maleimide, aldehyde, or epoxy) moiety.[9] The use of these reactions for surface functionalization limits the nucleophilic functional groups which can be included in the biomolecules of interest. These nucleophilic residues are commonly important for function, and their modification can reduce the bioactivity. Bioorthogonal strategies have been implemented, including copper-catalyzed[10] and strain-promoted alkyne-azide cycloadditions[11] and the Staudinger ligation.[12] However, these all suffer from limitations including extensive reaction times and the biologically damaging presence of copper(I).[13]

Our group have recently developed a mild oxidative coupling reaction that is compatible with various biomolecules and has been successfully used in the conjugation of gold-nanoparticles to biomolecules.[14–16] This reaction is completed at close to neutral pH values in water, making it particularly compatible with biomolecules. Continuing to demonstrate the versatility of this reaction, our group have immobilized peptidomimetic molecules on glass surfaces. *N*-substituted glycine oligomers, or peptoids,[17] were chosen as the target molecules due to (1) their promise as therapeutic molecules,[18–20] (2) the variety of nucleophilic side chains of interest, which cause the selection of a compatible immobilization strategy particularly challenging,[21] and (3) their compatibility with solid-phase synthesis – the platform developed should also be compatible with other molecules synthesized on solid phase. Peptoids have previously been conjugated to glass using thiol-maleimide reactions[22–25] and copper-catalyzed alkyne-azide cycloadditions,[26,27] Unfortunately the maleimide conjugation most commonly utilized is reversible at intracellular concentrations of glutathione.[28] The few equivalents required for the rapid oxidative coupling reaction and the stability of the iminoquinone product, will be advantageous for future immobilization of peptoids and other molecules.

6.2 Coupling Aniline-Containing Peptoids

To create *o*-aminophenol coated glass, an *o*-nitrophenol silane was designed (Figure 6.1a). In our previous work immobilizing biomolecules on gold nanoparticle surfaces, aniline, the opposite coupling partner was attached to the surface.[15] To minimize the purification steps required for

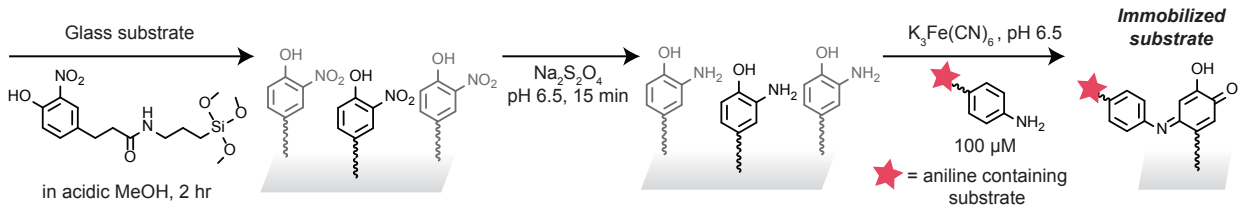

Figure 6.1. Functionalization of glass substrates using oxidative coupling of aniline and o-aminophenol moieties. Schematic of immobilization strategy. First the glass is silanized with a *o*-nitrophenol moiety. The nitrophenol is then reduced to an aminophenol and reacted with an aniline using potassium ferricyanide as a mild oxidant.

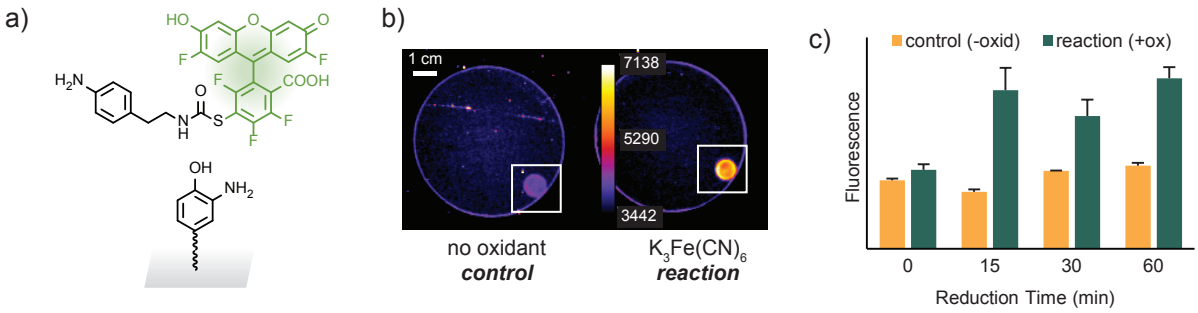

Figure 6.2. Quantification of reaction completion using fluorescence. Various reaction times were evaluated for the reduction of the nitrophenol immobilized on the glass bead (1 mm) to the aminophenol. a) Aniline-Oregon Green 514 was used as a model substrate to optimize the reaction conditions. The images show the fluorescence of 1 mm glass beads. The reaction is compared to a control that lacked the potassium ferricyanide oxidant. b) Fluorescence image taken with a typhoon imager showing the reaction of aminophenol-glass with the aniline-OG. The control reaction contained no oxidant. c) For each reduction time screened, the fluorescence was quantified from the typhoon images.

the peptoid, the aniline moiety was attached to the peptoid in this work. The *o*-nitrophenol silane was synthesized by coupling a nitrophenol carboxylic acid to the aminopropylsilane. Base-washed glass beads (1 mm) were exposed to the nitrophenol silane in acidified methanol and stored under vacuum. Immediately prior to further modification, the nitrophenol moieties were reduced to the aminophenol with sodium dithionite. To evaluate how the reaction rates on the surface varied from in solution, an aniline-Oregon Green 514 (aniline OG – Figure 6.2a) was synthesized by conjugating 4-(2-aminoethyl)aniline to NHS Oregon Green 514. This aniline-OG was used to evaluate the effect of the reaction time of the dithionite reduction by subsequently reacting the beads with the aniline-OG and quantifying the fluorescence with a laser scanning imager. The beads coupled to anilne-OG were compared to a set of control beads which had been exposed to the same reaction conditions with the exception of the oxidant (Figure 6.2b). The fluorescence of each bead was quantified (Figure 6.2c), and the average fluorescence of each control reaction was subtracted from the respective reaction at each time point (Figure 6.3a). The results indicate that similar to the reaction in solution, reducing the reaction for longer than 15 min does not increasee the amount of fluorophore attached.

Similar assays were performed to determine how the concentrations of the reactants affected the modification levels of the glass beads. The reaction is usually performed in solution at high micromolar concentrations,[14] and therefore concentrations surrounding that range were evaluated (Figure 6.3b). The modification increased with reactant concentration until 50 μM of the

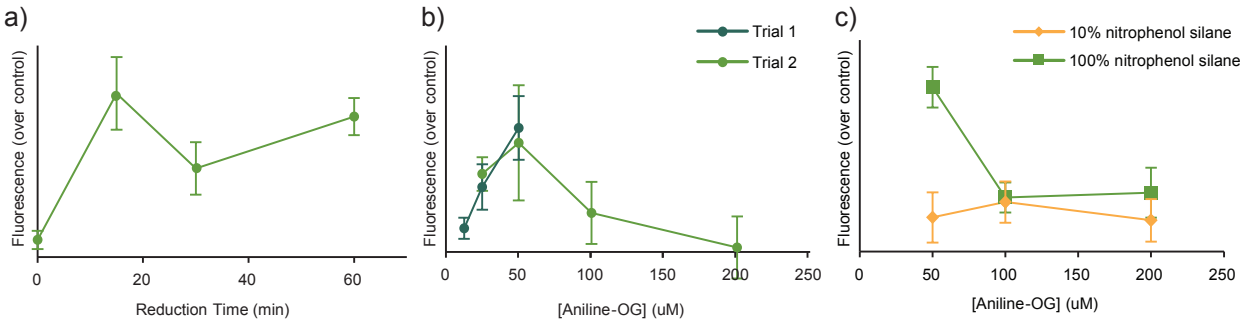

Figure 6.3. Optimization of the oxidative coupling reaction on the glass surface with the aniline-OG. a) Various times for the reduction of the nitrophenol with sodium dithionite were evaluated. b) Concentrations of the aniline for the oxidative coupling reaction were evaluated in two different trials (oxidant in 20x excess). All reactions were incubated for 1 hr. At concentrations above 50 uM the decrease in fluorescence was attributed to quenching. c) To evaluate whether the aminophenol moieties were reacting with each other on the surface, glass beads were coated with a 10:1 ratio of non-reactive moieties : aminophenols. The fluorescence signal after the oxidative coupling reaction was compared.

aniline, and then the fluorescent signal significantly dropped. We hypothesized that this drop could be due to either the aminophenol moieties reacting with each other on the surface at the higher concentrations of oxidant or that the higher levels of modification were leading to self-quenching of the fluorophore. To evaluate whether the surface functional groups were reacting with each other, glass beads were co-silanized with 2-[methoxy(polyethyleneoxy)propyl] trimethoxysilane (10:1 unreactive : reactive silane). If the reaction was hindered by reaction of the surface moieties with each other, this co-silanization should allow for higher or at least equivalent modification levels to be reached. The data in Figure 6.3c indicate that little modification was apparent on the co-silanized surfaces. Although the silanzation reaction itself will proceed at slightly different rates, the ratio of the two silanes on the glass surface should be comparable to 10:1. Therefore the decrease in fluorescence at higher concentrations was determined to be due to quenching, and in future surface conjugation reactions, the aniline substrate was reacted at a concentration of 100 μM.

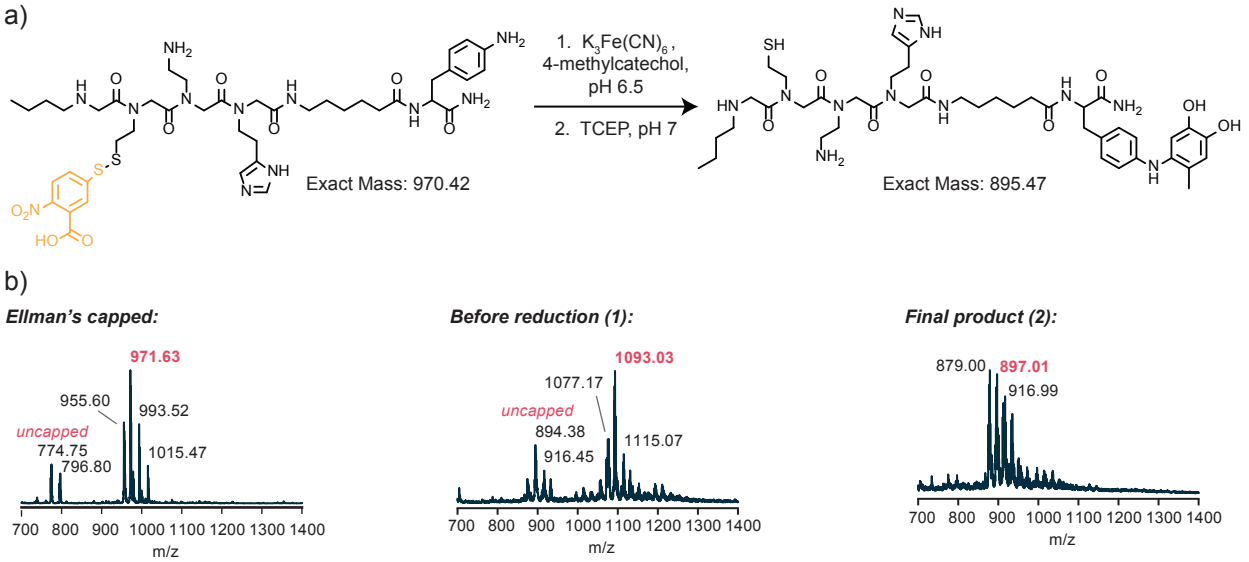

Figure 6.4. a) Schematic of oxidative coupling of aniline-linked peptoid to 4-methylcatechol. b) MALDI-TOF MS of the reaction stages. The thiol-containing peptoid was capped with Ellman's reagent and purified by HPLC (*left*). The peptoid was coupled to 4-methylcatechol with potassium ferricyanide (*center*). Tris(2-carboxyethyl)phosphine (TCEP) was used to remove the thiol protecting group and additionally reduced the iminoquinone product to the corresponding hydroquinone (*right*).

To confirm that a peptoid could be immobilized on glass, a previously identified chromium (VI)-binding structure with a variety of nucleophilic residues (Figure 6.4a) was evaluated.[29] It has been previously demonstrated that thiols must be capped before the reaction,[14] so the structure was capped with 5,5'-dithiobis-(2-nitrobenzoic acid) (Ellman's reagent) before purification. To confirm that only one product is formed, the peptoid was reacted with 4-methylcatechol (a small molecule mimic of the aminophenol silane). The reaction was characterized by MALDI-TOF MS (Figure 6.4b) before the reaction, after the reaction, and after the removal of the Ellman's reagent with tris(2-carboxyethyl)phosphine (TCEP). Due to the high charge of the peptoid, it was challenging to purify away excess reagents, but the mass spectra clearly indicate the formation of a single product. After the success of the solution reaction, the peptoid was reacted with the aminophenol coated glass beads. To confirm the presence of the immobilized peptoid, the surface was reacted with a maleimide fluorophore, and the fluorescence was compared to beads from which the Ellman's reagent had not been removed (Figure 6.5a). The higher fluorescence signal from the uncapped peptoid reactions demonstrates the success of conjucation using this technique.

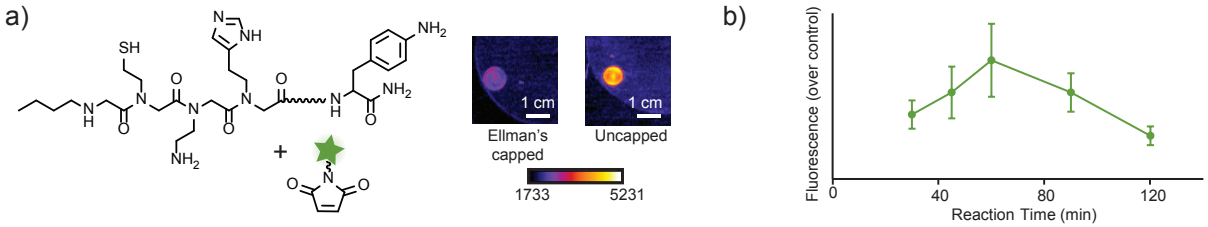

Figure 6.5. Immobilization of metal binding peptoids. a) The immobilization of a peptoid linked to an aniline is confirmed with a maleimide-Oregon Green 488. The control shown used a peptoid where the thiol was protected with Ellman's reagent. All images were taken with a Typhoon imager. b) To evaluate the reaction time required for maximum surface modification.

To evaluate the rate of the reaction with the peptoid substrate, the peptoid (100 μM) was incubated with the aminophenol-coated glass and ferricyanide oxidant for 30-120 min (Figure 6.5b). After the reaction the thiols were reduced and reacted with a maleimide fluorophore to compare the modification levels. The fluorescence peaks after 60 min, but as mentioned above, the decrease in fluorescence signal after that time point can be attributed to self-quenching. For this reason reaction times of 1-2 h are recommended for immobilizing peptoids with this reaction.

6.3 Conclusions and Future Outlook

In this work we have demonstrated the application of a mild bioconjugation reaction for the immobilization of aniline-containing peptidomimetic structures on glass surfaces. In future work we are working towards reacting the secondary *N*-terminal amine of the peptoid as the reactive moiety in the oxidative coupling. The expansion the biorthogonal reaction toolbox for immobilization of biological molecules on surfaces is essential for their integration into functional materials. These oxidative coupling reactions will allow for the development of high-throughput assays, silica-based delivery systems, and biosensors with nucleophilic functional groups that are imperative to their function.

6.4 Materials and Methods

General Procedures and Materials

Peptoid synthesis steps were performed in fritted disposable chromatography columns (Bio-Rad, Hercules, CA). During the reactions, the resin suspensions were slowly rotated using a nutator (Fisher Scientific, USA). Water (dd-H_2O) used was deionized using a Barnstead NANOpure purification system (ThermoFisher, Waltham, MA). All materials were purchased from commercial sources and used without further purification, except as noted below. Small scale centrifugation was performed in a Galaxy Mini Star (VWR, USA) and lyophilization was performed using a Labconco Freezone 4.5.

NMR Characterization

^{1}H and ^{13}C spectra were obtained on a Bruker AVQ-400 (400 MHz, 100 MHz) spectrometer. Peaks were calibrated using chloroform (7.26, s) and spectra were analyzed using TopSpin software.

Preparation of 3-(4-hydroxy-3-nitrophenyl)propionic acid

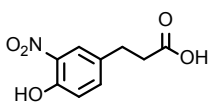

This was prepared according to a previously published protocol.[14] To a solution of 3-(4-hydroxyphenyl)propionic acid (5 g) was added fuming nitric acid (1.6 mL) in acetic acid (25 mL) and the reaction was stirred for 15 min. The product

was crashed out in ice water, filtered, and dried under vacuum. ^{1}H NMR ($CDCl_3$, 400 MHz): δ 10.494 (s, 1H), 7.961 (d, J = 2.0 Hz, 1H), 7.463 (dd, J = 2.0 Hz, 8.8 Hz, 1H), 7.110 (d, J= 8.8 Hz, 1H), 2.958 (t, J = 7.6 Hz, 2H), 2.701 (t, J = 7.6 Hz, 2H).

Preparation of 3-(4-hydroxy-3-nitrophenyl)-N-(3-(trimethoxysilyl)propyl)propanamide

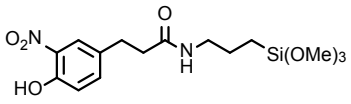

To a solution of 3-(4-hydroxy-3-nitrophenyl)proprionic acid (1 g, 4.74 mmol) and DIPEA (2.062 mL, 2.5 eq) in anhydrous tetrahydrofuran (150 mL) was added pentafluorophenyl trifluoroacetate (1.017 mL, 1.25 eq) dropwise over 20 min. The reaction mixture was stirred under nitrogen for 2 hours at room temperature. To this was added 3-aminopropyltrimethoxysilane (0.909 mL, 1.1 eq). The resulting solution was stirred under nitrogen for 18 hr at room temperature. The mixture was then concentrated using a rotary evaporator, and separated by flash chromatography (50:50 ethyl acetate:hexanes followed by 100% ethyl acetate). ^{1}H NMR ($CDCl_3$, 400 MHz): δ 10.450 (s, 1H), 7.910 (d, J = 2.3 Hz, 1H), 7.473 (dd, J = 2.3 Hz, 8.6 Hz, 1H), 7.062 (d, J= 8.6 Hz, 1H), 3.543 (s, 9H), 3.206 (q, J = 6.6, 2H), 2.948 (t, J = 7.4, 2H), 2.443 (t, J = 7.4 Hz, 2H), 1.561 (m, 2H), 0.548 (t, J = 8.1, 2H).

Silanization of glass surfaces

Glass beads (1 mm, Sigma Aldrich) were base-washed with KOH (1 M, 1 hr), rinsed with water and oven dried at 100 C (>1 h). The surfaces were then submerged and nutated in a 25 mM solution of 3-(4-hydroxy-3-nitrophenyl)-*N*-(3-(trimethoxysilyl)propyl)propanamide in methanol with 1% water (by volume) and 148 mM acetic acid. The surfaces were then rinsed first with methanol and then with 148 mM acetic acid in methanol, briefly dried under a stream of nitrogen gas, and fully cured in an oven at 100 °C (>13 h). The surfaces were stored at room temperature in a desiccator pending further modification.

Preparation of aniline-Oregon Green 514 (aniline-OG)

Oregon Green 514 carboxylic acid succinimidyl ester (5 mg, 8.2 umol) was dissolved in dimethylformamide (100 uL) in a brown 1.5 mL Eppendorf tube. To this solution was added 4-(2-aminoethyl)aniline (1.3 uL, 1.2 eq) and triethylamine (1.6 uL, 2 eq). The mixture was stirred for 30 minutes at room temperature and concentrated with a high vacuum rotary evaporator. The product was dissolved in a mixture of water (400 uL) and methanol (1.1 mL), spin filtered, and purified by HPLC. Purity was checked by MALDI-MS (detected m/z 630.9). Dye was lyophilized and stored at -20 °C until use.

Quantifying modification of glass surfaces with aniline-Oregon Green 514

The nitrophenol silanes on the glass surfaces were reduced by incubation in dithionite (60 mM, in 100 mM pH 6.5 phosphate buffer, 15 min). The surfaces were then washed with DPBS (x3) and water (x2). The surfaces were incubated in 100 uM aniline-Oregon Green with 2 mM $K_3Fe(CN)_6$ in 10 mM pH 6.5 phosphate buffer for (insert time here), resulting in an oxidative coupling between the fluorophore and the aminophenol silane. This was then washed with 0.4% SDS in water, DPBS, water, and methanol, and air dried. Fluorescence was imaged using a Typhoon 9410 variable mode imager (Amersham Biosciences) (excitation 532 nm, emission 555 nm).

Testing aniline-peptoids for reactivity in solution-based oxidative coupling reactions

Following solid phase synthesis and cleavage from the resin, aniline-sequence 10 was capped with Ellman's reagent. 2-amino-p-cresol (purified by sublimation and stored at -20 °C prior to use) was dissolved in acetonitrile to a concentration of 500 mM. Capped aniline-sequence 10 (1 eq, final concentration 100 uM), 2-amino-*p*-cresol (2 eq, 200 uM), and K_3FeCN_6 (20 eq, 2 mM) were then dissolved in 10 mM pH 6.5 phosphate buffer and were nutated for 30 min at room temperature. The desired oxidative coupling product was identified by MALDI-MS (predicted mass 1091, detected *m/z* 1093). This confirmed the viability of aniline-peptoids for glass modification.

Peptoid Synthesis

Of the seven amine monomers, piperonylamine, butylamine, and histamine were used as purchased and incorporated without protecting groups. *N*-boc-ethylenediamine was purchased and used as received. Before use, the glycine and β -alanine monomers (purchased as hydrochloric acid salts with *t*-butyl ester protecting groups) were treated with 1 M NaOH and extracted into a 15:85 v/v isopropanol-chloroform mixture which was dried over sodium sulfate and concentrated, yielding the monomers as the free bases. Cysteamine was protected with a trityl group using a procedure reported by Maltese.[48] The ability of each amine to incorporate into a peptoid using the chemistry described below was previously verified by synthesizing pentamers with alternating benzylamine groups and test monomers.[5,32] The initial fluorenylmethyloxycarbonyl (Fmoc) group was removed with 20% 4-methylpiperidine in DMF. Acylation and the addition of the first amine were performed according to the procedure developed by Zuckermann *et al.* for the incorporation of heterocyclic amines.[31] Acylation was achieved by gently agitating resin beads for 5 min with a solution of chloroacetic acid (6.8 eq, 0.4 M) in dimethylformamide (DMF) and a solution of diisopropylcarbodiimide (8 eq, 2 M) in DMF. The acylation solution was removed via filtration and the resin beads were rinsed with DMF. Next, the amines were added as 2 M solutions in DMF. After 2-12 h of gentle agitation at room temperature, the resin samples were isolated via filtration and rinsed with DMF. Following synthesis, a cleavage cocktail (95:2.5:2.5 trifluoroacetic acid:water:triisopropylsilane) was used to remove the peptoids from the resin, while also removing the protecting groups from the monomers. After evaporating the trifluoroacetic acid, the peptoids were precipitated from ether. The resulting precipitates were resuspended in water and purified using reversed phase chromatography on a semi-preparatory scale HPLC column (Agilent). The isolated fractions were concentrated using a speed vacuum (Labconoco, USA) and then lyophilized. The resulting sequences were stored dry at -20 °C before use in order to minimize disulfide formation.

Modification of glass surfaces with metal-binding peptoids

To protect the thiol before the oxidative coupling, the peptoid (approx. 1 mg) was dissolved in ethanol (100 uL) and combined with Ellman's reagent (5 mg in 1 mL EtOH). This was incubated for 30 min before evaporation and precipitation from cold ether. The product was purified by reverse-phase HPLC before immobilization on glass.

The silanes on the glass surfaces were reduced by incubation in dithionite (60 mM, in 100 mM pH 6.5 phosphate buffer, 15 min). After washing with DPBS (x3) and water (x2), the surfaces were incubated in 100 uM aniline-peptoid with 2 mM $K_3Fe(CN)_6$ in 10 mM pH 6.5 phosphate buffer for various amounts of time (30 min, 45 min, 60 min, 90 min, and 120 min), resulting in an oxidative coupling between the peptoid and the silane. This was then washed with 0.4% SDS in water, DPBS, water, and methanol, and dried under nitrogen before storing at room temperature in a dessicator.

The relative amount of modification attained for each of these timescales was evaluated using fluorescent dyes, as described below.

Quantifying modification of glass with metal-binding peptoids

The disulfides in the Ellman's capped peptoids were reduced by incubation with 10 mM TCEP in 10 mM pH 6.5 phosphate buffer (10 min), then washed with methanol and water. The surfaces were then incubated with 1 mM Alexafluor 488 maleimide dye in 25 mM pH 7.5 phosphate buffer (1.5 hr). The surfaces were washed with 0.4% SDS in water, DPBS, water, and methanol, air dried, and imaged using a Typhoon 9410 variable mode imager (Amersham Biosciences) (excitation 488 nm, emission 520 nm).

6.5 References

1. Henderson, G. & Bradley, M. Functional peptide arrays for high-throughput chemical biology based applications. *Curr. Opin. Biotechnol.* **18,** 326–330 (2007).

2. Lam, K. S. & Renil, M. From combinatorial chemistry to chemical microarray. *Curr. Opin. Chem. Biol.* **6,** 353–8 (2002).

3. Ma, H. & Horiuchi, K. Y. Chemical microarray: a new tool for drug screening and discovery. *Drug Discov. Today* **11,** 661–8 (2006).

4. Hong, J. A., Neel, D. V, Wassaf, D., Caballero, F. & Koehler, A. N. Recent discoveries and applications involving small-molecule microarrays. *Curr. Opin. Chem. Biol.* **18,** 21–8 (2014).

5. Yang, P., Gai, S. & Lin, J. Functionalized mesoporous silica materials for controlled drug delivery. *Chem. Soc. Rev.* **41,** 3679 (2012).

6. Tjong, V., Tang, L., Zauscher, S. & Chilkoti, A. 'Smart' DNA interfaces. *Chem. Soc. Rev.* **43,** 1612–26 (2014).

7. Magner, E. Immobilisation of enzymes on mesoporous silicate materials. *Chem. Soc. Rev.* **42,** 6213–22 (2013).

8. Lopez-Gallego, F. & Schmidt-Dannert, C. Multi-enzymatic synthesis. *Curr. Opin. Chem. Biol.* **14,** 174–83 (2010).

9. Kanoh, N. Small Molecule Microarrays. *Small* **669,** 17–23 (2010).

10. Fazio, F., Bryan, M. C., Blixt, O., Paulson, J. C. & Wong, C.-H. Synthesis of Sugar Arrays in Microtiter Plate. *J. Am. Chem. Soc.* **124,** 14397–402 (2002).

11. Manova, R., Vanbeek, T. a. & Zuilhof, H. Surface functionalization by strain-promoted alkyne-azide click reactions. *Angew. Chem. Int. Ed.* **50,** 5428–30 (2011).

12. Köhn, M. *et al.* Staudinger Ligation: A New Immobilization Strategy for the Preparation of Small-Molecule Arrays. *Angew. Chem. Int. Ed.* **42,** 5830–4 (2003).

13. Agard, N. J., Baskin, J. M., Prescher, J. A., Lo, A. & Bertozzi, C. R. A Comparative Study of Bioorthogonal Reactions with Azides. *ACS Chem. Biol.* **1,** 644–8 (2006).

14. Obermeyer, A. C., Jarman, J. B., Netirojjanakul, C., El Muslemany, K. & Francis, M. B. Mild bioconjugation through the oxidative coupling of ortho-aminophenols and anilines with ferricyanide. *Angew. Chem. Int. Ed.* **53,** 1057–61 (2014).

15. Capehart, S. L., Elsohly, A. M., Obermeyer, A. C. & Francis, M. B. Bioconjugation of Gold Nanoparticles through the Oxidative Coupling of ortho -Aminophenols and Anilines. *Bioconjugate Chem.* **25**, 1888-92 (2014).

16. Obermeyer, A. C., Jarman, J. B. & Francis, M. B. N-Terminal Modification of Proteins with o- Aminophenols. *J. Am. Chem. Soc.* **136**, 9572-9 (2014).

17. Simon, R. J. *et al.* Peptoids: a modular approach to drug discovery. *Proc. Natl. Acad. Sci. U. S. A.* **89,** 9367–71 (1992).

18. Zuckermann, R. N. & Kodadek, T. Peptoids as potential therapeutics. *Curr. Opin. Mol. Ther.* **11,** 299–307 (2009).

19. Astle, J. M., Udugamasooriya, D. G., Smallshaw, J. E. & Kodadek, T. A VEGFR2 Antagonist and Other Peptoids Evade Immune Recognition. *Int. J. Pept. Res. Ther.* **14,** 223–7 (2008).

20. Udugamasooriya, D. G., Dunham, G., Ritchie, C., Brekken, R. A. & Kodadek, T. The pharmacophore of a peptoid VEGF receptor 2 antagonist includes both side chain and main chain residues. *Bioorg. Med. Chem. Lett.* **18,** 5892–4 (2008).

21. Culf, A. S. & Ouellette, R. J. Solid-phase synthesis of N-substituted glycine oligomers (alpha-peptoids) and derivatives. *Molecules* **15,** 5282–335 (2010).

22. Reddy, M. M. *et al.* Identification of candidate IgG biomarkers for Alzheimer's disease via combinatorial library screening. *Cell* **144,** 132–42 (2011).

23. Kwon, Y.-U. & Kodadek, T. Encoded combinatorial libraries for the construction of cyclic peptoid microarrays. *Chem. Commun.* 5704–6 (2008).

24. Reddy, M. M. & Kodadek, T. Protein 'fingerprinting' in complex mixtures with peptoid microarrays. *Proc. Natl. Acad. Sci. U. S. A.* **102,** 12672–7 (2005).

25. Knight, A. S., Zhou, E. Y., Francis, M. B. & Zuckermann, R. N. Sequence Programmable Peptoid Polymers for Diverse Materials Applications. *Adv. Mater.* (2015). doi:10.1002/adma.201500275

26. Lim, H.-S. *et al.* Rapid identification of improved protein ligands using peptoid microarrays. *Bioorg. Med. Chem. Lett.* **19,** 3866–9 (2009).

27. Labuda, L. P., Pushechnikov, A. & Disney, M. D. Small molecule microarrays of RNA-focused peptoids help identify inhibitors of a pathogenic group I intron. *ACS Chem. Biol.* **4,** 299–307 (2009).

28. Baldwin, A. D. & Kiick, K. L. Tunable degradation of maleimide-thiol adducts in reducing environments. *Bioconjugate Chem.* **22,** 1946–53 (2011).

29. Knight, A. S., Zhou, E. Y., Pelton, J G. & Francis, M. B. Selective chromium (VI) ligands identified using combinatorial peptoid libraries. *J. Am. Chem. Soc.* **135**, 17488-93 (2013).